6504

Bayreuther

Bodenkundliche Berichte

Wenceslau Geraldes Teixeira

Land Use Effects on Soil Physical and Hydraulic Properties of a Clayey Ferralsol in the Central Amazon

Band 72

Bayreuth 2001

ISSN 0931-6442

CONTENTS

List of tables

List of figures

Acknowledgements

I thank Embrapa (Empresa Brasileira de Pesquisa Agropecuaria) – Amazônia Ocidental for the authorisation to complete my study in Germany.

I thank Prof. Dr. Bernd Huwe for having the confidence in me, and especially for the support, supervision and encouragement in the "hard" soil physics topics.

I am indebted to Prof. Dr. Wolfang Zech for inviting me to come to Bayreuth and your support during my period here.

Dr. Götz Schroth for his interest, suggestions and for critically reading the manuscripts.

Prof. Dr. Leonel Libardi (University of São Paulo – Brazil) for your technical assistance in the installation of the IPM experiment and to analyse the data, and Prof. Dr. Wolfgang Durner for sharing your expertise on pore size distribution analyses and helping me with actual literature.

Celso Paulo de Azevedo (Embrapa – Amazônia Ocidental) and Prof. Dr. Julio Silvio Bueno (University of Lavras – Brazil) for valuable discussion concerning the variance analysis.

Thanks to Eduard Arevalo for helping with the Fortran code.

Thanks also to Estevão Oliveira dos Santos, Jean Dalmo Marques, Max Sarrazin and Olivio Faccin for the technical assistance in the fieldwork and laboratory analyses.

Very special thanks to Hubert Wiedner and Dr. Marion Mertens for you help in the German abstract. Thanks all to Prof. Dr. Joao José Marques, Dr. Martin Schlather, Petra Schlegel for reviewing the English of parts of this manuscript.

Very special thanks to Sandra Iwata not only for reviewing English but specially for her strength and advices during my stay in Germany.

I grateful thank the financial support from DAAD (Deutscher Akademischer Austauschdienst).

AUSFÜHRLICHE DEUTSCHE ZUSAMMENFASSUNG

1 Enleitung

1.1 Amazonien

Im Zuge zahlreicher wirtschaftlicher Entwicklungsphasen in Amazonien haben große Probleme die Entwicklung einer intensiven landwirtschaftlichen Nutzung erschwert. Dadurch wurde das Wachstum der ansässigen Bevölkerung gebremst und die wirtschaftliche Unabhängigkeit des Gebiets behindert.

Seit dem Zusammenbruch des Kautschukbooms zu Beginn des letzten Jahrhunderts aufgrund des großmaßstäbigen Kautschukanbaus in Asien sind verschiedene Entwicklungsstrategien zur Verbesserung der landwirtschaftlichen Produktion ausprobiert worden. Die Kautschukgewinnung wurde teilweise mit Subventionen bis in die späten 70er Jahre aufrechterhalten, obwohl bereits intensive Ansiedlungsprogramme für Amazonien begonnen hatten. All diese Programme hatten zur Folge, dass Waldflächen in Weideflächen und Ackerland umgewandelt wurden. In den letzten Jahrzehnten rückten die Abholzung des Primärregenwalds und die daraus resultierenden ökologischen Konsequenzen verstärkt ins öffentliche Bewusstsein. Ein Aspekt sind die möglichen klimatischen Folgen: Die Landnutzungsänderungen können Veränderungen der Wasserbilanzen hervorrufen (Gash et al. 1996); außerdem könnte es zu signifikanten Kohlenstoff-Verlusten aus dem Boden in die Atmosphäre kommen (Moraes et al.; 1996; Fearnside und Barbosa, 1996), jedoch sind beide Hypothesen in wissenschaftlichen Kreisen noch umstritten.

Die Erhaltung der Biodiversität ist zweifellos ein guter Grund, den ursprünglichen Primärregenwald zu erhalten. Desweiteren müssen schützenswerte Flächen und Gebiete identifiziert und beschrieben werden. Es müssen Wege gefunden werden, die Biodiversität Amazoniens wirtschaftlich zu nutzen. Die Biodiversität darf zwar nicht nur unter dem Aspekt der wirtschaftlichen Nutzbarbeit gesehen werden, es muss jedoch auch der Nutzen für die ansässige Bevölkerung bedacht werden.

Ein weiterer Aspekt ist das landwirtschaftliche Potenzial der Hochlandböden in Zentral-Amazonien: Ihre geringe Fruchtbarkeit, ihr hohes Nährstoff-Auswaschungspotenzial und die für viele Pflanzenkrankheiten günstigen Bedingungen werfen die Frage auf, ob es wirtschaftlich sinnvoll ist in dieser Region Landwirtschaft zu betreiben.

In den meisten Regionen wird von den Kleinbauern immer noch traditioneller Brandrodungsfeldbau betrieben. Die typische Form dieses Bewirtschaftungssystems sieht folgendermaßen aus: Zuerst werden die vermarktungsfähigen Bäume gefällt und verkauft; die restlichen Bäume werden abgeholzt und liegengelassen, damit sie trocknen können. Danach wird die komplette Fläche abgebrannt. Die dann gepflanzten Feldfrüchte nutzen die Asche als Dünger. Im ersten Jahr sind die Feldfruchterträge in der Regel ziemlich hoch (hauptsächlich Reis, Bohnen, Mais und Maniok).

Allerdings gehen bereits im zweiten Jahr die Erträge sowohl in der Quantität als auch in der Qualität zurück, da die Verfügbarkeit der Nährstoffe abnimmt und gleichzeitig das Unkraut sehr stark zunimmt. In der Regel muss nach 3-5 Jahren die Fläche verlassen werden und es bildet sich wieder Sekundärwald (*capoeira*). Gleichzeitig wird wieder eine neue Fläche gerodet. Da sich die Bodenqualität nur langsam erholt, sollte der Boden nun über viele Jahre hinweg nicht landwirtschaftlich genutzt werden (*pousio*). Die Anzahl und Häufigkeit der Rotation hängt primär von der natürlichen Bodenfruchtbarkeit ab und kann zwischen 10-20 Jahren liegen. Deshalb benötigt der Brandrodungsfeldbau riesige Gebiete und ist bei der heutigen Bevölkerungsdichte ein nicht-nachhaltiges Landnutzungssystem. Die Fehlschläge vieler Landnutzungssysteme, die für Amazonien empfohlen wurden, lassen sich durch die Kombination von Umweltfaktoren mit ungeeigneten Anbaumethoden erklären. Dieselben Degradationsprozesse, die die Produktivität des Brandrodungsfeldbaus zurückgehen lassen, sind für den Produktivitäts-Rückgang fortschrittlicherer Landnutzungssysteme verantwortlich. Ein genaues Verständnis der zugrundeliegenden Prozesse ist daher ein Schlüsselfaktor für die Entwicklung nachhaltiger Anbaumethoden.

Viele Studien, die sich mit nachhaltiger Landnutzung in Amazonien beschäftigen, legen ihr Hauptaugenmerk vor allem auf die Umweltqualität und nicht auf die Bevölkerung Amazoniens, die *caboclos*. Die Kleinbauern im brasilianischen Amazonasgebiet sind beschuldigt worden, den Primärwald zu zerstören. Bislang gibt es jedoch kein geeignetes Landnutzungssystem, das den Brandrodungsfeldbau in den meisten Regionen Amazoniens ersetzen könnte. Deshalb ist der Brandrodungsfeldbau die bislang einzige Möglichkeit für diese Bauern, um zu überleben. Zudem ziehen die Kleinbauern bereits gerodete Flächen, die sich durch Brachlegung, die sogenannte *pousio*, wieder erholt haben, dem neu zu rodenden Primärwald vor.

Überlegungen zur Einführung geeigneter Landnutzungssysteme sollten, abgesehen von wirtschaftlichen Überlegungen, geo-politischen Motiven und militärischen Sicherheitsüberlegungen, auch die 600.000 Kleinbauern, die in dieser Gegend Brasiliens leben, mit einbeziehen. Deren Grundbedürfnis nach Nahrung, Kleidung, Wohnraum, Zugang zu Schulen für die Kinder, sowie zu medizinischen und sanitären Einrichtungen muss befriedigt werden.

Landnutzungssysteme mit mehrjährigen Kulturen werden als geeigneter für die *terra firma* (= nicht überschwemmte)-Böden Amazoniens angesehen, als Systeme mit einjährigen Kulturen. Sie erhalten die Bodenqualität, verbessern den Lebensstandard der örtlichen Bevölkerung und verbessern den Umweltzustand. Zudem können sie den Abholzungsdruck auf die Primärwald-Flächen lindern. Jedoch wird trotz der Vorteile mehrjähriger Kulturarten im Vergleich zu einjährigen Pflanzungen von mehreren Autorn über das Nachlassen der Bodenfruchtbarbeit auf derartigen Kulturen in den immerfeuchten Tropen berichtet.

Deshalb müssen die Bodendegradationsprozesse in diesen Landnutzungssystemen genauer untersucht werden.

1.2 Bodenqualität und nachhaltige Landnutzung

Die Begriffe Bodenqualität und nachhaltige Landnutzung werden schon seit mehreren Jahren verwendet und dementsprechend viele Definitionen sind vorgeschlagen worden. Die Begriffe dürfen nicht verwechselt werden und basieren auf verschiedenen Definitionen. In dieser Arbeit ist Bodenqualität wie folgt definiert:

> *"The capacity of a specific kind of soil to function within natural or managed ecosystem boundaries, to sustain plant and animal productivity, maintain or enhance water and air quality, and support human health and habitation "*
>
> *(Karten et al. 1997)*

und nachhaltige Landnutzung als:

> *"Combination of technologies, policies, and activities aimed at integrating socio-economic principles with environmental concerns so as to simultaneously maintain or enhance production, reduce the level of production risk, protect the potential of natural resources and prevent (buffer against) soil and water degradation, be economically viable, and be socially acceptable"*
>
> *(Smyth and Dumanski, 1993)*

Die Bodenqualität wird letztendlich von den Standort-Bedingungen bestimmt und kann auch untersucht werden, wenn nur Bodendaten vorliegen. Praxisrelevante Landnutzungsstudien müssen biophysikalische Daten mit wirtschaftlichen und sozialen Aspekten verbinden. Da in der vorliegenden Untersuchung nur Bodendaten analysiert wurden, beziehen sich die aus dieser Studie gewonnenen Erkenntnisse grundsätzlich nur auf die Bodenqualität.

Anbaumethoden wirken in entscheidender Weise auf die Bodenqualität. Ihre Beurteilung ist daher von fundamentaler Bedeutung, wenn die Nachhaltigkeit von Landnutzungssystemen bestimmt werden soll (Karten et al., 1997). Deshalb sollte die Wahl der Landnutzung und der Anbaumethode den Erhalt bzw. den Wiederaufbau einer hohen Bodenqualität berücksichtigen. Bodenqualität kann durch Monitoring von verschiedenen Indikatoren gemessen werden. Der gewählte Indikatortyp ist abhängig von der Bodenfunktion (landwirtschaftliche Produktion, Filterung und Pufferung von

Schadstoffen, etc.) und vom Maßstab (z.B. Feld, Bauernhof, Wassereinzugsgebiet), auf dem die Untersuchung durchgeführt wird (Mausbach und Seybold, 1998; Mohamemed et al. 2000).

Aus der Sichtweise der landwirtschaftlichen Produktion bezieht sich die Bodenfunktion auf die Fähigkeit, die Produktivität aufrecht zu erhalten. Die Bodenqualitäts-Indikatoren in dieser Studie sind darauf ausgerichtet, die physikalischen und hydraulischen Eigenschaften, sowie Prozesse, die mit der Anordnung von Bodenpartikeln und Poren zu tun haben (z.B. Porosität), zu erfassen. Um Indikatoren für die Abschätzung der Bodenqualität verwenden zu können, müssen Referenzwerte eingeführt werden (Mausbach und Seybold, 1998) oder es muss ein besseres Verständnis der dynamischen physikalischen Prozesse in Abhängigkeit der Parameter bekannt sein (Wagenet and Hudson, 1997). Die Analyse der Bodenqualität mit Hilfe eines physikalischen Prozessansatzes, wie sie bei Wagenet und Hudson (1997) vorgeschlagen wurde, könnte es erlauben, die Auswirkungen dynamischer Prozesse vorherzusagen, anstatt sie nur im Nachhinein zu messen.

1.3 Ziele der vorliegenden Arbeit

Diese Untersuchung ist Teil einer Langzeitstudie von SHIFT (**S**tudies of **Hu**man **I**mpact on **F**orest and floodplains in the **T**ropics) zur Rekultivierung von degradierten Monokulturflächen in Zentral-Amazonien. Sie soll nachhaltige Landnutzungssysteme auf abgeholzten und degradierten tonigen Ferralsol-Böden nahe Manaus entwickeln. Wobei es sich bei den Boden um tonige Hochland-Ferrasols handelt. Sollte dies erreicht werden, so besteht die Möglichkeit, diese Flächen wieder in den landwirtschaftlichen Produktionsprozess zurückzuführen.

Komplexere Simulationsmodelle für Wasserflüsse und Pflanzenwachstum benötigen räumlich repräsentative Parameter, die die physikalischen und hydraulischen Eigenschaften des Bodens in verschiedenen Tiefen beschreiben. Es sind bereits viele Modelle verfügbar und weitere werden entwickelt. Das Wissensdefizit bezüglich vieler bodenphysikalischer und –hydraulischer Eigenschaften beschränkt jedoch deren Nutzung für Simulationsstudien in Zentral-Amazonien wesentlich. Dieses Problem besteht vor allem für die tonigen Ferralsols, da fast nichts über deren physikalische und hydraulische Eigenschaften bekannt ist und vor allem nicht klar ist, wie sich diese Eigenschaften unter den verschiedenen Landnutzungssystemen verändern. Wegen des ungewöhnlichen Verhaltens der tonigen Ferralsols treten sowohl methodische als auch theoretische Probleme auf: Bei hohem Matrixpotenzial halten und leiten sie das Wasser wie typische Tonböden, aber die Infiltrationsraten und Wasserflüsse nahe der Sättigung sind eigentlich typisch für Sandböden.

Das Hauptanliegen dieser Arbeit ist:

- geeignete Methoden zu finden, um die bodenphysikalischen und –hydraulischen Eigenschaften von tonigen Ferralsols zu bestimmen und zu charakterisieren
- physikalische Bodenqualitäts-Indikatoren zu vergleichen, die in den verbreitetsten Landnutzungssystemen Zentral-Amazoniens gemesssen wurden. Dies könnte für die Entwicklung von nachhaltigen Landnutzungssystemen in dieser Region von Nutzen sein.

Die Arbeit gibt zu Beginn einen kurzen Überblick über die Landnutzungssysteme in Amazonien und die Bodenqualitätsparameter. Die mangelhaften Kenntnisse über die Eigenschaften der tonigen Ferralsols, die den Hauptanteil der Böden im Norden Brasiliens ausmachen, werden ebenso dargestellt. Im zweiten Kapitel werden Hintergrund-Informationen zu Klima, Vegetation, Geologie und den tonigen Ferralsols gegeben, sowie der Versuchsstandort mitsamt seiner Geschichte detailliert beschrieben. Das dritte Kapitel diskutiert die Messung einiger physikalischer Parameter, die der Charakterisierung der Bodenstruktur und ihrem Verhältnis zu chemischen Bodeneigenschaften dienen. Statistische Tests in Verbindung mit dem gewichteten Mittel werden als Instrument zum Vergleich von Bodenparametern vorgeschlagen, wobei verschiedene Werte innerhalb eines Landnutzungssystems angenommen werden. Das danach folgende vierte Kapitel stellt die Messung der Bodenporosität und ihre Interpretation in Bezug zur Wasserdynamik vor. In Kapitel 5 wird die Durchführbarkeit der Bodenwassergehalts-Messungen in tonigen Ferralsols mit Hilfe der TDR-Technik und die dazu notwendige Kalibrierung beschrieben. Außerdem werden die relevanten Einflussfaktoren auf die θ-Messung im Gelände diskutiert. Die Bestimmung der hydraulischen Eigenschaften ist das Thema des sechsten Kapitels. Hier werden mit unterschiedlichen Methoden und auf verschiedenen Landnutzungssystemen gemessene gesättigte und ungesättigte hydraulische Eigenschaften diskutiert und verglichen. Die neue inverse Methode zur Bestimmung hydraulischer Eigenschaften wird ebenfalls präsentiert. Es werden Rückschlüsse über die Funktionsweise von aus Mikro- und Makroporen aufgebauten bimodalen hydraulischen Sytemen abgeleitet. Allgemeine Schlussfolgerungen und Empfehlungen für weitere Untersuchungen werden in Kapitel 7 dargestellt. Alle in dieser Arbeit verwendeten Daten sind im Anhang des jeweiligen Kapitels aufgeführt. Einige statistische Methoden werden im Detail erläutert. Die Datenverarbeitung wird vollständig beschrieben. Im gesamten Text wurde Wert darauf gelegt, die Effizienz von komplexen statistischen und mathematischen Methoden (z.B. Skalierungstheorie, Tests zur Überprüfung von Modellübereinstimmungen, stückweise lineare Regression, log-Normal-Verteilungen und nicht-lineare Regression) zu demonstrieren. Diese werden normalerweise nicht bei der Erforschung von Landnutzungssystemen benutzt. Sie sind jedoch sehr nützlich, wenn nicht sogar absolut notwendig, um die hoch variablen bodenphysikalischen und –hydraulischen Parameter zu analysieren und zu interpretieren.

2 Beschreibung des Versuchsstandortes

2.1 Standort

Die Studie wurde auf der Versuchsstation der EMBRAPA–Westamazonien nahe Manaus im zentralen brasilianischen Amazonas-Gebiet durchgeführt (3° 8' S, 59° 52' W, 40-50 m a.s.l.). Zur Lage der Station s. Abbildung 2.1.

2.2 Klima

Die Monats-Mitteltemperaturen schwanken innerhalb Zentralamazoniens – zum Teil aufgrund fehlender Relief-Einflüsse - nur sehr wenig. In der Region um Manaus wird im September mit 28°C die höchste Monats-Mitteltemperatur gemessen. Die niedrigste Monats-Mitteltemperatur beträgt 26°C und tritt in den Monaten Februar bis April auf (Salati, 1985).
Das Verhältnis zwischen Intensität, Häufigkeit und Dauer von Niederschlagsereignissen wurde in der Region um Manaus von Paiva (1996), Marques Filho et al. (1981) und Ribeiro (1976) beschrieben. Ihre Ergebnisse zeigen eine durchschnittliche Jahresniederschlagsmenge von 2400 - 2500 mm und eine markante jahreszeitliche Abhängigkeit, wobei das monatliche Maximum im Februar bis März (durchschnittlich ca. 320 mm) und das Minimum im August bis September (durchschnittlich ca. 80 mm) liegt. Darüber hinaus treten die Niederschläge meist in Form sehr starker Regenfälle von kurzer Dauer auf.
Nach den Kriterien der Köppen-Klassifizierung in Critchfield (1993) sollte der Standort als Af und nicht, wie zuerst von Rodrigues et al. (1972) vorgeschlagen, als Aw klassifiziert werden, da die Niederschlagsmenge in den trockensten Monaten, normalerweise, mehr als 60 mm beträgt.
Die durchschnittliche Evapotranspiration für das gesamte Amazonas Becken wurde durch Verwendung der Penman-Gleichung berechnet: das ergab 1460 mm Jahr $^{-1}$ (Villa Nova et al., 1976). Ribeiro und Villa Nova (1979) benutzten Thornthwaite und Mather's Gleichung und schätzten die potenzielle Evapotranspiration auf 1536 mm Jahr $^{-1}$ bei einer durchschnittlichen jährlichen Niederschlagsmenge von 2478 mm. Sie schätzten eine aktuelle Evapotranspiration von 1508 mm Jahr $^{-1}$, wobei die Werte der potenziellen und aktuellen Evapotranspiration praktisch für das gesamte Jahr identisch waren. Ausgenommen hiervon sind die drei Monate August, September und Oktober, bei denen Bodenwassermangel auftritt. Unter Verwendung eines Wasserhaushaltsmodells schätzten Leopoldo et al. (1995) eine aktuelle Evapotranspiration von 1493 mm Jahr $^{-1}$. Sie folgerten daraus, dass die potenzielle und aktuelle Evapotranspiration die gleiche Größenordnung haben. Ähnliche Resultate erhielt Shuttleworth (1988), der die jährliche Evapotranspirationrate auf

1320 mm schätzte. 328 mm von dieser entfielen auf Interzeption im Bestand und 992 mm auf Transpiration.
Der größte Teil der standortspezifischen meteorologischen Untersuchungen in Manaus wurde im ca. 10 km von den Versuchsflächen entfernt liegenden Ducke Forest Reservat (Viswanadham et al., 1991; Shuttleworth et al., 1988; Marques et al., 1987, Villa Nova et al., 1976; Ribeiro et al., 1987) durchgeführt. Für die Jahre 1994 und 1995 wurden mikroklimatische Daten direkt von der Versuchsfläche ausgewertet (Cabral et al. 1997). Interzeption, direkt auf den Boden auftreffender Niederschlag und Stammabfluss wurden direkt am Standort untersucht (Schroth et al.; 1999); Interzeptions-Untersuchungen im Primärregenwald wurden von Leopoldo et al. (1987), Franken et al., (1982 a, b), Lloyd et al. (1988 a, b) und Northcliff and Thornes (1981) durchgeführt.

2.3 Geologie und Böden

Die über Sedimenten liegenden Böden in Zentralamazonien entstanden aus Verwitterungen tertiärer fluvial-limnischer Ablagerungen, die zur sogenannten "Barreiras Schicht" gehören. Diese besteht aus wechselgelagertem Sandstein mit eingesprengten Argiliten, wobei Quarz und Kaolinit dominieren und Feldspat und Muskovit in geringeren Mengen vorkommen (Chauvel, 1987).
Der Boden auf den Hochflächen und Oberhängen ist ein toniger, tiefgründig verwitterter Ferrasol (Cornu et al., 1998; Chauvel, 1982). Die starke Verwitterung resultiert aus Prozessen wie intensiver Quarz-Auflösung, Aluminiumhydroxid-Anreicherung und Kristallisation von Kaolinit (Cornu, 1998; Irion, 1984; Chauvel, 1987). Infolgedessen sind die Böden normalerweise sehr nährstoffarm (z.B. Phosphor, Calcium, Magnesium und Kalium).
Der Boden auf dem Versuchsstandort wird nach der FAO-Klassifizierung (FAO, 1990) als Xanthic Ferrasol angesprochen. Gemäß der Boden-Klassifikation des Soil Survey Staff (1999) handelt es sich um einen Xanthic Hapludox und nach der brasilianischen Klassifizierung (EMBRAPA, 1999) um einen Latosolo amarelo. Die tonigen Ferrasols sind repräsentativ für große Gebiete in Zentralamazonien (Vieira and Santos, 1987).
Die bodenpysikalischen und –chemischen Eigenschaften des Versuchsstandorts sind den von Camargo und Rodrigues (1979) und Rodrigues et al. (1972) beschriebenen Standorten sehr ähnlich. Sie haben mit 600 – 750 kg m^{-3} Ton in den ersten 30 cm einen hohen Tongehalt an der Oberfläche; darunter sind sie mit 750 - 850 kg m^{-3} Ton noch toniger. Die Tonfraktion besteht hauptsächlich aus Kaolinit und etwas Gibbsit (Camargo und Rodrigues, 1979; Rodrigues, 1998; Silva, 1997).
Die beobachtete starke Mikroaggretation entsteht wahrscheinlich als Folge der festen Bindung zwischen positiv geladenen Hydroxiden und negativ geladenen Kaoliniten sowie organischer Substanz (Sanches, 1986).

Der im Wasser gemessene pH von ca. 5 findet sich auch in tieferen Schichten des Profils. Die Kationen-Austausch-Kapazität (Ca^{++}, Mg^{++}, K^{+}, Na^{+}) ist mit ungefähr 0.60 cmolc kg^{-1} im A-Horizont sehr niedrig und sinkt bis auf 0.3 – 0.1 $cmol_c$ kg^{-1} in den darunter liegenden Horizonten. Verfügbares Phosphor ist nur im A-Horizont nachweisbar (3 ppm nach der Melhich II Methode), in tieferen Schichten des Profils sinkt die Konzentration rasch auf die Nachweisgrenze ab. Der organische Kohlenstoffgehalt liegt bei ca. 30 g kg^{-1} im A-Horizont, wobei die Gehalte mit zunehmender Tiefe rasch abnehmen: In 200 cm Tiefe g wurden noch ca. 2-3 g kg^{-1} gemessen.
Eine detaillierte Beschreibung der chemischen Eigenschaften des Untersuchungsstandorts findet sich in Preisinger (1997); Teixeira et al. (1997); Schroth et al. (1999b) and Schroth et al. (2000).

2.4 Vegetation

Die tonigen Ferrasols sind von einem dichten, feuchten und immergrünen Regenwald bedeckt, dem sogenannten Terra Firme-Wald. Obwohl in der gesamten Region das äußere Erscheinungsbild des Regenwaldes ziemlich ähnlich ist, zeigt eine detaillierte Untersuchung eine große Arten-Diversifizierung auf den verschiedenen Standorten (Murça Pires, 1984; Guillaument, 1987). Die Baumkronen des Primärregenwaldes reichen in etwa 30 m Höhe. Das unterste Stockwerk des dichten tropischen Waldes ist nur sehr schwach belichtet und daher im Allgemeinen frei von Lianen, Büschen, Kraut- und Zwergvegetation (Murça Pires, 1984). Die relative Luftfeuchtigkeit erreicht über der Baumkrone 100 %. Daher ist die direkte Verdunstung des Bodens nahe Null (Leopoldo et al., 1987).
Die Entwicklung eines dichten Waldes auf Böden, die nährstoffarmes Muttergestein als Grundlage haben, hat in den 60er Jahren die Aufmerksamkeit von vielen Forschern auf sich gezogen (Kitamura, 1996). Dies wurde durch die Tatsache erklärt, dass tropische Bedingungen mit hohen Temperaturen und hohem Niederschlag eine sehr intensive Photosyntheserate erlauben; da der tropische Wald ein hohes Alter besitzt, war genügend Zeit für die vorhandenen Nährstoffe, sich in der Biomasse der Pflanzen anzureichern (Murça Pires, 1984).
Die für diesen Prozess notwendigen Nährstoffe sind in der Biomasse des Waldes festgelegt und werden immer wieder durch die rege Pflanzen- und Faunaaktivität verrottet und resorbiert. Kleinere Nährstoffverluste werden durch mineralische Einträge durch den Regen ausgeglichen (Leopoldo et al., 1987).
Arbeiten von Nepstad (1994) zeigen außerdem, dass das Wurzelsystem der Waldpflanzen größere Tiefen erreichen kann und ein signifikanter Anteil des Bodenwassers aus Tiefen von mehr als 2 m entzogen wird. Das wiederum verringert den Wasserstress der Pflanzen in den Trockenzeiten.

2.5 Landnutzung, Versuchsanordnung und Flächen-Management

Einige Studien über pflanzenverursachte Bodenveränderungen sahen sich mit verblüffenden Effekten von Standortvariabilität und Bodennutzungsgeschichte konfrontiert. Eine Untersuchung, die die Einflüsse von Pflanzen auf Bodeneigenschaften exakt beurteilen will, kann genauere Schätzungen erzielen, wenn die Untersuchungen auf ursprünglich homogenen Substraten durchgeführt werden. Wenn der Boden am Anfang gut charakterisiert wird, können alle Unterschiede in den Bodeneigenschaften, die während der Versuchsdauer auf den verschiedenen Versuchsparzellen auftreten, Pflanzeneffekten zugeordnet werden. Deshalb folgt im Anschluss eine detaillierte Beschreibung der Standort-Geschichte. Einige Versuchsergebnisse lassen sich auf diese Weise erklären.

Der Primärregenwald wurde auf dem Versuchsstandort zum ersten Mal 1980 abgeholzt. Für das Abholzen und Entfernen der Baumstümpfe wurden schwere Maschinen eingesetzt. Die verbliebene Vegetation wurde verbrannt. Im Jahre 1981 wurde ein Versuchsfeld mit Gummibäumen (*Hevea brasiliensis*) angelegt und 1986 wieder eingestellt. Bis zur Vorbereitung der Fläche für die aktuellen Untersuchungen wuchs Sekundärvegetation zusammen mit den verbliebenen Gummibäumen. Der sich entwickelnde Sekundärwald wurde 1992 manuell abgeholzt und die Vegetation an Ort und Stelle verbrannt. Die Versuchsfläche wurde von Februar bis März 1993 mit Setzlingen bepflanzt.

Im Wesentlichen wurden vier wichtige regionale Baumarten für die Zusammenstellung der verschiedenen Landnutzungssysteme ausgewählt: i) die Palme *Bactris gasipaes* Kunt. (Pfirsichpalme; Pupunha; Arecaceae), die sowohl wegen der Früchte als auch für die Gewinnung Palmherzen genutzt wird; *Theobroma grandiflorum* (Willd. ex Spreng.) K. Schum. (Cupuaçu; Sterculiaceae), ein Baum der gleichen Gattung wie Kakao dessen Fruchtfleisch in der Region verbreitet zur Herstellung von Saft, Eiskrem und Bonbons verwendet wird. Außerdem können die Kerne möglicherweise zur Herstellung von Schokolade verwendet werden; ii) der Baum *Bertholletia excelsa* Humb, & Bonpl. (Brasilnuss, Paranuss; Lecythidaceae) der neben den wohlbekannten Nüssen auch hervorragendes Holz liefert; und iii) *Bixa orellana* L. (Annatto, Urucum; Bixaceae), der vor allem in den Tropen wegen seines ungiftigen roten Farbstoffs kultiviert wird.

Die Landnutzungssysteme waren Cupuaçu-Monokulturen und Pfirsichpalmen-Monokulturen zur Gewinnung von Palmherzen und Pfirsichpalmfrüchten. In den Pfirsichpalmen- und Cupuaçu-Monokulturen betrug die Pflanzdichte 2 x 2 m bzw. 7 x 6.4 m. Abbildung 2.2 und 2.3 zeigen den Aufbau der Flächen.

Im Agroforstsystem wurden die Bäume mit einem Reihenabstand von 4m gepflanzt. Eine Reihe Pfirsichpalmen (mit einem Abstand von 2 m innerhalb der Reihe) wechselt sich ab mit einer gemischten Reihe aus Cupuaçu und Paranuss (mit einem Baum-Abstand von 7 m innerhalb der Reihe), einer Reihe mit Annatto (mit einem Abstand von 4 m innerhalb der Reihe) und wieder einer gemischten Reihe aus Cupuaçu und Paranuss, nach der wiederum eine Reihe Pfirsichpalmen kommt. Zwischen den Bäumen wurde *Pueraria phaseoloides* Kunth (tropische Kudzu; Pueraria; Fabaceae) als Bodendecker angebaut. Im ersten Jahr wurde im Agroforstsystem Maniok mit einem Pflanzenabstand von 1.00 x 1.20 m angepflanzt. In Abbildung 2.3 wird der Aufbau des Agroforstsystems graphisch dargestellt.

Zum Vergleich wurden Flächen mit Wiederaufwuchs von spontaner Sekundärvegetation, die das gleiche Alter wie die landwirtschaftlichen Flächen aufwiesen, in die Studie mit aufgenommen. Die Sekundärvegetationsflächen wurden von *Vismia* spp. dominiert, einer charakteristischen Gattung für junge Brachen und degradiertes Land in dieser Region. Die Stammdichte auf den *Vismia* Flächen betrug 1.95 ± 0.17 pro m^2 (Schroth et al., 1999). Zusätzlich wurden zwei Baumarten eines nahegelegenen Primärregenwaldes für die Messungen einiger Parameter mit aufgenommen: ein zweikeimblättriger Baum, *Eschweilera sp.* (Matá-Matá, Lecythidaceae) und eine Palme, *Oenocarpus bacaba* (Bacaba, Arecaceae). Beide Arten kommen relativ häufig in diesem Wald vor und sind von kommerziellem Interesse, Matá-Matá wegen seines Holzes und Bacaba wegen seiner Früchte, aus denen Fruchtsaft gewonnen wird.

Für jede Art in jedem Landnutzungssystem wurden neben jeweils 3 gut entwickelten Pflanzen Bodenmessungen durchgeführt. Die Messflächen wurden - mit Ausnahme der Regenwaldflächen - als vollständig randomisierte Böcke mit drei Wiederholungen angelegt. Die Parzellengröße ist 24 x 32 m in der Pfirsichpalmen-Monokultur und 48 x 32 m im Agroforstsystem und im Sekundärwald.

Ca. 1 ½ Jahre nach der Pflanzung wurde der Hauptstamm der Pfirsichpalme abgeholzt und danach die Palmherzen drei Mal pro Jahr, immer wenn die Sprösslinge einen Durchmesser von 8 cm in einer Höhe von 1 m erreicht hatten, geerntet. Die Annattos wurden nach der Ernte ein Mal pro Jahr auf eine Höhe von 1.5 m zurückgeschnitten. Zwischen März und Mai wurden zur Erhöhung der Fruchtproduktion alle Blätter und kleinen Äste entfernt und diese zum Kompostieren unter die Bäume gelegt. Die Unterschiede in der Biomasseakkumulation wurden von Wolf (1997) beschrieben. In Shift (1997, 1998) und Schroth et al. (1999) wird die Höhe der Ersterträge diskutiert. Die Pflanzen wurden zweimal pro Jahr gedüngt: zu Beginn der Regenzeit im November – Dezember und am Ende der Regenzeit im Mai – Juni. Näheres hierzu siehe Schroth et al. (1999) und Shift (1996; 1997; 1998). Die Primär- und Sekundärwaldflächen wurden nie gedüngt.

3 Der Einfluss der Landnutzung auf bodenphysikalische Eigenschaften

Die Abnahme der Fruchtbarkeit tropischer Böden unter Ackernutzung, selbst bei entsprechender Ergänzungsdüngung, ist ein gut dokumentiertes Problem. Es gibt deutliche Hinweise darauf, dass die Produktivität eines tropischen Landnutzungssystems nicht nur von den Nährstoffvorräten und deren Verfügbarkeit, sondern in hohem Maße auch von der Erhaltung einer optimalen Bodenstruktur abhängt. Ein besseres Verständnis der Prozesse, die als Folge der Umwandlung von Wald in landwirtschaftlich genutzte Flächen die Bodeneigenschaften beeinflussen, ist sehr wichtig, um geeignete Managementsysteme zu finden, die die Produktivität der landwirtschaftlichen Flächen langfristig erhalten.

Die hier vorgestellte Studie befasst sich mit den Änderungen der Bodeneigenschaften als Folge von Boden-Pflanze-Interaktionen und spezifischem Bodenmanagement. Es wurden drei verschiedene Landnutzungssysteme untersucht: i) eine konventionelle Monokultur einer Palmenart zur Gewinnung von Palmherzen (*Bactris gasipaes*); ii) eine Monokultur mit Cupuaçu (*Theobroma grandiflorum*) und iii) ein komplexes Agroforstsystem mit Palmen, Cupuaçu, Paranuss (*Bertholletia excelsa*) und Annatto (*Bixa orellana*). Der Boden war in allen Nutzungssystemen mit Ausnahme der Palmen-Monokultur mit Pueraria (*Pueraria phaseoloides*) als Bodendecker bewachsen. Zum Vergleich wurden benachbarte Flächen des Primär- und Sekundärwaldes untersucht.

Die Messungen umfassten die Trockenraumdichte, die Textur, den Flockungsindex und die Substanzdichte sowie einige chemische Bodenparameter. Die Lagerungsdichten weisen mit 0.67 bis 1.08 Mg m^{-3} für Mineralböden niedrige Werte auf. Als Folge des schlechten Wuchses des Bodendeckers Pueraria in den Cupuaçu-Monokulturen konnte ein signifikanter Anstieg der Lagerungsdichten im Vergleich zum Primärwald beobachtet werden. In der unmittelbaren Umgebung der Palmen wurden die niedrigsten Lagerungsdichten festgestellt.

Dies ist eine unmittelbare Folge des dichten, gut entwickelten Wurzelsystems nahe der Bodenoberfläche. Zwischen dem Sekundär- und dem Primärwald konnten dagegen keine signifikanten Unterschiede festgestellt werden. Die Textur ist durch einen hohen Tongehalt von ≈ 600 g kg^{-1} an der Bodenoberfläche und einen leichten Anstieg mit der Tiefe charakterisiert. Während klassische Labormessungen der Korngrößenverteilung mit chemischen Dispersionsmitteln keine Unterschiede zwischen den Blöcken ergaben, zeigten die Flockungsindizes deutliche Unterschiede in der Aggregierung der Tonpartikel.

Die Verringerung des Aluminiumgehaltes und der Anstieg der Calcium- und Magnesiumgehalte sowie des pH waren korreliert mit zunehmender Dispersion der Tonpartikel an der Bodenoberfläche. Die Bestimmung der Lagerungsdichte und der Flockungsindizes stellen einfache und preisgünstige Indikatoren für das Monitoring der Stabilität der Bodenstruktur toniger Ferralsols bereit. Ein wesentlicher Faktor für die Nachhaltigkeit von Landnutzungssystemen auf stark aggregierten tonigen Ferralsols ist deren Strukturstabilität.

Es wird ein konzeptioneller Ansatz einer optimalen Bodenstruktur für bestimmte Landnutzungssysteme diskutiert. Die Verwendung einfacher und intuitiv verständlicher statistischer Modelle wird als Planungswerkzeug vorgeschlagen, um den Einfluss verschiedener Landbewirtschaftungssysteme, z.B. alternativer Anbaufrüchte und Bodenbearbeitungstechniken, auf die Bodenstruktur vorherzusagen.

4 Der Einfluss der Landnutzung auf die Gesamt-Porosität und die Porengrößenverteilung

Bodenporen variieren in Größe und Form und bilden ein zusammenhängendes Netzwerk, das zwar für jeden Bodentyp charakteristisch ist, sich jedoch als Folge verschiedener Landnutzungssysteme ändern kann. Die Porosität (ϕ) beeinflusst das Speichervermögen, die Verfügbarkeit und den Transport von Wasser und Luft im Boden. Diese Beeinflussung ist aber nicht nur vom Gesamtvolumen der Poren, sondern auch und vor allem von der Verteilung und Anordnung der Poren im Boden abhängig. Deshalb ist es wichtig, nicht nur die Porosität (ϕ) zu bestimmen, sondern auch die Porengrößenverteilung. Die Porengrößenverteilung kann mit Hilfe der Desorptionsmethode ermittelt werden. Hierbei werden an eine wassergesättigte Bodenprobe nacheinander unterschiedlich hohe Wasserdrucksäulen (h) angelegt. Es werden Datenpaare gesammelt, die den volumetrischen (θ) und h miteinander in Beziehung setzen.

Die Kapillartheorie wird dazu benutzt, den „äquivalenten Radius" der Porengrößen zu erhalten. Die Wasserspannungkurve (SWRC), bei der θ eine Funktion von h ist, ist eine der wichtigsten Hydraulikfunktionen, die die Bewegung von Wasser und gelösten Stoffen im Boden beschreibt. Die von van Genuchten (1980) aufgestellte Gleichung wird allgemein zur Anpassung experimenteller Wasserrückhaltedaten angewendet. Eine möglichst genaue Anpassung der experimentell ermittelten Wasserrückhaltedaten ist eine grundlegende Voraussetzung für die exakte Bestimmung der Kapazitätsfunktion und der kontinuierlichen Porengrößen-Verteilung. Theoretisch führt dies darüberhinaus zu einer besseren Abschätzung der gekoppelten Hydraulikfunktionen. In gut aggregierten Böden wird das Porensystem jedoch häufig in aggregatinterne Poren oder Texturporen und in Zwischenaggregat- oder Strukturporen unterteilt, so dass die Porengrößenverteilung bi- oder trimodale Verteilungen aufweist. Die Originalgleichung von van Genuchten hat nicht die nötige Flexibilität, um die gemessenen Daten sinnvoll anzupassen. Eine bessere Beschreibung der SWRC von Böden mit bimodaler Porengrößenverteilung wird durch zwei linear überlappende Funktionen der van Genuchten Gleichung erreicht.

Die tonigen Ferrasols in Zentralamazonien haben in ihrem Originalzustand eine hohe Porosität und eine bimodale Porengrößenverteilung, wobei ein hoher Anteil der Porosität auf die extrem feinen Poren und ein weiterer hoher Anteil auf die Groß- und größeren Mittelporen entfällt.

In diesem Kapitel soll die Porosität und die Porengrößenverteilung für die tonigen Ferrasols in Zentralamazonien für verschiedene Landnutzungssysteme charakterisiert werden. Daneben werden auch methodische Probleme sowie die Anwendbarkeit von flexibleren Rückhaltefunktionen zur Beschreibung der gemessenen Bodenwasserrückhaltedaten diskutiert. Die Diskussion konzentriert sich auf den Einfluss der Porengrößenverteilung auf die hydraulischen Bodeneigenschaften, praktische Auswirkungen auf das Verhältnis von Porengrößenverteilung zu Wasserverfügbarkeit bzw. –durchfluss werden aufgezeigt. Es wurden drei Landnutzungssysteme untersucht: i) eine konventionelle Monokultur mit Pfirsichpalme (*Bactris gasipaes*); ii) eine Monokultur mit Cupuaçu (*Theobroma grandiflorum*) und iii) ein komplexes Agroforstsystem mit Pfirsichpalme, Cupuaçu, Paranussbaum (*Bertholletia excelsa*) und Annatto (*Bixa orellana*). Der Boden war bei allen Nutzungssystemen mit *Pueraria phaseoloides* bedeckt, ausgenommen die Pfirsichpalmen-Monokultur, die keine Bodenbedeckung verträgt. Zum Vergleich wurden benachbarte Flächen von Primär- und Sekundärwald untersucht. Zusätzlich wurde ein Profil mit einer Tiefe von 100 cm genauer untersucht, wobei alle 10 cm Proben entnommen wurden.

Die Ergebnisse zeigen, dass durch die Verwendung des bimodalen VG-Ansatzes hervorragende Datenanpassungen und Ergebniskurven erhalten wurden: An der Bodenoberfläche wurden θ und h für verschiedene Landnutzungssysteme miteinander in Beziehung gesetzt, dies geschah außerdem für verschiedene Tiefen im Bodenprofil. Die Parameter n und α in den VG-Modellen wurden in ihrer physikalischen Bedeutung gebraucht. Sie erwiesen sich als nützlich beim Nachweis einer Schicht, die mit höherer Porosität und größerem Porenradius in mehr als 60 cm Tiefe in tonigen Ferrasols zwischen zwei dichteren Schichten liegt. Es wurden landnutzungs- und pflanzenspezifische Effekte auf die Gesamtporosität und Porengrößendichte untersucht. Für kurze Zeitspannen scheint Pueraria größere Poren, die das Wasser sehr schnell abführen, zugunsten von Porenradien zu verändern, die das Wasser effektiver zurückhalten und es pflanzenverfügbar halten. Im Boden in der Nähe von Pfirsichpalmen konzentrieren sich Poren mit reduziertem Radius.

Der Boden, der nicht ausreichend mit dem Bodendecker bewachsen war (unter Cupuaçu in der Monokultur), zeigt eine reduzierte Gesamtporosität und eine relativ ausgeprägte Reduktion im Großporenbereich. Im von Primärwald bedeckten Boden entfallen mehr als 30 % der Gesamtporosität auf Großporen. Das Großporensystem lässt das Wasser schnell abfließen und ist für die Bodenbelüftung und das tiefe Eindringen von Wasser und Nährstoffen (oder Pestiziden und Herbiziden) in den Boden verantwortlich. Der hohe Großporenanteil kann jedoch durch

Verringerung der durch die Matrix fließenden Wassermenge die Auswaschungsrate verringern, wenn die Nährstoffe (oder Pestizide und Herbizide) bereits in der Bodenmatrix sind.

Die Porengrößenverteilung des Ausgangszustands der tonigen Ferrasols (Boden mit Primärwald bedeckt) ist sehr gut an die klimatischen Bedingungen in diesem Gebiet angepasst. Sie erlaubt eine rasche Ableitung großer Wassermengen und vermeidet damit Abschwemmungen und die daraus resultierende Bodenerosion. Außerdem wird die Nährstoffauswaschung aus der Bodenmatrix reduziert, in dem Wasser durch die Großporen in tiefere Schichten geleitet wird. Außerdem fließt unter ungesättigten Bedingungen das Wasser in der Bodenmatrix schneller durch Mesoporen als durch kleine Poren. Der sehr kleine Radius der anderen Poren führt zu einer reduzierten hydraulischen Leitfähigkeit und geringeren Wasserflüssen durch die Bodenmatrix. Dabei erhöht sich die Aufenthaltsdauer des Wassers und der Nährstoffe und damit die Wahrscheinlichkeit, dass diese von Pflanzenwurzeln oder von Makro- und Mikrofauna aufgenommen werden. Die relativen Porenvolumenanteile im Primär- und Sekundärwald sind sehr ähnlich. Ursache hierfür ist, dass spontan entstehende Vegetation relativ schnell in der Lage ist, die Bodenporosität den Werten des Primärwalds wieder anzunähern. Die Messung der Porengrößenverteilung bestätigt die Feldbeobachtungen und ermöglicht Rückschlüsse auf das Verhalten von Wasser in verschiedenen Landnutzungssystemen. Die Verwendung der Porengrößenverteilung anstelle der Gesamtporosität ist daher sehr zu empfehlen.

5 Die TDR-Technik zur Bestimmung des Bodenwassergehalts – Eine Kalibrierungsstudie

Die Time-Domain-Reflectometrie (TDR)-Technik erlaubt schnelle, genaue und störungsfreie Messungen des volumetrischen Wassergehalts θ. Sie basiert auf der Messung der Dielektrizitäts-Konstanten des Bodens (ε) durch die Bestimmung der Ausbreitungsgeschwindigkeit von elektromagnetischen Wellen. In Forschungsprojekten und Monitoringprogrammen, die hohe Anforderungen an Messgenauigkeit und –zuverlässigkeit stellen, muss man die Fehlerquellen der TDR-Technik in Betracht ziehen, um diese ausschließen bzw. zumindest minimieren zu können (z.B. durch geeignete Kalibrierung und entsprechende Messungsdurchführung). Mehrere vorangegangene Studien haben gezeigt, dass empirische Gleichungen, die für Böden in gemäßigten Klimazonen entwickelt worden sind, nicht für die präzise Vorhersage des Wassergehalts tropischer Böden geeignet sind (Dirksen and Dasberg, 1993; Weitz et al., 1997). Daher soll in diesem Kapitel die Kalibrierung der TDR-Technik für die tonigen Ferrasols in Zentral-Amazonien durch die Verwendung von empirischen oder physikalischen Gleichungen beschrieben werden. Fehlerquellen, die bei Verwendung der TDR-Technik unter Freilandbedingungen auftreten können, werden hier ebenfalls unter besonderer Berücksichtigung des Untersuchungsgebiets diskutiert.

Die Ergebnisse deuten darauf hin, dass die Abschätzung von θ durch die direkte gravimetrische Bestimmung und die indirekte Abschätzung der ε –Determinanten in etwa die gleiche Genauigkeit haben. Die häufig benutzte Topp-Gleichung beschreibt die Daten nur sehr schlecht und tendiert zudem dazu, θ zu hoch zu schätzen. Unter den getesteten empirischen Gleichungen lieferten die quadratische Gleichung und die einfachste lineare Wurzel-Quadratgleichung die genauesten Abschätzungen für θ. Die Verbesserungen der θ-Abschätzung mit Hilfe der Multivariant-Funktion von ε und der Trockenrohdichte waren zu schwach, um empfohlen werden zu können.

Die Alpha-3-Gleichung könnte eine gute Alternative darstellen, wenn die Werte der Trockenrohdichte sehr stark schwanken und für die Dichte nur Schätzungen vorliegen. Die Sensitivitätsanalyse und die Validierung zeigten, dass die Alpha-3-Gleichung ein starkes Kalibrierungsgleichung ist, sogar dann, wenn nur eine Abschätzung der Trockenrohdichte vorliegt. Die physikalisch basierten Gleichungen, Alpha-4, mit α und ε_{BW} angepasst, gaben genaue θ_{TDR}-Abschätzungen und scheinen eine gute Alternative zu sein, wenn die gemessenen Werte vorwiegend im trockenen Bereich liegen. Weitere Untersuchungen über die dielektrischen Eigenschaften des an Tonminerale gebundenen Wassers sind notwendig, um die Alpha-4-Gleichung für fein gekörnte Böden zu verbessern. Die Schätzung von θ mit Hilfe der TDR-Technik ist im trockenen Bereich genauer.

Um die richtige Gleichung wählen zu können, müssen sowohl Bodeneigenschaften als auch die benötigte Genauigkeit bekannt sein. Nicht jede Studie benötigt Messungen mit einer Genauigkeit, die die beträchtlichen Aufwendungen an Zeit und Arbeit im Gelände für die Kalibrierung rechtfertigen.

6 Bodennutzungseffekte auf die hydraulischen Eigenschaften

Die Bestimmung von hydraulischen Eigenschaften ist zur Beantwortung vieler Fragen in der landwirtschaftlichen Forschung notwendig. Studien, die mit Wasserflüssen und Transport von Nährstoffen und Pestiziden durch das Bodenprofil, Änderungen der Bodenwasserspeicherung, dem Wasserhaushalt und Boden-Pflanzen-Wasser-Beziehungen zu tun haben, benötigen zuverlässige Abschätzungen der hydraulischen Eigenschaften. Hydraulische Eigenschaften sind räumlich und zeitlich variabel, infolgedessen ist eine verlässliche Charakterisierung der Bodenhydraulik sehr komplex und benötigt zeitaufwendige Messungen. Desweiteren werden viele hydraulische Eigenschaften besser von Funktionen beschrieben (z.B. ungesättigte hydraulische Leitfähigkeit und Bodenwasserrückhaltevermögen) als von Mittelwerten. Zudem sind die Ergebnisse von vielen Randbedingungen abhängig.

Die meisten ungestörten tropischen Böden sind durch eine dicke organische Auflageschicht mit beachtlicher biotischer Aktivität gekennzeichnet, von der sichtbar große Kanäle in den Böden führen, die eine rasche Wasserinfiltration erlauben. Zudem halten die Baumkrone und die Bodenstreu die Regentropfen auf und reduzieren deren kinetische Energie insbesondere während starker Gewitter. Die Entfernung von Vegetation und die Einführung mechanischer Bodenbearbeitung führen zu einer Störung des Bodens. Der direkte Aufprall von Regentropfen auf den ungeschützten Boden intensiviert die Zyklen von Bodendurchnässung und –trocknung, was häufig zu einem raschen Rückgang der Infiltrationsrate führt. Dies kann insbesondere auf hängigen Äckern zu Oberflächenabfluss und Bodenerosion führen. Obschon eine hohe Infiltrationsrate Wasserabfluss und Bodenerosion minimiert, kann durch die erhöhte Auswaschung die Effektivität von Düngern reduziert und das Grundwasser mit Nährstoffen und Pflanzenschutzmitteln verschmutzt werden. Überdies würden die Auswaschungsprozesse in tropischen Böden ohne Bypass-Systeme, in denen das gesamte Regenwasser durch die Bodenmatrix fließt, intensiviert werden.

In diesem Kapitel wird erstens ein Überblick über die benutzten Gleichungen zur Berechnung der Bodenwasserfunktionen gegeben und für tropische Böden geeignete Feldmethoden zur Bestimmung hydraulischer Eigenschaften vorgestellt. Außerdem wird auf spezifische Fehlerquellen und Verfahren zur Fehlervermeidung bzw. -begrenzung eingegangen. Zweitens werden die Messergebnisse der gesättigten hydraulischen Leitfähigkeit dargestellt. Diese wurde mit der Standard-Labormethode an Stechzylinderproben gemessen, im Gelände wurden Doppelring-Tensionsinfiltrometer verwendet. Außerdem werden Landnutzungssysteme miteinander verglichen und statistische Methoden zur Analyse von log-normalverteilten Daten präsentiert und anhand von Beispielen erläutert. Drittens werden zur Überprüfung der Messergebnisse der ungesättigten hydraulischen Leitfähigkeit Ergebnisse der Augenblicks-Profil-Methode analysiert. Die Umrechnung dieser Daten wird detailliert dargestellt und die Ergebnisse in Bezug auf die Homogenität der hydraulischen Eigenschaften innerhalb des Profils diskutiert. Außerdem wurden Messungen mit dem Tensionsinfiltrometer durchgeführt, um die ungesättigte hydraulische Leitfähigkeit zwischen und innerhalb verschiedener Landnutzungssysteme, sowie an verschiedenen Standorten in einem Landnutzungssystem vergleichen zu können. Skalierungstheorie und stückweise lineare Regression werden kurz beschrieben und zur Analyse der Ergebnisse benutzt. Schließlich wird die Eignung der Inversen Simulation, einer neuen Methode zur Bestimmung der hydraulischen Funktionen und zur mathematischen Beschreibung der Wasserbewegung, für tonige Ferrasols in verschiedenen Tiefen untersucht.

6.1 Bestimmung der gesättigten hydraulischen Leitfähigkeit

6.1.1 Stechzylinder-Methode (K_s)

Die Stechzylindermethode ist zur Bestimmung der gesättigten hydraulischen Leitfähigkeit wegen des kleinen Stichprobenumfangs, des Vorhanden- oder Nicht-Vorhandenseins von offenen Makroporen und der variablen Bodenverdichtung während der Probenahme nur begrenzt einsetzbar. Obwohl sich einige Trends identifizieren lassen, ist diese Methode wegen der geringen Zuverlässigkeit der Ergebnisse bei strukturierten Böden ungeeignet zur Bestimmung der gesättigten hydraulischen Leitfähigkeit von tonigen Ferrasols.

6.1.2 Doppelring-Infiltrometer (K_{fs})

Die hierm7it erzielten Messergebnisse sind viel weniger variabel als die Ergebnisse der Stechzylindermethode. Das ist möglicherweise darauf zurückzuführen, dass die Bodenstruktur weniger gestört wird und das von der Scheibe erfasste Probenvolumen das REV für die K-Bestimmung in den tonigen Ferrasols gut approximiert.

Die erhaltenen K_{fs}-Werte waren wesentlich niedriger als vorher beschriebene Werte, die für tonige Ferrasols in Zentralamazonien bestimmt wurden.

Im Agroforstsystem wiesen Böden unter Pueraria die höchsten K_{fs}-Werte auf, gefolgt von Kfs-Werten neben Cupuaçu-Stämmen. Die K_{fs} nahe an Pfirsichpalmen tendiert zu geringeren Werten. Diese niedrigen Werte stehen im Gegensatz zur geringeren Bodendichte, die neben den Palmen gemessen wurde. Diese Ergebnisse deuten darauf hin, dass die Bodendichte für viele Landnutzungssysteme ein irreführender Parameter zur Ableitung der hydraulischen Leitfähigkeit ist. Die erwartete Reduzierung der Kfs zwischen den Cupuaçus in der Monokultur als Folge der höheren Boden-Dispergierung und der Verringerung der totalen Porosität ließ sich nicht nachweisen. Dies ist wahrscheinlich auf das Vorkommen von kleinen Rissen zurückzuführen.

Das Vorhandensein großer Makroporen in tonigen Ferrasols führt zu dramatischen Änderungen der gesättigten hydraulischen Leitfähigkeit, sogar bei kleinen Veränderungen nahe der Sättigung. Die K-Werte steigen weiter merklich an, wenn die Wasserspannung kleine positive Werte annimmt. Dieses Phänomen, das durch die Standard-Hydraulikfunktion nicht gut beschrieben wird, kann bei Nichtberücksichtigung zu schwerwiegender Überschätzung der Bodenwasserflüsse führen, speziell beim Auftreten von Wasser-Überstau an der Bodenoberfläche.

Die mit dem Doppelring-Tensionsinfiltrometer gemessenen K_{fs}-Werte werden sinnvollerweise mit dem Hinweis versehen, dass die Messung ungefähr bei Matrixpotenzial gleich 0

($h \approx 0$) durchgeführt worden ist, aber dieser Wert nicht die maximale Infiltrationsrate für tonige Ferrasols repräsentiert.

Da die K-Werte log-normalverteilt verteilt sind, wurde zur Schätzung des ersten Moments und der Varianz die Maximum-Likelihood-Methode herangezogen.

Verlässlichere Methoden für Freilandbedingungen und mathematische Theorien zur Beschreibung von Böden mit Makroporen sind Gegenstand zukünftiger Untersuchungen.

6.2 Bestimmung der ungesättigten hydraulischen Leitfähigkeit (K)

6.2.1 Tensions-Infiltrometer (TI)

Tensions-Infiltrometer sind relativ billig, robust und eine einfache Feldmethode zur Bestimmung der ungesättigten hydraulischen Leitfähigkeit in tonigen Ferrasols. Da K nahe der Sättigung hoch variabel ist, werden die Daten besser unter Verwendung der relativen Wasserleitfähigkeit und der Skalierungstheorie ausgewertet.

Die stückweise lineare Regression erlaubt die Abschätzung eines Wendepunkts, der zwischen 15 ~ 40 mm Wasserspannung liegt. Dieser teilt zwei prozessual unterschiedliche Bereiche, die die hydraulische Leitfähigkeit der tonigen Ferrasols kontrollieren.

K schwankt zwischen 0-70 mm Matrixpotenzial um drei bis vier Größenordnungen. Unterschiedliche Landnutzungssysteme und Pflanzenarten hatten nachweislich Auswirkungen auf die ungesättigte hydraulische Leitfähigkeit. Diese Unterschiede können bei Nicht-Berücksichtigung eine Fehlerquelle in Wasser- und Stofftransport-Studien darstellen.

Der Boden nahe der Cupuaçustämme zeigt erhöhte K-Werte. Dies ist wahrscheinlich auf das besser entwickelte Feinwurzelsystem nahe der Bodenoberfläche zurückzuführen. Nahe an Pfirsichpalmen-Stämmen wurden die kleinsten K-Werte gefunden.

Eine Begrenzung der TI ist ihr geringer Messbereich. Allerdings können die mit TI gemessenen Daten mit den Ergebnissen anderer Methoden kombiniert werden, um einen Überblick über einen großen Messbereich ungesättigter Leitfähigkeiten zu erhalten.

6.2.2 Augenblicksprofilsmethode (IPM)

Die durch die lineare Form der Exponentialmodells geschätzte K-θ Funktion zeigt sehr gute Übereinstimmung mit den gemessenen Daten für die Tiefen 10, 20 und 40 cm, aber signifikante Abweichungen für die Tiefen 60, 80 und 90 cm.

Ähnlichkeiten zwischen den Gleichungen K(θ) oder K(h), wurden in Bezug auf Parallelität und Konkordanz getestet, um die Zahl der benötigten Gleichungen, die die Wasserflüsse in einem Bodenprofil beschreiben, zu reduzieren. Die Parallelität zwischen einigen K(h) Gleichungen zeigt, dass tonige Ferrasols ein ähnliches hydraulisches Verhalten haben. Der Nachweis eines lockeren Horizonts zwischen zwei kompakteren Horizonten, der durch die Analyse der Porengrößenverteilung festgestellt worden ist, konnte nochmals bestätigt werden.

6.3 Labor- und Feldbestimmung des Bodenwasserrückhaltevermögens [θ(h)]

Die Ergebnisse der θ - h Datenpaare zeigen nur für die Tiefenstufe 10 cm eine gute Übereinstimmung zwischen Feld- und Labordaten. Für die meisten Tiefen lässt sich tendenziell die Überschätzung der Felddaten durch die Labordaten beobachten. Die durch die Probenahme verursachte Bodenverdichtung könnte die höheren Werte von θ (bei gleichem h) für die Labordaten erklären. Die vielen Faktoren (Bodenvariabilität, Probenahmevolumen, Kalibrierung der Messinstrumente, Genauigkeit und Reaktionszeit der Tensiometer, Temperaturschwankungen, Hysterese und Lufteinschluss), die die Bestimmungsgenauigkeit des Bodenrückhaltevermögens verfälschen, wurden in dieser detaillierten Studie genau erörtert.

6.4 Inverse Simulation

Die Ergebnisse der inversen Simulation zur Vorhersage der Entwicklung der Wassergehalte in den mit der Augenblicks-Profilmethode gewonnenen Profilen [θ (t, z)] waren überraschend gut. Die inverse Simulation unter Verwendung der unimodalen van Genuchten – Mualem – Gleichung war in der Lage, den Versickerungsprozess bis zu einer Tiefe von 60 cm präzise zu beschreiben. Allerdings wurde für diese genaue Beschreibung der Bodenwasserdynamik eine hochaufgelöste Diskretisierung des Bodenprofils benötigt. Die Übereinstimmung zwischen der mit der inversen Methode geschätzten hydraulischen Leitfähigkeit und den mit der IPM-Methode berechneten Ergebnissen war ebenfalls gut. Die Bodenwasserrückhaltekurve ist nicht so genau, da die optimalen Werte während des Optimierungs- und Kalibrierungsverfahrens verändert wurden. Deshalb kann es vorteilhaft sein, das parametrische Modell von K(θ) oder K(h) anzuwenden, das nicht mit der θ (h)-Funktion gekoppelt ist; ansonsten sollten die Funktionen getrennt angepasst werden.

Die Ergebnisse zeigen die Durchführbarkeit der inversen Methode, sowie ihre Flexibilität und ihre Vorteile. Jedoch sollte der Erfolg der inversen Modellierung für die tonigen Ferrasols vorsichtig interpretiert werden. Er hängt wahrscheinlich von den verwendeten Daten ab, wo der vorherrschende Wasserfluss vermutlich nur durch die von Mikroporen durchzogene Bodenmatrix stattfand.

Die mit der inversen Methode bestimmten K-Funktionen sind nur für den untersuchten Bereich von θ gültig. Auf eine Extrapolation sollte insbesondere nahe der Sättigung und in tieferen Schichten verzichtet werden. Die Fähigkeit der inversen Methode, die hydraulischen Funktionen in einem weiten Gültigkeitsbereich unter Einschluss von Makroporen-Flüssen nahe der Sättigung zu bestimmen, ist Gegenstand weiterer Untersuchungen. Vorläufige Ergebnise, die Resultate von verschiedenen die inverse Methode benutzenden Untersuchungen einbeziehen, sind vielversprechend.

7 Schlussfolgerungen und Ausblick

Dieses Kapitel wird weder einen umfassenden Rückblick über Einzelaspekte der Ergebnisse noch über die Eignung der untersuchten Methoden geben. Die Ergebnisse und Schlussfolgerungen wurden am Ende des jeweiligen Kapitels erläutert. In diesem Kapitel habe ich versucht, die Ergebnisse in einer umfassenden Form zu interpretieren und einige Schlussfolgerungen gezogen. Zugleich gehe ich auf einige Aspekte ein, die zukünftig noch untersucht werden sollten.

7.1 Bodnennutzungeffekte auf die hydraulischen und bodenphysikalische Eigenschaften

Bodendichte und Flockungsindex haben sich als nützliche physikalische Indikatoren zum Monitoring der Bodenqualität erwiesen. Der Einsatz von Dünger und Kalk hatte Auswirkungen auf die Stabilität kleiner Bodenaggregate und die Bestimmung des Flockungsindex gibt Hinweise auf Veränderungen in der natürlichen Aggregierung von Tonpartikeln. Die Ergebnisse der Dichtemessungen schwanken zwischen 0.8 bis 1.1 Mg kg^{-1}, wobei niedrige Werte ein Hinweis auf stark aggregierte Böden sind. Außerdem sind die Bodendichten nicht invers mit den Infiltrationsraten korreliert, wie man es eigentlich erwarten würde. Als Folge der Flockung und der Aggregation in den Ferralsols verhalten sich diese Böden hinsichtlich Wasserinfiltration nahe der Sättigung wie Sand. Bei höheren Wasserspannungen verhalten sich Infiltrationsraten und Wasserspeichervermögen jedoch wie bei Tonböden. Dieses ungewöhnliche Verhalten der tonigen Ferralsols in Kombination mit der bimodalen Korngrößenverteilung, in dem sie Eigenschaften von Sand- und Tonböden vereinigen, führt dazu, dass viele Pedotransferfunktionen, die die Struktur und die Dichte als Inputparameter zur Bestimmung der hydraulischen Eigenschaften benutzen, fehlschlagen. Weitere Untersuchungen über Flockungs- und Aggregationsphänomene in

Zusammenhang mit organischer Substanz und speziell die Eisenoxid-Dynamik sollten verstärkt gefördert werden.

Die Porengrößenverteilung und ihre komplizierte Geometrie und Kontinuität kontrollieren die Wasserbewegung. Deshalb ist die genaue Kenntnis der Porositätseigenschaften und ihrer nutzungsbedingten Veränderungen ein Schlüsselfaktor, um Ferralsols mit guten bodenphysikalischen Qualitäten zu erhalten. Methodische Studien über die Bestimmung der Porengrößenverteilung, -kontinuität und –stabilität, sowie der für den Auf- und Abbau des Porensystems verantwortlichen Faktoren, sind faszinierende Fragestellungen für die Zukunft.

Die meisten Kalibrierungsfunktionen sind nicht in der Lage, die dielektrische Leitfähigkeit (ε) mit dem volumetrischen Wassergehalt (θ) in Beziehung zu setzen. Dies führt zu schwerwiegenden Schätzfehlern von θ in den tonigen Ferralsols, wenn die für die tonigen Ferralsols entwickelte spezifische Kalibrierung nicht angewandt wird. Das Versagen der Kalibrierungsfunktionen hängt mit der ungewöhnlichen Kombination von Dichte [ca. 1.00 Mg kg^{-1}] und hohem Tonpartikel-Anteil [> 600 g kg^{-1}] zusammen. Die Anwendung physikalisch-basierter Modelle, die ε mit θ in Beziehung setzen, könnte bei besserer Kenntnisse der an Tonpartikel gebundenen Wassermenge und der Menge des freien Bodenwassers optimiert werden. Untersuchungen, die die spezifische Bodenoberfläche mit ε in Beziehung setzen, können nicht nur zu einer genaueren Schätzung von θ führen, sondern auch den Restwasser-Gehalt (θr) besser bestimmen. Letzterer geht als Parameter in die meisten Wassertransport-Modelle ein. Die direkte Verwendung von ε in Studien zum Wassertransport anstelle direkter Kalibrierung von ε stellt ebenfalls eine Möglichkeit dar, die untersucht werden sollte.

Die Unsicherheiten zur Bestimmung der Wasserflüsse nahe der Sättigung unter Anwendung der $K(\theta)$ oder $K(h)$ Funktionen ergeben sich aus dem exponentiellen Verhalten nahe Sättigung (d.h. in den linearen Modellen, Hänge mit sehr hohen Werten). Dieses Problem ist sehr stark in sehr gut strukturierten Böden, wie es die tonigen Ferrasols im Zentralen Amazonas Gebiet sind. Daraus leitet sich als Konsequenz ab, dass bereits eine kleine Änderung von θ oder h eine dramatische Änderung von K zur Folge hat. Egal welche Gleichung benutzt wird, ist dies eine wesentliche Eigenschaft von tonigen Ferrasols (und anderen sehr gut strukturierten Böden). Somit ist bei der Bestimmung der Wasserflüsse bei beinahe Sättigung dieses Phänomen sehr aussagekräftig und kann zur höheren Unsicherheiten bei den bestimmten und geschätzten Werten führen.

Es ist schwer die Unsicherheiten der Bestimmungen abzuschätzen und diese in numerischen Simulationen anzuwenden, wenn man die hydraulische Gleichung anwendet, da sie von vielen

Parametern in strenger nichtlinearer Art und Weise abhängt. Die Anwendung von vielen Parametern macht die Modellierung und die statistische Analyse zu kompliziert und verwirrend. Andererseits ist es unrealistisch zu versuchen genaue Bestimmungen der hydraulischen Leitfähikeit durch den gesamten Wassergehaltsbereich zu erhalten und dafür nur eine einzige und einfache Bodengleichung zu verwenden.

Wahrscheinlich stellt eine Möglichkeit für die Modellierung der Wasserflüsse in strukturierten Böden, wie es die tonigen Ferrasols im Zentral Amazonas Gebiet sind, stückweise lineare Regression mit nur einem oder zwei Parametern für spezifische Bereiche von ausgepägten hydraulischen Verhalten zu entwicklen (z.B. der Domäne des Makroporenflusses; Kapillarfluss und Absorptionsdomäne). Die Teilgleichung könnte sicherlich die variablen Felddaten mit der gleichen Sicherheit als ausgeklügelte Funktionen beschreiben, allerdings müssen sie einfache analytische Lösungen und machbare statistische Analysen zulassen.

7.1 Bodenqualität und Nachhaltigkeit der Landnutzungssysteme

Allgemeine Aspekte der drei untersuchten Landnutzungssysteme, des Sekundär- und des Primärwaldes wurden bereits in vorangegangenen Kapiteln kurz diskutiert. Wie in der Einführung beschrieben, hängen mit dem Konzept der Nachhaltigkeit auch wirtschaftliche und soziale Fragen zusammen. In diesem Kapitel wird der Begriff Nachhaltigkeit jedoch auf bio-physikalische Aspekte beschänkt.

Die Versuchsergebnisse der Cupuaçu-Monokultur zeigen, dass die Bodenbedeckung zwischen den Baumreihen in den ersten Jahren nach Anlage der Plantage entscheidend für die Erhaltung der Bodenqualität ist. *Pueraria phaseoloides* scheint als Bodendecker gut geeignet zu sein, um die Porosität toniger Ferralsols wiederherzustellen.

In der Pfirsichpalmen-Monokultur konnte eine Reduktion der Wasserflüsse beobachtet werden. Die Pfirsichpalme reagiert sensibel auf unzureichende Bodenbelüftung. Die hydraulischen Eigenschaften sollten daher in Hinblick auf unterschiedliche Anbaumethoden untersucht werden, um diese so zu optimieren, dass die Bodendurchlüftung auf einem tolerierbaren Niveau bleibt. Um hydraulische und physikalische Parameter als Indikatoren für die Bodenqualität besser verwenden zu können, müssen jedoch das Wachstum der Pfirsichpalme limitierende kritische Werte eingeführt werden. Die Reduktion der Bodenleitfähigkeit wird offensichtlich durch die Wurzelsystem bedingte

Bodenverdichtung verursacht. Dieses Phänomen könnte in weniger durchlässigen Böden schwerwiegender als bei den Ferralsol sein.
In Agroforstsystemen erzeugen die verschiedenen Pflanzeneigenschaften und pflanzenartspezifische Anbaumethoden komplizierte Muster. Um Baumstämme herum entstehen kleine Flächen mit abweichenden Bodeneigenschaften. Die Messung von Bodenqualitätsparametern in einem komplizierten System, wie es die Agroforstsysteme darstellen, setzt ein durchdachtes Probenahmeschema voraus, dass eine Größenabschätzung der von den Baumstämmen beeinflussten Flächen erlaubt. Mit dem Probenahmeschema können möglicherweise wichtige Berechnungen, wie die Ermittlung von Extremwerten oder die Berechnung von gewichteten Mitteln für das ganze System durchgeführt werden. Gewichtete Mittel können zum Vergleich verschiedener Landnutzungssysteme herangezogen werden, indem sie die durchschnittliche Bodenstruktur als Referenz benutzen. Außerdem können Kombinationen verschiedener Pflanzen Anbaumethoden ausprobiert werden, um eine ideale Bodenstruktur zu erhalten. Die Erstellung einer Datenbank mit Baum- und Nutzpflanzen-Produktivitätsdaten in Abhängigkeit von Anbaumethoden und anderen Parametern erlaubt es, zukünftige oder hypothetische Szenarien zu simulieren. Diese können dann bei der Landnutzungs-Planung benutzt werden, um geeignete Kombinationen von Pflanzen und Anbaumethoden zu finden.

Der Sekundärwald scheint effiziente Mechanismen zur Wiederherstellung der Bodenqualität zu besitzen; viele Parameter in diesem System sind den Werten, die im Primärregenwald gefunden wurden, ähnlich. Zusätzlich zu Maßnahmen zur Steigerung der Biomasseanreicherung könnten weitere Untersuchungen Prozesse erforschen, die im von Sekundärwald bedeckten Boden ablaufen. Ein besseres Verständnis dieser Mechanismen könnte es erlauben, Ansätze zu finden, welche die Zeitspanne, die die Sekundärvegetation zur Wiederherstellung der Bodenqualität benötigt, verkürzt. Folglich könnten auch die Zeitintervalle der Rotationsflächen im Brandrodungsfeldbau reduziert werden.

Der Primärwald weist eine optimale Kombination von bodenphysikalischen und –hydraulischen Eigenschaften auf, um die knappen Nährstoffe in den tonigen Ferralsols zu erhalten. Das bimodale Porensystem erlaubt es dem Wasser nach einem heftigen Regenfall schnell durch die Makroporen abzufließen, indem es an der Bodenmatrix vorbeigeleitet wird. Das Restwasser im Boden fließt sehr langsam ab und ermöglicht es den gelösten Nährstoffen von der Bodenmatrix absorbiert oder durch die Pflanzenwurzeln aufgenommen zu werden. Die optimale Funktionsweise dieses Systems hinsichtlich der Auswaschungs-Reduzierung aus der Bodenmatrix ist mit der in Zentral-Amazonien üblichen hohen Niederschlagsintensität gekoppelt. Zudem ist das Mikroporensystem bei trockenem

Boden sehr effizient, um Wasser von unregelmäßigen Regenfällen aufzunehmen, die in Amazonien in der Trockenzeit auftreten.

Basierend auf den Erkenntnissen dieser Studie werden Praktiken zur Optimierung des Einsatzes von Düngemitteln und zur Reduzierung der Pflanzenschutzmittel-Auswaschung ins Grundwasser vorgestellt. Im Gegensatz zur Lehrmeinung kann Makroporenfluss die Auswaschungsraten verringern, wenn die Nährstoffe in der Bodenmatrix gebunden sind und das Wasser nicht durch die Matrix fließt. Aufbauend auf dieser Aussage ist die Untersuchung verschiedener Möglichkeiten die Nährstoffaufnahme in die Bodenmatrix zu verbessern sehr wichtig. Es sollten Studien gefördert werden die die Einarbeitung von Düngemitteln verbessern, z.B. durch direkte Einarbeitung in die Bodenmatrix, die Aufsplittung des Düngers in mehrere Teilgaben und durch den Gebrauch von feinkörnigem Mineraldünger, da dieser schneller mit der Bodenmatrix reagiert. Außerdem sollten Untersuchungen über die geeignete Bodenfeuchtigkeit während der Düngemittelverteilung gemacht werden.

Eine bessere Vorhersage der Wasserflüsse in tonigen Ferralsols wird möglich, wenn die Bedingungen unter denen Makroporenfluss auftritt bekannt sind. Dies ist sicherlich kein triviales Problem, da dieser Prozess nicht nur von der Niederschlagsrate, sondern auch von der aktuell vorhandenen Bodenfeuchtigkeit abhängt. Außerdem gibt es immer noch einen Bedarf an besseren mathematischen Gleichungen, die die Makroporenflüsse beschreiben. Sollte dies erreicht werden, könnte ein umsichtiger Gebrauch von Düngemitteln und Pestiziden vorausgesagt und empfohlen werden. Als Konsequenz daraus kann das Makroporensystem zu einer Reduzierung der Auswaschung beitragen.

Es ist fraglich, ob auf tonigen Ferralsols ein produktives Landnutzungssystem ohne externe Inputs langfristig aufrechterhalten werden kann. Umgekehrt können die Kleinbauern in Zentralamazonien keine hohen finanziellen Investitionen für die landwirtschaftliche Produktion tätigen. Das paradoxe Problem muss gelöst werden, damit ein alternatives Landnutzungssystem zum Brandrodungsfeldbau gefunden werden kann. Offensichtlich hängt die Einführung eines geeigneten Landnutzungssystems für Zentral-Amazonien nicht nur von geeigneten Anbautechniken, sondern auch von der Sozial- und Wirtschaftspolitik ab.

"It is entirely impossible in the Amazon to take stock of the vastness, which can be measured only in fragments; of the expansiveness of space, which must be diminished to be appraised, of an infinity which allows itself to be seen only by making itself tiny, through microscopes; and of an infinity which is meted out little by little, slowly, indefinitely, excruciatingly. The land is still mysterious ..."

Euclides da Cunha; 1904.

1 INTRODUCTION

1.1 The land use system in the Amazon

During the numerous economic cycles in the Amazon, serious difficulties hampered the development of intensive agricultural activity that would lead to expansion and economic independence of the local populations.

Since the collapse of the extractive rubber system from the forest due to production in large scale from plantations in Asia, at the beginning of the last century; different development policies to incentive agricultural production have been attempted. The rubber system was partly maintained through subsidies until the seventies, when more intensive programs of colonisation of the Amazon started. These programs have had as a consequence the conversion of forest areas to pasture and agricultural fields.

In the last decades the deforestation of Amazon primary forest and its potential environmental consequences got increasing public attention. One aspect is the possible climatic effect, in which changes of land use systems may lead to changes in water balance patterns (Gash et al. 1996), and may lead to significant soil carbon losses to the atmosphere (Fearnside and Barbosa, 1996; Moraes et al., 1996). However, both hypotheses have no scientific consensus.

Conservation of biodiverstiy is doubtless a good reason to preserve the primary forest. But, there is a need of identification and delineation of areas to be protected and a way of promoting practical use of Amazon biodiversity must be found. Biodiversity can not only be seen as a deposit of potential resources for future generations, but the economic benefit of the local population has to be regarded as well.

Another aspect concerns the agriculture potential of the upland soil in the central Amazon. Their low fertility, high nutrient leaching potential and ideal conditions for many plant diseases made it always doubtful whether it would be economically feasible to implement a productive agriculture in the region.

The traditional slash-and-burn method of agriculture is still practised by most of the small farmers in the Brazilian Amazon. The most typical way of this method is as follows: first trees with market demand are cut and sold. The remaining trees are slashed and left to dry, then the whole area is burned. Crops are then planted and the ashes provide the nutrients needed. The first-year crop production (mainly manioc, rice, beans or corn or manioc directly) is usually fairly high in yield. By the second year the quantity and quality of yield declines because of decreasing nutrient availability and weed encroachment. Usually after three to five years the area must be allowed to revert to secondary forest (*capoeira*) and a new area must be cleared. Since the soil quality does not regenerate quickly, the soil should not be used for agricultural production for many years (*pousio*). The frequency of rotations depends upon soil natural fertility, and varies between 10 – 20 years. Therefore, the slash-and-burn system needs large areas, and it is an unsustainable agriculture system nowadays because of the growth of the population.

The agronomic failures of many land use systems proposed to Amazon have been explained associating environmental factors with inadequate management. The same processes of degradation that diminish productivity in the traditional slash-and burn system are responsible for the decrease of productivity in more elaborate land use systems. A better understanding of these processes is therefore a key factor for managing a land use system in a sustainable manner.

In many studies concerning sustainable land use of the Amazon region, attention has been focused on environmental quality rather than on the Amazonian population, the *cabloclos*. The small farmers in the Brazilian Amazon have been accused of destroying the primary forest. But, the smallholders tend to prefer previously cleared and regenerated areas by the *pousio* than to clear new areas of primary forest to install their agricultural fields. Furthermore, until now a feasible land use system to substitute the traditional slash-and-burn system is not available for most areas in the Brazilian Amazon. Therefore, shifting cultivation still is the only chance of surviving from agricultural activities.

The challenge to formulate a suitable land use system, apart from economic considerations, geo-political motives and questions of sovereignty, should be addressed considering that in the Brazilian Amazon live about 600.000 small farmers (Homma et al., 1998 - p.132) who have the endless human need of food, home, clothes, schools for their children and medical and sanitation facilities.

Agricultural land use systems with perennial crops are considered more suitable for the upland soils of the Amazon than annual crops. They may maintain soil quality, improve living standards for the local population and improve environmental quality. Further, they can reduce the pressure of deforestation on areas of primary forest. However, despite the general advantages of perennial compared with annual cropping systems; symptoms of fertility decline have been reported also from tree crop based systems in the humid tropics (Caliman et al., 1987; Ekanade, 1987). Therefore, the processes of soil degradation in agriculture systems must be further investigated.

1.2 Soil quality and sustainable land use systems

The concepts of soil quality and land sustainability have been discussed for several years now and many definitions have been proposed. These concepts are not interchangeable and comprise different definitions. In this study, soil quality is defined as:

> *"The capacity of a specific kind of soil to function within natural or managed ecosystem boundaries, to sustain plant and animal productivity, maintain or enhance water and air quality, and support human health and habitation."*
>
> *(Karlen et al. 1997)*

and sustainable land management as:

> *"Combination of technologies, policies, and activities aimed at integrating socio-economic principles with environmental concerns so as to simultaneously maintain or enhance production, reduce the level of production risk, protect the potential of natural resources and prevent (buffer against) soil and water degradation, be economically viable, and be socially acceptable."*
>
> *(Smyth and Dumanski, 1993)*

Soil quality is effectively a condition of a site and it can be studied using only soil data. Suitable land management studies require the integration of biophysical data with economic and social demands. Because only soil data were analysed in this study the findings here refer basically to soil quality concerns.

Soil and land management practices are primary determinants of soil quality and its assessment is fundamental to determine the sustainability of land management systems (Karlen et al., 1997). Therefore, choice of land use and soil management practices should be made considering restoration and maintenance of high soil quality. Soil quality can be measured by monitoring several indicators. The type of indicator chosen depends on the soil function (agricultural production, filtering and buffering pollutants, etc) and scale (e.g. field, farm, watershed) in which the evaluation is made (Mausbach and Seybold, 1998; Doran et al., 1999).

In terms of agricultural production, the function of the soil refers to its ability to sustain productivity. Soil quality indicators in this study address to identify physical and hydraulic properties and processes related to the arrangement of soil particles and voids (i.e., soil porosity). However, for an indicator to be useful in assessing soil quality, reference values must be established

(Mausbach and Seybold, 1998) or a better understanding of the dynamic physical processes dependent on the parameter must be known (Wagenet and Hudson, 1997). The analysis of soil quality on a physical-process-approach as proposed by Wagenet and Hudson (1997) may permit to anticipate the effects of dynamic processes rather than just measuring them retrospectively.

1.3 Objectives of this study

This study is part of the long-term SHIFT program (Studies of **H**uman **I**mpact on **F**orest and floodplains in the **T**ropics) for the recultivation of degraded sites on upland clayey Ferralsols near Manaus. If this objective can be achieved, there is a chance to reintroduce those areas into the agricultural production process.

The use of more sophisticated simulation models of water fluxes or plant growth requires spatially representative parameters describing the soil physical and hydraulic properties at several depths. Nowadays, many models are available or may be developed. However, the gap of knowledge of many soil physical and hydraulic parameters limit their utilisation in simulation studies for the central Amazon. The problem is particularly serious for the clayey Ferralsols because little is known about their physical and hydraulic properties and how they change as a result of different land use systems. Methodological and theoretical problems arise because of their unusual behaviour. The clayey Ferralsols hold and transmit water at higher water potential like a typical clayey soil, but the infiltration rates and water fluxes near saturation are typical for sandy soils.

The overall objective of this work are i) to investigate suitable methods for evaluating and characterising soil physical and hydraulic properties of the clayey Ferralsol and ii) to compare physical indicators of soil quality evaluated in land use systems commonly used in the central Amazon. This knowledge might be useful for the development of sustainable, permanent land use systems for this region.

This study starts with this brief review about land use systems in the Amazon, soil quality parameters, and the lack of knowledge of the properties of clayey Ferralsols, which represent a large portion of the central Amazon soils. Chapter 2 presents some general aspects about climate, vegetation, geology and the clayey Ferralsols of the central Amazon, and a detailed description and history of the experiment site. Chapter 3 discusses the measurement of some physical parameters in order to characterise soil structure and its relation to some chemical aspects of the soil. The statistical contrast analysis technique conjoint with weighted average methods is proposed as a tool to compare soil parameters that assumes different values within a land use system. Chapter 4 discusses the evaluation of the soil porosity and its interpretation in relation to water dynamics. In Chapter 5 the viability of measurement of volumetric soil water content (θ) using TDR technique and its necessary calibration is shown. Relevant factors of influencing the θ evaluation in field conditions are also discussed. Evaluation of hydraulic properties is the topic of Chapter 6. Saturated and unsaturated hydraulic properties evaluated by different methods and on different land use systems are discussed and compared. The new inverse method of determining hydraulic properties is also presented. Inferences about the functioning of a dual hydraulic system composed of macropores and micropores are discussed. General conclusions and recommendations for further investigations are outlined in Chapter 7. All data used in this study are shown in appendices at the end of the respective chapter. Some statistical techniques are discussed in more details. Also, the complete handling of data is given. Throughout the text some effort was made to demonstrate the efficiency of using more advanced statistical or mathematical techniques (e.g., scaling theory, test for identity of models, piecewise regression, log-normal distributions and non-linear regression) which are not commonly used by researchers of land use systems, but however, are very useful, if not absolutely necessary to analyse and interpret the high variable soil physical and hydraulic parameters.

1.4 REFERENCES

CALIMAN J P.; OLIVIN J. AND DUFOUR. Dégradation des sols ferrallitiques sableux en culture de palmiers à huile par acidification et compaction. Oléagineaux, 42; 393 – 399, 1987.

EKANADE O. Spatio-temporal variations of soil properties under cocoa interplanted with kola in a part of the Nigerian cocoa belt. Agroforestry System, 5:419-428. 1987.

DORAN J W.; J H C.; JONES, A J.; ARSHAD M A AND GILLEY J E. Determinants of soil quality and health. In: Soil quality and soil erosion. Ed. Lal R. CRC Press. Boca Raton. 1999. 17-36p.

FEARNSIDE P. M. AND R I. BARBOSA. Soil carbon changes from conversion of forest to pasture in Brazilian Amazonian. Forest Ecology and Management, 108, 147–166. 1998

GASH J H C.; NOBRE C A.; ROBERTS J. M AND VICTORIA R L. An overview of Abracos. In: Amazonian deforestation and climate. Ed. GASH, J. H. C.; NOBRE C A.; ROBERTS, J. M AND VICTORIA R L. John Wiley & Sons. Chichester.1996. 1-14p

HOMMA; A. K. O.; WALKER R T.; SCATENA F. N.; COUTO A. J de; CARVALHO R. de A.; FERREIRA C. A. P and SANTOS A. I. M. do S. Reduçao dos desamatamentos na Amazônia: política agrícola ou ambiental. In: Homma, A. K. O. Amazônia – Meio ambiente e desenvolvimento agrícola. Embrapa. Brasília. 1998. p. 120-141.

KARLEN D L. ; MAUSBACH M J.; DORAN J W.; CLINE R G.; HARRIS R F. AND SCHUMAN G E. Soil quality: a concept, definition, and framework for evaluation. Soil Science Society America Journal. 61:4-10. 1997

MAUSBACH M J. AND SEYBOLD C A. Assessment of soil quality. In: Lal R. Soil Quality and agricultural sustainability. 2000. 33-43 p.

MORAES J F L; VOLKOFF B.; CERRI C AND BERNOUX J A. Soil properties under Amazon forest and changes due to pastures installation in Rondônia, Brazil. Geoderma. 70. 63-81. 1996

SMYTH, A J AND DUMANSKI, J. FESLM: An international framework for evaluating land management. World Soil Resources Report 73. FAO, Rome. 1993. 74p.

WAGENET R J. AND HUTSON J L. Soil quality and its dependence on dynamic physical processes. Journal of Environmental Quality. 26: 41-48. 1997.

Apart the references cited directly on the text, most of the information in this chapter comes from the following books:

ANDERSON, R L. Colonization as exploitation in the Amazon rain forest, 1758-1911. 1999. University Press of Florida. Gainesville. 1999. 197 p.

HOMMA A K O. Amazônia – Meio ambiente e desenvolvimento agrícola. Embrapa. Brasília. 1998. 386 p.

KITAMURA P C. A Amazônia e o desenvolvimento sustentável. Embrapa. Brasilia. 1994.182 p.

PRANCE G. T AND LOVEJOY T. E. Key environments Amazonia. Pergamon Press. Oxford. 1985. 442 p.

2 SITE DESCRIPTION

2.1 Location

The study was carried out on the research station of EMBRAPA - Amazônia Ocidental near Manaus in the central Brazilian Amazon (3° 8' S, 59° 52' W, 40-50 m a.s.l.).

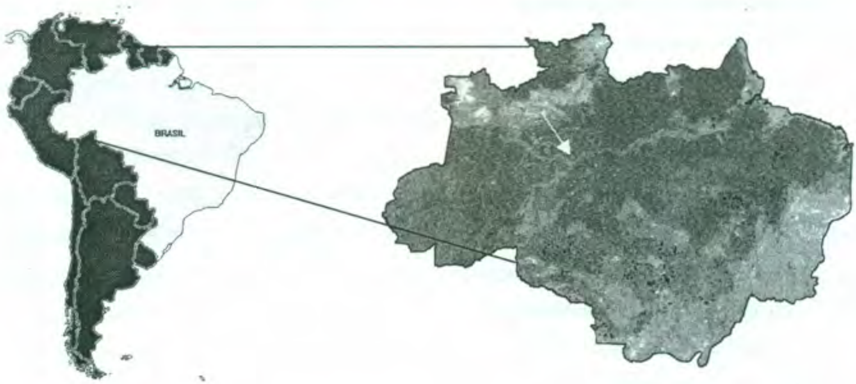

Figure 2.1 Map of Brazil in South America and the Brazilian Amazon. The arrow points to the location of the study area, near to the city of Manaus - Brazil.

2.2 Climate

The average monthly temperature varies very little throughout the central Amazon, in part because there are no relief effects. In the region of Manaus, the highest average monthly temperature, 28°C occurs in September and the lowest, 26°C, between February and April (Salati, 1985).

The relationship among intensity, frequency and duration of rainfall events was studied in the Manaus region by Marques Filho et al. (1981) and Paiva (1996). Their results show an average of the annual rainfall in the order of 2400 - 2500 mm and a marked seasonal dependence, with a monthly maximum in February – March (average around 320 mm) and a minimum in August – September (average around 80 mm). Moreover, the precipitation often occurs as a heavy rains of short duration. Following the criteria for the Köppen classification given by Critchfield (1983), the site should be classified as Af, and not as Aw as first proposed by Rodrigues et al. (1972), because the rainfall amount has normally more than 60 mm in the driest months.

The average potential evapotranspiration for the whole Amazon basin calculated by using Penman's equation resulted in 1460 mm year^{-1} (Villa Nova et al., 1976). Ribeiro and Villa Nova (1979) applying the Thornthwaite and Mather's method estimated a potential evapotranspiration of 1536 mm year^{-1} for an annual mean precipitation of 2478 mm. They estimated an actual evapotranspiration of 1508 mm year $^{-1}$. Their results shows that the values of potential and actual evapotranspiration are practically the same for the whole year, except for three months (August – September – October) when a soil-water deficit occurs. Using a water budget model, Leopoldo et al. (1995) estimated an actual evapotranspiration of 1493 mm year $^{-1}$. They concluded that the actual and potential evapotranspiration can be considered as being of the same magnitude. A similar result is given by Shuttleworth (1988) who estimate an annual evapotranspiration of 1320 mm, 328 mm of which stems from direct evaporation of the rainfall intercepted by the forest canopy, and 992 mm from forest transpiration.

Most part of the specific meteorological studies in Manaus were carried out in the Ducke Forest Reserve (Villa Nova et al., 1976; Ribeiro et al., 1987; Marques et al., 1987; Shuttleworth et al., 1988 Viswanadham et al., 1991) located about 10 km far away from this experiment. Specific microclimate data from this experiment from the years 1994 and 1995 were analysed by Cabral et al. (1997). The rainfall interception, throughfall and stemflow were studied in the present experiment (Schroth et al.; 1999 a). Interception studies for the primary forest were conducted by Northcliff and Thornes (1981); Franken et al. (1982); Leopoldo et al. (1987) and Lloyd et al. (1988 a, b).

2.3 Geology and the clayey Ferralsols

The soils covering sediments in the central Amazon results from the weathering of tertiary fluvio-lacustrine deposits, which belong to the so-called "Barreiras formation". It consists of cross-bedded sandstone with intercaled argilites, with predominance of quartz and kaolinite and with feldspar and muscovite as minor components (Chauvel, 1987).

The soil formed on the plateaux and on the upper part of the slopes is a clayey, deeply weathered Ferralsols (Chauvel, 1987; Cornu et al., 1998). This strongly weathering results from processes that involve intense dissolution of quartz, concentration of aluminium hydroxide, and crystallisation of kaolinite (Irion, 1984; Chauvel, 1987; Cornu, 1998). It has the consequence that the soil is normally very poor in nutrients (e.g., phosphorus, calcium, magnesium, and potassium).

The soil in the experiment is classified as Xanthic Ferralsol according to FAO legend (FAO, 1990). It is classified as a Xanthic Hapludox following the Soil taxonomy (Soil Survey Staff, 1997) or as Latossolo amarelo using the Brazilian classification system (EMBRAPA, 1999). The clayey Ferralsols is a representative soil of large areas in the central Amazon (Vieira and Santos, 1987).

The soil physical and chemical characteristics evaluated in the site where this study was carried out are very similar to those described by Camargo and Rodrigues (1979) and Rodrigues et al. (1972). It normally shows a high clay content on the surface, with 600 – 750 kg m^{-3} of clay in the first 30 cm; and very clayey down, with 750 - 850 kg m^{-3} of clay. The clay fraction is dominated by kaolinite with some gibbsite (Camargo and Rodrigues, 1979; Silva, 1997).

It shows a strongly microaggregation, possibly, as a consequence of the strong binding between positively charged oxyhydroxides and negatively charged kaolinite and organic matter (Sanches, 1976).

The pH measured in water has in the soil surface values of about 4.5 and it goes up in the lower parts of the profile. The sum of exchangeable bases (Ca^{++}, Mg^{++}, K^+, Na^+) is very low, about 0.60 $cmol_c$ kg^{-1} in the A horizon and goes down to 0.3 – 0.1 $cmol_c$ kg^{-1} below. Available phosphorus is only appreciable in the A horizon, 3 ppm according to Melhich II method and its decrease to the unit in depths part of the profile. The organic carbon is about 30 g kg^{-1} in the A horizon, however its values are reduced rapidly with depth, measuring about 2-3 g kg^{-1} at 200 cm deep. Detailed chemical characteristic of this experiment is given by Preisinger (1997); Teixeira and Villani (1997); Schroth et al. (1999 b) and Schroth et al. (2000 a, b).

2.4 Vegetation

The clayey Ferralsols are covered by a dense, humid, evergreen rain forest the so-called forest on terra-firme. Although, the physiognomy of the rain forest is quite uniform throughout the region, a detailed examination shows a great diversity of species between different sites (Murça Pires, 1984; Guillaument, 1987). The canopy of the primary forest has a height of $\approx$ 30 m. The understory of dense tropical forest is dimly illuminated and for this reason, generally free of vines, bushes, herb or low vegetation (Murça Pires, 1984). The relative humidity approaches 100 % above the canopy. Therefore direct evaporation from the soil is about zero (Leopoldo et al., 1987).

The development of a dense forest on soils formed from a nutrient poor parent rock poses a problem which had attracted the attention of the researchers in decade of 60 (Kitamura, 1994). It was explained by the fact that a tropical condition of high temperature and high precipitation allows for intense photosynthesis activity and since the tropical forest is a very old formation, there has been sufficient time for nutrients to be sequestered in the biomass of plants (Murça Pires, 1984).

The nutrients necessary to maintain this process are essentially tied up in the biomass of the forest and recycled once and again via decomposition and reabsortion by plant and fauna activity with small losses being compensated by the mineral input in the rain (Leopoldo et al., 1987; Cornu et al., 1998). Moreover, the works of Nepstad et al. (1994) show that the root system of the forest plants can reach greater depth and a significant proportion of the soil water is extracted from depths below 2 m, reducing the water stress in the dry periods.

2.5 Land use, experiment design and management

Some studies about plant-induced soil changes frequently encountered the confounding effects of site variability and land-use history. If soil is initially well characterised, then any differences in soil properties that arise over time among experimental treatments can be attributed to plant and management effects. Therefore, a detailed history of the site is described below, and allows explaining some results found in the actual experiments.

The study site was first cleared from primary forest in 1980, using heavy machinery for windrowing and the removal of tree stumps; the remaining vegetation was burnt. In 1981, an experiment with rubber trees (*Hevea brasiliensis*) was established, being abandoned in 1986. Until preparation of the area for the present experiment was carried out, secondary vegetation was growing together with the remaining rubber trees. The developing secondary forest was manually cleared in 1992 and the vegetation was burnt on the site. The experimental plots were planted with bag plants from February to March 1993.

Basically four regional important tree crop species were chosen to compose the agricultural land use systems: i) the palm *Bactris gasipaes* Kunt (peach-palm, pupunha; Arecaceae), which is managed for either fruits or heart of palm production; ii) *Theobroma grandiflorum* (Willd. ex Spreng.) K. Schum. (cupuaçu; Sterculiaceae), a tree from the same genus of cacao and whose fruit pulp is widely used in the region for the preparation of juice, ice-cream and sweets, further the seeds have a potential use to prepare chocolate; iii) a tree, *Bertholletia excelsa* Humb. & Bonpl. (Brazil nut, Para nut; Lecythidaceae) which, besides the well-known nuts, produces excellent wood; and iv) *Bixa orellana* L. (annatto or urucum; Bixaceae) which is widely cultivated in the tropics for its non-toxic red dye. The agricultural land use systems were monocultures of cupuaçu, peach palm for palm heart production and peach palm for fruits production. In the monocultures of peach palm and cupuaçu the planting density were, respectively, 2 x 2 m (Figure 2.2) and 7 x 6.4 m (Figure 2.3).

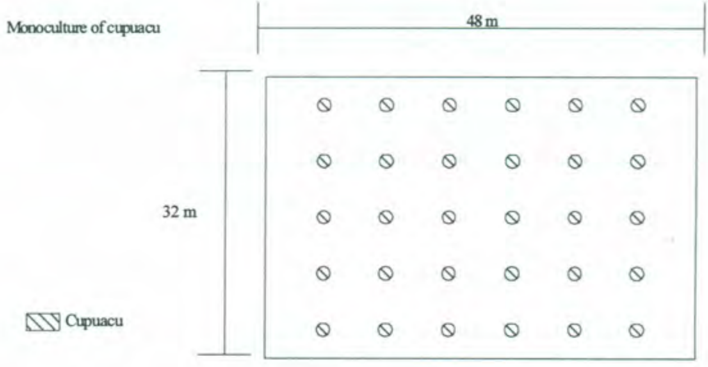

Figure 2.2 Layout of the plot of the cupuaçu (*Theobroma grandiflorum*) monoculture.

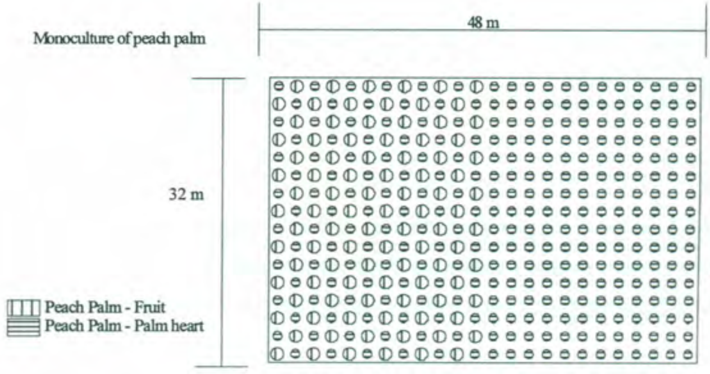

Figure 2.3 Layout of the plot of peach palm (*Bactris gasipaes*) monoculture for fruits and palm heart production.

In the agroforestry system, the trees were grown in rows spaced 4 m apart. A row of peach palm (at 2 m spacing within the row) was alternated with a mixed row of cupuaçu and Brazil nut (at 7 m spacing between the trees within the row), a row of annatto (at 4 m spacing within the row) and again a mixed row of cupuaçu and Brazil nut, after which the next row of peach palm followed. Between the trees, *Pueraria phaseoloides* Kunth (tropical kudzu; pueraria; Fabaceae) was grown as a cover crop. In the first year, in the agroforestry system, manioc (*Manhiot sp.*) was planted at the spacing of 1.00 x 1.20 m. The experimental layout of the agroforestry system is shown in Figure 2.4.

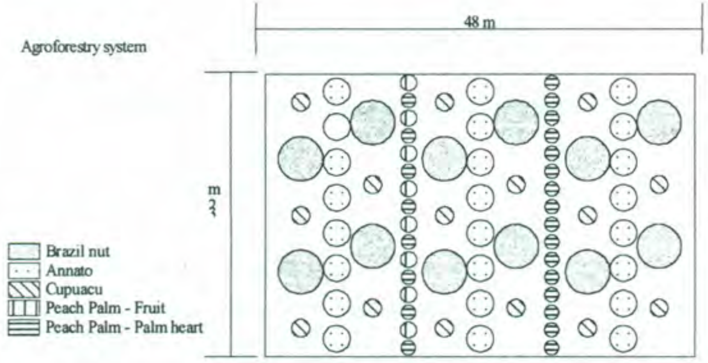

Figure 2.4 Layout of the plot of agroforestry system. The species are Brazil nut (*Bertholletia excelsa*), annatto (*Bixa orellana*), cupuaçu (*Theobroma grandiflorum*) and peach palm *(Bactris gasipaes*). The area between the species was covered by Pueraria (*Pueraria phaseoloides*).

For comparison, plots with regrowth of spontaneous secondary vegetation of the same age as the agricultural plots were included in the study. The secondary vegetation plots were dominated by *Vismia* spp., which is a characteristic genus in the vegetation of young fallow on degraded sites in the region. The stem density was 1.95 ± 0.17 per m^2 in the *Vismia* plots (Schroth et al., 1999 a). Additionally, two tree species from a nearby primary rainforest were included for the measurements of some parameters. A dicotyledoneous tree, *Eschweilera sp.* (matá-matá, Lecythidaceae), and a palm *Oenocarpus bacaba* (bacaba, Arecaceae). Both species are relatively frequent in the primary forest, and are of commercial interest, matá-matá for its wood and bacaba for its fruits used for juices. For each species, in all land use systems, the soil near three well developed specimens were included in the measurements. The measurement plots, except for the rainforest sites, were arranged in a randomised complete plot design with three replications. Plot size is 24 x 32 m in the peach palm monoculture, and 48 x 32 m in the monoculture of cupuaçu, agroforestry system and the secondary forest plots.

2.5.1 Management of the plots until the evaluations period

The peach palm was managed by cutting the main stem about 1½ years after planting and harvesting the palm hearts three times per year when the offshoots reached a diameter of 8 cm at 1 m height. The annattos were cut back about 1.5 m height once per year after the harvest, between March and May, to increase fruit production, removing all the leaves and small branches which were then left to decompose under the trees. Wolf (1997) gave the differences between the biomass accumulation. SHIFT (1996, 1997) discussed the initial crop yields.

Fertilisers were applied to the crops in two doses per year in November - December at the beginning of the rainy season and at the end of the rainy season and May – June (SHIFT 1996; 1997; 1998). The primary and secondary forest sites were never fertilised in the present experiment.

2.6 REFERENCES

CABRAL O M R. Climatological observation recorded during the period 1993 to 1995 at Shift project site in Manaus, central Amazonia. In: GASPAROTTO L. and LIEBEREI R. (eds). SHIFT ANNUAL REPORT 1996. Manaus, 1996. p.34-46.

CAMARGO M N and RODRIGUES T E. Guia de excursão. In: CONGRESSO BRASILEIRO DE CIÊNCIA DO SOLO, 17., 1979. Sociedade Brasileira de Ciência do Solo / Embrapa, Rio de Janeiro, 1979. p.1-72.

CHAUVEL A.; LUCAS Y. and BOULET R. On the genesis of the soil mantle of the region of Manaus, Central Amazonia, Brazil. Experientia. 43: 234-241, 1987.

CORNU S.; LUCAS Y.; AMBROSI J P. and DESJARDINS T. Transfer of dissolved Al, Fe and Si in two Amazonian forest environments in Brazil. European Journal of Soil Science. 49: 377-384, 1998.

CRITCHFIELD H J. General Climatology. 4.ed. Prentice Hall, Englewood Cliffs. 453 p.

EMBRAPA. Sistema brasileiro de classificação de solos. Embrapa, Brasilia, 1999. 257p.

FAO. Soil Map of the World, Revised legend. Roma, FAO, 1990. 119p.

FRANKEN W.; LEOPOLDO P R.; MATSUI E. and RIBEIRO M DE N G. Estudo da interceptação da água de chuva em cobertura florestal amazônica do tipo terra firme. Acta Amazonica. 12: 327-331, 1982.

GUILLAMENT J L. Some structural and floristic aspects of the forest. Experientia. 43: 241-290, 1997.

IRION G. Clay minerals of Amazonian soils. In: SIOLI H, ed. The Amazon: Limnology and Landscape Ecology of a mighty tropical river and its Basin. Dordrecht, W. Junk publisher, 1984. p.537-579.

KITAMURA P C. A Amazônia e o desenvolvimento sustentável. Brasilia, 1994. 182p.

LEOPOLDO P R.; FRANKEN W.; SALATI E. and RIBEIRO M DE N G. Towards a water balance in the Central Amazonian region. Experientia. 43: 222-233, 1987.

LEOPOLDO P R.; FRANKEN W. and VILLA NOVA N A. Real evapotranspiration and transpiration through a tropical rain forest in central Amazonia as estimated by the water balance method. Forest Ecology and Management. 73: 185-195, 1995.

LLOYD C R. and MARQUES A de O. Spatial variability of throughfall and stemflow measurements in Amazonian rainforest. Agricultural and Forest Meteorology. 42: 63-73, 1988.

LLOYD C R.; GASH J H C. and SHUTTLEWORTH W J. The measurement and modelling of rainfall interception by Amazonian rain forest. Agricultural and Forest Meteorology. 43: 277-294, 1988.

MARQUES A de O.; RIBEIRO M de N G.; SANTOS H M DOS. and SANTOS J M DOS. Estudos climatológicos da Reserva Florestal Ducke - Manaus-AM.IV. Precipitação. Acta Amazonica. 11: 759-768, 1981.

MURÇA PIRES J. The Amazonian forest. In: SIOLI H, ed. The Amazon: Limnology and Landscape Ecology of a mighty tropical river and its Basin. Dordrecht, W. Junk publisher, 1984. p.581-602.

NEPSTAD D C.; CARVALHO C R DE.; DAVIDSON E A.; JIPP P H.; LEFEBVRE P A.; NEGREIROS G H.; DA SILVA E D.; STPME T A.; TRUMBORE S E; et al. The role of deep roots in the hydrological and carbon cycles of Amazonian forest and pastures. Nature. 372: 666-669, 1994.

NORTCLIFF S. and THORNES J B. Seasonal variation in the hydrology of a small forested catchment near Manaus, Amazonas, and the implications for its management. In: LAL R. and RUSSEL E W, eds. Tropical agricultural hydrology. New York, John Wiley & Sons, 1981. p. 37-57.

PAIVA E M C D DE. Regime de precipitação na Amazônia e sua relação com o desmatamento e temperatura da superfície do mar. Universidade federal do Rio Grande do Sul, 1996. 297p. (Doctor)

PREISINGER H. Rekultivierung degradierter, brachliegender Monokultflächen in ausgewogene Mischkulturflächen unter besonderer Berucksichtigung bodenbiologische Faktoren. In: Anonymous.Forschungsprogramm SHIFT - ENV 23. Hamburg, Universität Hamburg, 1997. p.60-99.

RIBEIRO M DE N G. and VILLA NOVA N A. Estudos climatológicos da Reserva Florestal Ducke, Manaus, AM. III. Evapotranspiração. Acta Amazonica. 9: 305-309, 1979.

RODRIGUES T E.; REIS R S DOS. and MORIKAWA I K. Levantamento detalahdo dos solos do Instituto de pesquisas agropecuárias da Amazônia Ocidental. Manaus. IPEAAOc. 1972. 63p.

SALATI E. The climatology and hydrology of Amazonia. In: PRANCE G T. and LOVEJOY T E, eds. Key environments Amazonia. Oxford, Pergamon Press, 1985. p.18-48.

SANCHEZ P A. Properties and management of soils in the tropics. New York, John Wiley & Sons, 1976. 618p.

SCHROTH G.; DA SILVA, L. F..; WOLF M A.; TEIXEIRA W G. and ZECH W. Distribution of throughfall and stemflow in multi-strata agroforestry, perennial monoculture, fallow and primary forest in central Amazonia, Brazil. Hydrological Processes. 13: 1423-1436, 1999 a.

SCHROTH G.; SILVA L F DA.; SEIXAS R.; TEIXEIRA W G.; MACÊDO J L V. and ZECH W. Subsoil accumulation of mineral nitrogen under polyculture and monoculture plantations, fallow and primary forest in a ferralitic Amazonian upland soil. Agriculture, Ecosystem and Environment. 75: 109-120, 1999 b.

SCHROTH G.; TEIXEIRA W G.; SEIXAS R.; SILVA L F DA.; SCHALLER M.; MACÊDO J L V. and ZECH W. Effect of five tree crops and a cover crop in multi-strata agroforestry at two fertilization levels on soil fertility and soil solution chemistry in central Amazonia. Plant and Soil. 221: 143-156, 2000 a.

SCHROTH G; SEIXAS R.; SILVA L F DA.; TEIXEIRA W. G. and ZECH W. Nutrient concentrations and acidity in ferralitic soil under perennial, fallow and primary forest in central Amazonia. European Journal of Soil Science. 51: 219-231, 2000 b.

SHIFT ENV - 23. Recuperação de areas degradadas, através de sistemas de policultivo. Relatório Anual. Manaus - Hamburgo, Embrapa - CPAA and Universidade de Hamburgo, 1996. 69p.

SHIFT ENV - 23. Recuperação de areas degradadas, através de sistemas de policultivo. Relatório Anual. Manaus - Hamburgo, Embrapa - CPAA and Universidade de Hamburgo, 1997. 81p.

SHIFT ENV - 23. Recuperação de areas degradadas, através de sistemas de policultivo. Relatório Anual. Manaus - Hamburgo, Embrapa - CPAA and Universidade de Hamburgo, 1998. 80p.

SHUTTLEWORTH W J. Evaporation from Amazonian rainforest. Proc. R. Soc. Lond. B: 321-346, 1988.

SILVA M L N. Erosividade da chuva e proposição de modelos para estimar a erodibilidade de latossolos brasileiros, Lavras, University of Lavras - Brazil, 1997. 154p. (Doctor)

SOIL SURVEY STAFF. Key to soil taxonomy. 7.ed. Blacksburg, Pocahontas Press, 1997. 545p.

TEIXEIRA W G and VILLANI E M A. Variabilidade espacial de características químicas do solo em um Latossolo amarelo, com utilização agrícola anterior. In: REUNIAO BRASILEIRA DE FERTILIDADE DO SOLO E NUTRICAO DE PLANTAS. 22., 1996. Universidade do Amazonas - Embrapa /CPAA, Manaus, 1996. p.132-133.

VIEIRA L S and SANTOS P C T C. Amazônia: seus solos e outros recursos naturais. São Paulo, Ed. Agronômica Ceres, 1997.

VILLA NOVA N A.; SALATI E. and MATSUI E. Evapotranspiração da bacia Amazônica. Acta Amazonica. 6: 215-218, 1976.

VISWANDADHAM Y.; SILVA FILHO V P. and ANDRÉ R G B. The Priestley-Taylor parameter α for the Amazon forest. Forest Ecology and Management. 38: 211-225, 1991.

WOLF M A. Accumulation of biomass and nutrients in the aboveground organs of four local tree species in monoculture and polyculture systems in central Amazônia, Technische Universität Carolo-Wilhelmina. Braunschweig, 1997. 299p. (Diplomarbeit)

3 LAND USE EFFECTS ON SOIL PHYSICAL PROPERTIES OF A XANTHIC FERRALSOL IN THE AMAZON BASIN

3.1 INTRODUCTION

In order to define which land use systems may maintain or recuperate the agricultural potential of clayey Ferralsols in the central Amazon, a great number of physical, chemical and biological parameters must be assessed. Understanding the processes that lead to degradation is an essential element to define suitable land use systems for these soils. If these soils are cropped with little or no nutrient inputs other than the ashes of the previous vegetation, the yields of annual crops decline, and the land is often abandoned after a few years of cropping in the traditional "slash and burn" system.

Declining productivity of tropical soils under continuous cultivation, even with supplementary fertilisation, is well documented (Lal, 1979). This confirms that the productivity of tropical land use systems does not only depend on the stock of nutrients in the soil or the availability of commercial fertilisers, but is also related to the maintenance of soil physical and hydraulic qualities. Moreover, the maintenance or improvement of soil physical qualities for agriculture production, nutrients uptake and fertiliser use by plants will be more efficient, and consequently, crop production will be increased.

The structure of the soil surface tends to become massive by aggregate coalescence, and porosity is greatly reduced when the clayey Ferralsols are improperly managed (Medina, 1985; Chauvel, 1991; Teixeira et al., 1997). Leite and Medina (1984) and Medina (1985) also documented reduction in the water infiltration because of inappropriate soil management.

Under tropical conditions, available knowledge about plant-soil interactions in different land use systems is still limited. Also, the degree by which various agricultural systems may alter soil properties and processes is poorly understood and cannot be adequately predicted for the Ferralsols in the central Amazon.

In this chapter, bulk density, particle size distribution, index of flocculation and particle density are described and discussed for three different land use systems in the central Amazon. These studies investigate alterations of soil properties by measuring these physical parameters as affected by plant-soil interaction. The statistical contrast analysis technique conjoint with a weighted-average method is proposed as a tool to compare soil parameters that assumes different values within a land use system. In addition, some selected soil chemical parameters are also presented to better understand soil physical and hydraulic properties.

3.1.1 Evaluated physical properties

3.1.1.1 Bulk density (ρ)

The bulk density is a simple measure of soil structure which is used extensively for quantifying soil compactness and to predict soil strength and water retention. It is defined as the ratio of the mass of an oven-dry soil sample to its bulk volume. It is a temporally and spatially dynamic soil property commonly used as indicator of changes in soil structure due to tillage, root development and activity of soil fauna.

Although changes of ρ caused by soil tillage are well documented in the soil physics literature (e.g., in Ferralsols, Cassel (1982), Medina (1985), Chauvel et al. (1991)), only few examples are given where ρ changes are due to plants species effects. Such effects are specifically to be expected in complex land use systems, like the agroforestry system, in which a combination of different management practices are used and distinct plant species grow together in a plot. Examples of agroforestry studies in tropical climates in which management practices and different plant species caused significant alterations in ρ are summarised in Table 3.1. Likewise, Huxley et al., 1994; Mapa and Gunasena, 1995 and Torquebiau and Kwesiga, 1996 were also able to detect significant alterations in subsoil bulk densities. However, Kang et al., 1997 in southwest Nigeria on an Alfisol, and Hulugalle and Ndi, 1993 in southern Cameroon on a Typic Kandiudult could not find significant differences in soil bulk densities in agroforestry systems.

Table 3.1 Range of bulk density evaluated on different soil types in agroforestry systems on tropical climate.

Sampling depth (cm)	Range ($Mg\ m^{-3}$)	Location	Soil class	Reference
(0-5)	1.02 – 1.62	Ibadan, Nigeria	Oxic Kandiustalf	Juo et al., 1996
(-)†	1.26 – 1.53	Ibadan, Nigeria	Oxic Paleustalf	Yamoah et al., 1986
(0-5)	0.94 – 1.56	Ibadan,Nigeria	Oxic Paleustalf	Lal, 1989
(5-10)	1.06 – 1.70			
(0-10)	1.14 – 1.42	Ibadan, Nigeria	Oxic Paleustalf	Lal et al., 1979
(20)	1.25 – 1.30	Machakos, Kenya	Haplic Lixisol	Huxley et al, 1994
(50)	1.18 – 1.22			
(100) †	1.11 – 1.13			
(0-5)	1.27 – 1.41	Machakos, Kenya	Khandic Rhodustalfs	Jama et al. 1995
(0-5cm)	1.19 – 1.70	Madampe, Sri Lanka	red yellow Podzolic	Vidahama Arachchi and Liyanage, 1998
(0-15) ‡	1.10-1.38	Dambulla, Sri Lanka	Rhodustalf	Mapa and Gunasena,1995
(15-30) ‡	1.28-1.43			
(-)†	1.43-1.58	Misamfu, Zambia	Oxisol	Dalland et al., 1993
(0-10)	1.30 – 1.70	Yurimagas, Peru	typic Paleudult	Arevalo et al., 1998
(0-7.5)	1.43 – 1.29	Yurimagas, Peru	typic Paleudult	Alegre and Rao, 1996
(0-25)	1.12-1.32	Chipata, Zambia	Hulplustalfs	Torquebiau and Kwesiga, 1996
(25-50)	0.93-1.22			

† Information not available; ‡ core with 6 cm high.

A central biophysical agroforestry hypothesis is that trees and crops can grow together on the same site with increased productivity. Competition is reduced due to exploitation of water and nutrients at different soil layers and at different times, in a spatial or/and temporal complementarity (Sanchez, 1995; Rao et al., 1998;). Therefore, in order to develop productive and sustainable agroforestry systems for different pedoclimatic conditions, it is necessary to improve our knowledge not only about the competitive relations between the plant species for nutrients and water; but also to know how plants and their management changes soil properties. A reduction of ρ is frequently interpreted as an improvement of soil physical properties, which is usually true. Nevertheless, a reduction in ρ (i.e., an increase in porosity) can sometimes also be disadvantageous, e.g., when water infiltration and thus nutrient leaching increase. Also, the available water capacity of coarse textured soils can be reduced for low ρ and may, in fact, be increased by soil compaction (Archer and Smith, 1972). Moreover, high aeration porosity may result in considerable moisture loss through physical evaporation (Hillel, 1998).

Ideal structure

Nowadays, with the development of models for simulating plant growth or transport of solutes in soils, the concept of a static and qualitative description of soil structure is changing into the concept of finding ways of adjusting and optimising structure to achieve maximum yields or reduced leaching rates (Medvedev, 1991; Kuznetsova, 1991; Bouma et al., 1999).

With the purpose of developing productive and sustainable land use systems, the conceptual idea of an "optimum" or "ideal" structure for a land use system can be hypothesised. An ideal arrangement of the pores which give the ideal structure will result in an adequate retention and availability of water for plant uptake of nutrients with acceptable leaching rates, and simultaneously a soil aeration that is adequate for plants roots and micro-organisms development.

The optimal structure depends on many factors such as plants species, soil type, climatic conditions, field management, pore-size distribution, and hydraulical properties of the soil. However, determination of the ideal structure is complicated by conflicting criteria, for instance, the ideal structure for water uptake is probably not the ideal structure for reducing leaching risks. In such situations, a soil structure that maintains both criteria at satisfactory levels must be accepted.
The ideal structure is a dynamic and not a static value, which will be related to different stages of the agricultural fields. Furthermore, the combination of different factors to achieve an ideal structure has probably not a unique solution. For instance, many possible combinations of plant species, and different field management practices may result the ideal structure. Obviously, the ideal structure is dependent on the soil type and the climatic conditions. Bulk density measurement

is suggested as a rough indicator of the ideal structure for a land use system, and a simple statistical approach is proposed for comparing different scenarios of soil structure, using average weighted values of ρ as indicator parameter. The comparison of different scenarios may be used as a tool in planning experiments or in soil management decisions.

The concept for calculating weighted means, as used in this study, is a result of field observations and analyses of soil parameters, which shows that plants and their specific management create spot areas around the tree stems that have distinct soil properties. After estimating the radius of influence of these spots around a stem, and calculating their relative (weighted) means, plant species effects, and the whole land use systems can be compared using contrast analyses, and hypotheses of practical interest can be formulated in terms of the ρ-weighted values.

3.1.1.2 Particle size distribution

Particle size analysis or texture determination is the measurement of the relative proportions of the various sizes of the mineral soil particles. It is usually determined by their ability to pass through sieves of various mesh sizes and by their rates of settling in water (Stoke's law is applied in the calculations). Between the soil particles, the clay fraction has the most significant influence on physical and chemical processes in the soil, primarily because they have a large and reactive surface area per unit mass. In Ferralsols near Manaus, the predominant clay mineral is kaolinite (Irion, 1984; Rodrigues, 1998).

Although, the particle size distribution is a very stable soil property in structured clayey soils where the clay particles are strongly bound, the dispersion of the clay particles may cause some disturbances in the functionality of the soil structure (Raij and Peech, 1972; Castro and Logan, 1991, Tessier et al., 1998). Under field conditions, processes dependent on the soil structure may change significantly, as a consequence of the natural dispersion or flocculation of the clay particles, with are not be detected by the classical granulometric analyse with dispersion agents.

The surface charge of clayey Ferralsols in the Amazon is pH-dependent (Morais et al., 1976; Silva, 1996). The changes in the net charge of these soils can lead to an improvement or deterioration of the soil structure quality (El-Swaify, 1980; Castro and Logan, 1998) depending on the specific conditions and considering findings on short or long time basis. Since there are significant relations between particle-size and some physical, chemical and hydraulical properties, the former has been used to predict the others by using the so-called pedotransfer functions. Although, predictions of hydraulical parameter using particle size distribution have shown a reasonable agreement with experimental data for many temperate soils (e.g., Arya et al., 1999;

Schaap and van Genuchten, 1999); they do not give reasonable predictions for some Amazonian soils as showed by Tomasella and Hodenett (1997, 1998). The failure of the pedotransfer functions for the clayey Ferralsols may be because the oxides and kaolinite clay particles are strongly flocculated and aggregated. Therefore, for some processes they have a typical sandy behaviour. This phenomenon is discussed further in this chapter and throughout this study.

3.1.1.3 Particle density (ρ_p)

The particle density of a soil refers to the mean density of all solid particles. It is a function of the mineralogical composition of the particles and is expressed as the ratio of the total mass of the solid particles to their total volume, excluding the pore spaces between particles (Blake and Hartge, 1986). Often, the value of ρ_p is not evaluated, it is assumed to be 2.65 Mg m^{-3}, which is the value for the density of quartz particles (Carter and Ball, 1993; Skopp, 2000). However, the use of this value instead of its measurement can lead, especially for soils with high iron or organic matter content, to considerable estimation errors of the total porosity.

3.2 MATERIAL AND METHODS

3.2.1 Study area and site history

The study area and the site history of the selected plots have been described in details in Chapter 2.

3.2.2 Soil sampling and analysed parameters

Field evaluations were carried out from October 1996 to January 1997. The three land use systems investigated were: i) two monocultures of peach palm (*Bactris gasipaes*), for production of fruits and palm heart, respectively; ii) a monoculture of cupuaçu (*Theobroma grandiflorum*); and iii) a complex agroforestry system with peach palm, cupuaçu, Brazil nut (*Bertholletia excelsa*) and annatto (*Bixa orellana*). The soil was covered by *Pueraria phaseoloides* in all systems except the peach palm monoculture, which tolerates little ground vegetation. Adjacent areas of primary and secondary forest were investigated for comparison. A more detailed description of the experimental design and the plant species are given in Chapter 2. In the nearby primary forest, the sampling positions near the trunks of bacaba and matá-matá were included in the statistical analyses only for the ρ measurements. The other chemical and physical parameters evaluated in the primary forest are shown only for qualitative comparison.

Table 3.2 shows the sample points and their localisation relative to the land use system. The soil samples were collected at $\approx$ 40 cm from the trunk of the respective species as well as under the cover crop pueraria, in the agroforestry system and grasses and pueraria in the cupuaçu monoculture plots.

Table 3.2 Identification of the land use systems and plant species (scientific and common name) where the soil samples were collected.

Number	Land use system	scientific name	common name
1	Agroforestry	*Theobroma grandiflorum*	Cupuaçu
2	Agroforestry	*Bixa orellana*	Annatto
3	Agroforestry	*Bertholletia excelsa*	Brazil nut
4	Agroforestry	*Bactris gassipaes* (Fruit)	Peach palm – F
5	Agroforestry	*Bactris gassipaes* (Palm Heart)	Peach palm – P
6	Agroforestry	*Pueraria phaseoloides*	Pueraria
7	Monoculture	*Theobroma grandiflorum*	Cupuaçu
8	Monoculture	*Homolepsis sp and Pueraria phaseoloides*	Grasses and pueraria
9	Monoculture	*Bactris gassipaes* (Fruit)	Peach palm – F(m)
10	Monoculture	§	Peach palm – F(mb)
11	Monoculture	*Bactris gassipaes* (Palm heart)	Peach palm – P(m)
12	Monoculture	§	Peach palm –P(mb)
13	Secondary forest	*Vismia spp.*	Vismia
14	Primary forest	*Escheweleira sp.*	Matá-matá
15	Primary forest	*Oenocarpus bacaba*	Bacaba

§ Evaluation located in a position between the palms at a maximum distance from the trunks.
n = 9 samples ; SD = standard deviation; SE = standard error of the mean.
m = monoculture; b = between the palms; F = Peach palm for fruits production; P = Peach palm for palm heart production

In the monocultures of peach palm, further samples were collected in an intermediate position between the plants and at maximum distance from the trunks. Samples were also collected close to the trunks of *Vismia sp*, the dominant species in the secondary forest. The experimental design for statistical analysis was a randomised block design (RBD), and theoretical details are given in the Appendix 3-A. If the analyses of variance indicated a difference $\alpha < 0.05$, then Tukey's test was applied to compare soil properties as influenced by the specific plants and their specific agricultural management. In addition, the RDB allows to contrast the whole land use systems. This was performed by weighted means of each evaluated position within the land use system, and relating them to the surface area for which this mean was representative.

Weight-average method

The estimation of the weights of the spot areas proposed here is simple and straightforward. They are estimated based on the area of influence of a specific species, proportional to the entire area of the land use system. The domain of influence of a specific plant is a "disc" centred at the stem. The area of each of these disc areas around the stem was calculated based on: i) the crown area of the plants at that stage of growth (Schroth et al., 1999b); ii) results of selected soil physical properties in transects (data not shown); iii) the management practices, i.e., fertiliser rates and distribution around the stems, the weed control system adopted, pruning intervals for annatto and peach palm. These specific areas of influence of each species were then multiplied by the number of individuals in a specific area (e.g., one hectare). The remaining areas of bare soil or occupied by the cover crop, were calculated by subtraction. Table 3.3 shows the estimated total areas of influence of each species in relation to the whole system.

Table 3.3 Characteristics of the crown area (mean ± SD); the estimated radii of influence and the average area influenced by plants and its management in different land use systems in Manaus - Brazil.

System and plant specie	Number of plants per ha	Crown area per tree [m^2][¶]	Radii of influence [m]	Average area [m^2 ha^{-1}]	Percentile area [%]
Agroforestry system					
Cupuaçu	93	3.5 ± 2.3	1.2	421	~ 4
Annatto [†]	156	~ 12.5	1.5	1103	~ 11
Brazil nut	93	30.0 ± 13.4	2.5	1826	~ 18
Peach palm for fruit	78	19.5 ± 3.3	0.9	198	~ 2
Peach palm for palm heart	156	~ 4	0.8	313	~ 3
Pueraria – cover crop	n.d.	-	-	-	~ 62
Monoculture of cupuaçu					
Cupuaçu	223	4.2 ± 1.1	1.0	700	~ 7
Grasses and pueraria [§]	n.d.	-	-	-	~ 93[#]
Monoculture of peach palm for fruit and palm heart					
Peach palm for fruit	625	16.5 ± 1.7	0.7	962	~ 10
Peach palm for palm heart	1875	~ 4	0.6	2120	~ 20
Between palms	-	-	-	-	~ 70[#]
Monoculture of peach palm for palm heart					
Peach palm for palm heart	2500	~ 4	0.6	2120	~ 20
Between palms	-	-	-	-	~ 80[#]

[§] In the monoculture plots the cover crop of pueraria was not well established
[#] Estimated by subtraction; n.d – not determined.
[¶] Adapted from Schroth et al., 1999 b.
[†] The annatto crown was cut back one per year.

Figure 3.1 shows the spatial arrangement of the areas of influence. Following, several hypotheses of practical interest were formulated in terms of means of weighted-bulk density and were statistically compared using contrast analyses.

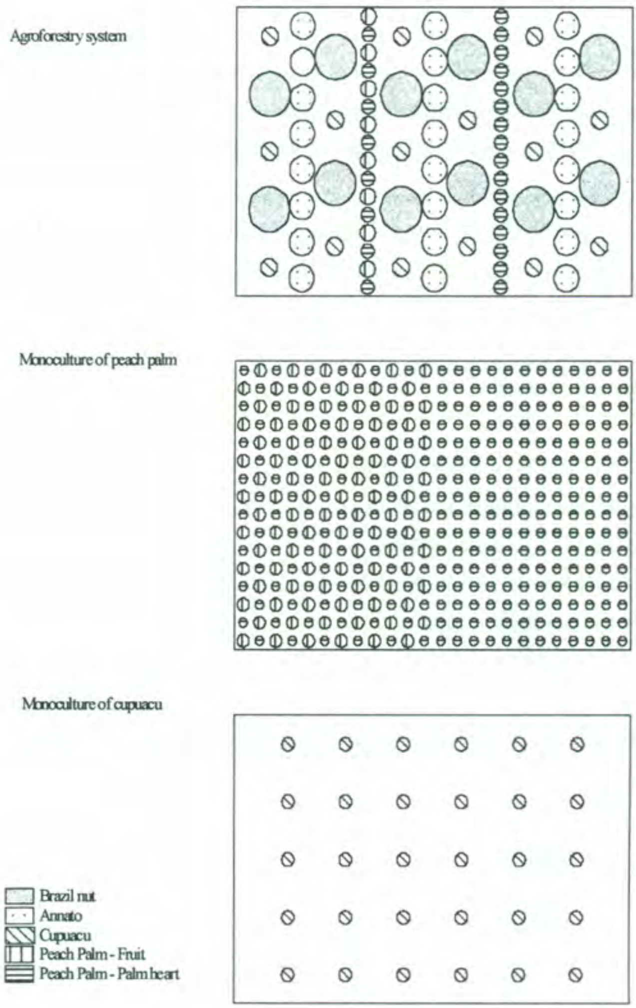

Figure 3.1 Layout of the experimental plots of the agroforestry system, the monoculture of peach palm and the monoculture of cupuaçu. The shadows areas represent the estimated "spots areas" around a stem, which are caused by specific interactions of soil-plant-management into the soil characteristics.

3.2.3 Evaluated parameters

3.2.3.1 Bulk density (ρ)

Undisturbed soil samples were collected at each position described in Table 3.2, with three subsamples within each plot. They were collected by hammering a steel cylinder into the soil to the desired depth, which was then removed to obtain an exact volumetric sample. The steel cylinders had 4.5 cm of inner diameter and 5 cm height, thus a volume of 100 cm^3. The samples were dried in laboratory in an oven at 105°C for 48 hours. McIntyre and Loveday (1974) and Blake and Hartge (1986) give details of the procedures for samples manipulation in the laboratory and the calculations to determine ρ by the core method.

3.2.3.2 Particle size distribution

Disturbed soil samples of about 1 kg were collected at ≈ 40 cm far from the trunks. In the laboratory they were homogenised and a subsample of 20.00 g was taken to be analysed. The positions of sampling are described in Table 3.2. The conventional sieve-pipette sedimentation method was used (EMBRAPA, 1997). Dispersion was carried out using 1N NaOH and mechanical agitation. The scheme and criteria used for classifying particle size limits followed the Brazilian classification system (EMBRAPA, 1997). Additionally, water dispersible clay was measured by repeating the above described texture analysis, except that the chemical dispersion agent was excluded. With the additional measurement of the natural clay content, indices of flocculation (IF) were calculated by

$$IF = 100\,[(a - b) / a] \qquad [3.1]$$

Here, "a" is the percentage of clay determined in the conventional analyses and, "b" is the percentage of clay dispersed in water.

In addition, a profile of 1 m depth was sampled in steps of 10 cm intervals and analysed for characterising the soil physical properties in the soil subsurface.

3.2.3.3 Particle density (ρ_p)

The particle density was evaluated with the balloon method (EMBRAPA, 1997). This method consist basically to transfer a weighted oven-dried soil sample to the balloon and then determine the volume of alcohol needed to fulfil the balloon. Organic carbon was not removed before the analysis. The removal of organic carbon is suitable for particle size studies, but may not give the correct values for calculating porosity (Skopp, 2000).

3.2.3.4 Chemical parameters

The soil samples analysed to determine chemical parameters were subsamples of the samples collected to determine texture. The procedure of sample collection in the field has already been described above.

The soil pH was measured with a glass electrode at a soil solution ratio of 1:2.5 in distilled water. The cations calcium (Ca^{2+}), magnesium (Mg^{2+}) and aluminium (Al^{3+}) were extracted by N KCl and determined by atomic absorption spectrometry (EMBRAPA, 1997). Organic carbon (OC) was measured by the method of Walkley with modifications described in EMBRAPA (1997).

3.3 RESULTS AND DISCUSSION

3.3.1 Bulk density (ρ)

An exploratory analysis of the data is shown in Table 3.4. The complete bulk density data set and the analyses to verify the assumptions to perform statistical analyses are shown in Appendix 3 –A.

Table 3.4 Exploratory analysis of bulk density [Mg m^{-3}] data set evaluated on different land use system in a clayey Ferralsols in the central Amazon – Brazil.

Number	Common name	Mean	S. D 10^{-2}	Median	S. E 10^{-2}	Minimum	Maximum	Kurtosis	Skewness
1.00	Cupuaçu	0.93 ab	6.15	0.91	2.05	0.84	1.02	-0.94	0.30
2.00	Annatto	0.90 ab	7.40	0.92	2.47	0.74	0.99	2.47	-1.34
3.00	Brazil nut	0.96 ab	6.64	0.95	2.21	0.88	1.07	-0.91	0.61
4.00	Peach palm – F	0.88 ab	6.86	0.86	2.29	0.80	1.00	-0.23	0.79
5.00	Peach palm – P	0.88 ab	0.00	0.94	3.55	0.67	0.98	-0.01	-1.02
6.00	Pueraria	0.88 ab	3.58	0.87	1.19	0.84	0.94	-1.05	0.42
7.00	Cupuaçu	0.93 ab	5.87	0.97	1.96	0.84	0.99	-1.24	-0.71
8.00	Grasses and pueraria	1.00 a	2.54	1.00	8.47	0.97	1.05	0.63	0.52
9.00	Peach palm – F(m)	0.86 ab	8.99	0.86	3.00	0.70	0.98	-0.10	-0.51
10.00	Peach palm – F(mb)	0.98 ab	6.36	0.99	2.12	0.86	1.08	0.49	-0.55
11.00	Peach palm –P(m)	0.91 ab	9.92	0.90	3.31	0.79	1.07	-0.70	0.55
12.00	Peach palm –P(mb)	0.97 ab	4.62	1.00	1.54	0.88	1.03	0.35	-0.93
13.00	Vismia	0.90 ab	8.70	0.92	2.90	0.78	1.01	-1.63	-0.25
14.00	Matá-matá	0.87 ab	5.74	0.89	1.92	0.77	0.94	-0.58	-0.73
15.00	Bacaba	0.82 b	9.25	0.82	3.08	0.65	0.95	-0.13	-0.38
Total		0.91	8.50	0.92	7.32	0.65	1.08	0.12	-0.50

n = 9 samples ; SD = standard deviation; SE = standard error of the mean.

m = monoculture; b = between the palms; F = Peach palm for fruits production; P = Peach palm for palm heart production

Means followed by the same letters, within the column, do not differ by Tukey's test ($\alpha < 0.05$).

The statistical results show that the assumption of normality, homogeneity of variance, additivity and independence hold. Moreover, graphical analysis of residuals does not show trends to invalidate the assumed statistical model. Consequently, the analysis of variance was performed using the randomised block design (RBD) with subsampling (Table 3.5).

Table 3.5 shows differences between the ρ evaluated near the different plant species ($\alpha < 0.05$) and does not indicate an variation between the blocks. The computation of the subsample variance, with three samples per position, shows that the sampling error contributes with 0.003 to the error variance of 0.010. The subsampling procedure may increase the sensitivity of the experiment by increasing the precision (by enhancing the number of samples participating in the mean calculation) of the mean estimation. The analyse of variance for a RBD with subsampling, the sums of squares of blocks, treatments and the total are computed as for RBD without subsampling, except that they are also divided by the number of subsamples. Consequently, the analysis for testing the hypothesis concerning treatments using F values are identical (Snedecor and Cochran, 1997; Steel et al., 1997).

Table 3.5 Analysis of variance using complete randomised block design with subsampling for the bulk density data set.

Source	Sum-of-Squares	df	Mean-Square	F-ratio	P
Land use and plant	0.341	14	0.024	2.465	0.020
Block	0.028	2	0.014	1.394	0.265
Error	0.277	28	0.010		
Subsampling	0.328	90	0.003		
subsampling	[0.009]	[2]	0.004	1.290	0.283
vs. land use and plant	[0.120]	[28]	0.004	1.271	0.220
vs. block	[0.010]	[4]	0.003	0.758	0.557
Error of subsampling	[0.189]	[56]	0.003		
Total	0.697	134			

The analysis of subsampling (i.e., the analysis of components of variance) was computed as an indication of the adequacy of the sampling scheme adopted in this study. It seems to be appropriate, because, if the number of samples were doubled, the sampling error contribution would be halved. Therefore, the main source of the variance are not from a presumed inadequate number of samples, and the reduction of the variance with increasing sampling (in this example, as well in many other situations) may not be worthwhile.

The mean values of ρ observed in Table 3.4 lie in the small range of 0.82 – 1.01 Mg m^{-3}, with a mean of 0.91 Mg m^{-3}. This range is not typical, considering that this Ferralsol has a clay content at the surface of about 600 g kg^{-1} (Figure 3.2) and the organic carbon content is not very high (Table 3.16). The reasons for this is that the clay particles in these soils are flocculated in microaggregates (intra-aggregate) and a secondary pore system (inter-aggregates) was established as a result from an intense biological activity and fissures (Chauvel et al., 1991; Chauvel, 1992).

The only significant difference in Table 3.4 is between the ρ near bacabas in the primary forest and the position between the cupuaçus in monoculture covered by grasses and pueraria. The higher values of ρ found between the cupuaçus are due to inadequate growth of the cover crop in this land use system, resulting, presumably, in compaction of the soil structure owing to direct impact of the tropical rain drops on the soil, and the more intensive cycles of heating and drying.

In the monoculture of peach palm for fruit and palm heart, the sample positions between the plants tend to show higher ρ values than the values near the trunks (Table 3.4). This agrees with the field observation of ponded water, for short periods, after intense rainfalls in those positions. This more compact structure is also indicated by a reduced saturated and unsaturated hydraulic conductivity evaluated at those positions (see Chapter 6). The apparent contradictory results of small values of ρ near the palms associated with a reduced hydraulic conductivity may be partially explained by a very intense and intricate root system developed by peach palms (Haag, 1997), which seems to compact the soil by mechanical compression. The high number of roots (with a low density) per volume maintains the ρ values low.

The smallest value of ρ was found near the trunks of the bacabas in the primary forest. It is explained by the high root concentration in the soil surface in tropical forests, and the normally high amounts of organic carbon, which contribute to reduce the value of the ρ. These facts may also explain the lower values of the ρ evaluated near the matá-matá in the primary forest. Further, the soil covered by the primary forest was never submitted a compaction processes as the other agricultural plots.

The results and discussion of comparison within and between the whole land use systems is divided in the three land use systems evaluated and presented below.

3.3.1.1 Agroforestry system

Although, within the agroforestry system the bulk density (ρ) near the peach palms and under the pueraria tends to show lower values of ρ no significant difference between the six plants growing within the agroforestry system were found (Table 3.4). The lower values of ρ near the palms were discussed above, and the effect of pueraria to recuperate the porosity of the soil and to maintain the soil structure quality in a good level confirms the results found in early experiments carried out in the Ferralsols in Manaus by Chauvel et al. (1991) and Teixeira et al. (1997).

Adapted plants for the central Amazon conditions (as cupuaçu, annatto, Brazil nut and peach palm) can grow very rapidly, hence this system is temporally very dynamic, and soil properties may change very quickly as a consequence of specific plant characteristics, (i.e., the superficial root development of peach palms) or management decisions as the pruning of annattos and peach palms. Examples of agroforestry studies in which management practices and different plant species caused significant alterations in ρ are shown in Table 3.1. Moreover, in Chapter 5 differences between plant species with respect to their effect on ρ are discussed, using another data set.

Practical hypotheses and its statistical formulation concerning the agroforestry system as a whole system are shown in Equations 3.2, 3.3 and 3.4. The results of the analyses of variance of the hypothesised contrasts are shown in Table 3.6.

Is there a significant difference in ρ between on the agroforestry and the primary forest?

$$H_1: 0.04\,\mu_1 + 0.11\,\mu_2 + 0.18\,\mu_3 + 0.02\,\mu_4 + 0.03\,\mu_5 + 0.62\,\mu_6 - 0.50\,\mu_{14} - 0.50\,\mu_{15} = 0 \quad [3.2]$$

Is there a significant difference in ρ between on agroforestry and the secondary forest?

$$H_1: 0.04\,\mu_1 + 0.11\,\mu_2 + 0.18\,\mu_3 + 0.02\,\mu_4 + 0.03\,\mu_5 + 0.62\,\mu_6 - 1\,\mu_{13} = 0 \quad [3.3]$$

Is there a significant difference in ρ between on agroforestry and the monoculture of cupuaçu?

$$H_1: 0.04\,\mu_1 + 0.11\,\mu_2 + 0.18\,\mu_3 + 0.02\,\mu_4 + 0.03\,\mu_5 + 0.62\,\mu_6 - 0.07\,\mu_7 - 0.93\,\mu_8 = 0 \quad [3.4]$$

Here, μ_i are mean values of ρ (the subscript i indicates from which mean the value is from), and the coefficients are the estimated weight factors (Table 3.3) for each mean in relation to the whole system.

Table 3.6 shows a significant difference (α'[1] > 0.01) between the agroforestry system and the cupuaçu monoculture. The other agricultural land use systems do not show significant differences at $\alpha' > 0.05$ in relation to the agroforestry.

Table 3.6 Analysis of variance for the hypothesis concerning agroforestry system.

Source of Variation	Sum of squares	Degrees of freedom	Mean Square	F	P
Agroforestry vs. primary forest	0.0100	1	0.0100	3.0038	0.0923
Agroforestry vs. secondary forest	< 0.0000	1	< 0.0000	0.0021	0.9640
Agroforestry vs. cupuaçu	0.0245	1	0.0245	7.4278	0.0109
Agroforestry vs. peach palm	0.0109	1	0.0109	3.3184	0.0792
Error	0.0922	28	0.0033		

The adjusted level (α') for $\alpha = 0.05$ is 0.0127 and for $\alpha = 0.01$ is 0.002. $F\,\alpha'\,[0.01;1,28] = 7.03$. $F\,\alpha'\,[0.002;1,28] = 10.56$. See Appendix 3-A for details.

[1] Adjusted level of significance for non-orthogonal contrasts. See Appendix 3-A.

It should be emphasised that the agroforestry system had been installed in the field only 3 to 4 years before. Thus, it did not yet represent a stabilised land use system. Specifically, plants like Brazil nut and cupuaçu were still small compared with their possible size in the mature age. Therefore, much free space existed between the plants. At the time of evaluation, the space between the trees was covered by pueraria, which in this system was growing well, and this is one reason for the relative good performance of the agroforestry system analysed as a whole system.

Simulations of two hypothetical scenarios were calculated and statistically compared. In the first simulation, the remaining areas between the trees in the agroforestry system, instead of being covered by pueraria, were covered by grasses (the mean and variance of the ρ for grasses, in this simulation were those found in the positions between the cupuaçu in monoculture), whereas the other means and the weight factors remained the same.

An opposite hypothetical situation, where a better structure was conceptualised, was the second scenario. In this theoretical land use system, the soil of the monoculture of cupuaçu was covered by pueraria instead of being covered by grass (here the values of ρ for pueraria were those evaluated in the agroforestry system). The results in Table 3.7 show that for the first scenario the agroforestry system shows a significant difference from the primary forest caused by the reduced values of ρ when the soil is not well covered. In the second scenario, an opposite effect was found with the improvement of the average soil structure in a hypothetical monoculture of cupuaçu system well covered by pueraria. In this scenario, the monoculture of cupuaçu would not show significant difference from the primary forest.

Table 3.7 Analysis of variance for hypothesis concerning hypothetical land use systems.

Source of Variation	Sum of squares	Degrees of freedom	Mean Square	F	P
Agroforestry[+] vs. primary forest	0.0585	1	0.0585	17.7518	0.0002
Cupuçu[¶] vs. primary forest	1.8092×10^{-5}	1	1.8092×10^{-5}	0.0055	0.9414
Error	0.0922	28	0.0033		

[+]Calculated with same weights showed in the Equation 3.2.
[¶] Calculated with same weights showed in the Equation 3.6.

The bulk density seems to be an appropriate physical indicator for the quality of the soil structure, or a mosaic of different soil structures within an agroforestry system. With accumulation of information about the response of the plants growth to soil structure, more sophisticated parameters (e.g., pore size distribution or soil water retention curve) or indexes could be used. Plant growth, yields and leaching rates may be used as indicators of the efficiency of the ideal structure for the suitability of a land use system.

A simple and useful tool to compare different combinations of plants or temporal scenarios are statistical models that combine contrast analysis with weighted means that represent the different spots within a land use system. The creation of a soil data bases with information about tree and crop performances as response to management practices and to other soil chemical properties related with soil structure and with other physical, hydrological and chemical properties in different types of soils and climates, will enable us to perform this kind of analysis. This technique may be incorporated in land use planning as an additional tool to define a suitable combination of plants and management practices. Although results of simulations of future scenarios cannot be immediately compared with measurements in the field, they can be used for exploratory modelling.

3.3.1.2 Monoculture of cupuaçu

The plots with monoculture of cupuaçu, at that stage of growth, the soil was covered to ≈ 80% by grasses and pueraria, and ≈ 20% of the area near the trunks was under the influence of the cupuaçu roots and canopy.

The research hypotheses and their statistical formulation for the monoculture of cupuaçu are shown in the Equations 3.5, 3.6 and 3.7. The results of the analyses of variance of these hypotheses are shown in Table 3.8.

Is there a significant difference in ρ between the monoculture of cupuaçu and the primary forest?

$$H_1: 0.2\,\mu_7 + 0.8\,\mu_8 - 0.5\,\mu_{14} - 0.5\,\mu_{15} = 0 \qquad [3.5]$$

Is there a significant difference in ρ between the monoculture of cupuaçu and the secondary forest?

$$H_1: 0.2\,\mu_7 + 0.8\,\mu_8 - 1\mu_{13} = 0 \qquad [3.6]$$

Is there a significant difference in ρ between the monoculture of cupuaçu and the monoculture of peach palm?

$$H_1: 0.2\,\mu_7 + 0.8\,\mu_8 - 0.20\,\mu_{11} - 0.80\,\mu_{12} = 0 \qquad [3.7]$$

Table 3.8 Analysis of variance for hypothesis concerning the monoculture of cupuaçu.

Source of Variation	Sum of squares	Degree of freedom	Mean Square	F	P
Cupuaçu vs. primary forest	0.0324	1	0.0324	9.8264	0.0040
Cupuaçu vs. secondary forest	0.0066	1	0.0066	1.9892	0.1694
Cupuaçu vs. peach palm	< 0.0000	1	< 0.0000	0.0023	0.9618
Error	0.0922	28	0.0033		

The adjusted level (α') for α = 0.05 is 0.0169 and for α = 0.01 is 0.0033. F α' [0.01;1,28] = 6.44
F α' [0.002;1,28] = 10.24. See Appendix 3-A for details.

Table 3.8 shows only a significant difference ($\alpha' > 0.01$) between the monoculture of cupuaçu and the primary forest. This difference was caused by the relative high values of ρ between the cupuaçus where the soil was not well covered by pueraria. Therefore, this result cannot be generalised for a monoculture of cupuaçu with the soil well covered.

An important aspect in the analysis of the monoculture of cupuaçu as an option of a suitable land use system for the clayey Ferralsols is related to the spacing between the plants (7 x 6.4 m, see Figure 3.1). Although this spacing is appropriate when the plants are mature, three years after the beginning of the experiment, much free space was still available. Thus, if it is decided not to use a cover crop between the plants, at least other cash crop as cassava, peanut, maize or papaya must be planted, not only for economical reasons but also to protect the soil.

3.3.1.3 Monoculture of peach palm

Table 3.9 shows no significant differences between the two monocultures of peach palms or between the positions within a monoculture plots. Until the period of this evaluation, no significant difference in palm heart yield per plant between cropping systems was found (Schroth et al., 2000), and their productivity were in a satisfactory level. On the other hand, fruit yields were very poor because of a non productive fruit variety that is better suited for palm heart production (Schroth et al., 2000). For this reason, the discussion will be focused on peach palm suited for production of palm heart.

The following hypotheses were concerned for the monoculture of peach palm and the statistical formulation is shown in Equations 3.8 and 3.9. The results of the analysis of variance of the contrasts are shown in Table 3.9.

Is there a significant difference in ρ between the monoculture of peach palm and primary forest?

$$H_1:\quad 0.20\,\mu_{11} + 0.80\,\mu_{12} - 0.5\,\mu_{14} - 0.5\,\mu_{15} = 0 \qquad [3.8]$$

Is there a significant difference in ρ between the monoculture of peach palm and secondary forest?

$$H_1:\quad 0.20\,\mu_{11} + 0.80\,\mu_{12} - 1\,\mu_{13} = 0 \qquad [3.9]$$

Table 3.9 shows a significant difference ($\alpha' > 0.05$) in ρ between the monoculture of peach palm and the primary forest. It is due to the reduction of ρ by the high number of roots in the cylinders. In a cylinder of 100 cm^3 used to evaluate ρ, the mass of fresh root of peach palms can reach values of ≈ 10 g. For comparison, the mass of fresh roots evaluated in the samples under grasses was twenty times lower.

Table 3.9 Analysis of variance for hypothesis concerning monoculture of peach palm, and primary forest and secondary forest.

Source of Variation	Sum of squares	Degrees of freedom	Mean Square	F	P
Peach palm vs. primary forest	0.0362	1	0.0362	11.0032	0.0025
Peach palm vs. secondary forest	0.0068	1	0.0068	2.0734	0.1610
Primary forest vs. secondary forest	0.0066	1	0.0066	2.0113	0.1672
Error	0.0922	28	0.0033		

The adjusted level (α') for $\alpha = 0.05$ is 0.0169 and for $\alpha = 0.01$ is 0.0033. $F\ \alpha'\ [0.01;1,28] = 6.44$ $F\ \alpha'\ [0.002;1,28] = 10.24$. See Appendix 3-A for details.

Among the land use systems analysed, the monoculture of peach palm was the only one that can be considered mature in its development. Nowadays, the production of palm heart offers a promising land use alternative for the central Amazon because of their good development and the potential to produce economical harvesting of palm hearts during the whole year (SHIFT 1997, 1998; Yuyama, 1997). However, the apparent soil compaction caused by the intense root systems near the soil surface indicates that the soil structure should be cautiously monitored because of the sensitivity of peach palm to soil compaction or poor drainage as reported by Bovi et al. (1998). Further, peach palms show extremely high values of stemflow (Schroth et al., 1999b), which increases the risks of leaching near the trunks or an accumulation of water in micro depressions in the soil surface, hence causing aeration deficiency. This problem may be more expressive in soils of lower permeability than the Ferralsols of the central Amazon.

3.3.1.4 Primary and secondary forest

In Table 3.9 the statistical result of the contrast of primary forest against the secondary forest is also shown. The mathematical hypothesis is presented in Equation 3.10.

$$H_1:\ 0.5\,\mu_{14} + 0.5\,\mu_{15} - 1\,\mu_{13} = 0 \qquad [3.10]$$

The ρ does not show a significant difference ($\alpha' > 0.83$) between the primary and secondary forest, indicating the capacity of the natural regrowth to recuperate or maintain the soil structure near the values found in the soil under primary forest. This trend that the soil returns to the original conditions under secondary forest is confirmed by the pore size distribution, which also shows similar results between the primary and secondary forest (see Chapter 4). This confirms the efficiency of the traditional shifting cultivation cycle to maintain favourable soil physical conditions if low population densities allow sufficient fallow lengths.

3.3.2 Particle size distribution

The particle size distribution show a predominance of clay particles near the soil surface (Figure 3.2) and an increase of clay content with depth (Table 3.10).

The complete data set of particle size distribution and the analyses to verify the assumptions to perform statistical analyses are shown in the Appendix 3-A.

The variations in sand, silt and clay contents are shown in Figure 3.2, the variance of the results are similar to the results found by Corrêa and Reichardt, 1989 in a similar Ferralsol. Non significant differences between positions for the different mineral particle sizes evaluated was found by F test at $p < 0.05$ (Table 3.11).

Table 3.10 Particle size distribution, index of flocculation, particle density and bulk density evaluated at each 10 cm until 1 m of depth in a profile on an clayey Ferralsol in Manaus – Brazil.

Depth	Coarse sand 2.00 – 0.2 mm	Fine Sand 0.2 – 0.05 mm	Silt 0.05 – 0.02 mm	Clay < 0.002 mm	Index Flocculation	Particle density	Bulk density⁺
cm			$g\ kg^{-1}$		%	$Mg\ m^{-3}$	
2.5-7.5	193.71	54.76	129.03	622.5	71.89	2.56	1.02
12.5-17.5	177.94	47.66	107.40	667.0	87.26	2.60	1.06
22.5-27.5	127.44	40.11	107.95	724.5	88.27	2.50	1.03
32.5-37.5	102.02	34.08	129.40	734.5	76.17	2.50	1.01
42.5-47.5	92.86	26.86	109.28	771.0	92.22	2.60	1.00
52.5-57.5	89.11	29.75	111.64	769.5	98.05	2.60	0.97
62.5-67.5	89.77	54.47	99.76	756.0	98.68	2.60	0.98
72.5-77.5	88.25	29.23	113.52	769.0	96.10	2.50	0.97
82.5-85.5	93.49	29.02	115.49	762.0	93.44	2.60	0.98
92.5-95.5	90.59	27.65	173.26	708.5	93.23	2.60	1.00

⁺ For each depth the value is a mean of 5 samples.

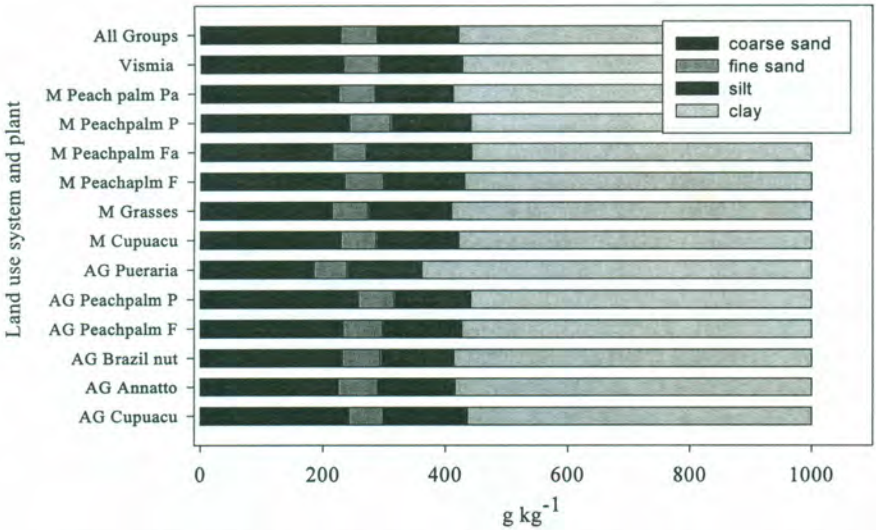

Figure 3.2 Stacked bar of the particle size distribution evaluated at different positions in an agroforestry system, monoculture of cupuacu, and peach palm and a secondary forest on a clayey Ferralsol in Manaus - Brazil.
[M is monoculture, AG is agroforestry system, F is fruit, P is palm heart and the letter [a] means evaluated between palms]

Table 3.11 Analysis of variance of particle size distribution evaluated in different land use system on a clayey Ferralsols in Manaus – Brazil.

Source	Sum-of-Squares	df	Mean-Square	F-ratio	P
		Coarse sand			
Land use and plants	10785.4026	12	898.7835	1.0000	0.4776
Block	10408.3221	2	5204.1610	5.7904	0.0089
Error	21570.2713	24	898.7613		
		Fine sand			
Land use and plants	602.3508	12	50.1959	0.8239	0.6261
Block	238.3774	2	119.1887	1.9564	0.1633
Error	1462.1692	24	60.9237		
		Silt			
Land use and plants	5885.2323	12	490.4360	0.7862	0.6596
Block	7336.7774	2	3668.3887	5.8808	0.0083
Error	14970.8692	24	623.7862		
		Clay			
Land use and plants	16670.5000	12	1389.2083	0.8966	0.5626
Blocks	16453.2821	2	8226.6410	5.3097	0.0123
Error	37184.3846	24	1549.3494		
		Index of flocculation			
Land use and plant	217.6680	12	18.1390	0.4378	0.9311
Block	1144.5102	2	572.2551	13.8132	0.0001
Error	994.2729	24	41.4280		

3.3.3 Index of flocculation (IF)

In Table 3.12, the high flocculation indexes indicate that most clay particles in field conditions are flocculated. As a consequence of this flocculation and the structured aggregates present in the Ferralsols, these soils behave like sand in terms of water infiltration near saturated conditions (see Chapter 6) but behave like clay soils at higher tensions with respect to infiltration rates and water holding capacity (see Chapter 4). Sharma and Uehara (1968) and Sanchez (1976) reported similar phenomenon for other tropical Ferralsols. This unusual behaviour of the clayey Ferralsols, combining the properties of sand and clay, in combination with a bimodal pore size distribution (see chapter 4) lead to the failure of many pedotransfer function which use texture or ρ values as input parameter to determine hydraulic properties for Ferralsols (Tomasella and Hodnett, 1997).

Table 3.12 Exploratory analysis indexes of flocculation [%] data set evaluated on different land use system in a clayey Ferralsol in the Central Amazon – Brazil.

Land Use System	Specie	mean	SE of mean	Median	Maximum	Minimum
Agroforestry	Cupuaçu	73.60	2.49	72.60	69.87	78.33
Agroforestry	Annatto	74.97	7.35	76.23	61.66	87.01
Agroforestry	Brazil nut	75.41	4.85	78.37	65.93	81.93
Agroforestry	Peach palm – F	75.72	2.69	74.96	71.50	80.71
Agroforestry	Peach palm – P	69.80	7.39	75.33	55.17	78.90
Agroforestry	Pueraria	75.46	4.71	79.82	66.04	80.52
Monoculture	Cupuaçu	72.13	4.02	72.49	64.99	78.91
Monoculture	Grasses and pueraria	70.11	5.96	64.64	63.68	82.01
Monoculture	Peach palm – F(m)	73.11	8.22	76.07	57.63	85.63
Monoculture	Peach palm – F(mb)	74.68	1.68	75.65	71.41	76.97
Monoculture	Peach palm –P(m)	73.98	1.65	74.68	70.84	76.41
Monoculture	Peach palm –P(mb)	68.32	4.10	70.39	60.41	74.16
Fallow	Vismia	75.23	6.87	80.12	61.66	83.91
Average		73.27	1.26	74.96	55.17	87.01

m = monoculture; b = between the palms; F = Peach palm for fruits production; P = Peach palm for palm heart production.
Means followed by the same letters within the column, do not differ by Tukey's test ($\alpha < 0.05$).

Table 3.11 does not show significant differences for IF between treatments, however, a highly significant difference between the blocks is shown. In blocks C and B the effect of liming and previous fertilisation promoted clay particle deflocculation near the soil surface (Figure 3.3). A similar effect on clay particle deflocculation by liming was reported by Roth and Pavan (1991). Deflocculation after liming is explained by substitution of Al^{3+} by Ca^{2+} and Mg^{2+} on the exchange complex. The ions of Al^{3+} had a greater flocculation power in the original soil conditions, because they are tightly absorbed and compress the electrical double layer. The higher the valence, the smaller the hydration radius and greater the flocculation power (Jury et al., 1991).

The percentage of dispersed clay is higher in the top horizons than in deeper ones (Table 3.10 and 3.12). Bravard and Righi, (1991) and Leite and Medina, (1984) found similar results in Ferralsols near Manaus. Goomber and D`Hoore (1971) suggested possible effects of organic compounds like the inactivation of polyvalent cations by soil organic matter to explain this fact.

The presence of H^+ or OH^- groups on the surface of the oxides and the broken faces of the kaolinite particles induce charges in Ferralsols to be dependent on pH, as identified in other highly weathered Ferralsols of the humid tropics by van Raij and Peech (1972) and Uehara and Gillman (1981). The point of zero charge (PCZ) is defined as the pH at which the net surface charge from all sources is zero (Sposito, 1989) and its knowledge is a very important property of soils with variable charge with respect to their management for agricultural purposes. Ferralsols normally have a PCZ between pH 3 - 4 (Raij and Peech 1972; Botschek et al., 1996; Silva et al., 1996). Moreover, Morais et al., (1976) found for a clayey Ferralsols near Manaus a PCZ of 3.2, and Silva (1997) a PCZ of 3.5. These values are probably related to the PCZ of kaolinite, which is the dominant clay particle in the Ferralsols in the central Amazon (Irion, 1984; Rodrigues, 1998; Silva, 1997) which shows a PCZ ranging from < 3.5 to 4.6 (El-Swaify, 1980). These values of pH are similar to the values presented in Table 3.14 for the soil covered by primary forest.

In the original conditions, i.e., when the soil is covered by primary forest, the clay particles on clayey Ferralsols near Manaus are almost totally flocculated (Camargo and Rodrigues, 1979 and Teixeira, et al., 1997). This is a consequence of the low pH and its relations with the surface charge of the clay colloids.

Table 3.13 Soil chemical characteristics evaluated on different land use systems in a clayey Ferralsol - Brazil.

Land Use System	Specie	mean	SD	Median	Maximum	Minimum
			pH			
Agroforestry	Cupuaçu	4.50 c	0.66	4.40	5.2	3.9
Agroforestry	Annatto	3.97 abc	0.50	3.90	4.5	3.5
Agroforestry	Brazil nut	4.33 abc	0.32	4.20	4.7	4.1
Agroforestry	Peach palm – F	4.20 abc	0.35	4.00	4.6	4
Agroforestry	Peach palm – P	4.13 abc	0.40	3.90	4.6	3.9
Agroforestry	Pueraria	4.17 abc	0.70	4.10	4.9	3.5
Monoculture	Cupuaçu	4.40 bc	0.40	4.40	4.8	4.0
Monoculture	Grasses and pueraria	3.80 abc	0.26	3.90	4.0	3.5
Monoculture	Peach palm – F(m)	4.17 abc	0.32	4.30	4.4	3.8
Monoculture	Peach palm – F(mb)	4.27 abc	0.42	4.40	4.6	3.8
Monoculture	Peach palm –P(m)	4.07 abc	0.47	3.90	4.6	3.7
Monoculture	Peach palm –P(mb)	4.57 c	0.55	4.60	5.1	4.0
Fallow	Vismia	3.77 a	0.25	3.80	4.0	3.5
			$Ca^{2+§}$	[$cmol_c\ dm^{-3}$]		
Agroforestry	Cupuaçu	1.41 ab	0.92	1.04	2.45	0.73
Agroforestry	Annatto	0.46 a	0.45	0.24	0.98	0.17
Agroforestry	Brazil nut	2.26 ab	1.01	1.77	3.42	1.59
Agroforestry	Peach palm – F	1.49 ab	1.06	1.21	2.66	0.60
Agroforestry	Peach palm – P	0.97 ab	0.87	0.61	1.96	0.34
Agroforestry	Pueraria	1.44 ab	1.66	0.94	3.29	0.09
Monoculture	Cupuaçu	1.61 ab	1.11	2.10	2.39	0.34
Monoculture	Grasses and pueraria	0.50 ab	0.45	0.33	1.01	0.15
Monoculture	Peach palm – F(m)	0.90 ab	0.57	1.12	1.33	0.25
Monoculture	Peach palm – F(mb)	0.67 ab	0.39	0.82	0.97	0.23
Monoculture	Peach palm –P(m)	1.69 ab	1.39	1.42	3.20	0.45
Monoculture	Peach palm –P(mb)	1.51 ab	0.74	1.54	2.23	0.75
Fallow	Vismia	0.19 b	0.13	0.16	0.33	0.08
			$Mg^{2§}$	[$cmol_c\ dm^{-3}$]		
Agroforestry	Cupuaçu	1.10 a	1.14	0.72	2.38	0.19
Agroforestry	Annatto	0.33 a	0.26	0.23	0.63	0.14
Agroforestry	Brazil nut	0.84 a	0.72	0.83	1.57	0.13
Agroforestry	Peach palm – F	0.93 a	0.88	0.76	1.88	0.15
Agroforestry	Peach palm – P	0.55 a	0.64	0.20	1.28	0.16
Agroforestry	Pueraria	1.25 a	1.55	0.62	3.02	0.12
Monoculture	Cupuaçu	1.07 a	0.70	1.42	1.53	0.26
Monoculture	Grasses and pueraria	0.30 a	0.24	0.21	0.58	0.12
Monoculture	Peach palm – F(m)	0.68 a	0.44	0.87	1.00	0.18
Monoculture	Peach palm – F(mb)	0.41 a	0.19	0.50	0.53	0.19
Monoculture	Peach palm –P(m)	1.20 a	1.04	1.12	2.28	0.21
Monoculture	Peach palm –P(mb)	1.07 a	0.69	1.30	1.61	0.29
Fallow	Vismia	0.18 a	0.04	0.19	0.21	0.14
			Al^{3+}	[$cmol_c\ dm^{-3}$]		
Agroforestry	Cupuaçu	0.99 abc	0.83	1.33	1.60	0.04
Agroforestry	Annatto	1.75 bc	0.84	1.96	2.47	0.83
Agroforestry	Brazil nut	0.68 ab	0.39	0.83	0.97	0.24
Agroforestry	Peach palm – F	0.73 ab	0.47	0.48	1.28	0.44
Agroforestry	Peach palm – P	1.06 abc	0.76	1.23	1.73	0.23
Agroforestry	Pueraria	1.17 abc	1.02	1.48	2.00	0.04
Monoculture	Cupuaçu	0.53 a	0.60	0.28	1.22	0.10
Monoculture	Grasses and pueraria	1.63 abc	0.04	1.63	1.67	1.60
Monoculture	Peach palm – F(m)	0.95 abc	0.65	0.88	1.63	0.33
Monoculture	Peach palm – F(mb)	1.36 abc	0.41	1.43	1.72	0.92
Monoculture	Peach palm –P(m)	0.74 ab	0.70	0.54	1.51	0.16
Monoculture	Peach palm –P(mb)	0.68 ab	0.64	0.33	1.42	0.30
Fallow	Vismia	1.95 c	0.33	1.99	2.26	1.60

m = monoculture; b = between the palms; F = Peach palm for fruits production; P = Peach palm for palm heart production.[§] - Original means (statistical analysis was carried out with transformed data), see Appendix A-3 for details. Means followed by the same letters within the column, do not differ by Tukey's test ($\alpha < 0.05$).

Table 3.14 Physical and chemical characteristics (mean ± standard error) of the soil covered by primary forest on a clayey Ferralsol in the central Amazon – Brazil.

Scient. name	Specie	Coarse sand 2.00 – 0.2 mm	Fine Sand 0.2 – 0.05 mm	Silt 0.05 – 0.02 mm	Clay < 0.002 mm	Particle density	pH	Ca^{2+}	Mg^{2+}	Al^{3+}
		g kg^{-1}				Mg m^{-3}		cmol $_c$ dm^{-3}		
Matá-matá	*Escheweilera sp*	321.10 ± 14.03	76.19 ± 2.94	125.57 ± 3.76	477.13 ± 14.12	2.46 ± 0.01	3.86 ±0.13	0.05 ± 0.01	0.08 ± 0.02	1.61 ± 0.12
Bacaba	*Oenocarpus bacaba*	294.04 ± 13.72	71.80 ± 3.50	120.51 ± 6.83	513.62 ± 14.66	2.44 ± 0.03	3.79 ±0.09	0.04 ± 0.00	0.08 ± 0.01	1.85 ± 0.16
Average		307.57 ± 10.07	73.99 ± 2.28	123.04 ± 3.83	495.38 ± 10.82	2.45 ± 0.01	3.82 ±0.08	0.04 ±0.00	0.08 ±0.01	1.73 ± 0.10

Mean of 9 samples for each species.

Further investigations are necessary to evaluate the effect of changing chemical properties on the soil surface of clayey Ferralsols on the flocculation of clay particles. Preserving the good structure quality of the clayey Ferralsols may be an essential factor in the sustainability of a land use system.

3.3.4 Chemical parameters

The complete soil chemical data set are shown in Appendix A-3. The residual analyses showed that, contrary to the assumptions, the variance is correlated with means for Ca^{2+} and Mg^{2+}. Box et al. (1978) show in details how to calculate variance stabilising transformations for this situation, the appropriate transformation is related to the kind of relation between variance and means. The power for a transformation to stabilise variances across groups was calculated using the lambda (λ) values of Box-Cox. The λ values were estimated using the Program Minitab 12.2 (Minitab Inc.; State Colege) and were 0.225 for Ca^{2+} and – 0.337 for Mg^{2+}.

The experiment was limed in November/December 1996 with 2.1 Mg ha^{-1} of dolomitic lime, which was broadcast in the plots. Soil sampling was conducted on block A before the application of lime, whereas blocks B and C were sampled in January 1997. Table 3.13 shows higher values of Ca^{2+}, Mg^{2+} and pH and reduced levels of Al^{3+} for block C. It was probably caused by a more intense use of lime and fertiliser in the previous rubber tree experiments (see history of the site in the chapter 2). The reduced levels may present near bacabas and matá-matás in the primary forest (Table 3.14) represent the original levels of these parameters.

In the secondary forest the plots were not limed or fertilised during the present experiment, the levels of Ca^{2+} and Mg^{2+} where not so high (Table 3.13), but confirms an anterior different use of the site197 because of the higher levels of the blocks B and C in relation to the original conditions of the soil covered by the primary forest. This fact is reflected in a highly significant effect of blocks for the chemical parameters (Table 3.15 and Figure 3.3). Variability between blocks clearly does not affect differences between treatment means, since each treatment appears the same number of times in every block. Nevertheless, significant treatment effects were found for pH, Al^{3+} and Ca^{2+}.

Table 3.15 Analysis of variance of soil chemistry properties determined in different land use system on a clayey Ferralsol in Manaus – Brazil.

Source	Sum-of-Squares	df	Mean-Square	F-ratio	P
		pH			
Land use and plants	2.1236	12	0.1770	4.1102	0.0016
Block	4.2867	2	2.1433	49.7806	0.0000
Error	1.0333	24	0.0431		
		Aluminium			
Land use and plants	7.4377	12	0.6198	3.8126	0.0026
Blocks	6.7849	2	3.3924	20.8680	0.0000
Error	3.9016	24	0.1626		
		Calcium §			
Land use and plant	12.8055	12	0.1230	2.5280	0.2600
Block	6.0502	2	0.4360	8.9890	0.0000
Error	16.1639	24	0.0048		
		Magnesium §			
Land use and plant	5.0471	12	0.9000	2.3670	0.0350
Block	7.3458	2	14.0840	37.053	0.0000
Error	8.2689	24	0.3800		
		Organic carbon			
Land use and plant	5.0471	12	0.3250	1.8150	0.1040
Block	7.3458	2	2.9400	2.9400	0.0720
Error	8.2689	24	0.1790		

§ - Analysis of variance performed with transformed data (power transformation). See appendix 3-A.

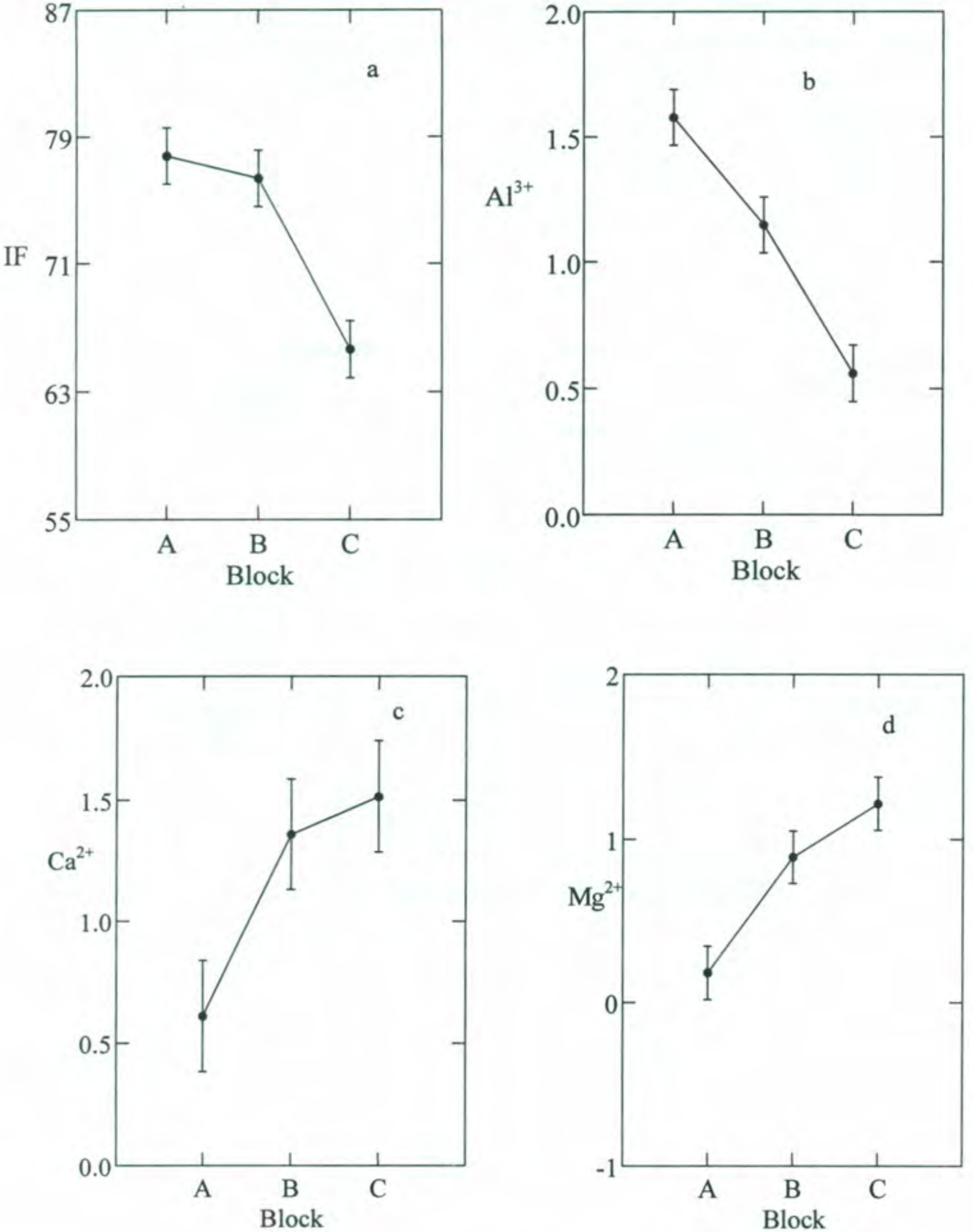

Figure 3.3 Graphical means of a) indexes of flocculation [%], b) concentration of aluminium [$cmol_c\ dm^{-3}$] c) concentration of calcium [$cmol_c\ dm^{-3}$] and d) concentration of magnesium [$cmol_c\ dm^{-3}$] evaluate in a clayey Ferralsol in the central Amazon.
Error bars represent the standard error of mean.

Table 3.16 Exploratory analysis of organic carbon [g kg^{-1}] data set evaluated on different land use system in a clayey Ferralsol in the central Amazon – Brazil.

Land Use System	Specie	mean	S. E of mean	Median	Minimum	Maximum
		g kg^{-1}				
Agroforestry	Cupuaçu	3.12 a	0.07	3.05	3.04	3.26
Agroforestry	Annatto	2.63 a	0.26	2.77	2.13	2.99
Agroforestry	Brazil nut	2.89 a	0.07	2.84	2.79	3.03
Agroforestry	Peach palm – F	2.42 a	0.04	2.39	2.36	2.50
Agroforestry	Peach palm – P	2.40 a	0.11	2.36	2.23	2.61
Agroforestry	Pueraria	2.78 a	0.34	2.77	2.19	3.37
Monoculture	Cupuaçu	2.41 a	0.02	2.40	2.39	2.44
Monoculture	Grasses and pueraria	2.48 a	0.25	2.54	2.01	2.88
Monoculture	Peach palm – F(m)	2.28 a	0.21	2.08	2.06	2.70
Monoculture	Peach palm – F(mb)	1.80 a	0.73	2.34	0.36	2.71
Monoculture	Peach palm –P(m)	2.68 a	0.09	2.73	2.51	2.80
Monoculture	Peach palm –P(mb)	2.86 a	0.15	2.80	2.65	3.14
Fallow	Vismia	2.57 a	0.13	2.54	2.36	2.80
Average		2.56	0.08	2.61	0.36	3.37

m = monoculture; b = between the palms; F = Peach palm for fruits production; P = Peach palm for palm heart production.

Means followed by the same letters, within the column, do not differ by Tukey's test ($\alpha < 0.05$).

The levels of Ca^{2+} show a significant difference between the extreme values of the data set (Table 3.13). The highest level was measured near the Brazil nut trees in the agroforestry system and the lowest level in the secondary forest. This can be explained with the fact that the secondary forest was not limed and fertilised in the present experiment, whereas the Brazil nut trees were limed and fertilised. With respect to pH and Al^{3+} levels, the clearest differences were between positions within the agricultural land use systems and the secondary forest, which shows lower levels of Ca^{2+} and pH, and higher Al^{3+} concentration. The differences between the positions on the agricultural plots are probably related to differences in the fertilisation levels used, which is specific for each species (SHIFT, 1996, 1997 and 1998). The reduced values of the flocculation indexes in the blocks B and C (Table 3.12) may be explained by increasing pH in blocks B and C (Table 3.13), which may have increased the net negative particle charge, resulting in particle repulsion and consequently the reduced flocculation index. An important implication of this fact is that certain management practices, which improve soil fertility, may be detrimental to soil structure (i.e., liming reduced intra-aggregate bonds by eliminating most positive charges). Fortunately, the origin of the inter-aggregate bonding is non-electrostatic in these Ferralsols, but are principally due to the activity of roots and earthworms (see, Chauvel, 1982). This fact tends to reduce the detrimental consequences of such changes in the functionality of the soil structure. Therefore, the most visible effects of the collapse of the soil structure, which are normally an expressive reduction of ρ, could not be observed yet. Further discussion about the pore-size distribution and saturated and unsaturated hydraulic conductivity evaluated in these land use systems can be found in Chapters 4 and 6.

Conversely, a increase in pH and higher concentration of mineral nutrients in the soil may result in more intense biological activity and the formation of polysaccharides, which promote aggregation (Tisdall and Oades, 1982). As a probable consequence, the opposite effect would be observed some time later, showing that the deflocculation of clay in the Ferralsols following liming was a temporary phenomenon. Further investigations are necessary to confirm or refute the hypothesis of a better aggregation on a long term basis from the increase of pH and reduction of Al^{3+}. The organic carbon values (Table 3.16) do not show significant differences between the positions evaluated (Table 3.17).

Doubtless, the maintenance of adequate levels of organic matter in the soil is an essential factor to maintain adequate chemical and physical properties of tropical soils for plant production (Zech et al., 1997; Tisdall and Oades; 1982). However, Lehmann et al., (2001) did not found positive relations between organic carbon and aggregate stability in this experiment. The driving force of aggregation in the clayey Ferralsols are probably more related to the dynamic of the aggregate-stabilising iron oxides (Sombroek, 1984; Oades and Waters, 1991).

A sustainable land use system for the clay Ferralsols must be designed for a reposition of organic matter from decomposing litterfall and dead roots and a positive net balance may be a fundamental factor to assure the quality of the soil structure.

Table 3.17 Analysis of variance of organic carbon content evaluated in different land use systems on a clayey Ferralsol in Manaus – Brazil.

Source	Sum-of-Squares	df	Mean-Square	F-ratio	P
Land use and plant	3.9041	12	0.3253	1.8145	0.1035
Block	1.0544	2	0.5272	2.9404	0.0721
Error	4.3031	24	0.1793		

3.3. 5 Particle density (ρ_p)

The results of ρ_p density are homogenous and reflected the predominance of kaolinite in the composition of the particles these Ferralsols (Table 3.10 and 3.18). The mean value for ρ_p of 2.52 Mg m^{-3} was used to estimate the total porosities in the soil surface (Table 3.18), which are discussed in the Chapter 4. In the subsurface layers the mean values were about 2.60 Mg m^{-3} (Table 3.10). The increase on the ρ_p values with depth is principally related to a reduction of organic carbon.

Table 3.18 Exploratory analysis of particle density [Mg kg^{-3}] data set evaluated on different land use system in a clayey Ferralsols in the Central Amazon – Brazil.

Land Use System	Specie	mean	SE of mean	Median	Maximum	Minimum
Agroforestry	Cupuaçu	2.54	0.04	2.50	2.63	2.50
Agroforestry	Annatto	2.50	0.00	2.50	2.50	2.50
Agroforestry	Brazil nut	2.49	0.06	2.50	2.59	2.38
Agroforestry	Peach palm – F	2.54	0.04	2.50	2.63	2.50
Agroforestry	Peach palm – P	2.50	0.00	2.50	2.50	2.50
Agroforestry	Pueraria	2.60	0.05	2.63	2.66	2.50
Monoculture	Cupuaçu	2.50	0.00	2.50	2.50	2.50
Monoculture	Grasses and pueraria	2.50	0.00	2.50	2.50	2.50
Monoculture	Peach palm – F(m)	2.50	0.00	2.50	2.50	2.50
Monoculture	Peach palm – F(mb)	2.56	0.05	2.53	2.66	2.50
Monoculture	Peach palm –P(m)	2.52	0.02	2.50	2.56	2.50
Monoculture	Peach palm –P(mb)	2.54	0.04	2.50	2.63	2.50
Fallow	Vismia	2.50	0.00	2.50	2.50	2.50
Average		2.52	0.01	2.50	2.66	2.38

m = monoculture; b = between the palms; F = Peach palm for fruits production; P = Peach palm for palm heart production.
Mean of 3 samples.

3.4 CONCLUSIONS

The agricultural use of clayey Ferralsols changes its bulk density and the natural flocculation of the clay particles, and this may affect other properties related to the structure, such as hydraulic conductivity and therefore transport processes in the soil.

Bulk densities in the ranges of 0.67 to 1.08 Mg m^{-3} indicate a highly structured soil.

A significant increase in the value of ρ was identified in the plots of monoculture of cupuaçu because the poor growth of the cover crop left part of the soil uncovered or under grass cover.

The soil under secondary forest does not show a significant difference in the bulk density values in relation to the soil under primary forest.

The soil near the palms (peach palm and bacaba) present lower values of bulk density because of a well developed root system near the soil surface.

Alteration of chemical properties of the clayey Ferralsols in the central Amazon, whose charge depends on pH, leads to a dispersion of clay particles near the soil surface.

While laboratory measurements of particle-size distribution using the classical method with chemical dispersion agent provides unchanged results about clay content, index of flocculation indicate changes in the natural aggregation of the clay particles.

Monitoring of bulk density and the index of flocculation are useful and cheap indicators of soil structure quality of the clayey Ferralsols.

A conceptual approach of an optimum structure for a land use system was discussed, and a simple and straightforward statistical model is proposed as an exploratory tool for predicting impacts of alternative crop and soil management practices on the average soil structure.

3.5 REFERENCES

ALEGRE J C. and RAO M R. Soil and water conservation by contour hedging in the humid tropics of Peru. Agriculture, Ecosystem and Environment. 57: 17-25, 1996.

AREVALO L A.; ALEGRE J C.; BANDY D E. and SZOTT L T. The effect of cattle grazing on soil physical and chemical properties in a silvopastoral system in the peruvian Amazon. Agroforestry Systems. 40: 109-124, 1998.

ARCHER J R. and SMITH P D. The relation between bulk density, available water capacity, and air capacity of soils. Journal of Soil Science. 23: 475-480, 1972.

ARYA L M.; LEIJ F J.; VAN GENUCHTEN M TH. and SHOUSE P J. Scaling parameter to predict the soil water characteristic from particle-size distribution data. Soil Science Society of America Journal. 63: 510-519, 1999.

BLAKE G R. and HARTGE K H. Bulk density. In: KLUTE A., ed. Methods of soil analysis - Part 1 Physical and mineralogical methods. 2. Madison, American Society of Agronomy, 1986. p.363-376.

BOTSCHEK J.; FERRAZ J.; JAHNEL M. and SKOWRONEK A. Soil chemical properties of a toposequence under primary rain forest in the Itacoatiara vicinity (Amazonas, Brazil). Geoderma. 119-132, 1996.

BOUMA J.; DROOGERS P. and PETERS P. Defining the "Ideal" soil structure in surface soil of a typic Fluvaquent in the Netherlands. Soil Science Society of America Journal. 63: 343-348, 1999.

BOVI M L A.; VIERIA S R.; SPIERING S H.; MONTEIRO S M G. and GALLO P B. Relações entre crescimento de pupunheira e alguns parâmetros físicos do solo. In: Congresso brasileiro de ciência do solo, 25., 1998. Sociedade Brasileira de Ciência do Solo / EMBRAPA - SOLOS, Rio de Janeiro, 1998. p.1-4.

BOX G E P.; HUNTER W G. and HUNTER J S. Statistics for experimenters. 1.ed. New York, John Wiley & Sons, 1978. 653p.

BRAVARD S. and RIGHI D. Characterization of fulvic and humic acids from an Oxisol-Spodosol toposequence of Amazonia, Brazil. Geoderma. 48: 151-162, 1991.

CABRAL O M R. Climatological observation recorded during the period 1993 to 1995 at Shift project site in Manaus, central Amazonia. SHIFT ENV 23- ANNUAL REPORT 1996, 34-46. 1996. Embrapa - CPAA. Manaus.

CAMARGO M N and RODRIGUES T E. Guia de excursão. In: congresso brasileiro de ciência do solo, 17., 1979. Sociedade Brasileira de Ciência do Solo / Embrapa, Rio de Janeiro, 1979. p.1-72.

CARTER M R. and BALL B C. Soil porosity. In: CARTER M R, ed. Soil sampling and methods of analysis. Boca Raton, Lewis publishers, 1993. p.581-588.

CASSEL D K. Tillage effects on soil bulk density and mechanical impedance. In: KRAL D M, ed. Predicting tillage effects on soil physical properties and processes. Madison, Soil Science Society of America, 1982. p.45-67.

CASTRO C. and LOGAN T J. Soil aggregation mechanisms affected by liming. In: World Congress of Soil Science.16, 1998. International Soil Science Society, Montpelier, 1998. p.1-8.

CASTRO C. and LOGAN T J. Liming effects on the stability and erodibility of some Brazilian Oxisols. Soil Science Society of America Journal. 55: 1407-1413, 1991

CHAUVEL A. Os latossolos amarelos, álicos, argilosos dentro dos ecossistemas das bacias experimentais do INPA e da região vizinha. Acta Amazonica. 12: 47-60, 1982.

CHAUVEL A.; GRIMALDI M. and TESSIER D. Changes in soil pore-space distribution following deforestation and revegetation: An example from the central Amazon basin, Brazil. Forest Ecology and Management. 38: 259-271, 1991.

CORRÊA J C. and REICHARDT K. The spatial variability of Amazonian soils under natural forest and pasture. GeoJournal. 19: 423-427, 1989.

DALLAND A.; VÅJE P I.; MATTHEWS R B. and SINGH B R. The potential of alley cropping in improvement of cultivation systems in the high rainfall areas of Zambia. III. Effects on soil chemical and physical properties. Agroforestry Systems. 21: 117-132, 1993.

EL-SWAIFY S A. Physical and mechanical properties of Oxisols. In: THENG B K G, ed. Soils with variable charge. Lower Hutt, New Zealand Society of Soil Science, 1980. p.303-324.

EMBRAPA. Manual de métodos de análise de solo. 2.ed. Rio de Janeiro, Centro nacional de pesquisa de solos, 1997. 212p.

GOOMBER R. and D'HOORE J. Induced migration of clay and other moderately mobile soil constituentes. Pedólogie. 30: 311-342, 1971.

HAAG D. Root distributions patterns in a polycultural system with local tree crops on an acid upland soil in central Amazonia, University of Bayreuth, 1997. 87p. (Diplomarbeit)

HILLEL D. Environmental soil physics. San Diego, Academic press, 1998. 771p.

HULUGALLE N R. and NDI J N. Effects of no-tillage and alley cropping on soil properties and crop yields in a typic Kandiudult of southern Cameroon. Agroforestry Systems. 22: 207-220, 1993.

HUXLEY P A.; PINNEY A.; AKUNDA E. and MURAYA P. A tree/crop interface orientation experiment with a *Grevillea robusta* hedgerow and maize. Agroforestry Systems. 26: 23-45, 1994.

IRION G. Clay minerals of Amazonian soils. In: SIOLI H, ed. The Amazon: Limnology and landscape ecology of a mighty tropical river and its basin. Dordrecht, Dr W. Junk Publishers, 1984. p.537-579.

JAMA B A.; NAIR P.K R. and RAO M R. Productivity of hedgerow shrubs and maize under alleycropping and block planting systems in semiarid Kenya. Agroforestry Systems. 31: 257-274, 1995.

JUO A S R.; FRANZLUEBBERS K.; DAIBIRI A. and IKHILE B. Soil properties and crop performance on a kaolinitic Alfisol after 15 years of fallow and continuous cultivation. Plant and Soil. 180: 209-217, 1996.

JURY W A.; GARDNER W R. and GARDNER W H. Soil physics. 5.ed. New York, John Wiley & Sons, 1991. 328p.

KANG B T. Alley cropping - soil productivity and nutrient cycling. Forest Ecology and Management. 91: 75-82, 1997.

KUZNETSOVA I V. Optimum bulk density. Eurasian Soil Science. 6: 74, 1991.

LAL R. Modifications of soil fertility characteristics by management of soil physical properties. In: LAL R. and GREENLAND D J, eds. Soil physical properties and crop production in the tropics. New York, John Willey and Sons, 1979. p.397-406.

LAL R.; WILSON G F. and OKIGBO B N. Changes in properties of an Alfisol produced by various cover crops. Soil Science. 127: 377-382, 1979.

LAL R. Agroforestry systems and soil surface management of a tropical Alfisol: IV. Effects on soil physical and mechanical properties. Agroforestry Systems. 8: 197-215, 1989.

LEHMANN J.; CRAVO M DA S. and ZECH W. Organic matter stabilization in a Xanthic Ferralsol of the central Amazon as affected by single trees: chemical characterization of density, aggregate, and particle size fractions. Geoderma. 99: 147-168, 2001.

LEITE J A. and MEDINA B F. Efeitos dos sistemas de manejo sobre as propriedades físicas de um latossolo amarelo do Amazonas. Pesquisa Agropecuária brasileira. 19: 1417-1422, 1984.

MAPA R B. and GUNASENA H P M. Effect of alley cropping on soil aggregate stability of a tropical Alfisol. Agroforestry Systems. 32: 237-245, 1995.

MCINTYRE D S. and LOVEDAY J. Bulk density. In: LOVEDAY J., ed. Methods of analysis of irrigated soils. Buchs, Commonwealth bureau of soils, 1974. p.38-42.

MEDINA B F. Influência de dois métodos de preparo de área na compactação de um latossolo amarelo. Revista Brasileira de Ciência do Solo. 9: 67-71, 1985.

MEDVEDEV V V. Variability of the optimal soil density and its causes. Eurasian Soil Science. 5: 65-75, 1991.

MORAIS I F.; PAGE A L. and LUND L J. The effect of pH, salt concentration, and nature of electrolytes on the charge characteristics of Brazilian tropical soils. Soil Science Society of America Journal. 40: 521-527, 1976.

OADES J M. and WATERS A G. Aggregate hierarchy in soils. Australian Journal of Soil Science. 29: 815-828, 1991.

RAIJ B. and PEECH M. Electrochemical properties of some Oxisols and Alfisols of the tropics. Soil Science Society American Proceedings. 36: 587-593, 1972.

RAO M R.; NAIR P K R. and ONG C K. Biophysical interactions in tropical agroforestry systems. Agroforestry Systems. 38: 3-50, 1998.

RODRIGUES M R L. Disponibilidade de micronutrientes em solos da Amazônia, University of São Paulo, 1998. 156p. (Doctor)

ROTH C H. and PAVAN M A. Effects of lime and gypsum on clay dispersion and infiltration in samples of a Brazilian Oxisol. Geoderma. 48: 351-361, 1991.

SANCHEZ P A. Properties and management of soils in the tropics. New York, John Wiley & Sons, 1976. 618p.

SANCHEZ P A. Science in agroforestry. Agroforestry Systems. 30: 5-55, 1995.

SCHAAP M G.; LEIJ F J. and VAN GENUCHTEN M TH. A bootstrap-neural network approach to predict soil hydraulic parameters. In: VAN GENUCHTEN M TH.; LEIJ F J. and WU L (eds.). Workshop Characterization and Measurements of the Hydraulic Properties of Unsaturated Porous Media. University of California, Riverside, 1999. p.1237-1250.

SCHROTH G.; SILVA L F DA.; SEIXAS R.; TEIXEIRA W G.; MACÊDO J L V. and ZECH W. Subsoil accumulation of mineral nitrogen under polyculture and monoculture plantations, fallow and primary forest in a ferralitic Amazonian upland soil. Agriculture, Ecosystem and Environment. 75: 109-120, 1999a.

SCHROTH G.; SILVA L F DA.; WOLF M A.; TEIXEIRA W G. and ZECH W. Distribution of throughfall and stemflow in multi-strata agroforestry, perennial monoculture, fallow and primary forest in central Amazonia, Brazil. Hydrological processes. 13: 1423-1436. 1999 b

SCHROTH G.; TEIXEIRA W G.; SEIXAS R.; SILVA L F DA.; SCHALLER M.; MACÊDO J L V. and ZECH W. Effect of five tree crops and a cover crop in multi-strata agroforestry at two fertilization levels on soil fertility and soil solution chemistry in central Amazonia. Plant and Soil. 221: 143-156, 2000.

SHARMA M L. and UEHARA G. Influence of soil structure on water relations in low humic latossols: II. Water movement. Soil Science Society American Proceedings. 32: 770, 1968.

SHELDRICK B H. and WANG C. Particle size distribution. In: CARTER M R, ed. Soil sampling and methods of analysis. Boca Raton, Lewis publishers, 1993. p.499-511.

SHIFT ENV - 23. Recuperação de areas degradadas, através de sistemas de policultivo. Relatório Anual. Manaus - Hamburgo, Embrapa - CPAA and Universidade de Hamburgo, 1996. 69p.

SHIFT ENV - 23. Recuperação de areas degradadas, através de sistemas de policultivo. Relatório Anual. Manaus - Hamburgo, Embrapa - CPAA and Universidade de Hamburgo, 1997. 81p.

SHIFT ENV - 23. Recuperação de areas degradadas, através de sistemas de policultivo. Relatório Anual. Manaus - Hamburgo, Embrapa - CPAA and Universidade de Hamburgo, 1998. 80p.

SILVA M L N.; CURI N.; MARQUES J J G S M.; GUILHERME L. R: and LIMA J M. Ponto de efeito salino nulo e suas relaçoes com propriedades mineralógicas e químicas de latossolos brasileiros. Pesquisa agropecuaria brasileira. 31: 663-671. 1996.

SILVA M L N. Erosividade da chuva e proposição de modelos para estimar a erodibilidade de latossolos brasileiros, Lavras, University of Lavras - Brazil, 1997. 154p. (Doctor)

SKOPP J M. Physical properties of primary particles. In: SUMNER M E, ed. Handbook of soil science. Boca Raton, CRC Press, 2000. p.A-3-A-17.

SNEDECOR G W and COCHRAN W G. Statistical methods. 8.ed. Ames, Iowa Sate University Press, 1989. 593p.

SOMBROEK W. The soils of the Amazon region. In: SIOLI H, ed. The Amazon: Limnology and landscape ecology of a mighty tropical river and its basin. Dordrecht, Dr W. Junk Publishers, 1984. p.521-537.

SPOSITO G. The chemistry of soils. New York, Oxford University Press, 1989. 277p.

STELL R G.; TORRIE J H. and DICKEY D A. Principles and procedures of statistics a biometrical approach. 3.ed. New York, Mc-Grawn Hill, 1997. 666p.

TEIXEIRA W G.; PEREIRA E G.; CRUZ L A. and BUENO N. Influência do uso nas característica fisico quimicas de um latossolo amarelo, textura muito argilosa, Manaus - AM. In: Congresso latino americano de ciência do solo, 13., 1997. Sociedade Brasileira de Ciencia do Solo, Campinas, 1997. p.1-4.

TESSIER D.; HARTMANN C. and TAVARES FILHO J. Changes in pore-space and microstructure of 1/1 clay soils: examples from Brazil and Africa. In: World Congress of Soil Science.16, 1998. International Soil Science Society, Montpelier, 1998. p.1-4.

TISDALL O M. and OADES J M. Organic matter and water-stable aggregates in soils. Journal of Soil Science. 33: 141-163, 1982.

TOMASELLA J. and HODNETT M G. Estimating unsaturated hydraulic conductivity of Brazilian soils using soil-water retention data. Soil Science. 162: 703-712, 1997.

TOMASELLA J. and HODNETT M G. Estimating soil water retention characteristics from limited data in Brazilian Amazonia. Soil Science. 163: 190-202, 1998.

TORQUEBIAU E F. and KWESIGA F. Root development in a *Sesbania seban* fallow-maize system in eastern Zambia. Agroforestry Systems. 34: 193-211, 1996.

UEHARA G and GILLMAN G P. The mineralogy, chemistry, and physics of tropical soils with variable charge clays. Boulder, Westview Press, 1981. 170p.

VIDHANA ARACHCHI L P. and LIYANAGE M DE S. Soil physical conditions and root growth in coconut plantations interplaned with nitrogen fixing trees in Sri Lanka. Agroforestry Systems. 39: 305-318, 1998.

YAMOAH C F.; AGBOOLA A A.; WILSON G F. and MURAYA P. Soil properties as affected by the use of leguminous shrubs for alley cropping with maize. Agriculture, Ecosystem and Environment. 18: 167-177, 1986.

YUYAMA K. Sistemas de cultivo para produção de palmito para pupunheira. Horticultura Brasileira. 15: 191-198, 1997.

ZECH W.; SENESI N.; GUGGENBERGER G.; KAISER K.; LEHMANN J.; MIANO T M.; MILTNER A. and SCHROTH G. Factors controlling humification and mineralization of soil organic matter in the tropics. Geoderma. 79: 117-161, 1997.

Analysis of variance

The randomised block design (RBD) is one of the most widely used experimental design in agriculture experiments. It permits a systematical control of the natural soil variability through blocking the treatments. The simplest type is set up by assigning treatments at random to a previously determined set of experimental units called block.

The objective of the blocking technique is to lead that the units in a block be as uniform as possible so that observed differences will be largely due to treatments. Ideally, the variability among experimental units is controlled so that the variation among blocks is maximised while the variation with is minimised (Steel et al., 1997). Variability among blocks clearly does not affect differences among treatments means, since each treatment appears the same number of time in every block.

If treatment-block interaction is present, the test on treatment means is unaffected by the interactions. The explanation for this fact is that both the expected mean squares of the treatments and experimental error contains the interaction effect. Details about its mathematical theory is given by and Graybill, (1976), Searle et al., (1992) and Montgomery, (1997) whereas and its application in agriculture experiments by Little and Hills, (1978), Snedecor and Cochran, (1989) and Gomes (1990).

The statistical model for the RBD is:

$$y_{ij} = \mu + \tau_i + \beta_j + \varepsilon_{ij} \qquad i = 1,2,\ldots, I$$
$$j = 1,2, \ldots, J$$

y_{ij} = is the observation for the i^{th} treatment on j^{th} block

μ = is the overall mean

τ_i = is the effect of the i^{th} treatment

β_j = is the effect from the j^{th} block, normally distributed with mean zero and variance $\sigma\beta^2$

ε_{ij} = is the random error, independently and identically distributed (iid) in a normal distribution with mean zero and variance σ^2

The parameters for the analysis of variance can be estimated directly using the equations below.

Source of variation	degree of freedom	Sums of squares
Blocks	J-1	$I\sum_{j}(\bar{y}_{.j}-\bar{y}_{..})^2$
Treatments	I-1	$J\sum_{i}(\bar{y}_{i.}-\bar{y}_{..})^2$
Experimental Error	(I-1)(J-1)	$\sum_{i,j}(y_{ij}-\bar{y}_{.j}-\bar{y}_{i.}+\bar{y}_{..})^2$
Total	IJ-1	$\sum_{i,j}(y_{ij}-\bar{y}_{..})^2$

The randomised block design with subsamples (RBDS) has more than one observation (subsampling) per treatment per block, i.e., the RBDS has k = 1,...,s subsamples (Hays, 1981; Snedecor and Cochran; 1989). The subsampling procedure may increase the sensitivity of the experiment by increasing the precision with which properties of each treatment is estimated.

Therefore, its analysis of variance contains an additional line – from the subsampling error, which can be calculated as show above.

Sampling error	IJ(s-1)	$\sum_{i,j}\sum_{k}(y_{ijk}-\bar{y}_{ij.})^2$

The sums of squares of RBDS for blocks, treatments and the total are computed as for RBD without subsampling, except that they are also divided by the number of subsamples (s) (Snedecor and Cochran, 1979; Steel et al. 1997). The experimental error is the appropriate error for testing hypotheses concerning treatments and block in both models if the subsampling and blocks are assumed to be random factors (Steel et al., 1997). Consequently, the analysis for test of hypothesis concerning treatments using F values would be identical (Hays, 1981; Steel et al. 1997).

The advantage of using the RBDS is that it permits to identify the effect of the sampling design in the experimental error. At the present work, the RBDS was computed to verify the effect of sampling and the interactions among sampling and treatments or blocks.

Because the F values and multicomparison tests would have identical results when using the simpler RBD, we perform the mean comparison tests using the sums of squares from the RDB model for its simplicity, although some statistical packages do not support comparison tests with multivariate models.

Model adequacy checking

An estimation of the residual (ε_{ij}) in the RBD can be calculated using the relation below (Montgomery, 1997).

$$\hat{\varepsilon}_{ij} = y_{ij} - \hat{y}_{i.} - \hat{y}_{ij} - \hat{y}_{.j} - \hat{y}_{..}$$

Where $\hat{y}$ (s) are the estimated observations using the statistical model.

Statistical Assumptions

Whereas, the assumptions to compute parametric statistical models are described by some authors in terms of the dependent variables, others describe them in terms of residuals. Although stating the assumptions in terms of the residual is more correct, the two approaches are, for practical purposes, equivalent. This is because the dependent variable can be expressed as the sum of a true value plus a random error; therefore, if the dependent variable meets the assumptions then so do the residuals (Kufs, 1991).

The premises for the variance analysis of RDB are that, the residuals [ε_{ij}] be independent and identically normally distributed with mean zero, the variance of the residuals within the treatments must be homogeneous, and the sample data should be obtained by random sampling (i.e., the residuals must be independent). Moreover, the effects of the factors must be additive (Graybill, 1977; Searle et al., 1977; Lindman, 1992; Steel et al., 1997).

Normality

The standard statistical procedure in variance analysis is based on the assumption of normal (Gaussian) distribution of the residuals. The major reasons for the dominance of the normal distribution in statistical analyses is that the Central Limit Theorem tells us that even if the distribution of the original population is far from normal, as sample size increases the distribution of the sample mean tends to the normal (Box et al. 1978; Montgomery 1997). In fact, many qualities whose variability results from the additive contributions of many effects are approximately normally distributed (Snedecor and Cochran, 1989; Draper and Smith, 1998).

However, the "correct" assumption of the statistical model is that the residuals must be independent and identically distributed (iid) within the treatments with normal distribution. In practice, it is very difficult to find an experiment with RBD design that permits investigating the normality assumption for each treatment. This is owed to the low numbers of repetition within each treatment, sometimes just one. However, a general inspection using an omnibus test with the residuals together may be appropriate to check the normality assumption (Miller, 1986); this approach is also showed by Montgomery (1997).

Procedures for ascertaining the type of probability distribution function (pdf) involve Shapiro-Wilk's W test; the Kolmogorov-Smirnov test with Liliefors corrections; Levene's median test (Parkin and Robison, 1989; Steel et al., 1997; Draper and Smith, 1998) or graphical methods like the fractile diagrams or quantile-quantile plot (Chambers et al. 1983; Jury et al. 1993), among many other methods.

Overall, the F test and planned comparison are remarkably robust to deviations from normality (Hays, 1981; Lindman, 1992). Tests based on studentized range are also robust to deviation of normality since the size of the design is not too small and if the violation is not to severe (Miller, 1986).

Failure of the normal approximation mostly occurs when the population contains some extreme individuals that dominate the sample average, causing a nonzero skewness (Beckett and Webster, 1971). In general, only the kurtosis of the distribution is likely to have any appreciable effect on F statistic. If the kurtosis is greater than zero, then the F tends to be too small and we cannot reject the null hypothesis although it is incorrect. The opposite is the case when the kurtosis is less than zero. The skewness of the distribution usually does not have a sizeable effect on the F statistic. A detailed discussion of the robustness of the F statistic can be found in Lindman (1974).

To verify normality, the Shapiro-Wilks' W test was chosen, because of its good power compared to a wide range of alternative tests. If the W statistic is significant, the hypothesis of normal distribution should be rejected. Details about the W statistic can be found in Gibbons (1994) and Steel et al. (1997).

The graphical method, normal quantile-quantile plot (qq-plot) was also used. It consists of a plot of the ordered values of the residuals versus the corresponding quantiles of a standard normal distribution. If the qq-plot is linear, the residuals (i.e. the data set) are reasonably Gaussian (Chambers et al., 1983).

Homogeneity of variances - Homoscedasticity

Homogeneity, equality of variances or homoscedasticity are synonyms for a basic assumption underlying statistical models, that the variances due to experimental errors within the treatments are homogeneous (Winer, 1971; Sokal and Rohlf, 1995).

The three univariate procedure most commonly used to test homoscedasticity are: the Hartley test (F- max statistic) which calculates the ratio of the largest to the smallest variance and compares it with a set of tabulated distributions; the Cochran test (C – statistic) which equals the ratio between the largest variance with the average of all variances; and the Bartlett test, which compares the logarithm of the mean of the sample variance with the mean of their logarithms (Winer, 1971; Seber et al. 1977).

However, they are all very sensitive to departures from normality in the population distribution, i.e., if the data are not normally distributed, the validity of the test is greatly affected. Aside from this, there are other arguments against the commonly used methods for testing homoscedasticity, and many statisticians do not recommend to perform these tests (Winer, 1972; Lindman, 1992; Draper and Smith, 1998).

In a certain degree, the consequences of the violation of homoscedasticity is not very critical, because the F test itself tends to be robust with respect to both non-normality and heterogeneity of variance for identical sample sizes (Hyan, 1985; Lindman, 1992;).

However, when the assumption of equal variances is severely violated, there is a tendency to reject the null hypothesis when it should be accepted (Little and Hills, 1978; Lindman, 1992;).

At the present work, tests of homoscedasticity of variance were performed applying Levene's test, using medians rather than means. It is relatively unaffected by non-normality, despite lowered testing power (Draper and Smith, 1998). If Levene's test is statistically significant, then the hypothesis of homoscedasticity should be rejected.

It is also important to examine any correlation between the means and the variances to verify independence between the means the variances of the samples. If means and variances are independent, these ratios will vary widely. Graphical analyses were also used to verify independence among means and variances.

Independence

Effects of land use systems on soil physical parameters are often noticed and experienced researchers and farmers are convinced of them, but statistical verification of these differences sometimes failed due to the spatial dependence among the observations.

Many soil physical properties vary with transient soil features and some are not normally distributed and rather systematically time and spatial dependent (Beckett and Webster, 1971; Jury et al., 1991; Warrick, 1998).

Special research on comparison among land use systems, has to cope with the soil variability, because the experiments normally are carried out at large treatment plots, with an inherent spatial variability between plots, while measurements among system components within the plots may be spatially dependent. Frequently, soil properties measured at nearby locations vary less than those measured further apart, indicating that the samples may be dependent of one another. This inherent soil variability may obscure treatment effects or lead to misinterpretations of results if not taken into account.

The distance between two sampling sites at which the respective samples are judged independent should be determined. This distance, called "the range of influence", characterises the spatial variability of the soil. Using geostatistical techniques it is possible to validate the basic assumptions of independence for many statistical analyses or to take into account possible autocorrelation between measurements when estimating the variance of the mean (Vauclin et al., 1984).

Gajem et al. (1981) studied the spatial dependence of 12 soil properties measured along different transects. They found that these soil properties were correlated over a distance that varied from a few centimeters to several meters.

Russo and Bresler (1981) determined that soil hydraulic properties were correlated over distances as follow: 21 m for saturated hydraulic conductivity, 55 m for saturated soil water content, 25 m for residual water content and 35m for sorptivity.

Campbel (1978) found ranges of 30 m and 40m for the sand content of two different soil types and Vieira et al. (1981) found the steady-state infiltration rates of Yolo loam soil to be spatially dependent within a 50 m range.

The spatial dependence may also be a function of time (Sadding et al. 1985), and most studies of the spatial variability of the soil physical properties have been done on bare soil; in studies with perennial species, the presence of plants may modify the structure of the spatial dependence.

In this study, it is assumed that the values of sample points were spatial independent. This assumption is based on a study carried out in Manaus on a Ferralsol by Côrrea and Richard (1989); their geostatistical analyses show that most soil physical variables are space independent for distances greater than 3 m. In the present study, the closest points within the agroforestry system were distanced about 6 m.

Furthermore, the measurements evaluated in the present study were carried out three years after the installation of the experiment at this stage of development of the plants, due to relatively large planting distances, interaction among individuals of the different species was found to be small and irrelevant for both the amounts of biomass accumulated until May 1996 (Wolf, 1997) and the roots interactions (Haag, 1997).

Therefore, the RBD design is appropriate to identify effects of a different species growing in determined land use system. In addition, planned comparisons using weighted mean of each land use system is calculated to compare the whole land use systems.

Apart from the natural soil variability, the differences among soil physical and hydrological parameters found in the present study are supposed to be caused by: i) the characteristics in the root development of each specie (Haag et al., 1997); ii) departures of rain water partitioned into throughfall, stemflow, and interception loss when passing through plant canopies (Schroth et al., 1999); iii) variations on the micro and macrofauna; iv) difference in the variations in the soil water content (see chapter 5 and 7); v) specific management practices which were differentiated among the species (e.g. fertiliser levels, harvesting or pruning intervals), but identical for the same species among the land use systems (see Chapter 2). Moreover, the differences among the different positions within a land use system are also a deterministic consequence of contrasting plant characteristics with respect to growth, litter production and rate of decomposition, the shadow caused by the canopy into the soil, among many other effects. Such small-scale deterministic differences would also be expected within natural vegetation communities such as tropical forest or fallow.

The variability of chemical properties near the different positions within the land use systems in the present experiment is given by Schoth et al., (1999; 2000).

Nevertheless, the sampling design for analysing agroforestry systems and monocultures with cover crops must take into account the interactions among the species in an advanced stage of development. In this situation, when plants are growing together and competing for nutrients, water and light, interaction among the individuals created an additional source of variability.

Evaluation of the competitive or complementary effects among the components of the system may be of special importance when the whole system is analysed. In this context, possible interaction among neighbours plants must be considered and the assumption of independence of the observation may be severely violated. In such circumstances, a more advanced statistical design must be used. Some statistical design to analysis crops growing together in the same plot is given by Federer (1993; 1998).

When analysing the normally large plots typical of experiment comparing land use systems, an additional complicating factor is the position of the plot in relation to its neighbour plots or the adjacent natural vegetation, i.e., forest or fallow.

The spatial positions of a plot may create additional microclimate sources of heterogeneity, even if the soil is considered homogeneous among the plots. Evidences of microclimate gradients from the border of the forest were found by Reisdorff et al., (2000), who show for the present experiment better development and productivity of cupuaçu plants growing in the plots near the adjacent forest, markedly in the dry years. This kind of phenomenon may be taken into account in the statistical techniques to control error and increase precision employing, for instance the nearest neighbour analysis (Brownie et al, 1993; Helms et al., 1999) or the classical covariance analysis (Snedecor and Cochran, 1989; Steel et al, 1997).

Additivity and residual analyses

The model is called additive because the effects of the fixed and random factors are added. For a randomised block design, any experimental observation is made up of the overall mean plus a treatment effect, plus a block effect, plus an error term. For instance, if the treatment (I) provided an increase of five units in the response and if the influence of the block (J) increased the response by four units, the increase of both together would be presumed to be nine. If an interaction occurs between blocks or treatments, the model is not additive anymore, and suitable transformations of the response variable should be considered to reduce the interaction effects. A method for testing nonadditivity for RDB was developed by Tukey and it is given in by Steel et al., 1997.

The analysis of residuals can reveal some violations of the assumption of additivity, and in some cases a transformation can lead to additive models. If the model is correctly designed and if the statistical assumptions are not severely violated, the residuals plotted versus the fitted values should be structureless, i.e., they should not reveal any obvious trend.

The residuals are the estimate of the errors and unlike the errors they estimate, they are not independent (Draper and Smith, 1998) and may have heteroscedastic variances, i.e., "the residual corresponding to observations with x values that are far from the centre of the range of x values tend to vary more from sample to sample than those corresponding to observations with x values that are closer to the centre, consequently they are not directly comparable with one another" (Graybill and Iyer, 1994). Before they are useful for checking for equality of the variances of the observations, they need to be standardised. Moreover, since methods for detecting nonnormality are often sensitive to inequality of variances, the use of ordinary residuals can lead to the assumption that errors are not normal even when they are (Christensen, 1991).

The standardised residual is the raw residual divided by its standard error. If the residuals are normally distributed about 66% of the standardised residuals have values between -1 and +1, and about 95% of the standardised residuals have values between -2 and +2. A larger standardised residual indicates an outlier (Montgomery, 1997).

A more powerful technique to identify outlier is the analysis of the studentized deleted residual. This procedure takes into account the differences in variability from point to point and allows to check the linearity assumption between the dependent and independent variables (Neter et al., 1989). Scatter plots of studentized residuals were also plotted for some graphical analysis in the present work. It is calculated subtracting the observed value (y_i) and a predicted value ($\square_i$), both corresponding to the i^{th} observation, when the i^{th} sample value is excluded from the analysis. This difference is then divided by an estimate of the standard deviation of the residual at that point (Graybill and Iyer, 1994). Thus, studentized deleted residual will at times identify outlying observations when ordinary residuals would not identify these (Neter et al., 1989).The concepts about graphical analysis of residuals can be found in the books of Neter et al., (1989), Graybill and Iyer (1994) and Draper and Smith (1998).

In this work transformations were used, when the analysis of residuals and the statistical tests showed great violations of the statistical assumptions. The Box-Cox power transformation was performed by the program Minitab Release 13 (Minitab Inc. 2000) to find the optimal power (lambda value in the Box-Cox method) to transform the data. Detailed discussion about suitable transformations can be found in Box et al., (1978) and Little and Hills (1978).

Multiple comparisons

The comparison among treatment averages was performed using two techniques. The first one has as objective to compare the means of the soil parameters evaluated near the different species among and within the plots, and it was done using the Tukey's test.

A second technique was used to compare the whole land use systems. In this context, weight factors relating the area of influence of a determined species on the measured parameter were estimated using maps of the spacing among the species within the plots. Subsequently, the weight factors were used in contrast analysis. The calculations of the weight factors for bulk density is explained in details on the Chapter 4.

In general, the multiple purpose tests for means have the same underlying assumptions as the analysis of variance and, ideally, a test of significance should reject the null hypothesis when it is false. The probability of this rejection to occur is called the power of the test.

The multiple comparison tests has received much attention in the statistical literature, and there is no agreement about the "best" procedure for routine use (Stell et al. 1997; Zar, 1999).

Tukey's tests were performed to compare the means of the parameters evaluated, and the confidence intervals of a difference between a pairwise comparison were determined.

While some authors have criticised the Tukey's test as being a little conservative (i.e., too few significant differences are concluded), others recommend it against other tests like the least square difference (LSD) or Student-Newman-Keuls (SNK) tests, because the last ones may falsely declare significant differences with a probability greater than α (Lindmann, 1994; Systat, 1998; Zar, 1999).

Objections to the use of LSD test in multiple comparisons have been found in the literature. It has a disadvantage of no attempt is made to adjust the observed significance level for multiple comparisons, therefore the test procedure loses its valuable property of protecting the investigator against making erroneous conclusions (Snedecor and Cochran, 1989). In resume, however, the LSD may be a valid test procedure for planned comparisons, it can be and often is misused, and some statisticians hesitate to recommend it (Snedecor and Cochran, 1989; Steel et al. 1994; Zar et al. 1999).

The Duncan's multiple range test is also regarded to be powerful, i.e., it is very effective at detecting differences between means when real differences exist (Carmer and Swanson, 1973; Montgomery, 1997). However, it gives even higher probabilities of Type I errors and is not recommended (Lindmann, 1994). Because SNK and Duncan test do not maintain their claimed protection level they have been excluded form some new versions of statistical packages, like Systat 9.0 ® (Systat, 1998) ; Minitab 12.2 (Minitab Inc. 2000) and S-Plus 2000 Professional (MathSoft Inc. 2000).

The Tukey's test or the honestly significant difference test (HSD) is based on a distribution known as studentized range distribution (q) (Lindman, 1992).

It requires a single value (q) for judging the significance of all differences. To perform the Tukey's test, a critical value of q is calculated using Equation [A.1]. If the calculated q value is equal to or greater than the critical value [$q_{\alpha, v, k}$], then the null hypotheses are rejected at the level α of significance. The degree of freedom of the experimental error is denoted by v, and k is the total number of means being tested.

The critical values of q can be found in and Lindman (1992) and Steel et al. (1997)

In the statistic q,

$$q = \frac{\bar{y}_1 - \bar{y}_2}{\sqrt{\frac{s^2}{n}}} \qquad [A.1]$$

Here value s^2 is the experimental error from the analysis of variance (MSerror) and n is the number of data in the treatments. The denominator is the difference between the means being compared.

It is also occasionally found that the overall F statistic in the analysis of variance is significant, but the comparison test fails to find any significant pairwise differences. This situation occurs because the F test is simultaneously considering all possible comparisons between the treatments means, not just pairwise comparisons (Montgomery, 1997).

Contrast analysis

A contrast or a planned comparison is any linear combination of the coefficients of the treatment whose sum is zero (Montgomery, 1997). It may include all treatment means or only some of the means, furthermore it also permits to give weights to the means.

A contrast (C) i.e., a hypothesis to be tested, may be formulate using the following rules:

$$C = \sum c_i y_{i.}$$

with the restriction that

$$0 = \sum c_i$$

Here, the $y_{i.}$ are the treatment totals and c_i are the coefficients for a hypothesis test.

A contrast allows the researcher to ask specific questions when analysing experimental effects. Although contrast analysis is a very useful technique, its use is not widespread in the agriculture research. This fact is probably related to a popular maxim that the contrasts must be orthogonal.

Orthogonal contrasts have the additional rule that the sum of the products of the corresponding coefficients in any two comparisons is zero. Moreover, they are independent if the data are normal (Snedecor and Cochran, 1989). Because of the independence, they have the advantage in the summary of results that each contrast deals with a distinctly different question and supplies different information. Although, orthogonal contrasts have many desirable mathematical qualities, they are not absolutely necessary, (Winer, 1971; Lindman et al., 1992; Sokal and Rohlf, 1995) and the results still interpretable if the orthogonality assumption is violated. Of course, when it is used indiscriminately to test all possible differences among several comparisons, certain differences will be significant but not at selected level of significance.

When the planned comparisons are not orthogonal is necessary to adjust the values of the probability level (α). Because if a result of a single such comparison is significant, the subsequent comparisons might more likely be significant as well, and decision based on conventional levels of significance might be in doubt.

To assure that the probability of making any type I error at all in the entire series of contrasts does not exceed α , an adjusted probability (α') of incorrectly rejecting at least one of the null hypotheses, can be calculate using the Equation [A.2]

$$\alpha' = 1 - 1(1-\alpha)^{1/k} \qquad [A.2]$$

Here, k is the number of tests and α is the significant level.

Although the probability calculate using the Equation A.2 is exact only for independent tests, this is a feature of any set of ordinary significance test on the same set of data, and employing α' for each comparison results in a conservative test and the probability that one or more test will be significant by chance will be less than α (Sokal and Rohlf, 1995).

In the present experiment, orthogonal contrasts do not allow to formulate all hypothesis of interest and some contrasts analysed are not orthogonal, however, the significant level for difference in a contrast group was differences was the adjusted α'.

An important observation when non-orthogonal sets of contrast are used is that they will not give sums of squares that add to the treatment sum of squares (Steel et al., 1997). Details about contrast analysis are given by Lindman, (1992), Sokal and Rohlf (1995), Stell et al., (1997) and Montogmery (1997).

The sum of squares for any contrast (SSc) for a balanced design, can be calculated using the Equation [A.3]. It has a single degree of freedom, so an F test may be used appropriately to verify the significance (Lindman et al, 1992; Steel et al., 1997). If the F is significantly, the null hypothesis is rejected at the specified α level or the adjusted level α'.

$$SSc = \frac{\left(\sum c_i y_{i.}\right)^2}{n \sum c_i^2} \qquad [A.3]$$

Where n is the number of observations in the mean. The SSc can be used directly as the numerator of an F test with the mean square error of treatments as denominator.

Confidence intervals following multiple comparisons

The confidence interval provides an assessment of how accurately we know the mean or a difference between means. The width of the confidence interval gives us some idea about how uncertain the knowledge of the parameter is. A very wide interval may show that more data should be collected before anything definite can be said about the parameter.

Therefore, confidence intervals are always more informative than tests, and simple results of hypothesis tests alone, without the accompanying confidence intervals, can be misleading (Graybill and Iyer, 1994).

Confidence intervals for the means are calculated using Equation [A.4], for a contrast using Equation [A.5], and for differences between pair of means related to Tukey's test by Equation [A.6]

$$\bar{y} \pm t_{\alpha,\upsilon} \frac{s}{\sqrt{n}} \qquad [A.4]$$

$$\bar{y}_1 - \bar{y}_2 \pm t_{\alpha,\upsilon}\sqrt{SSc * MSerror} \qquad [A.5]$$

$$\bar{y}_1 - \bar{y}_2 \pm q_{\alpha,\upsilon,k}\sqrt{\frac{MSerror}{n}} \qquad [A.6]$$

Here, s is the standard error of the mean; n is the number of the observations for each mean; $t_{\alpha,\upsilon}$ is the value of the t distribution with υ degrees of freedom, required for two-tailed significance at the α level. The parameter υ is the same as those in means square of experimental error (MSerror) in the analysis of variance. The others parameters were previously defined.

The interpretation of the p or value in comparison test

The p value is the likelihood of being incorrect in concluding that there is a true difference among the treatments (i.e., the probability of falsely rejecting the null hypothesis, or committing a Type I error). The smaller the p values, the greater the probabilities that the treatment effects are different. In most cases of this study, statistically significant difference was conclude if the α was smaller that 0.05 and $p > 0.95$.

REFERENCES

BECKETT P H T. and WEBSTER R. Soil variability: a review. Soils and Fertilizers., 34: 1-15, 1971.

BOX G E P.; HUNTER W G. and HUNTER J S. Statistics for experimenters. 1.ed. New York, John Wiley & Sons, 1978. 653p.

BROWNIE C.; BOWMAN D T. and BURTON J W. Estimating spatial variation in analysis of data from yield trials: a comparison of methods. Agronomy Journal., 85: 1244-1253, 1993.

CAMPBEL J B. Spatial variation of sand content and pH within single contiguous delineation of two soil mapping units. Soil Science Society of America Journal., 42: 460-464, 1978.

CARMER S G. and SWANSON M R. Evaluation of ten Pairwise multiple comparison procedures by Monte Carlo Methods. Journal of the American Statistical Association., 68: 66-74, 1973.

CHAMBERS J M.; CLEVELAND W S.; KLEINER B. and TUKEY PAUL A. Graphical methods for data analysis. Wadsworth International Group, Duxbury Press, 1983. 395p.

CÔRREA J C. and REICHARDT K. The spatial variability of amazonian soils under natural forest and pasture. GeoJournal., 19: 423-427, 1989.

DRAPER N R a nd SMITH H. Applied regression analysis. 3.ed. New York, Wiley, 1998. 820p.

FEDERER W T. Statistical design and analysis of intercropping experiments - 1 : Two crops. New York, Springer, 1993. 304p.

FEDERER W T. Statistical design and analysis of intercropping experiments - 2: Three or more crops. New York, Springer, 1998. 293p.

GAJEN Y M.; WARRICK A W. and MYERS D E. Spatial dependence of physical properties of a typic Torrifluvent soil. Soil Science Society of America Journal., 45: 709-715, 1981.

GIBBONS R D. Statistical methods for groundwater monitoring. New York, Wiley, 1994. 286p.

GOMES F P. Curso de estatística experimental. 13.ed. Piracicaba, Livraria Nobel, 1990. 468p.

GRAYBILL F A. Theory and application of the linear model. Pacific Grove, Wadsworth & Brooks, 1976. 704p.

GRAYBILL F A. and IYER H K. Regression analysis concepts and applications. Belmont, Duxbury, 1994. 699p.

HAAG D. Root distributions patterns in a polycultural system with local tree crops on an acid upland soil in central Amazonia, University of Bayreuth, 1997. 87p. (Diplomarbeit)

HAYS W L. Statistics for the social sciences. 3.ed. New York, Holt, Rinehart and Wiston, 1981. 713p.

HELMS T C.; SCOTT R A. and HAMMOND J J. Intrablock variance among duplicate treatments for nearest-neighbour analyses. Agronomy Journal., 91: 317-322, 1999.

JURY W A.; GARDNER W R. and GARDNER W H. Soil physics. 5.ed. New York, Wiley, 1991. 328p.

KUFS C T. Statistical modelling of hydrogeologic data - Part I: Regression and ANOVA models. Ground Water Monitoring Review., XII: 120-130, 1992.

LINDMAN H R. Analysis of variance in experimental design. New York, Springer, 1992. 531p.

LITTLE T M and HILL F J. Agricultural experimentation design and analysis. 6.ed. New York, Wiley, 1978. 350p.

MILLER R G. Beyond anova, basics of applied statistics. New York, Wiley, 1986. 317p.

MONTGOMERY D C. Design and analysis of experiments. 4.ed. New York, Wiley, 1977. 704p.

NETER J.; WASSERMAN W. and KUTNER M H. Applied regression analysis. 2.ed. Homewood, Irwin, 1989. 667p.

PARKIN T B. and ROBINSON J A. Analysis of lognormal data. In: STEWART B, ed. Advances in soil science. New York, Springer Verlag, 1992. p.193-233.

RUSSO D. and BRESLER E. Soil hydraulic properties as stochastic processes: I. An analysis of field spatial variability. Soil Science Society of America Journal., 45: 682-687, 1981.

SADDIQ M H.; WIERENGA P J.; HENDRICKS J M H. and HUSSAIN M Y. Spatial variability of soil water tension in an irrigated soil. Soil Science., 140: 126-132, 1985.

SEARLE S R. Linear models. New York, Wiley, 1972. 532p.

SEARLE S R.; COSELLA G. & MCCULLOCH C E. Variance components. New York, Wiley, 1992. 501p.

SEBER G A F. Linear regression analysis. New York, Wiley, 1977. 465p.

SNEDECOR G W and COCHRAN W G. Statistical methods. 8.ed. Ames, The Iowa University, 1989. 593p.

SOKAL R R and ROLHF F J. Biometrics. New York, Freeman, 1995. 887p.

STELL R G.; TORRIE J H. and DICKEY D A. Principles and procedures of statistics a biometrical approach. 3.ed. New York, Mc-Grawn Hill, 1997. 666p.

SYSTAT. Systat 8.0 Statistics. Chicago, SPSS Inc., 1998. 1086p.

VAUCLIN M.; VIEIRA S R.; BERNARD R. and HATFIELD J.L. Spatial variability of surface temperature along two transects of a bare soil. Water Resources Research., 18: 1677-1686, 1982.

VIEIRA S R.; NIELSEN D R. and BIGGAR J W. Spatial Variability of field-measured infiltration rate. Soil Science Society of America Journal., 45: 1040-1048, 1981.

WARRICK A W. Spatial variability. In: HILLEL D, ed. Environmental soil physics. San Diego, Academic Press, 1998. p.655-675.

WINER B J. Statistical principles in experimental design. 2.ed. New York, McGraw-Hill, 1971. 907p.

WOLF M A. Accumulation of biomass and nutrients in the aboveground organs of four local tree species in monoculture and polyculture systems in central Amazônia, University of Braunschweig, 1997. 298p. (Diplomarbeit)

ZAR J H. Biostatistical analysis. 4.ed. New Jersey, Prentice Hall, 1999. 663p.

A complete exemplification of an analysis of variance for a randomized block design with and without subsampling is given. The bulk density data set was used to exemplify step by step. The same test were performed for the other parameters, but are not shown. The theory of analysis of variance outlined here was used in other parts of this study.

Results of statistical analysis for bulk density

Randomized block design

Fix variable: Treatments (15) – Land use systems and positions within the land use.
Random variable: block (3) – Site
Subsampling: (3) – number of soil probes collected at each treatment

		Site 1 (Block A)			Site 2 (Block B)			Site 3 (Block C)				
Specie	Number	Rep 1	Rep 2	Rep 3	Rep 1	Rep 2	Rep 3	Rep 1	Rep 2	Rep 3	Total	Average
AG Theobroma	1	1.017	0.95	0.959	0.905	0.839	0.894	0.902	0.871	1.014	8.351	0.928
AG Bixa	2	0.737	0.866	0.858	0.927	0.934	0.921	0.964	0.989	0.902	8.098	0.900
AG Bertholetia	3	1.066	1.061	0.988	0.982	0.922	0.901	0.883	0.919	0.948	8.670	0.963
AG Bactris-F	4	0.835	0.818	0.800	0.861	0.815	0.948	0.897	1.004	0.905	7.883	0.876
AG Bactris-P	5	0.673	0.754	0.858	0.968	0.832	0.94	0.948	0.937	0.981	7.891	0.877
AG Pueraria	6	0.867	0.894	0.938	0.919	0.838	0.868	0.898	0.838	0.848	7.908	0.879
M Theobroma	7	0.981	0.869	0.92	0.987	0.982	0.984	0.886	0.969	0.835	8.413	0.935
M Grasses	8	1.028	1.005	1.001	0.985	0.997	0.967	1.021	1.054	0.997	9.055	1.006
M Bactris-F	9	0.895	0.769	0.954	0.858	0.698	0.848	0.825	0.920	0.983	7.750	0.861
M Bactris-bF	10	0.99	0.97	0.896	0.974	1.000	1.077	1.011	0.864	1.01	8.792	0.977
M Bactris-P	11	0.856	0.878	0.809	1.066	1.064	0.954	0.79	0.924	0.897	8.238	0.915
M Bactris-bP	12	0.882	0.935	0.995	1.014	0.999	1.003	0.949	0.957	1.026	8.760	0.973
Vismia spp	13	0.801	0.963	1.01	0.885	0.94	0.995	0.804	0.781	0.92	8.099	0.900
Eschweilera	14	0.860	0.770	0.843	0.890	0.940	0.793	0.910	0.900	0.913	7.819	0.869
Oenocarpus	15	0.750	0.900	0.650	0.740	0.890	0.813	0.830	0.820	0.950	7.343	0.816
Totals				40.12			41.56			41.39	123.070	
Averages				0.892			0.923			0.920		0.9916

AVERAGES PER SITE

Land use system and specie	Number	Site 1	Site 2	Site 3	Total	Average
AG Theobroma	1	0.975	0.879	0.929	2.784	0.928
AG Bixa orellana	2	0.820	0.927	0.952	2.699	0.900
AG Bertholetia	3	1.038	0.935	0.917	2.890	0.963
AG Bactris-F	4	0.818	0.875	0.935	2.628	0.876
AG Bactris-P	5	0.762	0.913	0.955	2.630	0.877
AG Pueraria	6	0.900	0.875	0.861	2.636	0.879
M Theobroma	7	0.923	0.984	0.897	2.804	0.935
M Grasses	8	1.011	0.983	1.024	3.018	1.006
M Bactris-F	9	0.873	0.801	0.909	2.583	0.861
M Bactris-bF	10	0.952	1.017	0.962	2.931	0.977
M Bactris-P	11	0.848	1.028	0.870	2.746	0.915
M Bactris-bP	12	0.937	1.005	0.977	2.920	0.973
Vismia spp	13	0.925	0.940	0.835	2.700	0.900
Eschweilera	14	0.824	0.874	0.908	2.606	0.869
Oenocarpus	15	0.767	0.814	0.867	2.448	0.816
Totals		13.373	13.852	13.798	41.023	
Averages		0.892	0.923	0.920		0.912

Estimated residual using the statistical model for RBD [pg 1 in this Appendix]

		Site 1			Site 2			Site 3		
Specie	Number	Rep 1	Rep 2	Rep 3	Rep 1	Rep 2	Rep 3	Rep 1	Rep 2	Rep 3
AG Theobroma	1	0.098	-0.062	-0.036	0.077	-0.053	-0.025	0.027	-0.066	0.039
AG Bixa	2	-0.117	0.025	0.092	-0.050	-0.001	0.050	-0.012	0.023	-0.011
AG Bertholetia	3	0.111	-0.021	-0.090	0.108	-0.050	-0.057	0.066	-0.049	-0.017
AG Bactris-F	4	-0.007	-0.029	0.036	-0.047	-0.069	0.116	-0.060	0.059	0.001
AG Bactris-P	5	-0.168	0.079	0.089	-0.073	-0.014	0.087	-0.044	0.009	0.035
AG Pueraria	6	-0.005	-0.002	0.007	0.051	-0.024	-0.028	0.077	-0.021	-0.056
M Theobroma	7	0.052	0.010	-0.062	-0.057	0.037	0.020	0.031	0.066	-0.097
M Grasses	8	0.039	-0.052	0.013	0.000	-0.027	0.026	0.037	-0.026	-0.011
M Bactris-F	9	0.058	-0.027	-0.031	-0.013	-0.103	0.115	0.050	-0.085	0.035
M Bactris-bF	10	0.021	-0.044	0.023	0.039	0.050	-0.090	-0.074	0.078	-0.004
M Bactris-P	11	-0.026	0.136	-0.110	-0.063	0.104	-0.040	-0.054	0.063	-0.009
M Bactris-bP	12	-0.044	0.040	0.004	-0.015	0.030	-0.016	0.011	-0.010	-0.001
Vismia spp	13	-0.007	0.029	-0.022	0.082	0.040	-0.123	0.059	0.015	-0.074
Eschweilera sp.	14	-0.004	-0.023	0.027	-0.086	0.065	0.021	0.017	-0.061	0.044
Oenocarpus	15	-0.001	-0.059	0.060	0.044	0.015	-0.059	-0.130	0.004	0.126

Estimated residuals from the RBD averaging the subsampling in only one mean per treatment per block.

Land use system and specie	Number	Site 1	Site 2	Site 3
AG Theobroma	1	-0.068	0.060	0.007
AG Bixa	2	0.059	-0.016	-0.044
AG Bertholetia	3	-0.095	0.040	0.055
AG Bactris-F	4	0.038	0.013	-0.051
AG Bactris-P	5	0.095	-0.025	-0.070
AG Pueraria	6	-0.041	0.016	0.026
M Theobroma	7	-0.009	-0.038	0.046
M Grasses	8	-0.025	0.035	-0.010
M Bactris-F	9	-0.032	0.072	-0.040
M Bactris-bF	10	0.005	-0.028	0.023
M Bactris-P	11	0.048	-0.101	0.053
M Bactris-bP	12	0.016	-0.020	0.004
Vismia spp	13	-0.045	-0.028	0.073
Eschweilera spp.	14	0.024	0.006	-0.031
Oenocarpus bacaba	15	0.029	0.013	-0.043

MODEL ADEQUACY CHECKING: TESTS FOR NORMALITY, HOMOCESDASTICITY AND INDEPENDENCE OF THE RESIDUALS

NORMALITY

Tests of Normality - Shapiro-Wilk

Specie	Statistic	df	Sig.
1.00	.941	9	.560
2.00	.898	9	.304
3.00	.911	9	.372
4.00	.925	9	.447
5.00	.874	9	.178
6.00	.932	9	.485
7.00	.837	9	.063
8.00	.966	9	.838
9.00	.975	9	.927
10.00	.925	9	.449
11.00	.922	9	.434
12.00	.915	9	.396
13.00	.913	9	.382
14.00	.924	9	.445
15.00	.972	9	.903

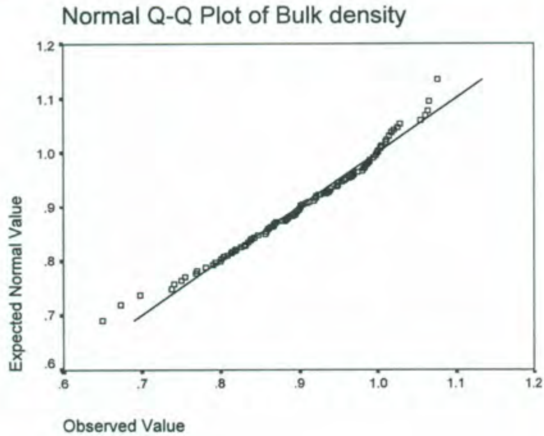

RESIDUAL ANALYSIS

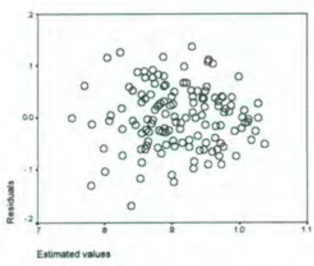

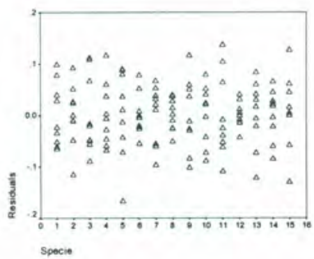

HOMOCEDASTICITY

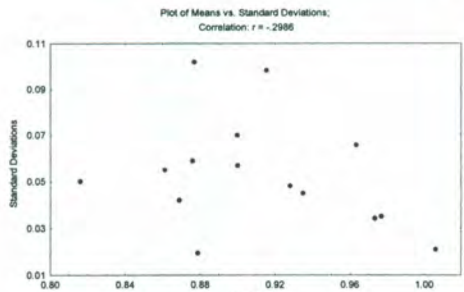

Levene's Test for Homogeneity of Variances

		Levene Statistic	df1	df2	Sig.
BD	Based on Mean	1.910	14	120	.032
	Based on Median	1.137	14	120	.334

Statistical analysis – Variance analyse

Randomised block design with subsampling

Source	Sum-of-Squares	df	Mean-Square	F-ratio	P
Plants	0.341	14	0.024	2.465	**0.020**
Site	0.028	2	0.014	1.394	**0.265**
Error	0.277	28	0.010		
Subsampling	0.328	90	0.003		
Subsampling	[0.009]	[2]	0.004	1.290	0.283
Plants	[0.120]	[28]	0.004	1.271	0.220
Sites	[0.010]	[4]	0.003	0.758	0.557
Error	[0.189]	[56]	0.003		
Total	0.697	134			

Randomised block design with one mean per treatment

Source	Sum-of-Squares	df	Mean-Square	F-ratio	P
Plants	0.114	14	0.008	2.465	**0.020**
Site	0.009	2	0.005	1.394	**0.265**
Error	0.092	28	0.003		
Total	0.215	44			

POST HOC TEST - Tukey HSD Multiple Comparisons.
Matrix of pairwise comparison probabilities:

	1	2	3	4	5	6	7	8	9	10	11	12	13	14	15
1	1.0000														
2	1.0000	1.0000													
3	1.0000	0.9850	1.0000												
4	0.9980	1.0000	0.8500	1.0000											
5	0.9980	1.0000	0.8590	1.0000	1.0000										
6	0.9990	1.0000	0.8760	1.0000	1.0000	1.0000									
7	1.0000	1.0000	1.0000	0.9920	0.9930	0.9950	1.0000								
8	0.9260	0.6180	1.0000	0.3130	0.3220	0.3430	0.9620	1.0000							
9	0.9770	1.0000	0.6740	1.0000	1.0000	1.0000	0.9510	0.1800	1.0000						
10	0.9990	0.9330	1.0000	0.6910	0.7020	0.7270	1.0000	1.0000	0.4890	1.0000					
11	1.0000	1.0000	0.9990	1.0000	1.0000	1.0000	1.0000	0.8160	0.9970	0.9890	1.0000				
12	0.9990	0.9520	1.0000	0.7370	0.7480	0.7710	1.0000	1.0000	0.5370	1.0000	0.9930	1.0000			
13	1.0000	1.0000	0.9850	1.0000	1.0000	1.0000	1.0000	0.6200	1.0000	0.9330	1.0000	0.9520	1.0000		
14	0.9920	1.0000	0.7720	1.0000	1.0000	1.0000	0.9790	0.2420	1.0000	0.5940	0.9990	0.6430	1.0000	1.0000	
15	0.5400	0.8830	0.1630	0.9910	0.9900	0.9870	0.4480	**0.0220**	0.9990	0.0910	0.7110	0.1060	0.8820	0.9970	1.0000

The confidence interval for the difference between the bulk density in the soil covered by grasses [8] and near the bacabas [15] in the primary forest is 0.190 ±. 0.185 with 95% confidence.

Table A-3.1 Particle size distribution, indexes of flocculation and particle density evaluated from soil samples taken at the soil surface near different species on a Ferralsol in the central Amazon

Land Use System	Specie	Coarse sand	Fine Sand	Silt	Clay	Index of Flocculation	Particle density
		2.00 – 0.2 mm	0.2 – 0.05 mm	0.05 – 0.02 mm	< 0.002 mm		
			$g\ kg^{-1}$			%	$Mg\ m^{-3}$
			Block A				
Agroforestry	*Theobroma grandiflorum*	237.9	56.0	117.6	588.5	78.33	2.63
Agroforestry	*Bixa Orellana*	210.5	59.2	110.8	619.5	87.01	2.50
Agroforestry	*Bertholletia excelsa*	265.8	58.9	110.8	564.5	81.93	2.50
Agroforestry	*Bactris gasipaes* †Fr	292.4	56.3	119.8	531.5	80.71	2.50
Agroforestry	*Bactris gasipaes* ‡	281.2	57.8	104	557.0	78.90	2.50
Agroforestry	*Pueraria phaseoloides*	216.1	56.6	55.8	671.5	79.82	2.63
Monoculture	*Theobroma grandiflorum*	246.9	58.2	128.4	566.5	78.91	2.50
Monoculture	*Pueraria phaseoloides*	251.4	57.7	149.9	541.0	63.68	2.50
Monoculture	*Bactris gasipaes* †Fr	245.2	53.6	130.7	570.5	76.07	2.50
Monoculture	†§	268.0	54.6	220.9	456.5	71.41	2.53
Monoculture	*Bactris gasipaes* ‡	273.0	52.4	106.6	568.0	76.41	2.56
Monoculture	‡§	189.6	51.6	116.3	642.5	74.16	2.63
Sec. Forest	*Vismia sp*	268.5	55.9	122.6	553.0	83.91	2.50
			Block B				
Agroforestry	Theobroma grandiflorum	219.8	50.2	137.0	593.0	72.60	2.50
Agroforestry	*Bixa Orellana*	212.4	55.2	134.9	597.5	76.23	2.50
Agroforestry	*Bertholletia excelsa*	200.9	59.6	108.5	631.0	78.37	2.59
Agroforestry	*Bactris gasipaes* †	195.6	76.7	124.7	603.0	74.96	2.63
Agroforestry	*Bactris gasipaes* ‡	215.9	52.6	131.5	600.0	75.33	2.50
Agroforestry	*Pueraria phaseoloides*	165.5	44.6	153.4	636.5	80.52	2.50
Monoculture	*Theobroma grandiflorum*	196.3	57.9	130.3	615.5	64.99	2.50
Monoculture	*Pueraria phaseoloides*	235.0	60.0	93.5	611.5	82.01	2.50
Monoculture	*Bactris gasipaes* †F	200.7	74.3	119.5	605.5	85.63	2.50
Monoculture	§	195.7	55.6	145.2	603.5	76.97	2.50
Monoculture	*Bactris gasipaes* ‡	227.2	62.1	122.2	588.5	74.68	2.50
Monoculture	‡§	251.8	63.9	98.3	586.0	70.39	2.50
Sec. Forest	*Vismia sp*	210.3	49.1	134.6	606.0	80.12	2.50
			Block C				
Agroforestry	Theobroma grandiflorum	269.8	61.6	159.1	509.5	69.87	2.50
Agroforestry	*Bixa Orellana*	253.7	76.2	134.1	536.0	61.66	2.50
Agroforestry	*Bertholletia excelsa*	229.9	64.1	144.0	562.0	65.93	2.38
Agroforestry	*Bactris gasipaes* †	211.1	57.8	145.1	586.0	71.50	2.50
Agroforestry	*Bactris gasipaes* ‡	277.8	59.8	144.9	517.5	55.17	2.50
Agroforestry	*Pueraria phaseoloides*	175.6	57.0	159.4	608.0	66.04	2.66
Monoculture	*Theobroma grandiflorum*	246.5	53.4	147.6	552.5	72.49	2.50
Monoculture	*Pueraria phaseoloides*	159.2	56.1	166.7	618.0	64.64	2.50
Monoculture	*Bactris gasipaes* †	260.7	59.6	148.7	531.0	57.63	2.50
Monoculture	†§	184.8	52.5	150.7	612.0	75.65	2.66
Monoculture	*Bactris gasipaes* ‡	230.2	84.3	166.0	519.5	70.84	2.50
Monoculture	‡§	237.9	60.5	168.6	533.0	60.41	2.50
Sec. Forest	*Vismia sp*	224.5	64.3	155.7	555.5	61.66	2.50

§ Evaluated between the palms

† *Peach* palm for fruit production

‡ Peach palm for palm heart production

Table A 3.2 Soil chemical characteristics evaluated from soil samples taken at the soil surface near different species on an clayey Ferralsol in Manaus –Brazil.

Land Use System	Specie	Carbon	pH	Ca^{2+}	Mg^{2+}	Al^{3+}
		%	-		$cmol_c\ dm^{-3}$	
			Block A			
Agroforestry	Theobroma grandiflorum	3.04	3.9	0.73	0.19	1.60
Agroforestry	*Bixa Orellana*	2.99	3.5	0.17	0.14	2.47
Agroforestry	*Bertholletia excelsa*	2.84	4.1	3.42	0.13	0.83
Agroforestry	*Bactris gasipaes* †Fr	2.39	4.0	0.6	0.15	1.28
Agroforestry	*Bactris gasipaes* ‡	2.23	3.9	0.61	0.16	1.23
Agroforestry	*Pueraria phaseoloides*	2.19	3.5	0.09	0.12	2.00
Monoculture	*Theobroma grandiflorum*	2.44	4.0	0.34	0.26	1.22
Monoculture	*Pueraria phaseoloides*	2.01	3.5	0.15	0.12	1.63
Monoculture	*Bactris gasipaes* †Fr	2.08	3.8	0.25	0.18	1.63
Monoculture	†§	3.06	3.8	0.23	0.19	1.43
Monoculture	*Bactris gasipaes* ‡	2.51	3.9	0.45	0.21	1.51
Monoculture	‡§	2.65	4.0	0.75	0.29	1.42
Sec. Forest	*Vismia sp*	2.80	3.5	0.16	0.19	2.26
			Block B			
Agroforestry	Theobroma grandiflorum	3.05	4.4	1.04	0.72	1.33
Agroforestry	*Bixa Orellana*	2.77	3.9	0.24	0.23	1.96
Agroforestry	*Bertholletia excelsa*	3.03	4.2	1.59	0.83	0.97
Agroforestry	*Bactris gasipaes* †	2.36	4	2.66	1.88	0.44
Agroforestry	*Bactris gasipaes* ‡	2.61	3.9	0.34	0.2	1.73
Agroforestry	*Pueraria phaseoloides*	3.37	4.1	0.94	0.62	1.48
Monoculture	*Theobroma grandiflorum*	2.39	4.4	2.39	1.42	0.28
Monoculture	*Pueraria phaseoloides*	2.88	4	1.01	0.58	1.67
Monoculture	*Bactris gasipaes* †F	2.7	4.3	1.12	0.87	0.88
Monoculture	§	2.34	4.4	0.82	0.5	1.72
Monoculture	*Bactris gasipaes* ‡	2.73	3.7	3.2	2.28	0.16
Monoculture	‡§	3.14	4.6	2.23	1.3	0.3
Sec. Forest	*Vismia sp*	2.36	3.8	0.08	0.14	1.99
			Block C			
Agroforestry	Theobroma grandiflorum	3.26	5.2	2.45	2.38	0.04
Agroforestry	*Bixa Orellana*	2.13	4.5	0.98	0.63	0.83
Agroforestry	*Bertholletia excelsa*	2.79	4.7	1.77	1.57	0.24
Agroforestry	*Bactris gasipaes* †	2.50	4.6	1.21	0.76	0.48
Agroforestry	*Bactris gasipaes* ‡	2.36	4.6	1.96	1.28	0.23
Agroforestry	*Pueraria phaseoloides*	2.77	4.9	3.29	3.02	0.04
Monoculture	*Theobroma grandiflorum*	2.40	4.8	2.10	1.53	0.10
Monoculture	*Pueraria phaseoloides*	2.54	3.9	0.33	0.21	1.60
Monoculture	*Bactris gasipaes* †	2.06	4.4	1.33	1.00	0.33
Monoculture	†§	2.71	4.6	0.97	0.53	0.92
Monoculture	*Bactris gasipaes* ‡	2.80	4.6	1.42	1.12	0.54
Monoculture	‡§	2.80	5.1	1.54	1.61	0.33
Sec. Forest	*Vismia sp*	2.54	4.0	0.33	0.21	1.60

§ Evaluated between the palms
† *Peach* palm for fruit production
‡ Peach palm for palm heart production

4 LAND USE EFFECTS ON TOTAL POROSITY AND PORE SIZE DISTRIBUTION

4.1 INTRODUCTION

The measurement of total porosity (ϕ) is a quantitative, indirect approach to soil structure analysis. Soil pores vary in size and shape, and manifest an interconnected framework typical for each particular soil type, which, however, may change as a consequence of different land use systems.

Porosity controls the storage, availability and transport of water and air in the soil. However, this control depends not only on the total volume occupied by pores, but also and specifically on how the porous space is distributed and connected. It is therefore important to determine not only ϕ, but also pore-size distribution. In summary, the pore size distribution, the relative number, volume, morphology, stability, connectivity of the pores and the history of wetting and drying processes determine the ability of a soil to store and transmit water. This ability compared to that of rainfall intensity is an important property that influences the soil water balance and controls runoff and erosion.

Techniques have been elaborated to determine ϕ based on image analysis using the microscopical evaluation of soil thin sections (Chauvel, 1982; Moran et al., 1989) and computerised tomography (Warner et al., 1989; Macedo and Crestana, 1999). However, the most common method to estimate ϕ is still based on bulk density measurements in combination with particle density measurements.

The pore-size distribution can be evaluated by the pressure-intrusion method, in which a nonwetting liquid, generally mercury, is forced into the pores of a predried sample (Lawrence, 1977; Danielson and Sutherland, 1986; Carter and Ball, 1993). Chauvel et al., 1991 used this technique to evaluate soil samples from the clayey Ferralsols in the central Amazon. In the mercury intrusion technique errors can arise especially from the drying methods employed and from deviations from the assumed contact angles between the mercury and the pore walls (Marshal et al., 1996, pg. 211). Lawrence (1977) has reviewed some other techniques to describe the pore-size distribution, such as non-polar liquid desorption and nitrogen sorption. Another approach to evaluate pore-size distribution is called desorption method, where a saturated soil sample is subjected to a stepwise series of incremental water pressure head (h), and the paired data are collected relating the volumetric water content (θ) and the h during the drying phase (i.e., the evaluation of how much water is retained at each successively lower matric potential). This information is related to the distribution of the pore radii and can be interpreted in relation to water availability for plants, for water flow and infiltration. The capillary theory is used to obtain the "equivalent radius" of the soil pore sizes.

The soil water retention curve (SWRC) or soil water desorption curve (SWDC) in which θ is a function of h is one of the most important hydraulic functions governing the movement of water and solutes in the soil. The equation proposed by van Genuchten (1980) is widely adopted to fit the experimental water retention data and is generally combined with Mualem's estimation of hydraulic conductivity. A good fitting of the experimental water retention data is fundamental in the evaluation of the capacity function and the continuous pore-size distribution, further it theoretically leads to better estimates of coupled hydraulic functions.

In well-aggregated natural soils the pore system is frequently partitioned into intraaggregate or textural pores and interaggregate or structural pores (Sharma and Uehara, 1968; Chauvel et al., 1991), resulting in bi- or tri-modal pore-size distribution. Further, the soil aggregates show frequently a steep slope of water retention near saturation (see e.g., Durner, 1994), which the original van Genuchten equation has not the necessary flexibility to fit (Smettem and Kikby, 1990; Durner, 1994; van Genuchten and Leij, 1999). A better description of the SWRC of soils exhibiting bimodal pore-size distributions has been given by linearly overlapping two Van Genuchten equations (Othmer et al., 1991; Durner, 1994; Mallants et al., 1997; Coppola, 2000).

The clayey Ferralsols in the central Amazon show in their original conditions a high ϕ (Côrrea, 1985; Camargo and Rodrigues, 1979; Teixeira et al., 1997) and their pore-size distribution was shown to be clearly bimodal by Chauvel et al. (1991), with a large proportion of the ϕ concentrated in extremely fine pores and further a large proportion concentrated in the macro and large mesopores. These heterogeneous pore systems are a consequence of the pore genesis. One peak or mode represents the interaggregate pores caused by bonding the clay particles, the other creates from biological activity; evidence of these processes for the clayey Ferralsols in the central Amazon is given by Chauvel (1982). Moreover, a study of the soil hydraulic properties conducted by Tomasella and Hodnett (1996) showed the inability of the original van Genuchten equation (unimodal) to fit a soil SWRC for the clayey Ferralsols in the central Amazon as a probably consequence of the bimodal pore size distribution.

The objective of this chapter is to characterise ϕ and the pore-size distribution of the clayey Xanthic Ferralsol in the central Amazon on different land use systems. Methodological problems and the capacity of more flexible retention functions to describe the measured soil water retention data are also reviewed and discussed. The discussion is focused on the consequences of Φ on hydraulic properties but practical inferences about the pore size distribution in relation to water availability and fluxes are pointed out.

4.2 MATERIAL AND METHODS

4.2.1 Study area and site history

The study area and the site history of the selected plots have been described in detail in Chapter 2.

4.2.2 Soil sampling

The soil sampling scheme and the positions sampled was the same as described to collect samples to determine soil bulk density in Chapter 3 (Table 3.2). The steel cylinders to collect the samples for SWRC were similar to those described in the bulk density determination.

4.2.3 Evaluated parameters

4.2.3.1 Total porosity [ϕ]

The total porosity (ϕ) of a soil sample is the volume of the pores related to the total volume of the sample. It is calculated from measurements of bulk density (ρ – M L^{-3}) and average particle density (ρ_P - M L^{-3}) using Equation 4.1.

$$\Phi = 1 - \frac{\rho}{\rho_P} \qquad [4.1]$$

4.2.3.2 Soil water retention curve (SWRC)

For the evaluation of SWRCs five samples were collected at each position described in Table 3.2. The samples were taken in the same area concentrated in the area where the disc infiltrometer were installed. It was an attempt to permit posterior comparisons between the results from the direct evaluation of the hydraulic properties and indirect estimation from SWRC. This topic is discussed in Chapter 5. Soil samples were collected on the same or the next day after the evaluation of the infiltration, determined with the disc infiltrometer.

The samples, collected with steel cylinders of 100 cm^3, were wrapped into plastic for a convenient transport to the Soil Physics Laboratory at the Embrapa – Amazônia Ocidental station in Manaus, where the SWRCs were determined. Initially, the soil cores were saturated in a shallow bath and, after saturation had been reached, the water retention data were determined successively at 0, 0.5, 1.0, 1.5, 1.8, 2.0 and 2.2 *pF ($\log_{10}$ cm H_2O) employing the tension-plate method. Afterward, the soil water retention was determined in a pressure-plate apparatus for h of 2.5, 3.0 and 3.5 pF. Finally, the samples were removed from the cylinders and disturbed soil samples were put into rubber rings and submitted to an h of 4.2 pF in a special pressure-plate apparatus. Details about the measurement of SWRCs with desorption method from soil cores are given by Klute and Dirksen (1986); Topp et al. (1993), Mathieu and Pieltain (1997).

The evaluation of the complete SWRC lasted about 2 months. The time to reach equilibrium ranged from few days for the low h to more than a month for the last one.

In addition, a profile of 100 cm depth was sampled in steps of 10 cm intervals and analysed for characterising SWRC in the subsurface layers. The profile was located at the centre of the experimental area. Methodological limitations of the evaluation of SWRC by desorption are given by Hillel and Mottes (1966), Madsen et al. (1986), Ball and Hunter (1988), Klute and Dirksen (1986) and Moraes and Libardi (1993a, b).

Fitting equation to SWRC

The SWRC, which relates θ and h, can be parameterised to obtain a simple description of a comprehensive set of measurements. Several parametric functions have been proposed to describe empirically SWRC. Most popular are the piecewise equation of Brook and Corey and the equation of van Genuchten (1980) further referred as VG-equation. The VG equation is now widely used in numerical simulation of water fluxes, with no sharp transition at the air entry value as produced by the

* The water potential is the potential energy per unit volume (or mass) of water in a system. It has in the S.I the units of J m^{-3} or J kg^{-1}, which are dimensionally equivalent to N m^{-2} or Pascal. To facilitate comparisons with other studies the pF unit was adopted. The following relations are useful to convert units: 1 J kg^{-3} ≈ 1000 Pa ≈ 0.1 bar ≈100 cm of water.

Brooks and Corey equation. Two equivalent forms of the VG- equation are shown in Equations 4.2 and 4.3.

$$\theta = \theta_r + \frac{\theta_s - \theta_r}{\left[1 + (\alpha|h|)^n\right]^m} \qquad [4.2]$$

$$S_e = \frac{\theta - \theta_r}{\theta_s - \theta_r} = \left[1 + (\alpha|h|)^n\right]^m \qquad [4.3]$$

Here, θ_s and θ_r are the saturated and residual water content, respectively ($L^3\ L^{-3}$- $m^3\ m^{-3}$); h is the pressure head (cm water – which is in absolute value, to simplify notation), α, n and m are fitting parameters, and Se is the relative saturation. The parameter α (L^{-1} - cm^{-1}) is inversely related to the air entry-pressure (van Genuchten and Nielsen, 1985), and n represents the slope of the SWRC and is associated with the width of the pore size distribution (Russo, 1988). The parameter θ_s should not be equated with porosity, because under field conditions, porosity is generally about 5 to 10% smaller because of entrapped or dissolved air (van Genuchten et al., 1991). Moreover, in this chapter both θ_s and θ_r are viewed as being essentially empirical constants in SWRC and hence without much physical meaning.

A restriction [m = 1 – 1/n] was imposed, because this leads to a relatively simple expression for the hydraulic conductivity function when Equation 4.2 is combined with the theoretical pore-size distribution model of Mualem (van Genuchten and Nielsen, 1985). The values for the parameters (θ_s, θ_r, α and n) were obtained by simultaneously fitting the above expression to the experimental soil water retention data (i.e., the paired θ (h) data).

Better descriptions of the SWRC of soils exhibiting bimodal pore-size distributions have been given by linearly overlapping two functions of VG-equations (Othmer et al., 1991; Durner, 1994). This approach can also be used for more modes by overlapping more functions.

The overlapping van Genuchten's equation proposed by Durner (1994) is shown in Equation 4.4

$$S_e = \sum_{i=1}^{k} w_i \left[1 + (\alpha|h|)^{n_i}\right]^{-m} \qquad [4.4]$$

Here, Se is as defined previously, k is the number of subcurves, set at two in this study (for bimodal distribution), w_i are weighting factors indicating the fraction of the total pore space occupied by each distribution, with $[0 < w_i < 1]$ and the sum of the weight factors equal to one. For each subcurve, parameters (α_i, n_i, and m_i) are defined similarly to the corresponding parameters in the unimodal VG-equation, which was previously defined. The eight unknown parameters in the bimodal approach (θs, θr, α_1, α_2, n_1, n_2, w_1 and w_2) were fitted simultaneously. The Fortran code SHYPFIT (Soil **H**ydraulic **P**roperties **F**itting) (Durner, 1995) was used to obtain the solution of Equations 4.3 and 4.4 Shiypfit uses the algorithms of Levenberg-Marquardt (Press et al., 1986) for optimising parameters in non linear equations.

Nowadays another computer program is available to fit dual porosity model of SWRC, the RETC 6.0 code which provides the dual porosity options with until eight parameters to be simultaneously optimised for describing or predicting the hydraulic properties of unsaturated soils. The RETC 6.0 is a public domain software developed by Salinity Laboratory of the United States and a description of its functions and the Fortran code is given by van Genuchten et al. (1991).

Pore size distribution from SWRC

From the measurement of the discrete paired data of θ and h, the equivalent pore size distribution curve is calculated based on the capillary equation described as Equation 4.5.

$$r = \frac{2\gamma\cos\zeta}{(\rho_l - \rho_a)gh} \qquad [4.5]$$

Where, r is the radius (L; m) of the biggest pore which remains filled with water after a water pressure head (h) has been applied to the soil; h is expressed as equivalent height in a capillary tube (hydrostatic tension) (L - m); (γ) is the surface tension between the liquid and the air (M T^{-1} - 0.0728 N m^{-1} at 20°C); ξ is the contact angle between the liquid and the solid, or the pore wall, normally considered 0° hence its cosine assumes the value one; ρ_l is the water density (M L^{-3} - 998 kg m^{-3} at 20°C); ρ_a is the air density (M L^{-3} - 1 kg m^{-3} a 20°C), which is generally neglected, and g is the acceleration of gravity (L T^{-2} - 9.81 m s^{-2}).

Although [r] in the capillary theory represents the radius of a capillar, at the scale of soil pores it is normally called the "equivalent radius", with no attempt made to quantify the real radius of the soil pores (Kutilek and Nielsen, 1994).

Equation 4.5 may be approximated for most cases (using typical values at room temperature) by calculating only

$$r = \frac{0.149}{h} \qquad [4.6]$$

Here, h is water pressure head (tension) applied in centimetres of water and r is the radius of the equivalent pore in centimetres.

The pore size distribution is commonly calculated from the specific moisture capacity [C], which is the slope of the soil-moisture characteristic curve and represents the change of θ per unit change of h. It is calculated deriving the function of θ(h).

Another approach to visualise the pore-size distributions in continuous form was presented by Durner (1994) and Mallants et al. (1997) and can be calculated using Equation 4.7. The retention characteristics are frequently plotted on a logarithmic pressure head scale, which is conveniently expressed in pF [log10 (-h)], where h is expressed in centimetres.

$$\frac{d\theta(h)}{d\log_{10}|h|} = \left[\log_e(10)|h|C\right] \qquad [4.7]$$

The Fortran code Shypfit was used to obtain the parameter C. The discrete results evaluated with Equation 4.5 agree with the estimates given by Equation 4.7 (obviously, at the discrete measured values of h). Therefore, our discussion concentrates on the continuous distribution of the pore-size frequency, they are mathematical abstraction and do not necessarily describe the real situation.

Moreover, the density function estimated was normalised for values of pF between -3 to 7 in one hundred intervals, and the total area covered by the curve is regarded as one. It simplifies the comparison between the curves and allows calculating the percentile contributions of determined range of pore radii to ϕ.

The criteria applied in the discussion of the results to classify the equivalent pore-size are shown in Table 4.1.

Table 4.1 Pore size classification and pressure range (After Brewer, 1964 and Kusnetsova, 1991)

Class	Equivalent pore diameter, range [μm]	†Pressure range, [pF]	†Pressure range, [cm H_2O]
Macropores			
coarse	> 5000	> 1.47	30
medium	5000-2000	1.48 - 1.87	30 – 75
fine	2000-1000	1.88 -2.17	75 – 150
very fine	1000-75	2.18 - 3.30	150 – 2000
Mesopores	75-30	3.31 - 3.70	2000 – 5000
Micropores	30-5	3.71 - 4.47	5000 –30000
Ultramicropores	5-0.1	4.48 - 6.17	30000 –1500000
Cryptopores	< 0.1	< 6.17	1500000

† Estimated with Equation 4.6.

The normalisation of the pore size density (i.e. the area below the curve equals one) allows the comparison of released water in a determined range of pore radii. It was calculated using the trapezoidal rule to estimate a specific area (range). The ranges selected representing the relative water released following the criteria proposed in Table 4.1 are: i) by coarse macropores (> 5000 um); ii) by medium, fine and very fine macropores (pore radii between 5000 and 75 um); iii) mesopores (pore radii between 75 and 30 um); iv) micropores (pore radii between 30 and 5 um) and v) ultramicropores and cryptopores (pore radii < 5 um). This calculation allows subdividing the ϕ of a soil into size classes of pores, which may differ in their ecological functions in the soil.

The discussion of the results was focused differently for the results from the soil profile and the results from the superficial measurement carried out on the different land use systems. For the results on the soil profile, the discussion stresses the fitted parameter and problems in the methodology itself. For the results evaluated on the soil surface the discussion focus on the pore size distribution in terms of water supply characteristics, based on the pore-size classification presented in Table 4.1, current concepts of the role of pores of different sizes in the migration and retention of water, gas exchange to the plant roots and microorganisms.

4.2.4 Statistical analysis

The statistic results for ϕ are the same as presented for the bulk density in Chapter 3. This is because estimation of ϕ was done using a fixed number for particle density (for the soil surface of 2.50 Mg m^{-3} and 2.60 Mg m^{-3} for the subsurface layers).

The calculation of ϕ, using Equation 4.1, does not change the statistical results showed for the bulk density analysis in Chapter 3. It is because the bulk density data set was divided by a constant value (particle density) and then subtracted of one. These operations have the effect of coding the original bulk density. Therefore, the F value and the statistical significance shown for the bulk densities remain unchanged. Details of the effect of coding on the parametric ANOVA are given by Zar (1999).

As measure of the goodness of fit, the average deviation (AD) was calculated using Equation 4.8. The code Shypfit calculates AG automatically

$$AD = \frac{1}{n}\sum_{i}^{n}\left|y_i - \hat{y}_i\right| \qquad [4.8]$$

Here, n is the number of parameters used in the optimisation, y_i is the i^{th} measured value and $\hat{y}$ is the estimation of y_i.

Finally, because of possible problems related to convergence and parameter uniqueness, some equations were recalculated using different constraints, and in some cases, when θ_s was fixed (at the maximal value measured) the program converges to better results.

4.3 RESULTS AND DISCUSSION

4.3.1 Profile

The location and complete experimental data set to estimate Φ is given in Appendix 3-A (data from bulk density measurements and particle density). The complete data set of measured water retention from the soil profile is given in Appendix 4-A. The mean values and standard error for the measured retention data are shown in Table 4.2 and the fitted parameters for SWRC are given in Table 4.3.

Figure 4.1 (a) shows a box plot of Φ on the soil profile until 100 cm depth. Figures 4.2, 4.3 and 4.4 show the measured water retention data, the fitted functions of VG and VG- bimodal and the pore size distribution, respectively. The box plot for the soil profile (Figure 4.1 a) shows a drift owing to the existence of a more porous layer placed at $\approx$ 60 cm depth, which is situated between two more compact layers. Chauvel (1982) and Tomasella and Hoddnet (1986) also reported a similar trend in a clayey Ferralsols near Manaus. Differences in the depth of this layer were more clearly identified by analysing the pore-size distribution (Table 4.3 and Figure 4.4), which show pores with radii larger than those in the layers above and below. Table 4.2 also indicates some differences between the first layer (10 cm) and the other ones, with the first one showing reduced water content at low h (i.e. because of its greater macroporosity).

Table 4.3 shows another slight trend towards an increase of the water holding capacity with depth. Apart from an increase in the clay content with depth (see Table 3.1 in Chapter 3 for values of the clay). A higher macro and mesoporosity in the superficial layers may be explained by a higher biological activity near the soil surface or because of cracks because of a more intense drying and wetting. This phenomenon, which happens in the dry season in the central Amazon is only observed in the first layers of the soil, because deeper layers never seem to be dry enough for the occurrence of cracks (see results about water dynamic in the Chapter 7 and also the results of soil water monitoring carried out in Manaus by Cabral, 1991; Hoddnet et al., 1996; Teixeira et al. 1997).

In Figures 4.2 and 4.3, the SWRC for the lower h range resembles SWRCs for a coarse textured soil, although this soil has over 600 g kg^{-1} clay. In the dry range, the magnitudes of the values resemble typical clayey soils. This paradoxical behaviour was partially explained in Chapter 3 by the strong aggregation of the clay particles and the formation of two pore systems. In this chapter, these phenomena are further discussed in relation to their consequences for the water fluxes.

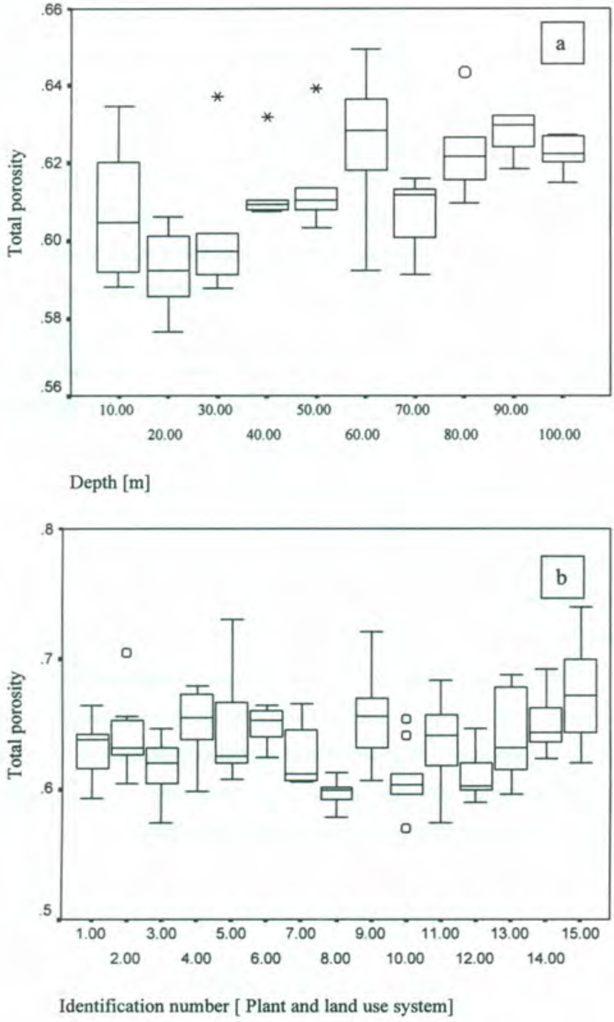

Figure 4.1. Box plot of the estimation of the total porosity on an clayey Ferralsol in the central Amazon a) at a soil profile of 100 cm depth evaluated at each 10 cm, b) at different positions within three land use system. The dark horizontal line shows the median of the porosity. The top and bottom lines of the box show the 25th and 75th percentiles — half the porosity values fall within this range. The "whiskers" show the highest and lowest porosity (not considered outliers). The stars show the outliers (i.e. the values that fall outside ± 1.5 the height of the box). The empty circles, called far outside values, show extreme values. (i.e., ± 3.0 the height of the box).The identification is given in Table 3.1.

Table 4.2 Volumetric water content [lines] and soil water pressure head [columns] evaluated in soil samples from a profile of 1m depth evaluated at each 10 cm depth in a clayey Ferralsol.

Depth	Statistics	pF 0.0	pF 0.5	pF 1.0	pF 1.5	pF 1.8	pF 2.0	pF 2.2	pF 2.5	pF 3.0	pF 3.5	pF 4.2
cm		θ [m3 m^{-3}]										
10	Mean	0.5735	0.5381	0.5006	0.4392	0.4260	0.4099	0.4033	0.3927	0.3780	0.3648	0.2188
	SE	0.0057	0.0050	0.0049	0.0043	0.0051	0.0049	0.0049	0.0050	0.0050	0.0050	0.0085
20	Mean	0.5377	0.5128	0.4909	0.4568	0.4446	0.4296	0.4226	0.4122	0.3983	0.3875	0.2453
	SE	0.0084	0.0065	0.0035	0.0024	0.0028	0.0032	0.0025	0.0026	0.0024	0.0025	0.0045
30	Mean	0.5353	0.5117	0.4927	0.4619	0.4510	0.4359	0.4302	0.4209	0.4067	0.3942	0.2643
	SE	0.0104	0.0111	0.0106	0.0117	0.0115	0.0124	0.0121	0.0121	0.0120	0.0121	0.0048
40	Mean	0.5414	0.4991	0.4816	0.4482	0.4396	0.4267	0.4184	0.4117	0.3994	0.3825	0.2516
	SE	0.0062	0.0105	0.0108	0.0119	0.0122	0.0101	0.0118	0.0117	0.0118	0.0117	0.0038
50	Mean	0.5424	0.5022	0.4851	0.4507	0.4409	0.4279	0.4188	0.4095	0.3960	0.3830	0.2583
	SE	0.0139	0.009	0.0096	0.0089	0.0086	0.0089	0.0085	0.0083	0.0084	0.0081	0.013
60	Mean	0.5524	0.5096	0.4886	0.4499	0.4388	0.4224	0.4149	0.4057	0.3891	0.3753	0.2530
	SE	0.0139	0.009	0.0096	0.0089	0.0086	0.0089	0.0085	0.0083	0.0084	0.0081	0.0132
70	Mean	0.5314	0.5024	0.4844	0.4461	0.4291	0.4204	0.4093	0.4037	0.3885	0.3754	0.2635
	SE	0.0082	0.0068	0.0059	0.0061	0.0047	0.0061	0.006	0.0059	0.0056	0.0050	0.0073
80	Mean	0.5383	0.5126	0.4965	0.4555	0.4370	0.4281	0.4153	0.4093	0.3927	0.3784	0.2849
	SE	0.0052	0.0037	0.0061	0.0067	0.0088	0.0086	0.0089	0.0093	0.0089	0.0082	0.0038
90	Mean	0.5493	0.5176	0.5019	0.4617	0.4434	0.4333	0.4211	0.4146	0.3949	0.3801	0.2741
	SE	0.0069	0.0074	0.0074	0.0083	0.0087	0.0086	0.0086	0.0091	0.0093	0.0095	0.0071
100	Mean	0.5409	0.5170	0.5026	0.4817	0.4576	0.4461	0.4376	0.4250	0.4073	0.3885	0.2949
	SE	0.0065	0.0048	0.0031	0.0029	0.0022	0.0023	0.0024	0.0026	0.0029	0.0028	0.0045

Table 4.3 Soil water retention measured at the soil surface on different positions within land use systems in a clayey Ferralsol.

Plant and land use system	Statistics	pF 0	pF 0.5	pF 1.0	pF 1.5	pF 1.8	pF 2.0	pF 2.2	pF 2.5	pF 3.0	pF 3.5	pF 4.2
Cupuaçu – AG	Mean	0.558	0.5162	0.461	0.3963	0.3727	0.3617	0.3470	0.3357	0.3254	0.311	0.199
[1]	SE	0.0113	0.0101	0.009	0.0111	0.0116	0.0104	0.0099	0.0098	0.0103	0.011	0.023
Annatto – AG	Mean	0.5708	0.532	0.4824	0.4193	0.3989	0.3875	0.3725	0.3565	0.3463	0.331	0.2265
[2]	SE	0.0079	0.0053	0.010	0.0133	0.0136	0.0141	0.0144	0.0125	0.0118	0.0128	0.0105
Brazil nut – AG	Mean	0.5627	0.5275	0.484	0.4201	0.3950	0.3836	0.3680	0.3552	0.3381	0.3132	0.2118
[3]	SE	0.0132	0.0113	0.006	0.0097	0.0113	0.0121	0.0121	0.0123	0.0112	0.0103	0.0040
Peach palm – AG - F	Mean	0.5646	0.5101	0.4490	0.3944	0.3763	0.3620	0.3471	0.3359	0.3260	0.3123	0.2067
[4]	SE	0.0095	0.0088	0.0084	0.0093	0.0103	0.0100	0.0105	0.0104	0.0113	0.0130	0.0108
Peach palm – AG -P	Mean	0.5570	0.5207	0.4717	0.4126	0.3904	0.3763	0.3638	0.3479	0.3307	0.3164	0.2094
[5]	SE	0.0058	0.0101	0.0151	0.0195	0.0201	0.0201	0.0199	0.0195	0.0187	0.0201	0.0122
Pueraria – AG	Mean	0.5760	0.5526	0.5251	0.4790	0.4576	0.4473	0.4307	0.4150	0.3938	0.3612	0.2255
[6]	SE	0.0082	0.0089	0.009	0.0077	0.0089	0.0098	0.0091	0.0096	0.0068	0.0058	0.0082
Cupuaçu - M	Mean	0.5733	0.5330	0.4822	0.4286	0.4036	0.3904	0.3789	0.3693	0.3536	0.3307	0.2228
[7]	SE	0.0134	0.0150	0.0107	0.0104	0.0097	0.0101	0.0098	0.0099	0.0078	0.0075	0.0070
Grass – M	Mean	0.5533	0.5289	0.503	0.4643	0.4447	0.4279	0.4123	0.3996	0.3897	0.3675	0.2441
[8]	SE	0.0104	0.0095	0.0093	0.0085	0.0084	0.0077	0.0077	0.0081	0.0071	0.0064	0.0057
Peach palm – M - F	Mean	0.5982	0.563	0.5023	0.4391	0.4160	0.4030	0.3835	0.3634	0.3415	0.3281	0.2127
[9]	SE	0.0134	0.0099	0.019	0.0214	0.0203	0.0203	0.0225	0.0156	0.0154	0.0155	0.0115
Peach palm – M – bF	Mean	0.5677	0.5439	0.5080	0.4653	0.4476	0.4333	0.4161	0.3995	0.3756	0.3643	0.2404
[10]	SE	0.0073	0.0060	0.0070	0.0073	0.0071	0.0085	0.0095	0.0075	0.0077	0.0073	0.0089
Peach palm – M – P	Mean	0.5925	0.5535	0.5005	0.4392	0.4194	0.4061	0.3910	0.3672	0.3489	0.3367	0.2165
[11]	SE	0.0153	0.0110	0.0172	0.0187	0.0181	0.0187	0.0181	0.0170	0.0146	0.0146	0.0092
Peach palm – M – bP	Mean	0.5755	0.5525	0.5257	0.4790	0.4626	0.4506	0.4361	0.4153	0.3895	0.3761	0.2397
[12]	SE	0.0060	0.0071	0.0064	0.0065	0.0065	0.0065	0.0065	0.0071	0.0055	0.0054	0.0055
Vismia - Sec. Forest	Mean	0.5690	0.5340	0.5044	0.4685	0.4479	0.4318	0.4156	0.3995	0.3849	0.3505	0.2102
[13]	SE	0.0153	0.0176	0.0181	0.0191	0.0193	0.0162	0.0165	0.0163	0.0157	0.0152	0.0090
Matá matá - Prim. Forest	Mean	0.5762	0.5306	0.4748	0.4095	0.38850	0.3744	0.3601	0.3471	0.3233	0.3088	0.1685
[14]	SE	0.0078	0.0091	0.0090	0.0090	0.0102	0.0098	0.0092	0.0087	0.0080	0.0076	0.0049
Bacaba – Prim. Forest	Mean	0.5772	0.5275	0.4859	0.4325	0.4138	0.4011	0.3884	0.3728	0.3519	0.3339	0.1706
[15]	SE	0.0073	0.0077	0.0090	0.0083	0.0091	0.0091	0.0086	0.0088	0.0088	0.0084	0.005

AG = agroforestry system; M = monoculture system; b = between the palms; F = Peach palm for fruits production; P = Peach palm for palm heart production

The discussion about SWRC will be concentrated on data evaluated between pF 1.5 and pF 3.5. Capillary pores compose this range, and the fluid permeating them generally obeys the laws of capillary and Darcy flow. Moreover, most processes of water redistribution occur in this range, and the flow can be considered laminar.

The data evaluated at h of 0, 0.5 and 1.0 pF were an attempt to enlarge the range of the SWRC and to give some idea about the magnitude of these values. Accurate evaluation of the water holding capacity at low water potentials is an unsolved problem in soil physics. The empty macropores constitute barriers to capillary flow, permitting only very slow film of water creep along their walls. When filled with water, however, macropores permit very rapid flow, often turbulent rather than strictly laminar (see, e.g., Beven and German, 1982; McCoy et al., 1994; Myasaki, 1995). Therefore, these data have many uncertainties. Specifically, at pF = 0 the saturated samples were subjected to a quick drainage and have lost some amount of water during the weighting procedures. The gradient in a soil core, for instance, when it was equilibrated at pF 0.5 ($\approx$ 32 mm of water pressure at the centre of the core), and considering that the steel cylinder had 5 cm high, actually the soil core had at the upper surface a pressure head potential of $\approx$ 57 mm and at the bottom $\approx$ 17 mm, yielding a relatively large percentile variation across the core. The same calculations of gradient apply to the water determined at samples submitted to pF 1.0. Moreover, Corey (1992) asserted that at conditions above 85 % of the soil saturation capacity, the nonwetting phase is not continuous and the air is not free to enter all parts of the porous medium, and the regions of the soil matrix containing some of the larger pores may be entirely isolated from the air phase surrounding water filled pores. The problem is further complicated by the large presence of macropores in the clayey Ferralsols.

Recently, methods have been developed to even out gravitational gradients in evaluation of low h in the laboratory (Rosenberg and McCoy, 1990; Logsdon et al., 1993); they showed positive air entry values for some soils. The phenomenon of positive air entry values was also observed in the present project, when determinations were carried out in field conditions using a tension infiltrometer. The positive air entry values means that at zero water potential (h = 0) some pores are still empty.

The most promising field technique for the evaluation of macroporosity distribution is tension infiltrometry, where the field near-saturated hydraulic conductivity and sorptivity have been used to distinguish infiltration in the macropores from that of the soil matrix (Messing and Jarvis, 1993; Wilson and Luxmoore, 1988; Watson and Luxmoore, 1986). The tension infiltrometer method is further discussed in Chapter 6.

The magnitude of the value obtained from at pF 4.2 in both data sets analysed [0.20 – 0.30 m^3 m^{-3}] show lower values of water retained than previously published data (Camargo and Rodrigues, 1979). Apart from differences in the clay content of the soil profiles evaluated by the different studies, errors may arose from the transformation of soil mass base into soil volume base (pF 4.2 is evaluated with disturbed samples, see details in the methodology). Further, because of an extremely low unsaturated hydraulic conductivity at pF 4.2, the soil samples need a long time to achieve the equilibrium at pF 4.2. The indication of equilibrium is normally the stop of outflow flux from the sample. However, because of the low flux, sometimes it seems that the outflow flux stopped and the analyses are finished, but, actually the equilibrium was not achieved. Many researchers working with samples from clayey Ferralsols have found greater values of water retained with increasing h, which is theoretically impossible. The reasons for that are probably related to insufficient time for the equilibrium to be achieved and variations in the temperature in laboratory, which may have a significant effect on the values of water surface tension (see Equation 4.5). Lack of equilibrium may also be a result of poor contact between the sample and the porous plate. The use of a linear scaling approach was proposed by Moraes and Libardi (1996) to recuperate part of the physically incorrect values in the soil water retention measurements.

The amount of water held by soils at higher water pressure heads is fairly well correlated with the surface area of a soil and would represent molecular layers of water around the soil particles (Hillel, 1998), therefore, it is improbable that capillary models and Darcian flow apply for these slight films of water subjected to adsorptive force fields (Corey, 1992; Iwata et al, 1995).

Table 4.3 and Figures 4.2 and 4.3 show that the original VG equation does not have enough flexibility to fit reasonably the experimental water retention data. Better fits (see also statistical parameter in Table 4.3) were achieved using the VG-bimodal, which had enough flexibility to fit the two pore systems present in the clayey Ferralsols in the central Amazon. A better fit could be achieved by optimising the VG equation without constraining the m parameter or employing more modes. However, if the objective of the fitting procedure also includes to use the fitted model in numerical simulations or inverse method to determine hydraulic functions, keeping the equations with a small number of parameters may avoid considerable numerical problems (van Genucthen and Nielsen, 1985; Durner, 1994). The small n values presented in Table 4.3 and in Table 4.5 indicate a relatively broad pore-size distribution (van Genuchten and Nielsen, 1985). The α values equal approximately the inverse of the pressure head at the inflection point where [$d\theta$ / dH] has its maximum value (van Genuchten and Nielsen, 1985; Wösten and van Genuchten, 1988).

The VG parameters can be physically interpreted in both Tables 4.2 and 4.3 as well in both approaches of VG and the VG – bimodal. In a comparison between two layers in Table 4.2, the smaller α indicate that the air began to enter at lower h (relatively more saturated conditions). It can be visualised in Figures 4.2 and 4.3. These results agree with the results of Φ (Figure 4.1) indicating a soil with higher porosity in the layers at 10 and 60 cm (i.e., the smaller α indicate that the porosity is composed by large pores in relation to the other layers). Evidently, completely different pore systems are represented when using different models (see, in Figure 4.4 the representation of the pore size distributions from unimodal and bimodal distribution for the depths of 10 and 60 cm). The unimodal distributions are fairly similar in the location of the maximum pore size (Table 4.3), but because it was not able to fit reasonably the measured data set, it is not discussed further.

Better fits were obtained using the VG – bimodal approach (Table 4.3 and Figure 4.2 and 4.3). Pore size distributions based on the bimodal retention curve display a secondary structural pore system at the left side of the primary (textural) pore system (Figure 4.4). The secondary pore system is due to the effect of aggregation of the clay particles, which was discussed in the Chapter 3. It shows basically two principal air entry points; one for the interaggregate porosity and another for intraaggregate porosity. The interaggregate pores include macropores, mesopores and part of the micropores range (probably with adjacent aggregates intimately continuos); the intraaggregate pores include micropores, ultramicropores and cryptopores (see Table 4.1 for the division of the pore classes).

The clearly bimodal pore size distribution of the clayey Ferralsols is shown in Figure 4.4 for the profile and Figures 4.7 and 4.8 for the samples collected at the soil surface.

4.3.2 Soil surface

The complete data set of measured water soil retention from the fifteen positions in the soil surface is given in Appendix 4-A. The mean values and standard error for the measured retention data are shown in Table 4.4. Figure 4.1 (a) shows that the effect of the exposition of the soil in the position between cupuaçus growing in monoculture (position 8) had as a consequence the lowest value of ϕ. In contrast, the soil under primary forest (positions 14 and 15)] shows the highest ϕ, the causes for this difference have already been discussed in Chapter 3. As for bulk density, statistical tests were only able to detect a significant difference between the position between the cupuaçus in the monoculture and the bacabas, indicating a difference between the lower porosity of 0.08 Mg m^{-3} for the soil near bacabas.

Table 4.4 Estimated hydraulic parameters from soil samples taken in different land use systems in a clayey Ferralsol in the central Amazon.

Parameters	Cupuaçu AG	Annatto AG	Brazil nut AG	Peach palm F AG	Peach palm P AG	Pueraria AG	Cupuaçu M	Grasses AG	Peach palm F M	Peach palm aF M	Peach palm P M	Peach palm aP M	Vismia	Matá-matá	Bacaba
	1+	2+	3	4+	5	6	7+	8	9	10	11	12	13	14†	15
							unimodal								
θ_s (m^3 m^{-3})	0.56	0.57	0.61	0.56	0.61	0.57	0.57	0.65	0.56	0.57	0.65	0.57	0.56	0.62	0.59
θr (m^3 m^{-3})	0.19	0.09	0.00	0.12	0.00	0.00	0.00	0.00	0.00	0.00	0.00	0.00	0.00	0.00	0.00
α (cm-1)	0.41	0.52	1.42	0.66	1.88	0.13	1.09	1.51	0.24	0.30	1.68	0.16	0.14	1.31	0.63
n	1.20	1.11	1.09	1.14	1.09	1.09	1.08	1.09	1.08	1.08	1.09	1.09	1.09	1.10	1.10
SAG	0.0134	0.0148	0.0122	0.0164	0.0118	0.0160	0.0160	0.0116	0.0134	0.0117	0.0112	0.0144	0.0175	0.0151	0.0196
							bimodal								
θ_s (m^3 m^{-3})	0.57	0.58	0.57	0.59	0.57	0.58	0.59	0.55	0.61	0.58	0.61	0.58	0.58	0.49	0.60
θr (m^3 m^{-3})	0.12	0.06	0.10	0.12	0.08	0.06	0.09	0.06	0.07	0.09	0.00	0.02	0.00	0.01	0.00
α_1 (cm^{-1})	0.29	0.30	0.26	0.54	0.32	0.22	0.33	0.20	0.32	0.29	0.36	0.27	0.52	0.26	0.49
n_1	1.46	1.40	1.38	1.39	1.35	1.26	1.41	1.31	1.32	1.23	1.31	1.19	1.18	1.42	1.28
w_1	0.60	0.50	0.57	0.62	0.56	0.47	0.51	0.42	0.59	0.56	0.50	0.51	0.49	0.49	0.49
α_2 (cm^{-1})	0.09×10^{-3}	0.07×10^{-3}	0.12×10^{-3}	0.09×10^{-3}	0.08×10^{-3}	0.12×10^{-3}	0.11×10^{-3}	0.08×10^{-3}	0.07×10^{-3}	0.07×10^{-3}	0.06×10^{-3}	0.06×10^{-3}	0.10×10^{-3}	0.09×10^{-3}	0.09×10^{-3}
n_2	1.25	2.37	1.99	2.87	2.68	1.90	1.89	2.28	3.86	5.17	5.47	5.78	2.00	2.23	2.44
w_2	0.40	0.50	0.43	0.38	0.44	0.53	0.48	0.58	0.41	0.44	0.50	0.49	0.51	0.51	0.51
SAG	0.0020	0.0022	0.0021	0.0017	0.0017	0.0016	0.0014	0.0028	0.0015	0.0019	0.0024	0.0024	0.0029	0.0029	0.0021

AG = agroforestry system; M = monoculture system; b = between the palms; F = Peach palm for fruits production; P = Peach palm for palm heart production
+ Fixed θs at the maximum value measured (unimodal). † Fixed θs at the maximum measured (bimodal).

The difference between the bulk density of the soil near bacabas and between the cupuaçus is contained within the interval [0.02 to 0.15 Mg m^{-3}] at 95% of confidence (details about how to calculate confidence intervals using the Tukey's test are given in Appendix 3-A).

Analysing the heights of boxes and whiskers in Figure 4. 1 (b) (see legend on Figure 4.1 for a statistical explanation) they show a high variability of ϕ in some positions, especially near the peach palms. This is probably not only due to a higher soil variability near peach palms in comparison to the other sampling position, but it is also a consequence of the methodology employed to take the samples. The insertion of the soil cylinders into the soil was done by hammering the cylinder into the soil, which is the most usual method to collect soil samples to evaluate bulk density and SWRC. However, these processes cause some disturbance in the soil, especially, when a higher concentration of roots is present. In order to reduce the variability and increase the reliability of the measurements more refined methods like hydraulic jacks should be used.

On the other hand, the small range evaluated in the soil covered by pueraria in the agroforestry system (position 6 on Figure 4.1 b) confirms field observations that the well developed canopy of pueraria created a partial buffer against weather variations, and probably a better environment for fauna activities, leading to a homogenisation of the soil at that position. The homogeneity is also corroborated by smaller variations of the water holding capacities at different h at those positions (Table 4.4).

Table 4.5 Estimated parameters for soil water retention curves at different depths in a clayey Ferralsols in the central Amazon.

Parameters	Depth (cm)									
	10	20	30	40	50	60	70	80	90	100
	unimodal – van Genuchten									
θ_s (m^3 m^{-3})	0.57	0.53	0.51	0.52	0.52	0.55	0.53	0.55	0.55	0.54
θr (m^3 m^{-3})	0.00	0.00	0.00	0.00	0.00	0.00	0.00	0.00	0.00	0.00
α (cm^{-1})	0.45	0.08	0.02	0.03	0.05	0.56	0.07	0.33	0.13	0.05
n	1.08	1.08	1.08	1.08	1.07	1.06	1.07	1.06	1.08	1.07
	bimodal – van Genuchten									
SAG	0.0188	0.0186	0.0198	0.0225	0.0211	0.0177	0.0190	0.0135	0.0158	0.0133
θ_s (m^3 m^{-3})	0.56	0.54	0.53	0.54	0.54	0.58	0.54	0.54	0.55	0.54
θr (m^3 m^{-3})	0.08	0.07	0.23	0.18	0.20	0.07	0.21	0.15	0.12	0.11
α (cm^{-1})	0.20	0.18	0.09	0.31	0.35	1.06	0.16	0.12	0.16	0.11
n_1	1.52	1.30	1.40	1.26	1.28	1.25	1.38	1.53	1.36	1.24
w_1	0.39	0.35	0.40	0.42	0.43	0.42	0.41	0.37	0.36	0.41
α_2	0.09 x 10^{-3}	0.07 x 10^{-3}	0.12 x 10^{-3}	0.10 x 10^{-3}	0.11 x 10^{-3}	0.07 x 10^{-3}	0.12 x 10^{-3}	0.10 x 10^{-3}	0.09 x 10^{-3}	0.07 x 10^{-3}
n_2	2.72	3.20	3.80	3.63	3.52	3.73	3.28	2.05	2.34	2.39
w_2	0.61	0.65	0.60	0.58	0.57	0.58	0.59	0.51	0.64	0.59
SAG	0.0028	0.0021	0.0025	0.0021	0.0018	0.0026	0.0015	0.0023	0.0019	0.0036

SAG : Statistic average deviation

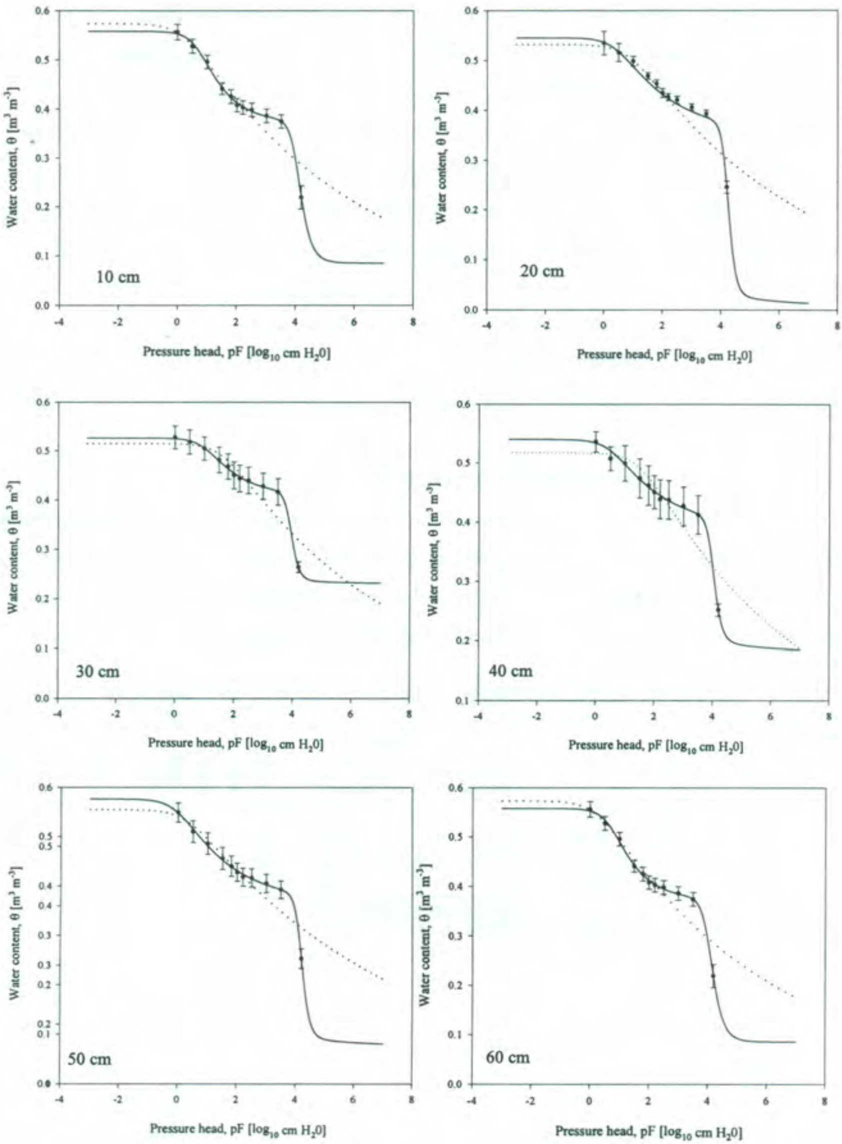

Figure 4.2 Measured values and fitted soil water retention curve of soil samples collected at different dephts on an clayey Ferralsol in the central Amazon. Error bars represent the confidence intervals at 95 % of the measured values. Dotted line are the predicted van Genuchten unimodal. Continuous line are the predicted bimodal.

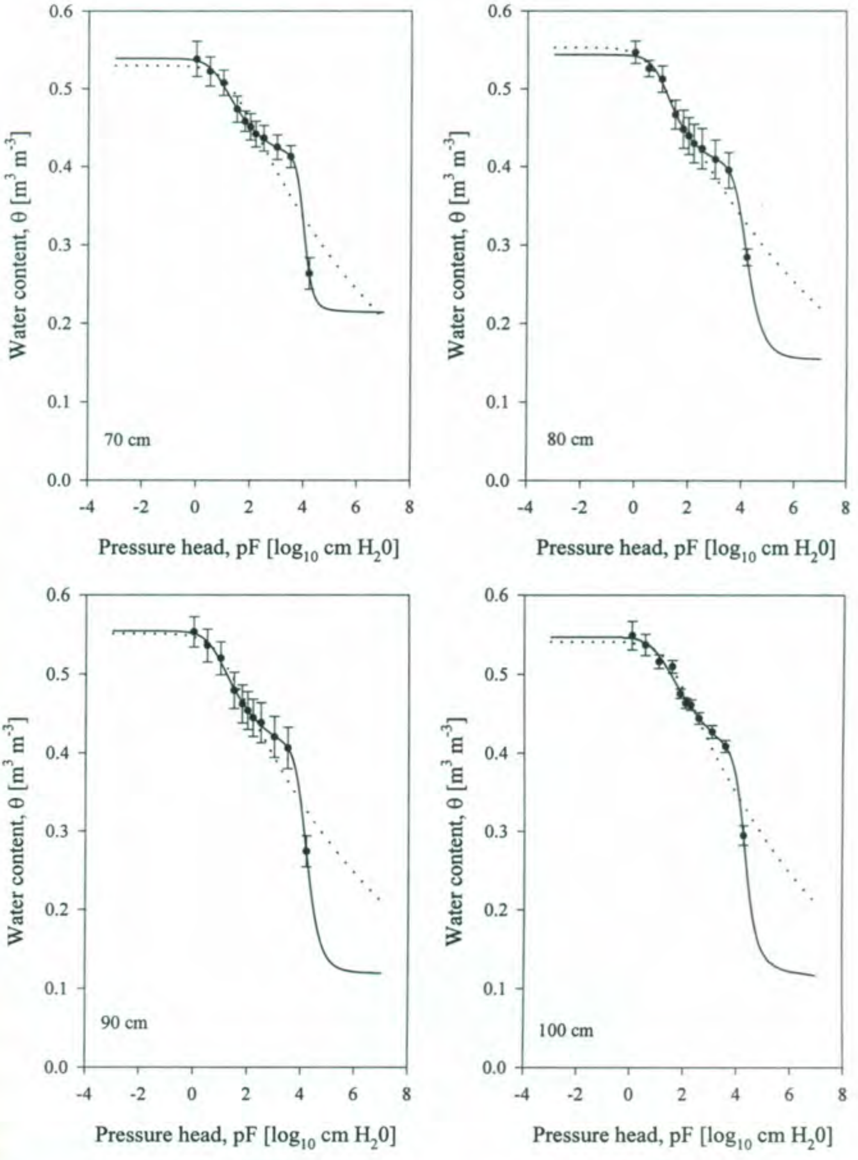

Figure 4.3 Measured values and fitted soil water retentios curves of soil samples collected at different dephts on an clayey Ferralsol in the central Amazon. Error bars represent the confidence intervals at 95 % of the measured values. Dotted line are the predicted van Genuchten unimodal. Continuous line are the predicted bimodal.

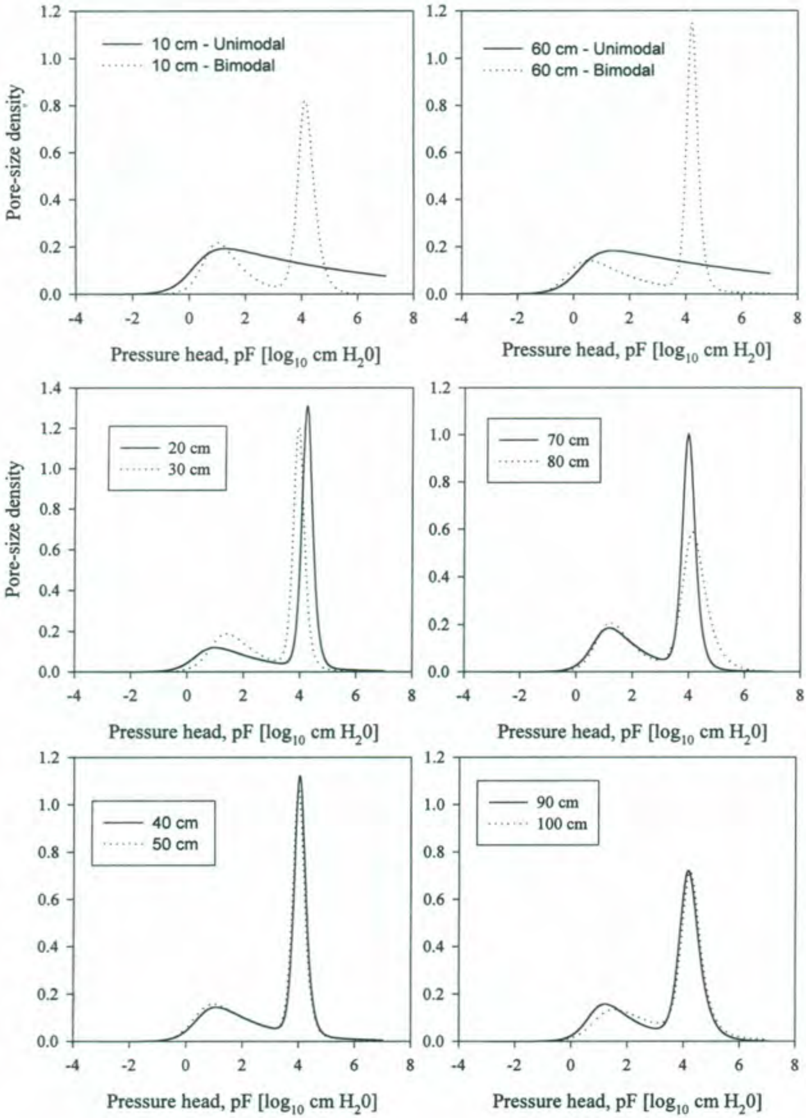

Figure 4.4 Pore-size density estimated from the fitted soil water retention curves from soil samples collected at different depths in a soil profile on an clayey Ferralsol in the central Amazon.

4.3.3 Land use effects on pore size distribution

Table 4.4 shows the measured soil water retention evaluated in soil samples collected near different plants species growing in the agroforestry system, monoculture of cupuaçu, monoculture of peach palm, secondary forest and primary forest. Table 4.5 shows the estimated parameters of the fitted VG and VG-bimodal equations. Figure 4.1 shows ϕ and Figures 4.5 and 4.6 the fitted equations for the models of VG and VG- bimodal. As for the soil profile, only the VG – bimodal was able to fit reasonably the measured water retention data and these results will not be discussed further. Figures 4.7 and 4.8 show the continuous pore-size distribution evaluated from the VG – bimodal model.

The analysis of the pore size distribution was more effective to detect some differences that were indistinct when the pore system was analysed pooling the pore sizes (i.e., ϕ).

For explanatory reasons, the discussion of the pore size distribution was divided according to the land use systems.

4.3.3.1 Agroforestry system

Table 4.6 shows that the macropores represent as much as 40% of ϕ near all plants in the agroforestry system. The plotted pore-size distribution in Figure 4.7 shows a peculiar pore-size distribution for the cover crop pueraria. It changes to the lower curve in the macropore range to the higher curve in the mesopore range (this phenomenon is pointed by arrows in Figure 4.7). Macropores are the least stable of all pore size classes, and are very sensitive to management and collapse when they experience stress (Kay and Angers, 2000). For instance, the degradation of the macroporosity because of agricultural use was clearly shown on clayey Ferralsols by Medina (1985), Chauvel et al. (1991), and Teixeira et al. (1996). Pueraria creates a higher percentile of pores with radii in the mesopore range that are more effective to hold water and maintain it available for the plants. A higher percentile of the pore size in the mesopore range could help plants to tolerate water-limiting situations, as the mesopores are more effective in water storage than the macropores. Moreover, water is not held in the mesopores with so high energy that are unavailable to the plants, as happens in micropore range. The more efficient storage of water from the irregular rainfalls that occur in the central Amazon in the dry season can be very important when water availability seems to be a limiting factor for many plant species. Conversely, under dry conditions, transmission of water across the matrix potential occurs more rapidly in the mesopore range than in the small ones as presented in the primary forest.

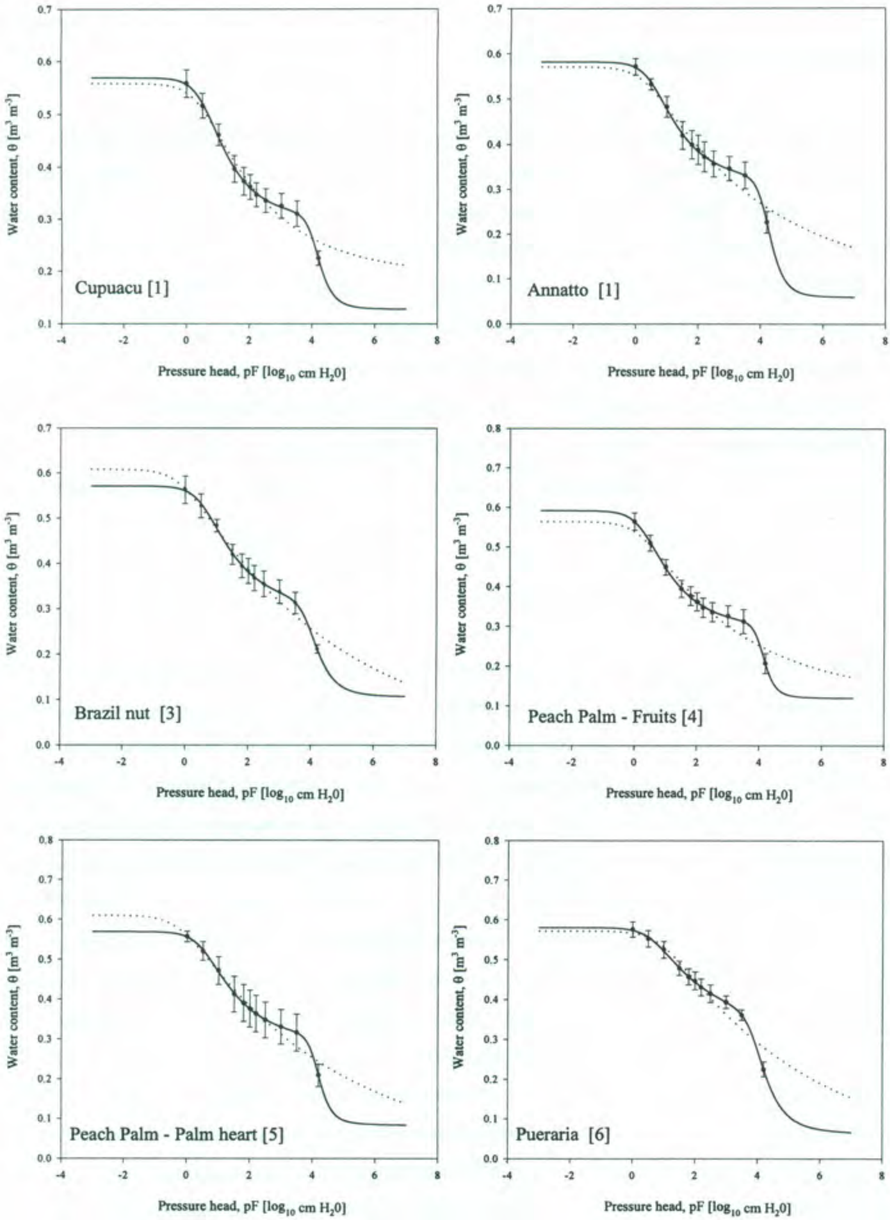

Figure 4.5 Measured values and fitted soil water retention curves from soil samples collected at the soil surface near different species of plants growing in an agroforestry system on an clayey Ferralsol in the central Amazon. Error bars represent the confidence interval at 95 %.

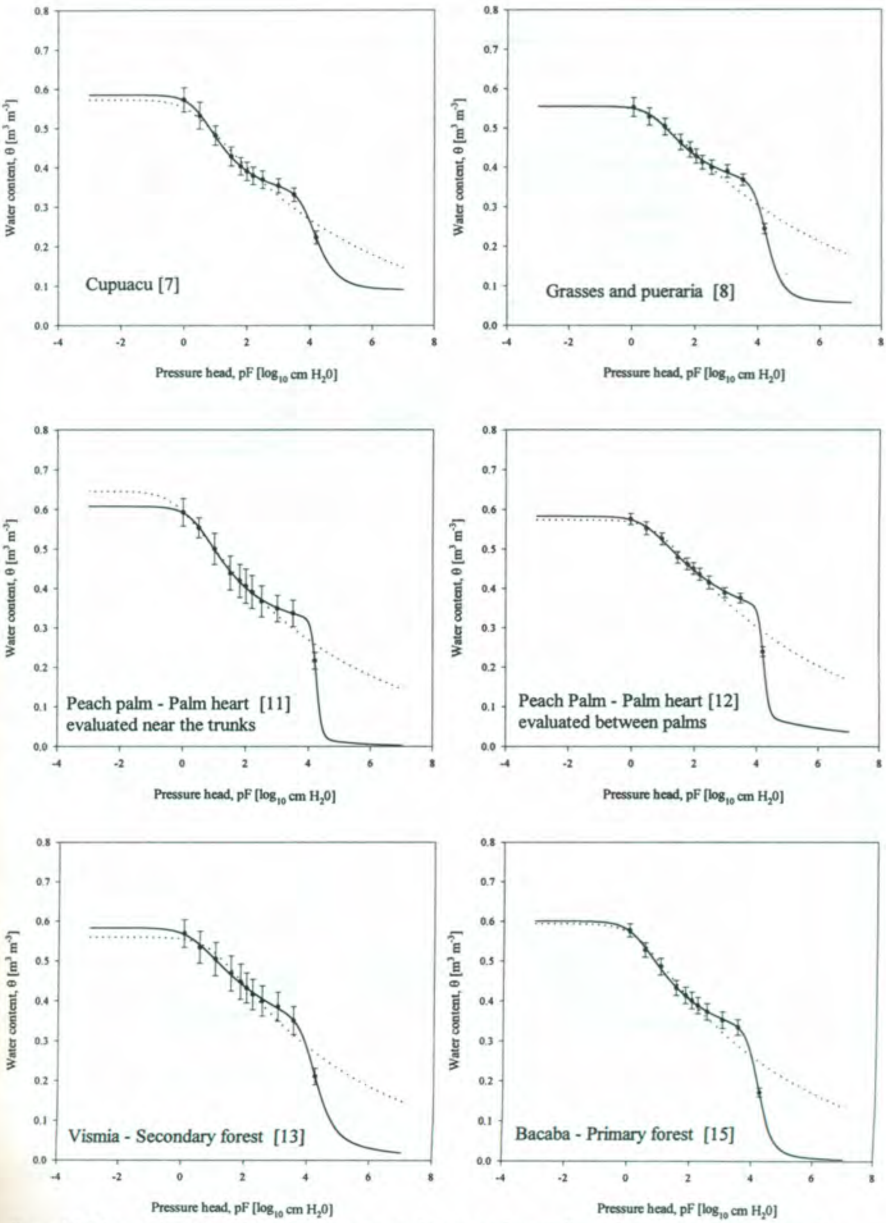

Figure 4.6 Measured values and fitted soil water retention curves from soil samples collected at the soil surface near different species of plants growing in a monocultures of cupuacu, a monoculture of peach palm, in a secondary and primary forest on an clayey Ferralsol in the central Amazon.
Error bars represent the confidence interval at 95 %.

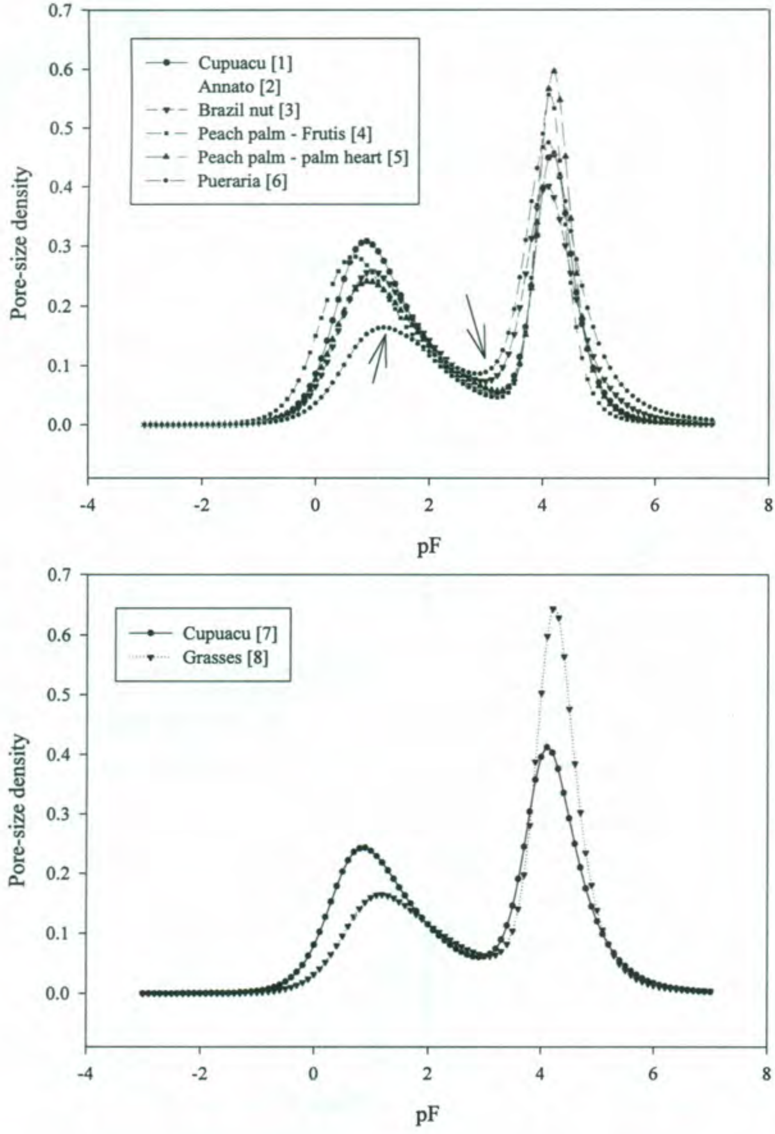

Figure 4.7 Pore-size density estimated from the fitted soil water retention curves from samples collected near different species of plants growing in an agroforestry system and a monoculture of cupuacu on a clayey Ferralsol in the central Amazon.

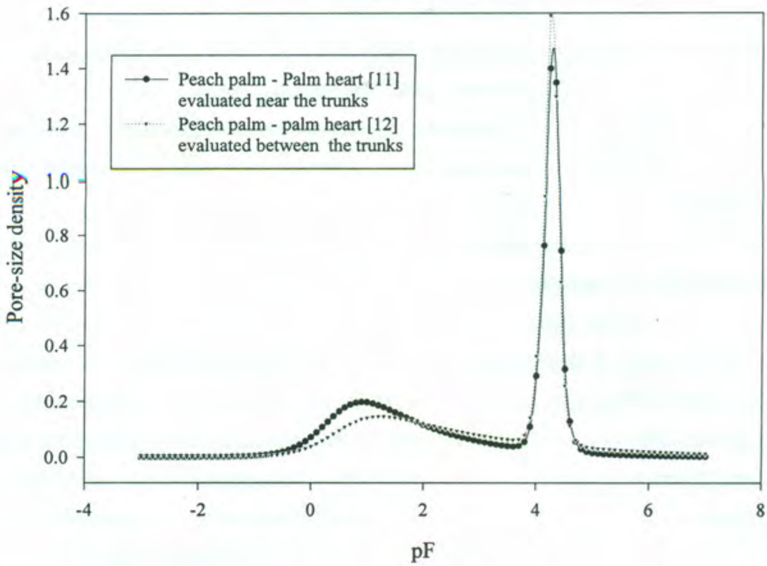

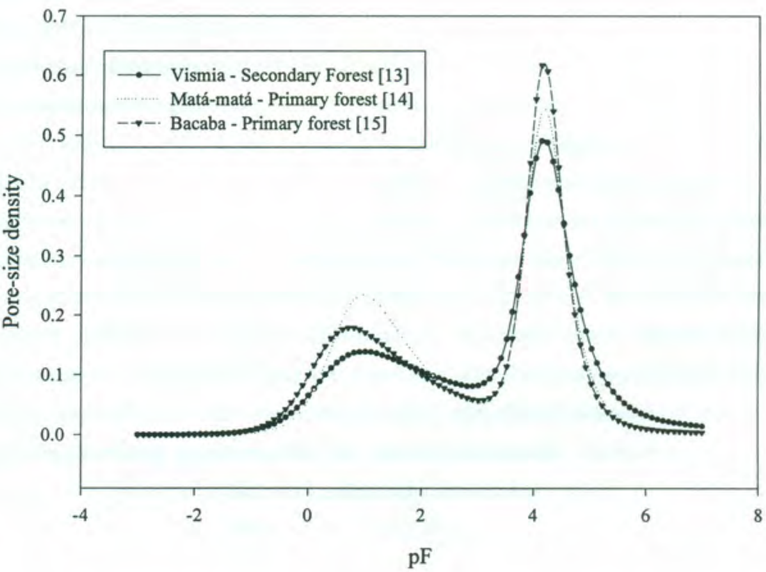

Figure 4.8 Pore-size density estimated from the fitted soil water retention curve from samples collected near different species of plants in an monoculture of peach palm, and secondary and primary forest on an clayey Ferralsol in the central Amazon.

The controversial advantages and disadvantage of changing the pore size distribution is discussed further in the primary forest results. Nevertheless, pueraria seems to be a good option to maintain or rehabilitate the soil porosity of clayey Ferralsols. Certainly, other processes like connectivity and tortuosity of pores also influence the soil water retentivity evaluated in different pore-size arrangements.

4.3.3.2 Monoculture of cupuaçu

Table 4.6 shows a greater reduction of pores in the macropore range in the position between the cupuaçus covered basically by grass and some plants of pueraria. However, the analysis of ϕ could not identify a clear difference between the soil near the cupuaçus and between them; the distribution of ϕ was more efficient to explain some field observations. The pore size distribution clearly indicated a rearrangement of the pore space with probable consequences for the water dynamics. The porosity in the soil covered partially by grasses between the cupuaçus was not only reduced in magnitude (Figure 4.1) with a greater reduction of the macroporosity (Table 4.6), but also shows an enlargement of the percentage of ultramicropores and cryptopores. In those pore ranges, water is not only located in pores but the most part is adsorbed on the surface of clay particles with completely different properties in comparison to free water (see, discussion about free water and bound water in Chapter 5). Little amount of this water is available to plants and its flow rate is very slow.

A complex process may explain the observed effects of the water deficit on plants growing between the cupuaçus in the dry season. As a general rule, roots of plants penetrate pores larger than 10 µm (Kay and Angers, 2000), but these pores need to be easily expandable for the roots to grow through them, and continuous for the root to extend normally (Greenland, 1979). With reduction of the porosity in the soil covered by grasses between the cupuaçus only few roots could penetrate the remaining small pores (because they are too small) and could not use a part of the water (i.e., water held with high energy by the soil forces) by simply interception between roots and water. Probably, in the compacted sites between the cupuaçus with reduced porosity, only few roots may penetrate small pores and the interception mechanism of the root growth is blocked.

4.3.3.3 Monoculture of peach palm

In Table 4.4 and Figures 4.5 and 4.6, the high amount of water retained by samples collected near the peach palms when submitted to increasing water potential in relation to the other plants can be seen. Apart from some bias introduced by the core sampling method, a rearrangement of the pore size classes occurred on the soil surface near the peach palms. The field observations indicating that the aggressive superficial and coarse root system of the peach palm which seems to compact the soil have already been discussed in Chapter 3. The rearrangement of the porosity in other classes with small pores is shown in Table 4.6. It indicates that even if ϕ remains practically unchanged (Figure 4.1), alteration in the pore distributions can have a considerable effect on the water dynamics, because the radii of the pores govern not only the rate of water movement but also the availability of water to these palms. The smaller the pore, the greater the suction by which water is held. It is frequently observed that weed plants are less common near the peach palms, which is in part explained by light competition, which is usually a correct explanation. A reduced soil water content (Teixeira et al., 1997; Renck, 2000) due to a high absorption by the palms is also another explanation. However, it is also important to point out that not only the amount of water is reduced near the peach palms, but also a large amount of the water is strongly held by the soil, which could cause drought conditions for many weed plants. The explanation given above, concerning the reduction of root growth in the soil owing to the small size of the pores is also valid in this situation. However, the phenomenon of redistribution of the porosity near the peach palms seems to be distinct from that in the soil covered partially only by grass in the monoculture of cupuaçus. The range where the porosity increases near the peach palms was between 30 and 5 µm and in the grasses the highest range is in the pores > 5 µm. This fact indicates that, probably, distinct processes of degradation of the soil structure occurred.

The highest peak in the micropore range in the monoculture of peach palm in Figure 4.8 is presumably a consequence of a specific process of compression of the soil, leading to concentrate the pore in a small group of radii, with a specific air entry value. The analysis of the VG – bimodal parameters show that the n_2 parameters for the peach palms assume high values. The n_2 value represents the slope of the second peak, and a greater value can be interpreted as an indication that the pores are concentrated in a specific radius or small radii of pores. In the soil between the cupuaçus it seems to be more an effect of the water absorbed on the surface of the clay particles (i.e., the peak is from the addition of ultramicropores and cryptopores which are pooled together in the last category of pores > 5µm inTable 4.6).

4.3.3.4 Primary and secondary forest

Between the land use systems analysed in this study, probably only the porosity in the soil under primary forest (Figure 4.8) can be considered to be in a dynamic equilibrium, with a rate of formation and destruction controlled basically by the soil fauna and by plant roots. Any change in soil conditions may affect that balance. Macropores formed by shrinkage resulting from desiccation of the first layers by plant roots is probably another explanation for the porosity in the clayey Ferralsol (Chauvel, 1982). However, the forest canopy creates a layer with saturated air humidity, which operates as a buffer system against the direct evaporation of the soil water (Leopoldo et al, 1997). The reduced rainfall and the continuous evapotranspiration at high rates during the dry season in the central Amazon (normally on July until September) lead the first layers of soil under the primary forest to be dry, due to the continuos uptake of water by the plant roots. Some climate aspects are discussed in Chapters 2.

Pores with diameters > 300 μm support infiltration when large amounts of water reach the soil surface (Kay and Angers, 2000). Therefore, the existence of pores with greater diameters is essential to infiltrate large rainfalls, for instance with an intensity of 70 mm h^{-1} for more than an hour (Marques et al., 1981). The existence of this large pore system, which represents about 40% of the ϕ in the primary forest (Table 4.6), is responsible for the higher hydraulic conductivity at and near saturation shown by the clayey Ferralsols (see Chapter 5) and is essential for the maintenance of a system of rapid drainage into this soil to avoid runoff and hence water erosion processes. The macropores drain water rapidly and are responsible for soil aeration and the deep penetration of water and nutrients (or pesticides, herbicides) into the soil. However, the macroporosity can also reduce the leaching rate when the nutrients are already in the soil matrix (Larsson and Jarvis, 1999), because it diminishes the amount of water that percolates through the soil. This fact may indicates that the pore-size distribution under original conditions in the clayey Ferralsol seem to be very well adapted to the climate conditions in that region. It allows a rapid drain of water, avoiding runoff and consequently erosion process and also reduces nutrient leaching from the soil matrix bypassing the water to deep layers through the macropores. On the other hand, the very small radius of the other pores as a consequence of a reduced hydraulic conductivity and fluxes through the soil matrix increases the residence time of water and nutrients to be absorbed by plant roots, macro and micro fauna in the soil matrix.

The results between primary and secondary forest are similar for the measured water retention data (Table 4.4), ϕ (Figure 4.1), the VG parameters (Table 4.5) and the relative volumetric fraction of the pores within the macropore and mesopore range (Table 4.6). This fact indicates a relative fast capacity of the natural regrowth of the spontaneous vegetation to rehabilitate soil porosity to values found in the original conditions when the primary forest covers the soil. Further, it also indicates the resilience of the clayey Ferralsol. However, the limit of disturbance at which the clayey Ferralsol is able to return to its original pore-size distribution need to be established. The concepts and processes involved in soil resilience and soil rehabilitation are given by Blum (1998).

Table 4.6 Relative volumetric fractions of the pores within various size ranges for a clayey Ferralsol with different land use systems in the central Amazon.

Relative volumetric fraction with radii	Cupuaçu AG	Annatto AG	Brazil nut AG	Peach palm F AG	Peach palm P AG	Pueraria AG	Cupuaçu M	Grasses AG	Peach palm F M	Peach palm aF M	Peach palm P M	Peach palm aP M	Vismia	Matá-matá	Bacaba
Coarse Macropores															
> 5000 µm	0.39	0.30	0.32	0.42	0.32	0.19	0.32	0.19	0.32	0.23	0.27	0.18	0.21	0.29	0.28
Macropores															
between 5000 and 75 µm	0.16	0.15	0.19	0.15	0.17	0.19	0.16	0.16	0.18	0.19	0.15	0.17	0.16	0.15	0.14
Mesopores															
between 75 and 30 µm	0.03	0.03	0.05	0.03	0.03	0.07	0.05	0.04	0.02	0.01	0.02	0.02	0.06	0.04	0.04
Micropores															
between 30 and 5 µm	0.23	0.27	0.22	0.27	0.29	0.26	0.23	0.23	0.32	0.33	0.42	0.43	0.47	0.28	0.32
† Ultramicropores and cryptopores															
> 5 µm	0.19	0.25	0.22	0.13	0.19	0.29	0.24	0.62	0.16	0.24	0.14	0.20	0.10	0.24	0.22

AG = agroforestry system; M = monoculture system; a = between the palms; F = Peach palm for fruits production; P = Peach palm for palm heart production

† Rounding errors adjusted at this level

4.4 CONCLUSIONS

4.4.1 Soil water retention curve (SWRC)

Because the structured clayey Ferralsols have two pore systems, one from the intraaggregate and the other from the interaggregate porosity, the original single sigmoidal model of van Genuchten VG could not satisfactorily relate the measured volumetric water content (θ) and water pressure head (h).

The results show that using the VG-bimodal approach, excellent fits were obtained, characterising the θ and h relationships for the soil surface in different land use systems, and also for different depths in a soil profile.

The parameters n and α in the VG models interpreted in its physical meaning were useful to confirm the presence of a layer with higher porosity and pores with higher radius about 60 cm deep in the clayey Ferralsols, located between two more compact ones.

It is emphasised that the VG and VG – bimodal model are empirical models to represent the SWRC, and the continuos pore size distributions derived from that function are probably a good approximation to the real pore size distributions.

The development of physically based models taking into account different physical laws for the range near saturation and the dry range, when the capillary law is not applicable anymore, could improve the understanding of soil water retentivity processes.

4.4.2 Pore size distribution

Pueraria seems to change the pores for the mesopore range, which appears to be more effective to hold and maintain water available for plants than the macropores.

The soil near the peach palms has a concentration of pores with a reduced radius in the micropore range, apparently originating from the pressure exerted by the root development on the soil structure.

The soil, which was not well covered by cover crops (between the cupuaçus growing in monoculture), shows a reduced total porosity and a relative pronounced reduction in the macropore range.

The soil covered by the primary forest shows more than 30% of the total porosity in the macropore range, this macropore system which drains water rapidly and is responsible for the soil aeration and the deep penetration of water and nutrients (or pesticide, herbicides) into the soil. It appears to be very well adapted to the climate conditions in that region. It allows a rapid drain of large amount of water, and avoids runoff and consequently erosion process. Further, it also may reduce the nutrient leaching of the soil matrix bypassing the water to deep layers through the macropores. Furthermore, under unsaturated conditions, the very small radius of the other pores has as a consequence a reduced hydraulic conductivity and fluxes through the soil matrix enhancing the residence time of water and nutrients and the likelihood of be absorbed by plant roots, macro and micro fauna.

The relative volumetric fractions of the pores between the primary and secondary forest are very similar. It shows a relative fast capacity of the spontaneous vegetation to rehabilitate the soil porosity near the values found under the original conditions.

The evaluation of the pore size distribution permits to explain field observation and to do some inferences about water behaviour on the different land use systems, and its use instead the total porosity is strongly recommended.

4.5 REFERENCES

BALL B C. and HUNTER R. The determination of water release characteristics of soil cores at low suctions. Geoderma. 43: 195-212, 1988.

BEVEN K. and GERMANN P. Macropores and water flow in soils. Water Resources Research. 18: 1311-1325, 1982.

BLUM W H. Soil resilience, rehabilitation. In: LAL R.; BLUM W H.; VALENTINE C. and STEWART B A, eds. Methods for assessment of soil degradation. Boca Raton, CRC Press, 2021. p.1-16.

BREWER R. Fabric and mineral analysis of soils. Chichester, John Wiley & Sons, 1964.

CABRAL O M R. Armazenamento de água no solo da floresta e de terra firme e seringal implantado, São José dos Campos, INPE, 1990. 103p. (Master)

CAMARGO M N and RODRIGUES T E. Guia de excursão. In: congresso brasileiro de ciência do solo, 17., 1979. Sociedade Brasileira de Ciência do Solo / Embrapa, Rio de Janeiro, 1979. p.1-72.

CARTER M R. and BALL B C. Soil porosity. In: CARTER M R, ed. Soil sampling and methods of analysis. Boca Raton, Lewis publishers, 1993. p.581-588.

CHAUVEL A. Os latossolos amarelos, álicos, argilosos dentro dos ecossistemas das bacias experimentais do INPA e da região vizinha. Acta Amazonica. 12: 47-60, 1982.

CHAUVEL A.; GRIMALDI M. and TESSIER D. Changes in soil pore-space distribution following deforestation and revegetation: An example from the central Amazon basin, Brazil. Forest Ecology and Management. 38: 259-271, 1991.

COPPOLA A. Unimodal and bimodal descriptions of hydraulic properties for aggregated soils. Soil Science Society of America Journal. 64: 1252-1262, 2000.

COREY A T. Pore-size distribution. In: VAN GENUCHTEN M TH.; LEIJ F J. and LUND L J (eds.). workshop on indirect methods for estimating the hydraulic properties of unsaturated soils, 1., 1992. University of California, Riverside, 1992. p.37-44.

CORRÊA J C. Características físicas de um latossolo amarelo muito argiloso (typic Acrorthox) do Estado do Amazonas, sob diferentes sistemas de preparo do solo. Pesquisa Agropecuária brasileira. 20: 1381-1387, 1985.

DANIELSON R E. and SUTHERLAND P L. Porosity. In: KLUTE A, ed. Methods of soil analysis. Part 1 - Physical and mineralogical methods. 2. Madison, SSSA, 1986. p.443-460.

DURNER W. Hydraulic conductivity estimation for soils with heterogeneous pore structure. Water Resources Research. 30: 211-223, 1994.

DURNER W. Shypfit 0.22 User's Manual. Bayreuth, University of Bayreuth, 1995. 25p.

GREENLAND D J. Structural organization of soils and crop production. In: LAL R. and GREENLAND D J, eds. Soil physical properties and crop production in the tropics. Chichester, John Wiley & Sons, 1979. p.47-56.

HILLEL D. and MOTTES J. Effect of plate impedance, wetting method and aging on soil moisture retention. Soil Science. 102: 135-140, 1966.

HILLEL D. Environmental soil physics. San Diego, Academic press, 1998. 771p.

HODNETT M G.; OYAMA M D.; TOMASELLA J. and MARQUES A DE O. Comparisons of long-term soil water storage behaviour under pasture. In: GASH J H C.; NOBRE C A.; ROBERTS J M. and VICTORIA R L, eds. Amazonian deforestation and climate. Chichester, John Wiley & Sons, 1986. p.57-78.

IWATA S.; TABUCHI T. and WARKENTIN B P. Soil-water interactions: mechanisms and applications. 2.ed. New York, Marcel Dekker, 1995. 440p.

KAY B D. and ANGERS D A. Soil structure. In: SUMNER M E, ed. Handbook of soil science. Boca Raton, CRC Press, 2000. p.A-229-A-276.

KLUTE A. and DIRKSEN C. Hydraulic conductivity and diffusivity: laboratory methods. In: KLUTE A., ed. Methods of soil analysis. Part 1. Physical and mineralogical methods. 2. Madison, American Society of Agronomy; Soil Science Society of America, 1986. p.687-734.

KUTÍLEK M. and NIELSEN D R. Soil hydrology. Cremlingen-Destedt, Catena, 1994. 370p.

KUZNETSOVA I V. Optimum bulk density. Eurasian Soil Science. 6: 74, 1991.

LARSSON M H. and JARVIS N J. A dual porosity model to quantify macropore flow effects on nitrate leaching. Journal of Environmental Quality. 28: 1298-1307, 1999.

LAWRENCE G P. Measurements of pore sizes in fine-textured soils: a review of existing techniques. Journal of Soil Science. 28: 527-540, 1977.

LEOPOLDO P R.; FRANKEN W.; SALATI E. and RIBEIRO M DE N G. Towards a water balance in the Central Amazonian region. Experientia. 43: 222-233, 1987.

LOGSDON S D.; M$_c$COY E L.; ALLMARAS R R. and LINDEN D R. Macropore characterisation by indirect methods. Soil Science. 155: 316-324, 1993.

MACEDO A. and CRESTANA S. Avaliação da macroporosidade e da densidade de partículas do solo através da microtomografia de raios X. Revista Brasileira de Ciência do Solo. 23: 763-772, 1999.

MADSEN H B.; JENSEN C R. and BOYSEN T. A comparison of the thermocouple psychrometer and the pressure plate methods for determination of soil water characteristics curves. Journal of Soil Science. 37: 357-362, 1986.

MALLANTS D.; TSENG P H.; TORIDE N.; TIMMERMAN A. and FEYEN J. Evaluation of multimodal hydraulic functions in characterizing a heterogeneous field soil. Journal of Hydrology. 195: 172-199, 1997.

MARQUES A DE O.; RIBEIRO M DE N G.; SANTOS H M DOS. and SANTOS J M DOS. Estudos climatológicos da Reserva Florestal Ducke - Manaus-AM.IV. Precipitação. Acta Amazonica. 11: 759-768, 1981.

MARSHALL T J.; HOLMES J W. and ROSE C W. Soil physics. 3.ed. Cambridge, Cambridge University Press, 1996. 453p.

MATHIEU C and PIELTAIN F. Analyse physique des sols. Paris, Lavoisier, 1998. 275p.

M$_C$COY E L.; BOAST C W.; STEHOUWER R C. and KLADIVKO E J. Macropore hydraulics. Taking a sledgehammer to classical theory. In: LAL R. and STEWART B A, eds. Soil processes and water quality. Boca Raton, Lewis Publishers, 1994. p.303-348.

MEDINA B F. Influência de dois métodos de preparo de área na compactação de um latossolo amarelo. Revista Brasileira de Ciência do Solo. 9: 67-71, 1985.

MESSING I. and JARVIS N J. Temporal variation in the hydraulic conductivity of a tilled clay soil as measured by tension infiltrometers. Journal of Soil Science. 44: 11-24, 1993.

MIYAZAKI T. Water flow in soils. New York, Marcel Dekker, 1993. 296p.

MORAES S O. and LIBARDI P L. Problemas metodológicos na obtenção da curva de retenção da água pelo solo. Scientia agricola. 50: 383-392, 1993a.

MORAES S O.; LIBARDI P L. and REICHARDT K. Heterogeneidade dos pontos experimentais de curvas de retenção da água no solo. Scientia agricola. 50: 393-403, 1993b.

MORAES S O and LIBARDI P L. Utilização da técnica de "scaling" para recuperação de resultados fisicamente incorretos em curvas de retenção de água no solo. In: Congresso latino americano de ciência do solo, 13., 1996. Sociedade Brasileira de Ciência do Solo, Campinas, 1996. CD ROM

MORAN C J.; MCBRATNEY A B. and KOPPI A J. A rapid method for analysis of soil macropore structure. I. Specimen preparation and digital binary image production. Soil Science Society of America Journal. 53: 921-928, 1989.

OTHMER H.; DIEKKRÜGER B. and KUTÍLEK M. Bimodal porosity and unsaturated hydraulic conductivity. Soil Science. 152: 139-149, 1991.

PRESS W.; TEUKOLSKY S A.; VETTERLING W T. and FLANNERY B P. Numerical recipes in Fortran - The art of scientific computing. 2.ed. Cambridge, Cambridge University Press, 1992. 963p.

RENCK A. Wasser-und Stickstoffflüsse unter verschiedenen tropischen Nutzbäumen in Zentralamazonien. University of Bayreuth, Bayreuth. 2000. 99 p. (Diplomarbeit)

ROSEBERG R J. and M$_C$COY E L. Measurement of soil macropore air permeability. Soil Science Society of America Journal. 54: 969-974, 1990.

RUSSO D. Determining soil hydraulic properties by parameter estimation: on the selection of a model for the hydraulic properties. Water Resources Research. 24: 453-459, 1988.

SHARMA M L. and UEHARA G. Influence of soil structure on water relations in low humic latossols: II. Water movement. Soil Science Society American Proceedings. 32: 765-771, 1968.

SMETTEM; K R J and KIRKBY C. Measuring the hydraulic properties of a stable aggregated soil. Journal of Hydrology. 177: 1-13, 1990.

TEIXEIRA W G.; PEREIRA E G.; CRUZ L A. and BUENO N. Influência do uso nas característica fisico quimicas de um latossolo amarelo, textura muito argilosa, Manaus - AM. In: Congresso latino americano de ciência do solo, 13., 1996. Sociedade Brasileira de Ciência do Solo, Campinas, 1996. p.1-4. CD ROM.

TEIXEIRA W G.; SCHROTH G.; FACCIN O. P. HUWE B. and ZECH W. Avaliação de parâmetros físico-químicos e hídricos do solo como indicadores da recuperação de áreas degradadas na Amazônia Ocidental. IN: Simpósio Nacional de Recuperação de áreas degradadas. 3. Ouro Preto, Viçosa, Sobrade / UFV. 1997. p. 166-174.

TOMASELLA J. and HODNETT M G. Soil hydraulic properties and van Genuchten parameters for an Oxisol under pasture in Central Amazonia. In: GASH J.H.C.; NOBRE C.A.; ROBERTS J.M. and VICTORIA R.L., eds. Amazonian deforestation and climate. West Sussex, John Wiley, 1996. p.101-124.

TOPP G C.; GALGANOV Y T.; BALL B C. and CARTER M.R. Soil water desorption curves. In: CARTER M R, ed. Soil sampling and methods of analysis. Boca Raton, Lewis, 1993. p.569-580.

VAN GENUCHTEN M TH. A closed-form equation for predicting the hydraulic conductivity of unsaturated soils. Soil Science Society of America Journal. 44: 892-898, 1980.

VAN GENUCHTEN M TH. and NIELSEN D R. On describing and predicting the hydraulic properties of unsaturated soils. Annales Geophysicae. 3: 615-618, 1985.

VAN GENUCHTEN M TH.; LEIJ F J. and YATES S R. The RETC code for quantifying the hydraulic functions of unsaturated soils. Ada, US Enviromental Protection Agency, 1991. np.

VAN GENUCHTEN M TH and LEIJ F J. Estimating the hydraulic properties on unsaturated soils. In: VAN GENUCHTEN M TH.; LEIJ F J. and WU L (eds.) . workshop on indirect methods for estimating the hydraulic properties of unsaturated soils, 2., 1997. University of California, Riverside, 1999. p.1-13.

WARNER G S.; NEIBER J L.; MOORE I D. and GIESE R A. Characterizing macropores in soil by computed tomography. Soil Science Society of America Journal. 53: 653-660, 1989.

WATSON K W. and LUXMOORE R J. Estimating macroporosity in a forest watershed by use of a tension infiltrometer. Soil Science Society of America Journal. 50: 578-582, 1986.

WHITE R E. The influence of macropores on the transport of dissolved and suspended matter through soil. Advance in Soil Science. 3: 94-120, 2021.

WILSON GV. and LUXMOORE R J. Infiltration, macroporosity, and mesoporosity distributions on two forested watersheds. Soil Science Society of America Journal. 52: 329-335, 1988.

WÖSTEN J H M. and VAN GENUCHTEN M TH. Using texture and other soil properties to predict the unsaturated soil hydraulic functions. Soil Science Society of America Journal. 51: 1762-1770, 1988.

ZAR J H. Biostatistical analysis. 4.ed. New Jersey, Prentice-Hall, 1999. 663p.

Table A.4.1 – Volumetric water contents related with water pressure head evaluated in samples collected at different depths in a profile on a clayey Ferralsol in the central Amazon. Bulk density - BD [Mg kg^{-3}]

Depth	pF0	pF0.5	pF1.0	pF1.5	pF1.8	pF2.0	pF2.2	pF2.5	pF3.0	pF3.5	pF 4.2	BD
0-10	0.5615	0.5197	0.4876	0.4387	0.4194	0.4025	0.3978	0.3934	0.3804	0.3689	0.2191	0.95
0-10	0.5424	0.5287	0.5072	0.4552	0.4395	0.4237	0.4194	0.4156	0.4037	0.3926	0.2320	1.07
0-10	0.5489	0.5252	0.4827	0.4284	0.4110	0.3942	0.3894	0.3852	0.3733	0.3628	0.2316	0.99
0-10	0.5756	0.5464	0.5067	0.4418	0.4340	0.4116	0.4048	0.3983	0.3870	0.3744	0.2251	1.03
0-10	0.5534	0.5185	0.4953	0.4431	0.4238	0.4082	0.4035	0.3997	0.3868	0.3740	0.1861	1.06
10-20	0.5302	0.5085	0.4962	0.4679	0.4480	0.4294	0.4221	0.4154	0.4010	0.3858	0.2548	1.02
10-20	0.5566	0.5338	0.5077	0.4717	0.4548	0.4436	0.4280	0.4239	0.4098	0.3970	0.2485	1.10
10-20	0.5448	0.5213	0.5026	0.4743	0.4605	0.4386	0.4321	0.4272	0.4123	0.3992	0.2514	1.04
10-20	0.5370	0.5212	0.4997	0.4707	0.4580	0.4368	0.4316	0.4250	0.4089	0.3957	0.2430	1.08
10-20	0.5061	0.4958	0.4867	0.4601	0.4461	0.4259	0.4194	0.4144	0.4006	0.3900	0.2289	1.06
20-30	0.5323	0.5203	0.5059	0.4852	0.4683	0.4483	0.4430	0.4397	0.4299	0.4173	0.2812	1.07
20-30	0.5073	0.4987	0.4854	0.4660	0.4538	0.4366	0.4306	0.4268	0.4133	0.4001	0.2597	1.04
20-30	0.5057	0.5000	0.4917	0.4604	0.4500	0.4333	0.4243	0.4197	0.4070	0.3970	0.2665	0.94
20-30	0.5630	0.5595	0.5452	0.5254	0.5129	0.4990	0.4910	0.4865	0.4736	0.4633	0.2528	1.06
20-30	0.5301	0.5119	0.4965	0.4718	0.4576	0.4360	0.4318	0.4275	0.4170	0.4065	0.2615	1.05
30-40	0.5542	0.5483	0.5285	0.5085	0.4989	0.4825	0.4747	0.4726	0.4624	0.4470	0.2448	1.01
30-40	0.5347	0.5215	0.5064	0.4792	0.4636	0.4463	0.4398	0.4388	0.4276	0.4120	0.2481	1.02
30-40	0.5433	0.5279	0.5120	0.4851	0.4733	0.4630	0.4501	0.4489	0.4379	0.4259	0.2515	1.02
30-40	0.5306	0.4925	0.4686	0.4383	0.4270	0.4240	0.4038	0.4024	0.3915	0.3782	0.2662	0.96
30-40	0.5170	0.4950	0.4810	0.4589	0.4466	0.4380	0.4260	0.4250	0.4150	0.3993	0.2473	1.02
40-50	0.5629	0.5260	0.5144	0.4887	0.4767	0.4740	0.4579	0.4546	0.4458	0.4333	0.2266	1.01
40-50	0.5202	0.5178	0.5033	0.4799	0.4688	0.4601	0.4505	0.4480	0.4387	0.4247	0.2594	1.02
40-50	0.4976	0.4825	0.4646	0.4408	0.4284	0.4215	0.4097	0.4075	0.3978	0.3868	0.2830	1.03
40-50	0.5212	0.5047	0.4835	0.4574	0.4465	0.4395	0.4281	0.4261	0.4176	0.4047	0.2918	0.94
40-50	0.5704	0.5341	0.5132	0.4805	0.4627	0.4505	0.4382	0.4367	0.4254	0.4125	0.2306	1.01
50-60	0.5503	0.4985	0.4719	0.4333	0.4179	0.4065	0.3969	0.3949	0.3833	0.3718	0.2532	0.91
50-60	0.5356	0.5106	0.4831	0.4582	0.4437	0.4349	0.4223	0.4198	0.4085	0.3971	0.2536	0.99
50-60	0.5737	0.5398	0.5160	0.4830	0.4637	0.4467	0.4373	0.4361	0.4245	0.4100	0.2281	1.06
50-60	0.5504	0.5073	0.4833	0.4564	0.4420	0.4266	0.4215	0.4199	0.4087	0.3975	0.2569	0.97
50-60	0.5346	0.4948	0.4754	0.4497	0.4343	0.4255	0.4144	0.4131	0.4017	0.3884	0.2733	0.95
60-70	0.5630	0.5458	0.5284	0.4950	0.4727	0.4721	0.4622	0.4560	0.4439	0.4294	0.2853	1.06
60-70	0.5371	0.5194	0.5077	0.4751	0.4624	0.4545	0.4447	0.4411	0.4271	0.4137	0.2404	1.04
60-70	0.5449	0.5203	0.5047	0.4656	0.4507	0.4407	0.4310	0.4249	0.4136	0.3979	0.2606	1.00
60-70	0.5340	0.5227	0.5048	0.4722	0.4580	0.4488	0.4405	0.4356	0.4248	0.4103	0.2615	1.01
60-70	0.5124	0.5033	0.4918	0.4588	0.4456	0.4378	0.4289	0.4235	0.4130	0.4113	0.2697	1.01
70-80	0.5514	0.5188	0.4997	0.4454	0.4177	0.4103	0.3993	0.3920	0.3786	0.3671	0.2900	0.93
70-80	0.5609	0.5306	0.5191	0.4697	0.4513	0.4431	0.4336	0.4261	0.4123	0.3981	0.2938	1.00
70-80	0.5304	0.5171	0.5014	0.4598	0.4433	0.4325	0.4235	0.4164	0.4049	0.3911	0.2714	0.97
70-80	0.5508	0.5372	0.5327	0.4859	0.4712	0.4617	0.4528	0.4480	0.4322	0.4163	0.2859	0.98
70-80	0.5409	0.5268	0.5096	0.4723	0.4557	0.4477	0.4384	0.4325	0.4185	0.4042	0.2834	1.01
80-90	0.5568	0.5327	0.5159	0.4760	0.4554	0.4488	0.4397	0.4320	0.4149	0.3997	0.2792	0.96
80-90	0.5370	0.5189	0.5044	0.4672	0.4493	0.4417	0.4325	0.4298	0.4058	0.3924	0.2789	0.98
80-90	0.5666	0.5413	0.5296	0.4755	0.4572	0.4473	0.4381	0.4256	0.4078	0.3922	0.2476	0.96
80-90	0.5369	0.5251	0.5062	0.4669	0.4522	0.4431	0.4345	0.4295	0.4162	0.4032	0.2747	0.99
80-90	0.5686	0.5615	0.5437	0.5115	0.4967	0.4879	0.4785	0.4746	0.4568	0.4432	0.2903	0.96
90-100	0.5311	0.5261	0.5141	0.5090	0.4806	0.4705	0.4683	0.4536	0.4378	0.4193	0.2977	0.99
90-100	0.5655	0.5505	0.5256	0.5191	0.4811	0.4679	0.4661	0.4466	0.4301	0.4101	0.2831	0.97
90-100	0.5376	0.5268	0.5066	0.5012	0.4700	0.4589	0.4561	0.4396	0.4225	0.4050	0.3080	1.00
90-100	0.5599	0.5450	0.5188	0.5112	0.4730	0.4601	0.4579	0.4405	0.4234	0.4062	0.2991	0.98
90-100	0.5501	0.5371	0.5154	0.5088	0.4741	0.4607	0.4586	0.4415	0.4232	0.4040	0.2869	0.97

Table A 4.2 – Soil water retention curve from collected near different plant species – Block A

pF0	pF0.5	pF1	pF1.5	pF1.8	pF2	pF2.2	pF2.5	pF3	pF3.5	pF 4.2
					1 [Cupuacu – AG]					
0.5320	0.5060	0.4760	0.4208	0.4002	0.3862	0.3730	0.3600	0.3530	0.3330	0.2495
0.5130	0.4600	0.4150	0.3628	0.3424	0.3325	0.3190	0.3070	0.2980	0.2810	0.2139
0.5460	0.5060	0.4590	0.3988	0.3724	0.3625	0.3440	0.3280	0.3240	0.3030	0.2166
					2 [Annato – AG]					
0.5680	0.5100	0.4220	0.3478	0.3290	0.3156	0.2980	0.2860	0.2820	0.2570	0.1748
0.5820	0.5390	0.4920	0.4149	0.3913	0.3784	0.3560	0.3420	0.3370	0.3190	0.2209
0.5640	0.5282	0.4538	0.3886	0.3734	0.3470	0.3290	0.3170	0.3120	0.3020	0.2129
					3 [Brazil nut – AG]					
0.5280	0.5150	0.4760	0.4160	0.3840	0.3691	0.3490	0.3340	0.3280	0.3030	0.2273
0.5330	0.5220	0.4830	0.4021	0.3707	0.3496	0.3360	0.3170	0.3150	0.2900	0.2123
0.5370	0.5010	0.4570	0.3868	0.3622	0.3509	0.3350	0.3190	0.3140	0.2920	0.2013
					4 [Peach palm – Fruit – AG]					
0.5520	0.4880	0.4330	0.3694	0.3484	0.3407	0.3190	0.3090	0.3070	0.2840	0.1651
0.5390	0.4970	0.4410	0.3845	0.3630	0.3501	0.3310	0.3190	0.3160	0.2880	0.1742
0.5420	0.4700	0.4210	0.3668	0.3457	0.3314	0.3170	0.3010	0.2990	0.2750	0.1741
					5 [Peach palm – AG]					
0.5470	0.4720	0.4000	0.3287	0.3033	0.2853	0.2720	0.2580	0.2560	0.2350	0.1510
0.5500	0.4740	0.4050	0.3286	0.3077	0.2945	0.2810	0.2690	0.2650	0.2470	0.1756
0.5530	0.5180	0.4440	0.3732	0.3504	0.3371	0.3240	0.3100	0.3060	0.2860	0.1830
					6 [Pueraria – AG]					
0.5430	0.5091	0.4776	0.4453	0.4237	0.4100	0.3970	0.3760	0.3720	0.3430	0.2247
0.5800	0.5435	0.5028	0.4593	0.4316	0.4180	0.4030	0.3850	0.3750	0.3390	0.2418
0.5500	0.5273	0.4987	0.4625	0.4380	0.4230	0.4090	0.3910	0.3880	0.3600	0.2647
					7 [Cupuaçu – M]					
0.543	0.519	0.477	0.432	0.405	0.394	0.382	0.366	0.364	0.345	0.2371
0.655	0.604	0.509	0.451	0.419	0.407	0.399	0.385	0.381	0.358	0.1956
0.594	0.575	0.489	0.441	0.399	0.388	0.369	0.356	0.353	0.332	0.2192
					8 [Grass]					
0.512	0.492	0.467	0.436	0.418	0.409	0.388	0.374	0.372	0.360	0.2401
0.550	0.535	0.496	0.448	0.425	0.413	0.398	0.381	0.377	0.359	0.2822
0.537	0.511	0.484	0.455	0.437	0.427	0.415	0.398	0.395	0.376	0.2380
					9 [Peach palm – F - M]					
0.575	0.554	0.439	0.364	0.347	0.332	0.278	0.309	0.298	0.290	0.2033
0.615	0.590	0.426	0.345	0.328	0.314	0.300	0.299	0.281	0.271	0.1816
0.549	0.527	0.431	0.373	0.359	0.346	0.326	0.323	0.322	0.313	0.2178
					10 [Peach palm – between F]					
0.578	0.560	0.516	0.469	0.451	0.434	0.414	0.395	0.382	0.369	0.2214
0.539	0.529	0.479	0.430	0.413	0.390	0.368	0.366	0.341	0.333	0.2023
0.564	0.552	0.491	0.435	0.414	0.394	0.371	0.365	0.340	0.329	0.2000
					11 [Peach palm – PH - M]					
0.553	0.528	0.451	0.392	0.378	0.358	0.344	0.337	0.323	0.312	0.2068
0.554	0.524	0.453	0.376	0.355	0.341	0.329	0.308	0.301	0.289	0.2044
0.543	0.508	0.410	0.344	0.327	0.311	0.298	0.271	0.270	0.256	0.1604
					12 [Peach palm – between PH - M]					
0.611	0.601	0.555	0.509	0.495	0.475	0.456	0.442	0.421	0.405	0.2261
0.575	0.561	0.504	0.445	0.432	0.418	0.408	0.403	0.379	0.363	0.2379
0.553	0.541	0.502	0.465	0.448	0.432	0.416	0.415	0.389	0.377	0.2556
					13 [Vismia]					
0.601	0.529	0.456	0.419	0.386	0.381	0.366	0.350	0.348	0.309	0.1645
0.557	0.518	0.496	0.469	0.448	0.438	0.427	0.405	0.398	0.369	0.2275
0.540	0.528	0.517	0.489	0.464	0.448	0.430	0.406	0.404	0.388	0.2420

AG = Agroforestry, M = monoculture; F = Fruits; PH = Palm heart

Table A 4.3 – Soil water retention curve – Block B

pF0	pF0.5	pF1	pF1.5	pF1.8	pF2	pF2.2	pF2.5	pF3	pF3.5	pF 4.2
					1					
0.5680	0.5278	0.4508	0.3712	0.3463	0.3401	0.3265	0.3204	0.3028	0.2898	0.2206
0.5662	0.5074	0.4428	0.3627	0.3361	0.3310	0.3193	0.3133	0.2961	0.2817	0.1993
0.5207	0.4929	0.4481	0.3782	0.3518	0.3459	0.3334	0.3237	0.3139	0.2997	0.2230
					2					
0.5933	0.5344	0.4835	0.4068	0.3833	0.3781	0.3654	0.3607	0.3437	0.3278	0.2181
0.5579	0.5221	0.4665	0.3932	0.3695	0.3645	0.3564	0.3483	0.3337	0.3181	0.2293
0.6165	0.5638	0.5065	0.4355	0.4075	0.4028	0.3907	0.3816	0.3615	0.3436	0.1980
					3					
0.6164	0.6066	0.5189	0.4507	0.4309	0.4180	0.4078	0.3976	0.3790	0.3629	0.2217
0.6002	0.5518	0.4869	0.3932	0.3615	0.3502	0.3341	0.3248	0.2963	0.2743	0.1962
0.6220	0.5276	0.4648	0.3867	0.3575	0.3480	0.3342	0.3277	0.3007	0.2856	0.1946
					4					
0.5402	0.5050	0.4477	0.3807	0.3556	0.3477	0.3331	0.3277	0.2997	0.2876	0.2075
0.5637	0.5116	0.4398	0.3856	0.3721	0.3355	0.3232	0.3155	0.2926	0.2887	0.1939
0.5444	0.5066	0.4582	0.4067	0.3881	0.3814	0.3671	0.3564	0.3356	0.3210	0.2396
					5					
0.5509	0.5221	0.4965	0.4276	0.4037	0.3946	0.3800	0.3678	0.3307	0.3187	0.2290
0.5553	0.5434	0.4702	0.3969	0.3718	0.3613	0.3583	0.3335	0.2917	0.2760	0.1832
0.5945	0.5639	0.5217	0.4564	0.4246	0.4130	0.4131	0.3826	0.3393	0.3254	0.2233
					6					
0.5790	0.5640	0.5376	0.4842	0.4660	0.4608	0.4477	0.4350	0.4065	0.3900	0.2461
0.6131	0.5874	0.5416	0.4638	0.4355	0.4237	0.4066	0.3950	0.3646	0.3476	0.2146
0.5912	0.5828	0.5521	0.4935	0.4695	0.4608	0.4397	0.4251	0.3995	0.3783	0.241
					7					
0.5767	0.5296	0.4776	0.4215	0.3964	0.3781	0.3693	0.3558	0.3425	0.3242	0.213
0.5640	0.5105	0.4592	0.4045	0.3816	0.3575	0.3510	0.3400	0.3266	0.3069	0.237
0.5857	0.5562	0.5163	0.4521	0.4213	0.3985	0.3865	0.3758	0.3621	0.3426	0.235
					8					
0.6183	0.5848	0.5506	0.5082	0.4859	0.4458	0.4263	0.4111	0.3973	0.3735	0.220
0.5515	0.5300	0.5034	0.4702	0.4488	0.4162	0.4025	0.3924	0.3767	0.3548	0.243
0.5632	0.5267	0.4840	0.4473	0.4262	0.4025	0.3905	0.3787	0.3666	0.3383	0.235
					9					
0.5910	0.5740	0.5491	0.4824	0.4437	0.4249	0.4081	0.3912	0.3496	0.3300	0.2012
0.6571	0.5759	0.5228	0.4236	0.3911	0.3836	0.3789	0.3309	0.2871	0.2639	0.1603
0.6622	0.6192	0.5843	0.4991	0.4591	0.4440	0.4283	0.4087	0.3724	0.3584	0.2022
					10					
0.5667	0.5434	0.5091	0.4665	0.4468	0.4335	0.4169	0.4041	0.3601	0.3491	0.2479
0.5933	0.5771	0.5508	0.4995	0.4764	0.4639	0.4463	0.4308	0.3864	0.3730	0.2579
0.5618	0.5395	0.5229	0.4871	0.4640	0.4514	0.4324	0.4219	0.3839	0.3750	0.2505
					11					
0.5597	0.5351	0.5139	0.4497	0.4272	0.4194	0.4061	0.3980	0.3672	0.3571	0.2451
0.6014	0.5768	0.5510	0.4870	0.4627	0.4491	0.4373	0.4241	0.3906	0.3794	0.2462
0.6202	0.5890	0.5455	0.4625	0.4307	0.4174	0.3986	0.3828	0.3470	0.3345	0.2071
					12					
0.5614	0.5439	0.5178	0.4692	0.4483	0.4369	0.4217	0.4112	0.3684	0.3556	0.2062
0.5794	0.5429	0.5262	0.4810	0.4618	0.4523	0.4373	0.4242	0.3816	0.3636	0.2413
0.5715	0.5603	0.5535	0.5013	0.4833	0.4737	0.4660	0.4521	0.4058	0.3942	0.2526
					13					
0.6366	0.6141	0.5630	0.5285	0.5050	0.4692	0.4523	0.4355	0.4132	0.3639	0.1898
0.5983	0.5767	0.5578	0.5046	0.4858	0.4562	0.4384	0.4238	0.4056	0.3660	0.2265
0.6048	0.5862	0.5683	0.5416	0.5250	0.4956	0.4840	0.4729	0.4526	0.4176	0.2233

Table A 4.4 – Soil water retention curve – Block C

pF0	pF0.5	pF1	pF1.5	pF1.8	pF2	pF2.2	pF2.5	pF3	pF3.5	pF 4.2
					1					
0.5824	0.5542	0.4726	0.4033	0.3800	0.3666	0.3508	0.3343	0.3204	0.3087	0.2302
0.6213	0.5484	0.4763	0.4020	0.3792	0.3611	0.3448	0.3315	0.3273	0.3148	0.2132
0.5725	0.5434	0.5095	0.4670	0.4463	0.4296	0.4120	0.4033	0.3933	0.3835	0.2567
					2					
0.5553	0.5326	0.5064	0.4613	0.4452	0.4325	0.4176	0.3871	0.3776	0.3671	0.2544
0.5345	0.5155	0.4975	0.4682	0.4519	0.4416	0.4293	0.4030	0.3965	0.3857	0.2784
0.5656	0.5421	0.5135	0.4575	0.4392	0.4272	0.4101	0.3831	0.3723	0.3584	0.2515
					3					
0.5647	0.5217	0.4963	0.4448	0.4268	0.4189	0.4003	0.3901	0.3681	0.3340	0.2120
0.5299	0.4962	0.4819	0.4446	0.4249	0.4184	0.4043	0.3898	0.3715	0.3449	0.2203
0.5331	0.5057	0.4912	0.4563	0.4366	0.4290	0.4110	0.3971	0.3702	0.3319	0.2205
					4					
0.6144	0.5126	0.4256	0.3788	0.3633	0.3555	0.3415	0.3282	0.3224	0.3160	0.2207
0.5845	0.5457	0.4989	0.4499	0.4366	0.4175	0.4002	0.3906	0.3883	0.3821	0.2597
0.6011	0.5547	0.4758	0.4271	0.4135	0.3978	0.3917	0.3753	0.3736	0.3687	0.2259
					5					
0.5543	0.5285	0.4920	0.4497	0.4322	0.4142	0.3922	0.3862	0.3833	0.3714	0.2389
0.5737	0.5387	0.5114	0.4739	0.4564	0.4368	0.4241	0.4076	0.4014	0.3913	0.2458
0.5344	0.5253	0.5042	0.4782	0.4636	0.4501	0.4299	0.4164	0.4033	0.3965	0.2550
					6					
0.5574	0.5483	0.5341	0.4958	0.4796	0.4710	0.4528	0.4357	0.4047	0.3532	0.2023
0.6064	0.5750	0.5590	0.5193	0.5037	0.4954	0.4743	0.4602	0.4275	0.3756	0.1900
0.5640	0.5356	0.5227	0.4864	0.4700	0.4624	0.4456	0.4322	0.4061	0.3647	0.2050
					7					
0.5272	0.4566	0.4307	0.3757	0.3601	0.3551	0.3454	0.3360	0.3265	0.3047	0.2547
0.5890	0.5547	0.5290	0.4777	0.4632	0.4564	0.4436	0.4355	0.3927	0.3600	0.2245
0.5250	0.4910	0.4521	0.4019	0.3872	0.3788	0.3640	0.3733	0.3342	0.3030	0.1891
					8					
0.5335	0.5124	0.4972	0.4592	0.4416	0.4336	0.4190	0.4111	0.4022	0.3792	0.2542
0.5338	0.5092	0.5000	0.4509	0.4324	0.4252	0.4081	0.3968	0.3840	0.3602	0.2484
0.5808	0.5593	0.5459	0.5043	0.4868	0.4788	0.4634	0.4536	0.4364	0.4066	0.2363
					9					
0.5995	0.5401	0.5105	0.4674	0.4521	0.4388	0.4202	0.3933	0.3678	0.3576	0.2202
0.5772	0.5524	0.5415	0.5144	0.4987	0.4856	0.4686	0.4146	0.4015	0.3862	0.2558
0.5581	0.5334	0.5163	0.4826	0.4660	0.4570	0.4440	0.4008	0.3952	0.3826	0.2719
					10					
0.5562	0.5315	0.5079	0.4727	0.4605	0.4511	0.4412	0.4127	0.4040	0.3922	0.2705
0.6061	0.5453	0.5004	0.4654	0.4529	0.4413	0.4280	0.3988	0.3913	0.3784	0.2440
0.5444	0.5167	0.4944	0.4623	0.4487	0.4406	0.4276	0.4019	0.3923	0.3798	0.2692
					11					
0.6704	0.5895	0.5348	0.4886	0.4692	0.4554	0.4376	0.3957	0.3770	0.3649	0.2057
0.5817	0.5386	0.4959	0.4499	0.4393	0.4305	0.4169	0.3768	0.3624	0.3503	0.2397
0.6492	0.5920	0.5491	0.5044	0.4853	0.4731	0.4518	0.4111	0.4034	0.3878	0.2331
					12					
0.5965	0.5577	0.5348	0.4869	0.4733	0.4659	0.4535	0.4061	0.3937	0.3815	0.2410
0.5630	0.5327	0.5175	0.4717	0.4535	0.4429	0.4282	0.3847	0.3738	0.3645	0.2371
0.5686	0.5319	0.5207	0.4819	0.4677	0.4586	0.4387	0.3998	0.3934	0.3804	0.2598
					13					
0.5056	0.4580	0.4260	0.3871	0.3712	0.3641	0.3475	0.3335	0.3169	0.2876	0.1862
0.5057	0.4619	0.4381	0.3906	0.3735	0.3672	0.3476	0.3365	0.3157	0.2870	0.1937
0.5719	0.5343	0.5182	0.4873	0.4725	0.4665	0.4475	0.4326	0.4099	0.3663	0.2379

Table A 4.5 – Soil water retention curve – samples collected in the primary forest.

pF0	pF0.5	pF1	pF1.5	pF1.8	pF2	pF2.2	pF2.5	pF3	pF3.5	pF 4.2
					mata- mata [14]					
0.5880	0.5424	0.4887	0.4268	0.4105	0.3964	0.3779	0.3640	0.3358	0.3207	0.1956
0.6236	0.5702	0.5184	0.4322	0.4124	0.3947	0.3730	0.3586	0.3283	0.3093	0.1651
0.5973	0.5726	0.5136	0.4423	0.4238	0.4062	0.3866	0.3722	0.3424	0.3206	0.1810
0.5682	0.5232	0.4503	0.3782	0.3549	0.3434	0.3370	0.3261	0.3083	0.2985	0.1538
0.5530	0.5190	0.4753	0.4267	0.4108	0.3964	0.3879	0.3656	0.3442	0.3291	0.1745
0.5676	0.5091	0.4574	0.3840	0.3653	0.3464	0.3301	0.3124	0.2895	0.2740	0.1501
0.5540	0.5011	0.4680	0.4197	0.3961	0.3859	0.3751	0.3678	0.3482	0.3419	0.1601
0.5567	0.5011	0.4422	0.3652	0.3345	0.3232	0.3100	0.3028	0.2831	0.2769	0.1601
0.5771	0.5365	0.4593	0.4107	0.3886	0.3768	0.3631	0.3548	0.3296	0.3078	0.1765
					bacaba [15]					
0.6016	0.5598	0.5285	0.4769	0.4606	0.4472	0.4310	0.4187	0.3972	0.3776	0.1726
0.5602	0.5428	0.5198	0.4541	0.4358	0.4212	0.4022	0.3881	0.3607	0.3422	0.2003
0.6132	0.5605	0.5100	0.4352	0.4181	0.4011	0.3883	0.3672	0.3429	0.3262	0.1559
0.6014	0.5409	0.4779	0.3913	0.3699	0.3511	0.3368	0.3204	0.2970	0.2820	0.1544
0.5555	0.5107	0.4781	0.4289	0.4077	0.4006	0.3811	0.3718	0.3509	0.3373	0.1752
0.5682	0.5071	0.4790	0.4453	0.4351	0.4186	0.4075	0.3873	0.3692	0.3500	0.1627
0.5700	0.5121	0.4651	0.4174	0.3974	0.3893	0.3841	0.3655	0.3505	0.3305	0.1714
0.5663	0.5060	0.4521	0.4125	0.3908	0.3805	0.3739	0.3594	0.3439	0.3262	0.1636
0.5584	0.5080	0.4626	0.4307	0.4092	0.4004	0.3911	0.3765	0.3548	0.3333	0.1792

5 EVALUATION OF SOIL WATER CONTENT IN THE CLAYEY FERRALSOLS USING TDR TECHNIQUE – A CALIBRATION STUDY

5.1 INTRODUCTION

Volumetric soil water content (θ) can be evaluated in the field by direct or indirect methods. The direct gravimetric method is regarded as highly reliable and thus often preferred. Its main disadvantages are that the sampling and laboratory procedures are labour intensive, and that the method is destructive, what makes resampling the same point impossible.

Time domain reflectometry (TDR) is increasingly used as a non-invasive technique for the estimation of volumetric water content (θ_{TDR}). It is based on the determination of the dielectric number (ε) of the soil through the measurement of the propagation velocity of electromagnetic waves, using the large difference of ε between water (≈81), air (≈1), mineral constituents of the soil (3-30), and frozen or bound water (≈3.2) (Lide, 1999). ε is measured with probes that are installed in the soil (down to several meters deep, if required) and that are either permanently connected to an automatically data-logger, or temporarily connected to a mobile device. It was initially believed that a single universal equation could be found relating θ to ε. However, subsequent work showed that various factors may influence the measurement of ε so that site-specific calibrations may be necessary for improving the accuracy of θ_{TDR}, especially in clayey soils or soils with low bulk density (Roth et al., 1992; Dirksen and Dasberg, 1993; Malicki et al., 1996) and soils with high organic matter content (Herkelrath et al., 1991; Roth et al., 1992).

The temperature effect on determination of ε is reported to be linear (Pepin et al., 1995; Persson and Berndtsson, 1998; Wraith and Or, 1999; Or and Wright, 1999) and should be corrected where large temperature fluctuations occur, especially near the soil surface. Saline conditions or presence of large amounts of fertilizers can interfere in ε measurements (Dalton, 1992; Ferré et at., 1998; Kim et al., 1998). In some tropical soils, the high amounts of iron components and the presence of magnetic minerals can likewise interfere in ε determinations (Roth et al., 1992; Robinson et al., 1994) as well as technical characteristics of the measurement device, such as the length, diameter and geometry of the rods (Zegelin et al., 1992; Knigth, 1992; Petersen et al., 1995; Rothe et al.; 1997) and the signal frequency used (Hook and Livingston, 1995). Another factor influencing the accuracy of ε measurements is the sampling procedure used, such as the direction (i.e., vertical or horizontal) along which the TDR probes are installed (Ferré et al., 1996; Zegelin et al., 1992; Topp and Davis, 1985), the mode of insertion of the probes into the soil (Rothe et al., 1997) and the time elapsed between the installation of the probes and the beginning of the measurements (Jacobsen and Schjønning, 1993 and Rothe et al., 1997).

In research and monitoring projects which aim to analyse the soil water dynamics at high levels of precision and accuracy, it is necessary to take into account the sources of error in the TDR technique, so that they can be excluded or minimised, (e.g., through appropriate calibration and measurement procedures).

Some studies have shown that empirical equations generated in temperate soils frequently correlate unsatisfactorily θ_{TDR} and θ_{Grav} in tropical soils (Dirksen and Dasberg, 1993; Tomasseli and Bachi, 1996; Weitz et al., 1997).

The fine texture and low bulk density values that are typical characteristics of the clayey Ferralsols in the central Amazon conducted to failure of most equations of TDR calibration to provide accurate estimates of θ_{TDR} (Teixeira et al., 1997). Therefore, the objectives of this work were to calibrate the TDR technique using either empirical or physically based equations for the clayey Ferralsols in the central Amazon. Sources of errors, which may arise when using the TDR technique under field conditions, are also discussed with particular reference to the study region.

5.2 MATERIALS AND METHODS

5.2.1 Site characteristics

The study was carried out within selected plots of the experiment detailed in the Chapter 2. The plots comprising the monoculture of cupuaçu, peach palm and the agroforestry system.

Records of ε were taken with the TDR probes inserted vertically into the soil at ≈ 40 cm from the trunk of trees of cupuaçu and peach palm which were grown either in monoculture or in an agroforestry system, as well as under the leguminous pueraria used as cover crop in the monoculture of cupuaçu and the agroforestry system. Measurements were also made close to two species in the adjacent primary forest, the palm bacabeira and the dicotyledoneous tree matá-matá. In addition, a soil pit was opened and measurements and samples were taken from the subsoil. The samples were collected during both the dry and the rainy season of the year 1996.

The ε measurements were carried out with a commercial device (EASY TEST®, Lublin - Poland) with the following technical specifications: pulse rate 250 ps, probes with two transmission rods of 0.10 m length and 2.0 cm diameter, spaced 1.6 cm from each other. Details about the volume assessed by the TDR probes are given by Teixeira et al. 2001.

Immediately after the evaluation of ε, a layer of ≈ 2 cm was removed and steel cylinders were driven vertically into the soil so that their geometric center coincided with that of the TDR probe. Then the soil samples were collected and carried to the laboratory. The steel cylinders were 5 cm long and had a volume of 100 cm^3. The soil samples were dried in an oven at 105°C for 48 hours for determination of bulk density (ρ) and volumetric water content determined gravimetrically (θ_{Grav}). To calculate θ_{Grav}, a water specific gravity of 1000 kg m^{-3} was assumed. The water content determined in this way (θ_{Grav}) was considered the "correct value" of θ. The data set characteristics are summarised in Table 5.1; the complete data set is shown in Appendix 5 –B.

5.2.2 Calibration Equations

5.2.2.1 Empirical equations

Univariate equations

The commercial TDR device used has a built-in calibration for mineral soils that give directly the volumetric soil moisture θ_{TDR} in % (Equation 5.1 in Table 5.2). However, for mineral soils where ρ differs by more than $\pm$ 0.2 Mg $m^{-3}$from the range 1.4 Mg $m^{-3} < \rho <$ 1.8 Mg m^{-3}, the manufacturer suggests the use of the equation given by Malicki et al. (1996) (Equation 5.2 in Table 5.2).

In addition to these empirical equations, the suitability of the empirical equation given by Topp et al. (1980) was tested (Equation 5.3 in Table 5.2). All these empirical equations tested matched θ_{Grav} and θ_{TDR} unsatisfactorily (Figure 5.1, 5.2 and Table 5.2). Therefore, linear, quadratic and cubic regression equations were calculated in an attempt to obtain a better accuracy in the θ_{TDR} estimates (Equations 5.4, 5.5 and 5.6 in Table 5.2). Additionally, a linear regression between the square root of ε and θ_{Grav} was also computed (Equation 5.7 in Table 5.2).

Table 5.1 Volumetric soil moisture assessed gravimetrically [θ_{Grav}]. apparent dielectric number [ε]. soil bulk density [ρ] and porosity [ϕ] measured on primary forest and cultivated areas close to different plant species (≈ 40 cm) and at one soil profile on a clayey Ferralsol in the central Amazon.

Sampling point	n	θ_{Grav} $m^3\ m^{-3}$				ε [-]				ρ $Mg\ m^{-3}$				ϕ [-]			
		Mean	SD	Min	Max	Mean	SD	Min	Max	Mean	SD	Min	Max	Mean	SD	Min	Max
Primary forest - sampled at ≈ [0.02 -0.07 m] depth																	
Matamatá (*Eschweilera spp*)	19	0.341	0.065	0.254	0.477	17.31	4.87	10.77	25.49	0.785	0.112	0.620	0.980	0.67	0.04	0.61	0.75
Bacaba (*Oenocarpus bacaba*)	18	0.414	0.058	0.302	0.487	21.29	3.95	14.79	26.16	0.808	0.102	0.630	1.000	0.68	0.04	0.60	0.58
Cultivated area - sampled at ≈ [0.02 -0.07 m] depth																	
Peach palm (*Bactris gasipaes*)	58	0.319	0.072	0.203	0.478	15.97	4.91	8.55	26.69	0.920	0.111	0.710	1.200	0.63	0.04	0.51	0.72
Cupuaçu (*Theobroma grandiflorum*)	33	0.418	0.026	0.347	0.468	22.43	2.58	16.08	27.47	1.103	0.212	0.910	1.540	0.56	0.08	0.64	0.38
Pueraria (*Pueraria phaseoloides*)	20	0.376	0.029	0.308	0.425	20.35	2.54	16.50	25.02	1.049	0.060	0.930	1.180	0.58	0.02	0.53	0.63
Soil profile. [three depths]																	
0.30 m	26	0.436	0.031	0.345	0.474	23.02	2.56	15.15	26.45	1229	0.064	1.060	1.330	0.51	0.03	0.47	0.58
0.90 m	27	0.483	0.031	0.408	0.534	26.11	2.64	20.45	29.43	1211	0.060	1.050	1.300	0.52	0.02	0.48	0.58
1.50 m	25	0.483	0.002	0.445	0.532	28.22	2.51	24.00	31.61	1220	0.063	1.140	1.290	0.51	0.02	0.48	0.54
Total	226	0.399	0.078	0.203	0.534	21.21	5.46	8.55	31.61	1041	0.195	0.620	1.540	0.58	0.08	0.38	0.75

SD = standard deviation. Min = minimum datum; Max = maximum datum; n = number of data

Table 5.2 Empirical equations to estimate the volumetric soil water content [θ_{TDR} – $m^3\ m^{-3}$] with the apparent dielectric number [ε] as predictor variable. As goodness of fit are shown the coefficient of determination [R^2]. adjusted coefficient of determination [R^2_a] and root mean square of error [RMSE].

Eq.	Type or Name	Soil characteristics were the model was developed and coefficients of equations	Equation	R^2	R^2_a	RMSE
5.1	Easy Test ©	$1400 < \rho < 1800$ kg m^{-3}	$\theta_{TDR} = 17.54 \times \sqrt{\varepsilon} - 57.21 \text{ if } \varepsilon \leq 36$ $\theta_{TDR} = 10.64 \times \sqrt{\varepsilon} - 15.82 \text{ if } \varepsilon > 36$	0.6236	0.6219	0.0760
5.2	Malicki et al.	$0.20 < \theta < 0.53$ $m^3\ m^{-3}$ $1200 < \rho < 1400$ kg m^{-3}	$\theta_{TDR} = \dfrac{\sqrt{\varepsilon} - 0.819 - 0.168\rho - 0.159\rho^2}{7.170 + 1.180\rho}$	0.7603	0.7582	0.0364
5.3	Topp et al.	$0.10 < \theta < 0.53$ $m^3\ m^{-3}$ $1300 < \rho < 1400$ kg m^{-3} $\beta_0 = -5.3 \cdot x10^{-2}$; $\beta_1 = 2.92 \text{ x } 10^{-2}$; $\beta_2 = -5.5 \text{ x } 10^{-4}$; $\beta_3 = 4.3 \text{ x } 10^{-6}$	$\theta_{TDR} = \beta_0 + \beta_1\varepsilon + \beta_2\varepsilon^2 + \beta_3\varepsilon^3$	0.7195	0.7157	0.0536
5.4	linear	$\beta_0 = 1.0879^{**} \text{ x } 10^{-1}$; $\beta_1 = 1.3690^{**} \text{ x } 10^{-2}$	$\theta_{TDR} = \beta_0 + \beta_1\varepsilon$	0.9080	0.9076	0.0239
5.5	quadratic	$\beta_0 = 4.6367^{**} \text{ x } 10^{-2}$; $\beta_1 = 2.0444^{**} \text{ x } 10^{-2}$; $\beta_2 = -1.6852^{**} \text{ x } 10^{-4}$	$\theta_{TDR} = \beta_0 + \beta_1\varepsilon + \beta_2\varepsilon^2 +$	0.9124	0.9116	0.0233
5.6	cubic	$\beta_0 = 1.4252^{**} \text{ x } 10^{-1}$; $\beta_1 = 4.2068^{ns} \text{ x } 10^{-3}$; $\beta_2 = 6.8439^{ns} \text{ x } 10^{-4}$; $\beta_3 = -1.41527^{ns} \text{ x } 10^{-5}$	$\theta_{TDR} = \beta_0 + \beta_1\varepsilon + \beta_2\varepsilon^2 + \beta_3\varepsilon^3$	0.9134	0.9122	0.0232
5.7	Root square	$\beta_0 = -1.4747^{**} \text{ x } 10^{-1}$; $\beta_1 = 1.1980^{**} \text{ x } 10^{-1}$	$\theta_{TDR} = \beta_0 + \beta_1\sqrt{\varepsilon}$	0.9113	0.9109	0.0234

** and *: significant at the 1% and 5% probability levels respectively [F test]. Equation of Easy test and Malicki in the original form, the units are Mg m^{-3} and θ in %.

Table 5.3 Comparison among several procedures of computing multivariate regressions of the apparent dielectric number [ε] and bulk density [ρ – kg m^{-3}] as predictor of volumetric soil water content [θ_{TDR} - $m^3\ m^{-3}$] on a Xanthic Ferralsol in Manaus – Brazil. As goodness of fit is shown the significance of coefficients. coefficients of determination [R^2]. adjusted coefficients of determination [R^2_a] and root mean square error [RMSE].

Eq.	Parameters	Procedure	Model	R^2	R^2_a	RMSE
5.8¶	$\beta_0, \varepsilon^2, \varepsilon^3, \rho^2$	All subset	$\theta_{TDR} = 1.5620^{**} \text{ x } 10^{-1} + 8.7019^{**} \text{x } 10^{-4}\varepsilon^2 - 1.7399^{**} \text{ x } 10^{-5}\varepsilon^3 + 2.0799^{**} \text{ x}10^{-2}\rho^2$	0.9212	0.9202	0.0222
5.9	$\beta\ \varepsilon^2, \varepsilon^3, \rho$		$\theta_{TDR} = 1.3493^{**} \text{ x } 10^{-1} + 8.6733^{**} \text{ x } 10^{-4}\varepsilon^2 - 1.7322^{**} \text{ x } 10^{-5}\varepsilon^3 + 4.3316^{**} \text{ x } 10^{-2}\rho$	0.9209	0.9199	0.0222
5.10	$\beta_0, \varepsilon^2, \varepsilon^3, \rho, \rho^2$		$\theta_{TDR} = 1.6680^{**} \text{ x } 10^{-1} + 8.7199^{**} \text{ x } 10^{-4}\varepsilon^2 - 1.7441^{**} \text{ x } 10^{-5}\varepsilon^3 - 2.1266 \text{ x } 10^{-2}\rho - 3.0740 \text{ x } 10^{-2}\rho^2$	0.9212	0.9198	0.2222
5.11	$\beta_0, \varepsilon, \varepsilon^3, \rho, \rho^2$	†Forward	$\theta_{TDR} = 5.5489^{**} \text{ x } 10^{-2} + 1.6769^{**} \text{ x } 10^{-2}\varepsilon - 3.1217^{**} \text{ x } 10^{-6}\varepsilon^3 + 2.0916^{*} \text{ x } 10^{-2}\rho^2$	0.9207	0.9197	0.0222
5.8¶	$\beta_0, \varepsilon^2, \varepsilon^3, \rho^2$	†Backward	$\theta_{TDR} = 1.5620^{**} \text{ x } 10^{-1} + 8.7019^{**} \text{ x } 10^{-4}\varepsilon^2 - 1.7399^{**} \text{ x } 10^{-5}\varepsilon^3 + 2.0799^{**}10^{-2}\rho^2$	0.9212	0.9202	0.0222
5.12	$\beta_0, \varepsilon, \varepsilon^2, \varepsilon^3, \rho, \rho^2$	Standard	$\theta_{TDR} = 1.3947^{*} \text{x } 10^{-1} + 4.4956^{ns} \text{x}10^{-3}\varepsilon + 6.4057^{ns} \text{ x } 10^{-4}\varepsilon^2 - 1.3670^{ns} \text{ x } 10^{-5}\varepsilon^3 - 2.1064^{ns} \text{ x } 10^{-2}\rho - 3.0659^{ns} \text{ x } 10^{-3}\rho^2$	0.9213	0.9195	0.0223

† - F to enter 11 and 4 – F to remove 10.9 and 3.9, respectively. Both procedures with the same results; * and ** respectively significant at p>0.05 and p>0.01 respectively. by F test. ¶ The same equation obtained using different approaches.

Multiple regression

Diverse statistical multiple regression procedures were computed, assuming that both predictor variables (ε and ρ) could be included or excluded from the equation. The original data set of measured variables (Table 5.1) was extended with other variables calculated from them, which included the squares of ε and ρ, and the cube of ε. First, all subset regressions were performed and the best three subsets were selected based on the criteria discussed below (Equations 5.8, 5.9 and 5.10 in Table 5.3). Afterwards, the following procedures were performed: the stepwise procedure with forward selection (Equation 5.11 in Table 5.3); stepwise procedure with backward elimination (Equation 5.8 in Table 5.3); and standard multiple regression (Equation 5.12 in Table 5.3). The stepwise procedure with forward selection and backward elimination evaluates the independent variables at each step, adding or deleting variables in the equation. Two specified F values criteria to remove or enter variables in the equations were tested, respectively 10 – 9 and 4 – 3.9; these values determined how significant the contribution of a variable to the equation had to be in order for it to be added or removed in the equation by using the partial F-test (Draper and Smith, 1998; Graybill and Iver, 1994). Multiple regression analysis were performed using the computer package Statistica® for Windows 6.0 (StatSoft, 1998, Tulsa).

5.2.2.2 Physically based equations

Physically based equations are an alternative approach to obtain θ from measured ε. Their advantage is that the description of the relationship between the soil characteristics is selected not only by the mathematical procedures, but it also has a physical meaning. The physically based equations assume that ε is a function of a multiphase mixture dependent on their dielectric numbers, shapes and geometrical arrangement relative to the applied electromagnetic field, and volume fractions of the soil components (Ansoult et al., 1984; De Loor, 1990). The Alpha-3, Alpha-4 and Maxwell-De Loor equations were calculated and statistically tested.

Alpha-3 Equation

In the Alpha-3 Equation, the ε is divided into three compontents: i) the dielectric number of water (ε_w), ii) the dielectric number of the solid phase (ε_s), and iii) the dielectric number of the air phase (ε_a) (Equation 5.13 in Table 5.5). The respective volume fractions are calculated from soil porosity (ϕ).

The parameter α phenomenally summarizes the geometry of the medium in relation to the applied electric field (Ansoult et al, 1984; Roth et al., 1990). Several researchers assume α as being a constant value of 0.5 which corresponds to the refractive mixing model (Alharti and Lange, 1987; Roth et al., 1990; Whalley, 1993; Heimovaara et al., 1994; White et al., 1994). In another interpretation, α is considered an empirical factor and requires fitting (Roth et al., 1990 Dasberg and Hoppmans, 1992; Dirksen and Dasberg, 1993; Yu et al., 1997; Yu et al., 1999). Both procedures were investigated (Equation 5.13 A, 5.13 B and 5.13 C in Table 5.5). First, the optimum value of α was found using the minimization procedures of the Levenberg-Marquardt method for nonlinear regression (Press et al., 1992). In another attempt α was optimized and subsequently, the optimized value was fixed and ε_s was optimized. Values assumed and constraints (used to avoid unrealistic values) are shown in Table 5.6. The Marquardt-Levenberg algorithm basically seeks the values of the parameter(s) that minimize the sum of the squared differences between the values observed and predicted. The process of calculation is iterative, the curve fitter begins with the initial parameters given, checks how well the equation fits, then continues to make change until the differences between the residual sum of squares no longer decrease significantly (i.e., the equation converged to a solution). The initial parameters ideally should be as close to the real value as possible, and an adequate selection of them may be critical for a successful convergence (Press et al., 1992; Draper and Smith, 1998). False convergence to a local minimal instead of a global minimal (i.e., the correct solution) is an associated problem using "bad" initial parameters.

Alpha - 4 Equation

Soils with a low clay content have a tendency to show higher ε values at water contents around 0.10-0.30 $m^3\ m^{-3}$ than clayey soils (Topp et al., 1980; Jacobsen and Schjønning, 1995). This phenomenon is caused by layers of water bound to colloidal particles, which induce a restricted rotational freedom of water molecules in these layers lowering their dielectric number (Bohl and Roth, 1994). The magnitude of this effect depends on the surface area and surface charge. Therefore, related to texture and mineralogy of the soil (Dirksen and Darsberg, 1995; Hall and Rose, 1977).

The Alpha-4 Equation considers this phenomenon and divides the water component into free water (θ_{fw}) and bound water (θ_{bw}). This equation may potentially improve the estimation of θ in fine textured soils, especially in the dry range, where θ_{bw} assumes an important role in ε determinations (Bohl and Roth, 1994; Heimovaara et al., 1994; Jacobsen and Schjønning, 1995; Weitz et al., 1997). To calculate θ_{bw} the Equation 5.16 was used (Dirksen and Dasberg, 1993)

$$\theta_{bw} = \iota \delta \rho S \qquad [5.16]$$

where ι is the number of molecular layers of tightly bound water, δ is the thickness of one molecular water layer (L – 3 x 10^{-10} m), S is the specific surface of soil (L^2 M^{-1} - m^2 kg^{-1}) and ρ is the bulk density (M L^3 - kg m^{-3}) (Dirksen and Darsberg, 1993; Bohl and Roth, 1994; Jacobsen and Schønning 1995).

Firstly, the Alpha-4 was calculated assuming α = 0.5 (Equation 5.14 in Table 5.4). Subsequently, the Alpha-4 was computed in three different combinations of parameters (Equations 5.14 A; 5.14 B and 5.14 C in Table 5.5).

Maxwell-De Loor Equation

The Maxwell-De-Loor Equation uses only physical parameters and assumes that ε consists of a homogeneous mixture of one or more substances randomly distributed in an isotropic dielectric medium, the solid phase (De Loor, 1990). This equation was calculated with the same values for the dielectric components of the soil used in the Alpha-4. Then various combinations of parameters were performed (Equation 5.15 in Table 5.4 and Equations 5.15 A, 5.15 B and 5.15 C in Table 5.6). Additionally, a curtailed data set formed only with $\theta_{Grav} \leq 0.30$ was also used to test this equation (Equation 5.15 D in Table 5.5).

Table 5.4 Physically based equations to estimate the volumetric soil water content [θ_{TDR}] in a clayey Ferralsol in Manaus using the apparent dielectric number [ε] of soil components, bulk density [ρ] or porosity [ϕ] as predictor variables. The root mean square error (RMSE) is shown as measure of accuracy.

Eq.	Type	Parameter	Equation	R^2	R^2_a	RMSE
5.13	Alpha 3	‡$\varepsilon_s = 4$; $\varepsilon_a = 1$; $\varepsilon_w = 81$; $\alpha = 0.5$	$\theta_{TDR} = \dfrac{\varepsilon^{\alpha} - (1-\varphi)\varepsilon_s^{\alpha} - \eta\varepsilon_a^{\alpha}}{\varepsilon_w^{\alpha} - \varepsilon_a^{\alpha}}$	0.8759	0.8732	0.274
5.14	† Alpha 4	‡$\varepsilon_s = 4$; $\varepsilon_a = 1$; $\varepsilon_{fw} = 81$; $\varepsilon_{bw} = 3.2$ $\alpha = 0.5$	$\theta_{TDR} = \dfrac{\varepsilon^{\alpha} - \theta_{bw}(\varepsilon_{bw}^{\alpha} - \varepsilon_{fw}^{\alpha}) - (1-\varphi)\varepsilon_s^{\alpha} - \varphi\varepsilon_a^{\alpha}}{\varepsilon_{fw}^{\alpha} - \varepsilon_a^{\alpha}}$	0.8155	0.8130	0.391
5.15	† M.-De Loor	‡$\varepsilon_s = 4$; $\varepsilon_a = 1$; $\varepsilon_{fw} = 81$; $\varepsilon_{bw} = 3.2$	$\theta_{TDR} = \dfrac{3\cdot(\varepsilon_s - \varepsilon) + \theta_{bw}\cdot\left[2\cdot(\varepsilon_{bw} - \varepsilon_{fw}) - \varepsilon\cdot\varepsilon_s\left(\frac{1}{\varepsilon_{bw}} - \frac{1}{\varepsilon_{fw}}\right)\right] + \varphi\cdot\left[2\cdot(\varepsilon_a - \varepsilon_s) - \varepsilon\cdot\varepsilon_s\left(\frac{1}{\varepsilon_a} - \frac{1}{\varepsilon_s}\right)\right]}{\varepsilon\cdot\varepsilon_s\left(\frac{1}{\varepsilon_{fw}} - \frac{1}{\varepsilon_a}\right) + 2\cdot(\varepsilon_a - \varepsilon_{fw})}$	0.8282	0.8235	0.312

†: θ_{bw} [soil bound water] calculated with Equation 5.16 assuming that $S = 13 \times 10^{4}\ m^2\ kg^{-1}$; $\delta = 3 \times 10^{-10}$ m; and one monomolecular layer of bound water.

‡: ε = apparent dielectric number of the soil; ε_s = apparent dielectric number of solid phase; ε_a = apparent dielectric number of air phase; ε_{fw} = apparent dielectric number of free water, ε_{bw} = apparent dielectric number of bound water.

5.2.3 Data analysis

5.2.3.1 Criterions for goodness of fit

The following criteria were used to assess the goodness of fit of the equations: root mean square of residual (RMSE), coefficient of correlation (R^2), adjusted coefficient of correlation (R^2_a), average deviation (AD) and statistical significance of β coefficients on regression analyses (Draper and Smith, 1998; Graybill and Iyer, 1994).

The RMSE statistic measures the dispersion of the observed values around the regression line. The RMSE is an estimate of the uncertainties of the regression coefficients. It was calculated with the Equation 5.17.

$$\mathrm{RMSE} = \frac{\sqrt{\sum_{i=1}^{n}(y_i - \hat{y})^2}}{n-1} \qquad [5.17]$$

Where y_i is the measured value (e.g., θ_{Grav}), $\hat{y}$ is the predicted value by the calibration equation (e.g., θ_{TDR}), and n is the number of data used in the calibration. This criterion was used in TDR calibration studies by Bohl and Roth (1994) and Jacobsen and Schjønning, (1995).

The R^2 measures the reduction in the total variation of the dependent variable due to the independent variables (Draper and Smith, 1998 and Graybill and Iyer, 1994). It is calculated with the Equation 5.18

$$R^2 = \frac{\sum_{i=1}^{n}(\hat{y}_i - \bar{y}_i)^2}{\sum_{i=1}^{n}(y_i - \bar{y}_i)^2} \qquad [5.18]$$

Here, y is the mean value of the measured data, the other parameters are as defined above.

The R^2_a is a measure of how well the regression equation describes the data as the R^2 criterion, but it takes into account the number of dependent variables (e.g.; ε; ε^2, ρ). It is used to compare equations fitted with different number of variables (Draper and Smith, 1998 and Graybill and Iyer, 1994). It is calculated with the Equation 5.19.

$$R_a^2 = 1 - \frac{n-1}{n-p} \cdot [1 - R^2] \qquad [5.19]$$

Where p is the number of parameters in the equation.

The AD is an estimation of the mean residual in absolute values. It is calculated using the Equation 5.20

$$AD = \frac{1}{n}\sum_{i}^{n}|y_i - \hat{y}_i| \qquad [5.20]$$

The residuals ($\theta_{Grav} - \theta_{TDR}$) were plotted as ordinate against the corresponding fitted values θ_{TDR}, using the fitted equation, and the corresponding ε values. Although, it is a procedure commonly used, the residuals were not plotted against θ_{Grav} because, while the residuals and estimator (θ_{Grav}) are usually correlated, residuals and estimated values (θ_{TDR}) are not (Draper and Smith, 1998). Further details about residual analyses are given in the Appendix 3-A.

5.2.3.2 Sensitivity analysis and validation

Sensitivity analysis was carried out to test the impact of different values of ρ on the results of the Malicki Equation, and the impact of φ on the Alpha-3 Equation. It was carried out to estimate the impact of inaccuracies on the measurements of ρ and ϕ or of the use of their mean values on the θ_{TDR} estimates. The graphical results of sensitivity analyses are illustrated on Figure 5.3 and 5.7.

To validate the predictive capacity and the accuracy of the calibration equations, an independent data set, which had not been used in the calibration, was used. This data set was obtained on a parallel study about soil variability carried out on the same experiment. In this study, the same steel cylinder used in calibration studies was employed to obtain soil samples for bulk density and volumetric water content determinations. The soil samples were collected at the surface with the cylinder inserted at $\approx$ 2-7 cm depth and the ε measurements were carried out with the same TDR device, with the probe inserted vertically until 10 cm into the soil. The data set characteristics are summarised in Table 5.6. The complete data set is shown in the Appendix 5 –A.

5.4 RESULTS AND DISCUSSION

5.4.1 Variability of bulk density

In this project, significant patterns of throughfall, stemflow (Schroth, et al.1999a) nutrients (Schroth et al., 1999b) and ρ (Chapter 3) in relation to the proximity to different plant species have been described. In Chapter 3 and Table 5.1 differences of ρ and consequently of ϕ are shown. The difference are caused by different soil management, and the presence of different plant species; as well as differences on ρ and ϕ between sampling points measured at the surface and subsurface were found. The values of ρ increase with depth at all sampling points (Tables 5.1) but very small differences were found within subsurface sampling layers.

In the primary forest, the lower values of ρ than in agriculture areas are a consequence of the high concentration of roots and intense biological activities near the soil surface. The subsurface values of ρ show higher uniformity than the soil surface values, shown by smaller standard deviations and a reduced range (Table 5.1). Among the sampled points in the cultivated area, the smallest values of ρ were found near trunks of peach palm. Similar results about bulk density and more detailed discussion about ρ are shown in Chapter 3.

5.4.2 Calibration with empirical equations

5.4.2.1 Linear univariate equations

Table 5.2 shows the empirical equation used in this calibration study, the conditions assumed to perform the equations and, as measure of the goodness of fit, RMSE, R^2 and R^2_a.

Figure 5.1 shows the values of ε and the corresponding θ_{Grav} determined gravimetrically from the soil sampled with cylinders and also the fitted equation proposed by Topp et al., 1980. Although, the Topp equation has been used successfully by many researchers in temperate conditions, it has been shown to underestimate θ_{TDR} in clayey soils (Dasberg and Hopmans, 1992; Dirksen and Dasberg, 1993; Jacobsen and Schjønning, 1993). An underestimation of θ can be observed in Figure 5.1, where practically all data are above the fitted Topp Equation. This fact is probably related to the anomalous behaviour of the dielectric properties of water bound in colloidal particles (clay and organic matter), which is discussed in detail below with the physically based methods.

A scatter plot between θ_{Grav} and θ_{TDR}, either by direct reading from the display of the EASY TEST device (Equation 5.1 in Table 5.2) or by calculation with the equation proposed by Malicki et al., (1996) is presented in Figure 5.2. The matching of θ_{Grav} by θ_{TDR} is unsatisfactory and the RMSE was unacceptably high for the EASY TEST equation (Table 5.2).

The Malicki Equation shows reasonable matching in the Figure 5.2 and acceptable value of RMSE (Table 5.2). The partial failure of the Malicki Equation for our data set is probably because it was developed with a data set with a range of ρ between 1200 kg m^{-3} and 1400 kg m^{-3}, whereas the clayey Ferralsols show values of ρ below this range (Table 5.1). The sensitivity analysis of the Malicki Equation in relation to the range of ρ found in these experiment shows that when using the Malicki equation, larger errors would be expected with small ρ values when the soil is wet (Figure 5.3). This condition is commonly found in Amazonian Ferralsols. Therefore, the Malicki Equation may be used and will provide reasonable predictions of θ_{TDR} on clayey Ferralsols when accurate ρ data are available.

The results between the linear, quadratic and cubic regressions are shown in Table 5.2. Small differences between the linear and the quadratic equations using the RMSE criterion were found, whereas the cubic equation contained non-significant coefficients, therefore is not further discussed. Therefore, the quadratic Equation, which shows slightly higher R^2_a and a smaller RMSE, is a suitable relationship for predicted θ_{TDR}. This is a partial conclusion that applies to the polynomial regressions using only ε as variable predictor.

A comparison among the RMSE values in Table 5.2 shows results with a similar accuracy were obtained with the simple linear relationship between the square root of ε and θ_{Grav} (Equation 5.7 in Table 5.2). This linear equation has not only the advantage of mathematical simplicity, but has also a physical meaning. It is equivalent to a linear relationship between ε and the travel time of the electromagnetic waves in the soil (Ledieu et al., 1986; Alharti and Lange, 1987; Yu et al., 1997).

The residual analysis plotted in Figures 5.5 and 5.6 exhibits a small scattering with no trends, showing also no lack of fit for this equation. Other parameters to measure the goodness of fit, such as R^2 and R^2_a, also indicate that the linear-root-square Equation is also a suitable option to calibrate ε as a function of θ_{TDR}. The linear-root-square Equation was also found by Yu et al., (1997 and 1999) to be the best choice for the TDR calibration. Moreover, a potential advantage of using a linear equation is the theoretically need of sample points only at the dry and wet end to estimate the coefficient for a calibration equation.

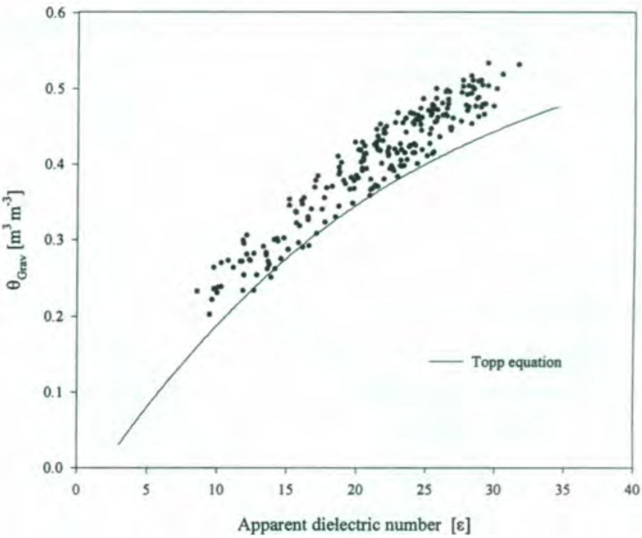

Figure 5.1 - Scatter plot between apparent dieletric number [ε] and volumetric soil water content determined gravimetrically [θ_{Grav}] on a clayey Ferralsol in the central Amazon.
A curve fitted from the Topp Equation is also plotted.

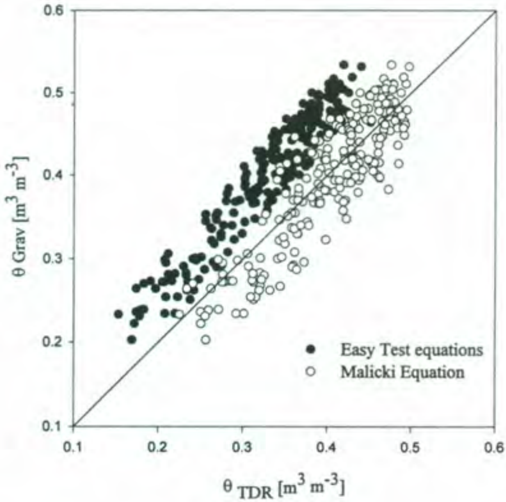

Figure 5.2 - Scatter plot 1:1 between volumetric soil water content determined gravimetrically [θ_{Grav}] and volumetric soil water content [θ_{TDR}] estimated with Easy Test Equation and Malicki Equation on a clayey Ferralsol in the central Amazon.

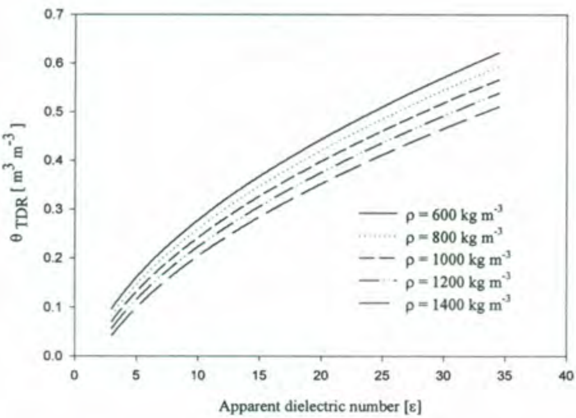

Figure 5.3 - Sensitivity analysis of the influence of bulk density [ρ] on the estimated volumetric soil water content [θ_{TDR}] with the Malicki Equation.

5.4.2.2 Multivariate equations

Table 5.3 shows the results obtained from various multivariate regression procedures. Following the criteria R^2_a and RMSE, the Equation 5.8 in Table 5.3 was chosen as the most suitable between the multivariate equations tested. The same equation was obtained through the stepwise procedure with backward elimination. Table 5.3 shows that different equations may be obtained from the same data only by using different type of multiple regression procedure. Although, for some practical purposes the differences between the values predicted from these equations may not be significant, some of them are statistically different. Furthermore in studies involving many predictors the facilities for using multiple regression in software packages can be misleading and easily misapplied. In some statistical packages the forward selection and backward elimination procedures have the disadvantage that they do not eliminate variables, what can become non-significant after other variables have been added to or removed from the equation (Draper and Smith, 1998).

The multivariate equation obtained from the standard multiple regression (including obligatorily all variables in the equation) shows the highest R^2 within all subsets selected (Equation 5.12 in Table 5.3). This result exemplifies that by forcing additional variable into the calibration equation the resultant estimates might become increasingly unreliable. The larger values of R^2 do not always necessarily implicate the best prediction equation, and its relevance may be questionable and a misleading criterion. Figure 5.4 shows that R^2_a does not necessarily increase with increasing number of variables, as does R^2, because of the correction for number of parameters included in the equation. Therefore, R^2_a may be a better criterion to compare subsets when the equations have a different number of predictor variables.

Figure 5.5 shows the scatter plot of residuals of the quadratic Equation, the linear-root-square Equation and the multivariate Equation (Equation 5.8). It shows a similar scatter among theses equations. A slight improvement on the accuracy by inclusion of ρ into the calibration equation is shown by a reduced RMSE, which does not justify the measurement of ρ only to improve the θ_{TDR} predictions on the clayey Ferralsols (Table 5.3). Multiple regression was used in TDR calibration approaches by Tommaselli and Bacchi (1996) and by Jacobsen and Schjønning (1993), who also found slightly better adjustments when including ρ into the multivariate equation. Contrasting, Malicki et al. (1996) obtained a significant improvement by including ρ into their bivariate equation.

Table 5.5 Parameters used in physical models to calibrate the relationship between dielectric number [ε] and volumetric water content determined gravimetrically [θ_{Grav}]. Values assumed, constraints used and result of parameter optimization with non-linear procedures of Levenberg - Marquardt. As goodness of fit are shown the significance of coefficients, coefficients of determination [R^2]. adjusted coefficients of determination [R^2_a] and root mean square error [RMSE].

Number	Parameters assumed	Parameter optimized	Constraints	R^2	R^2_a	RMSE
		Alpha-3				
13 A	$\varepsilon_s = 3.2; \varepsilon_a = 1; \varepsilon_{fw} = 81$	$\alpha = 0.4859$	$-1 \le \alpha \ge 1$	0.8780	0.8780	0.0272
13 B	$\varepsilon_a = 1; \varepsilon_{fw} = 81$	$\alpha = 0.5233; \varepsilon_s = 4$	$-1 \le \alpha \ge 1; 3 \le \varepsilon_s \ge 30$	0.8944	0.8939	0.0256
13 C	$\varepsilon_s = 4; \varepsilon_a = 1; \varepsilon_w = 81; \alpha = 0.4859$	$\varepsilon_s = 3.7449$	$3 \le \varepsilon_s \ge 50$	0.8807	0.8807	0.0269
		Alpha-4				
14 A	$\varepsilon_s = 4; \varepsilon_a = 1; \varepsilon_{fw} = 81; \iota = 1; \delta = 3x\ 10^{-10}; S = 13 \times 10^{-4}$	$\alpha = 0.5977; \varepsilon_{bw} = 2.00$	$-1 \le \alpha \ge 1; 2 \le \varepsilon_{bw} \ge 50$	0.9147	0.9143	0.0236
14 B	$\varepsilon_s = 4; \varepsilon_a = 1; \varepsilon_{fw} = 81; \alpha = 0.50$	$\alpha = 0.6719; \varepsilon_{bw} = 2.00; \iota = 1$	$-1 \le \alpha \ge 1; 2 \le \varepsilon_{bw} \ge 50; 1 \le \iota \ge 10$	0.9235	0.9228	0.0231
14 C	$\varepsilon_a = 1; \varepsilon_{fw} = 81; \alpha = 0.50; \varepsilon_{bw} = 3.2$	$\alpha = 0.6718; \iota = 1.2253; S = 122533;$ $\delta = 36 \times 10^{-9}; \varepsilon_s = 4$	$-1 \le \alpha \ge 1; 2 \le \varepsilon_{bw} \ge 50; 1 \le \iota \ge 10;$ $3x\ 10^{-10} \le \delta \ge 3x\ 10^{-5};$ $5 \times 10^4 \le S \ge 17 \times 10^4$	0.9235	0.9220	0.0232
		Maxwell-De-Loor				
15 A	$\varepsilon_a = 1; \varepsilon_{fw} = 81; \varepsilon_s = 4; \iota = 1; \delta = 3x\ 10^{-10}; S = 13x\ 10^4$	$\varepsilon_{bw} = 2.00$	$2 \le \varepsilon_{bw} \ge 50$	0.8328	0.8328	0.0313
15 B	$\varepsilon_a = 1; \varepsilon_{fw} = 81; \varepsilon_s = 4; \delta = 3x\ 10^{-10}; S = 13x\ 10^4$	$\varepsilon_{bw} = 2.00; \iota = 1.0$	$2 \le \varepsilon_{bw} \ge 50; 1 \le \iota \ge 10$	0.8328	0.8320	0.0313
15 C	$\varepsilon_a = 1; \varepsilon_{fw} = 81; \varepsilon_s = 4; \iota = 1; \delta = 3x\ 10^{-10}; S = 13 \times 10^4$	$\varepsilon_{bw} = 2.00; \iota = 1.0; S = 13 \times 10^4$	$-1 \le \alpha \ge 1; 2 \le \varepsilon_{bw} \ge 50; 1 \le \iota \ge 10;$ $5 \times 10^4 \le S \ge 17 \times 10^4$	0.8327	0.8312	0.0314
15 D	$^{\dagger}\varepsilon_a = 1; \varepsilon_{fw} = 81; \varepsilon_s = 4; \iota = 1; \delta = 3x\ 10^{-10}; S = 13x\ 10^4$	$\varepsilon_{bw} = 20.00$	$2 \le \varepsilon_{bw} \ge 50$	0.6078	0.6078	0.0315

† - Curtailed data set using only data with $\theta_{Grav} > 0.30$. Values of dielectric constants of different materials were taken from Lide et al. 1999.

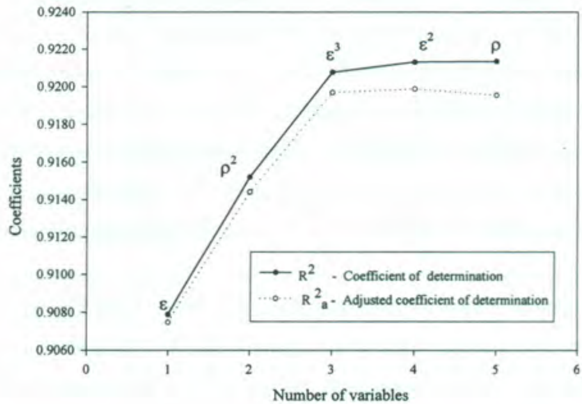

Figure 5.4 - Coefficient of determination [R^2] and adjusted coefficient of determination [R^2_a] in relation to the number of variables in the multivariate equation to predict volumetric soil water content [θ_{TDR}] with apparent dieletric number [ε] and bulk density [ρ] as predictors in an clayey Ferralsol in the central Amazon.

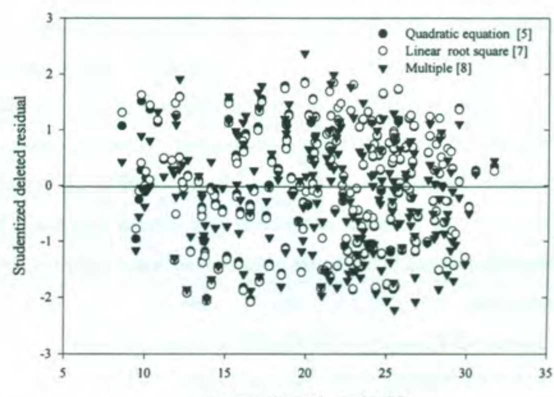

Figure 5.4 - Studentized deleted residual of the volumetric water content [θ_{TDR}] estimated with the quadratic Equation [5]; linear root square Equation [7] and the multiple Equation [8] against apparent dielectric number [ε] measured on a clayey Ferralsol in the central Amazon.

5.4.3 Calibration with physically based Equations

Physically based or mixing equations were first applied assuming ε values of 1.0 for soil air, 3.2 for the solid phase, and 81 for free water. For the Alpha-4 the bound water was calculated following Equation 5.16, whereas the specific surface of the clayey Ferralsol in the central Amazon was estimated to be 130 x 10^{-3} m^2 kg^{-1} (Morais et al., 1976). Table 5.4 shows the results from physically based equations without optimization procedures. The Alpha-3 yielded the most accurate results showed by the lowest RMSE and higher R^2_a. Other experiments have also shown that the Alpha-3 is a robust calibration approach (Roth et al., 1990; Bohl and Roth, 1994; Weitz et al., 1997; Yu et al. 1999). The relative small sensitivity of the Alpha-3 to inaccuracies in soil porosity determinations is shown in Figure 5.7.

The optimized α value in Alpha-3 was found be 0.4859 (Table 5.4). This value is in accordance with the arguments of Yu et al. (1997), who suggested that for TDR probes vertically inserted into the soil, the electromagnetic field is perpendicular to soil layers with different water contents and, in such cases, it can be expected that the fitted α value should be less than 0.5. When ε_s and α were optimized simultaneously, values of 4 and 0.5233 were found, respectively, but with a negligible improvement in the predictions (Table 5.4). Other optimization approaches of the Alpha-3 with simultaneous or subsequent optimization using parameters previously optimized did not give significant improvements in the predictions (Table 5.5).

The Alpha-4 without optimization procedures did not match the data better then the simpler Alpha-3, and showed a large RMSE (Table 5.4). However, when the α and ε_{bw} were optimized simultaneously, Alpha-4 gave more accurate results than Alpha-3 (Table 5.5 and Figure 5.8). Other parameters in several approaches were optimized subsequently, however, changing more parameters did not significantly improve the predictions of θ_{TDR}. Heimovaara et al. (1994) used a sensitivity analysis to show the impact of the different parameters in a refined Alpha-4. They showed that the Alpha-4 is mainly sensitive to changes in thickness of the bound water layer (δ), in the specific surface of soil (S) and bulk density (ρ).

Although, the theoretical Equation of Maxwell-De-Loor has been successfully used in TDR calibration studies (Dirksen and Dasberg, 1993; Bohl and Roth, 1994; Jacobsen and Schjønning, 1995; Weitz et al, 1997), it did not yield accurate θ_{TDR} predictions for our data set. This is probably because the accuracy of this equation decreases when the water content increases beyond a third of the total volume (De Loor, 1990). Therefore, a curtailed data set taking only with values of θ_{Grav} above 0.30 m^3

m^{-3} was tested, but this did not improve the θ_{TDR} predictions (Equation 15 D in Table 5.5). Some other optimizations were also tested but the R^2 and RMSE values are too low to consider the Maxell-De Loor Equation acceptable.

A major problem in applying the Alpha-4 and Maxwell-De-Loor Equations is assigning values to the volume fraction of θ_{bw}, and its average relative dielectric number, ε_{bw}. The number of water layers (ι) to estimate bound water properties in Equation 5.16 is probably larger than 1, with a smooth change between the apparent dielectric number of bound and free water. Further research is needed about the dielectric properties of bound water to improve the performance of the Alpha-4.

The Alpha-4 with α and ε_{bw} fitted to the data showed the best performance among the mixing equations tested. This is in contrast with the results obtained by Dirksen and Dasberg (1993), who did not find an accommodation for the apparently anomalous ε behavior in Ferralsols using the Alpha-4.

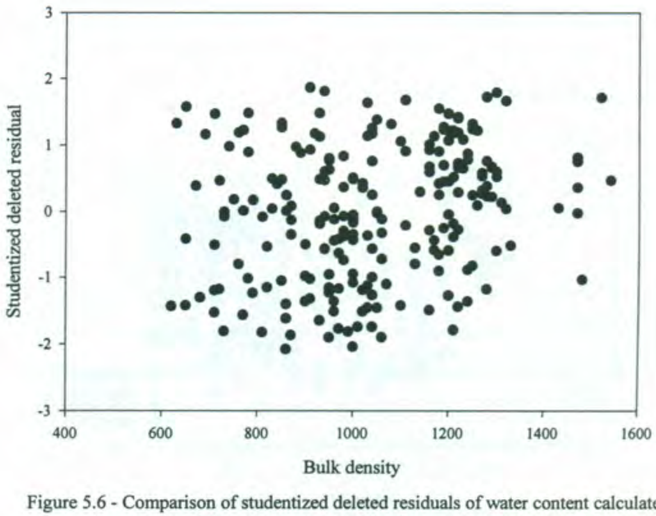

Figure 5.6 - Comparison of studentized deleted residuals of water content calculated with the Linear root square model [7] against bulk density [ρ] on a clayey Ferralsol in the central Amazon.

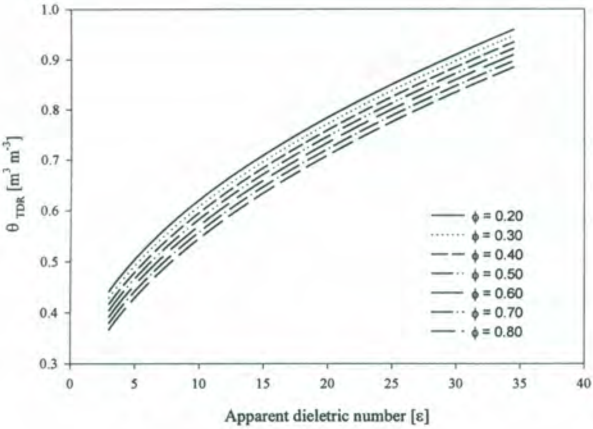

Figure 5.7 - Sensitivity analysis about the influence of porosity [ϕ] on apparent dieletric number [ε] estimated with TDR probes and its effects on estimation on volumetric soil water content [θ_{TDR}] with Alpha-3 Equation [13].

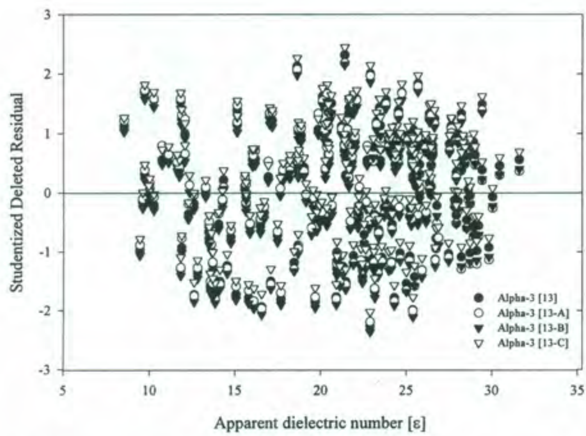

Figure 5.8 Studentized deleted residuals of water content calculated with Alpha 3 Equation using different parameters (Equation 13 in Table 5.4 and Equations 14 A, 14 B and 15 C in Table 5.5) against apparent dielectric number [ε] on an clayey Ferralsol in the central Amazon.

5.4.4 Accuracy

The range of the RMSE of the θ_{TDR} estimations (Tables 5.3 to 5.5) is approximately of the same magnitude as those found by other authors: - Herkelrath et al. (1991) [0.02]; Bohl and Roth, (1994) [0.02 to 0.03 for mineral soils and 003 to 0.07 for organic soils]; Topp et al. (1980) [0.013]; Jacobsen and Schjønning (1995) [0.01to 0.18] and Weitz et al. (1997) [0.02 to 0.52]. Moreover, the accuracy of θ_{TDR} for the best equations in Table 5.4 to5.5 are of the same magnitude as the accuracy showed by θ_{Grav} measurements (about 0.02 – Gardner (1986) pg. 56). However, the validation study below, shows reduced accuracy than the calibration results, this fact is discussed below. The sources of error of gravimetric methods - normally taken as the „corrected" value of θ are discussed in details by Gardner (1986) and errors in the determination of ρ by Blake and Hartge (1986).

5.4.5 Validation

The quadratic Equation, the linear-root-square Equation and the multivariate fitted for the clayey Ferralsol showed the smallest RMSE in the validation study (Table 5.7). This is not surprising since these equations were developed for this soil, but confirms the reliability of these calibration equations. Moreover, Table 5.7 gives the field accuracy with which the volumetric soil water content can be estimated with TDR probes. The lower accuracy [ca. 0.05] in comparison to the values found in the calibration study [ca 0.02] is probably related to the fact that the validation data set was obtained exclusively at the soil surface. Therefore, the high variability normally found at the soil surface might introduce more uncertainties either in the ε determinations (e.g.., because of air gaps around the TDR rods) or in the gravimetric determination (Teixeira et al. 2001). Furthermore, this data set contains more values in the dry range than the data set used in calibration studies and, as shown on Figure 5.9 (in the dry range the accuracy of TDR estimations is lower. see discussion on the section range of water content).

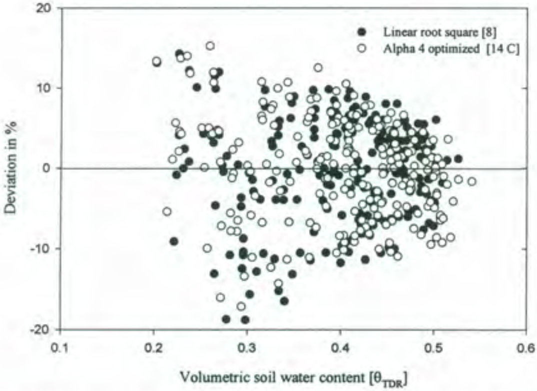

Figure 5.9 - Deviations of raw residues (%) of volumetric water content (θ_{TDR}) estimated with Linear root square Equation [8] and Alpha 4 Equation optimized [14 C] against the estimated volumetric soil water content [θ_{TDR}] on a clayey Ferralsol in the cetral Amazon

Table 5.6 Volumetric soil moisture assessed gravimetrically [θ_{Grav}], apparent dielectric number [ε], soil bulk density [ρ] and porosity [ϕ] measured on a clayey Ferralsol in the central Amazon.

θ_{Grav} $m^3 m^{-3}$				ε				ρ $Mg\ m^{-3}$				ϕ %			
μ	SD	Min	Max	μ	SD	Min	Max	μ	SD	Min	Max	μ	SD	Min	Max
0.3868	0.0858	0.2080	0.5256	18.38	4.03	11.14	26.45	1.008	0.084	0.800	1.183	0.60	0.03	0.53	0.67

μ = Mean; SD = Standard deviation; Min = Minimum datum; Max = Maximum datum; data set of 81 samples

The Alpha-3 and the optimized Alpha-4 for the clayey Ferralsol [Eq. 14 C] showed similar accuracy with smaller RMSE and AD in the validation study (Table 5.7).

In addition, the θ_{TDR} estimates from the Alpha-3 and Alpha-4 Equations were recalculated using only an average value of ρ [1.00 Mg kg^{-3}] and ϕ [0.60 %]. The results [RMSE 0.0764 and 0.0707 for the Alpha 4 and Alpha 3, respectively] show that using an estimated value of ρ and ϕ the accuracy remains in the same order of magnitude. When ρ measurements are available from the site of measurement, they should be used, but the improvement might not justify the effort for their determination. Reliable estimates of ρ and ϕ can be used without loss of accuracy if the range of variation is not so large.

Table 5.7 Root mean square error[RMSE] and average deviation (AD) as statistics to estimate the accuracy of different calibration equations for estimation of volumetric soil water content (θ_{TDR}) in a clayey Ferrralsol in the central Amazon.

Statistical parameters	Topp [3]	Malicki [2]	Quadratic [6]	Linear root square [7]	Multivariate [8]	Alfa-3 [13]	Alfa-4 [14 c]
RMSE	0.0852	0.0691	0.0675	0.0674	0.0668	0.0760	0.0707
AD	0.0750	0.0483	0.0480	0.0470	0.0420	0.0411	0.0030

5.4.6 Influence of soil characteristics on ε determination under field conditions.

5.4.6.1 Range of water contents

In the calibration procedure with regression analysis, the regression coefficients depend, among other factors, on the range of θ used. In the present study, a range of θ between 0.20 – 0.53 m^3 m^{-3} was used (Table 5.1). Similar ranges of θ were obtained with the neutron probe technique by Cabral (1991) and by Hodnett et al. (1996) in field studies on similar soils in the central Amazon. Therefore, the range used in our calibration corresponds to its normal range encountered under field conditions.

In laboratory calibrations, such as those performed by Topp et al. (1980) and Malicki et al. (1996), a larger range of θ can be obtained, even if it does not occur in the field. The use of an increased range of water contents in TDR calibration procedures can lead to changes in the coefficients of the equations. It should occur principally in clayey soils, due to an increase of the relative contribution of bound water to ε in the dry range. At low soil moisture values, ε increases slowly with increasing soil water content, but after passing a certain soil moisture whose value depends strongly on soil texture or organic matter content, a pronounced increase in the inclination of this relationship may occur.

A better accuracy of the θ_{TDR} predictions in the wet range by the Linear-root-square Equation and the Alpha 4 is shown in Figure 5.9. It may be explained due to a better contact of the rods with the surrounding soil and a consequent reduced occurrence of discontinuities, such as air-inclusions and water gaps near the probes. Furthermore, at high water content the relatively lower velocity of propagation may facilitate the determination of ε (Amato and Ritchie, 1993). Therefore θ_{TDR} values are less reliable for the dry range than in the intermediate to wet range.

5.4.6.2 Temperature effects

In this calibration study, ε measurements were taken on sites relatively protected from direct radiation. Hence, temperature was probably not a significant source of error. Soil variability among different probe locations probably causes larger errors in the θ measurements than temperature (Yu et al., 1999; Roth et al., 1990). Consequently, for absolute measurements, temperature does not need to be considered. However, it should be kept in mind that ε is also a function of temperature (Lide, 1999; Pepin et al., 1995), and errors could be introduced into ε measurements when measuring the relative changes in θ using a single probe permanently installed. In this situation, temperature effects may assume importance and, if not accounted for, they will impose an apparent change in θ between, e.g., day and night, especially in the topsoil or where significant temperature gradients occur during the evaluated period.

5.4.6.3 Soil electrical conductivity

Soil bulk electrical conductivity can cause an overestimation of θ (Persson and Berndtsson, 1998) if the soil solution has an electrical conductivity greater than about 8 dS m^{-1} (Dalton, 1992).
In parallel studies of this project, the maximal values of soil electrical conductivity were found to be about 2 dS m^{-1} in brief period after the twice-yearly fertilisation. Therefore, the electrical conductivity effects in ε determinations were not considered in this study.

5.4.6.4 Technical characteristics and installation procedures

The measurements of ε were taken immediately after installing the probes into the soil. This procedure may introduce errors due to the compression of the water around the steel rods during the installation (Jacobsen and Schjønning, 1993; Rothe et al., 1997). However, this effect had certainly a reduced importance in this study because of the small diameter of the rods (2 mm) used, but it may be relevant for rods with larger diameter, especially in clayey soils close to saturation.

Ease of insertion and minimising soil disturbance dictate that the probe wires should have as small a diameter as possible. Against this, the effect of air gaps, the volume measured and mechanical strength of the soil requires large diameter rods (Zegelin et al., 1992). A disadvantage of rods with small diameter is the occurrence of a short circuit when the probe is being installed into the soil in the dry range, such as when the mechanic resistance of the clayey Ferralsols is very high in dry conditions. A short circuit causes a downward deviation of the propagation signal that could lead to a subestimation of θ (Amato and Ritchie, 1993). It is recommended to check for drifts in the equipment by reading the ε value in air and pure water before starting the measurement in soil.

5.4.6.5 Magnetic effects

In this study, the employed pulse travel time of 250 ps was presumably too small to cause changes in the process of magnetic polarisation of the soil (Roth et al., 1990). Furthermore, the clayey Ferralsols on the central Amazon have apparently not enough iron and magnetic minerals for the occurrence of the polarisation phenomenon.

5.5 CONCLUSIONS

Accurate predictions of θ for the clayey Ferralsols in the central Amazon may be obtained with the quadratic Equation or using the simplest linear-root- square Equation .

The commonly used Topp Equation poorly fitted the data and tends to overestimate θ.

The Malicki Equation could give accurate results if reliable estimates of bulk density are available.

The improvement of the θ predictions using empirical multivariate functions of ε and ρ was small.

The Alpha-3 Equation might be a good alternative, if the bulk density values change in a large range and only estimate of these values are available. Sensitivity analysis and a validation study showed that the Alpha-3 is a robust calibration procedure that can yield satisfactory accuracy even if only an estimate of bulk density is available.

The physically based equation Alpha-4, with α and ε_{bw} fitted, gave accurate θ_{TDR} estimations and seems to be a good option if the measured data are concentrated in the dry range. Further research is needed about the dielectric properties of bound water in order to improve the performance of the Alpha-4 Equation for fine textured soils.

The accuracy of the estimates of θ using the TDR technique is higher in the ~~dry~~ range.

wet

The choice of a specific equation requires the knowledge of soil characteristics and the required accuracy; not every study requires precise absolute measurements that justify the considerable investment in time and labour for a field calibration.

5.6 REFERENCES

ALHARTI A. and LANGE J. Soil water saturation: dielectric determination. Water Resources Research. 23: 591-595, 1987.

AMATO M. and RITCHIE J T. Small spatial scale soil water content measurement with time-domain reflectometry. Soil Science Society of America Journal. 59: 325-329, 1995.

ANSOULT M.; BACKER L W DE. and DECLERQ M. Statistical relationship between apparent dielectric constant and water content in porous media. Soil Science Society of America Journal. 48: 47-50, 1984.

BLAKE G R. and HARTGE K H. Bulk density. In: KLUTE A., ed. Methods of soil analysis, Part 1: Physical and Mineralogical methods. 2. Madison, ASA and SSSA, 1986. p.363-375.

BOHL H and ROTH K. Evaluation of dielectric mixing models to describe the $\theta(\varepsilon)$-relations. North Western University, Evanston, 1994. p.309-319.

CABRAL O M R. Armazenamento de água no solo da floresta e de terra firme e seringal implantado, São José dos Campos, INPE, 1990. 103p. (Master)

DALTON F N. and VAN GENUCHTEN M TH. The time domain reflectometry method for measuring soil water content and salinity. Geoderma. 38: 237-250, 1986.

DALTON F N. Development of time-domain reflectometry for measuring soil water content and bulk soil electrical conductivity. In: TOPP G C.; REYNOLDS W D. and GREEN R E., eds. Advances in measurements of soil physical properties: bringing theory into practice. Madison, SSSA, 1992. p.143-168.

DASBERG S. and HOPMANS J W. Time domain reflectometry calibration for uniformly and nonuniformly wetted and clayey loam soils. Soil Science Society of America Journal. 56: 1341-1345, 1992.

DE LOOR G P. The dielectric properties of wet soils. Report 90-13, -41. 1990. The Hague, Netherlands Remote Sensing Board.

DIRKSEN C. and DASBERG S. Improved calibration of time domain reflectometry soil water content measurements. Soil Science Society of America Journal. 57: 660-667, 1993.

DRAPER N R and SMITH H. Applied regression analysis. 3.ed. New York, Wiley, 1998. 820p.

EMBRAPA. Manual de métodos de análise de solo. 2.ed. Embrapa-CNPS, 1997. 212p.

FERRÉ P A.; RUDOLPH D L. and KACHANOSKI R G. Spatial averaging of water content by time domain reflectometry: Implications for twin rod probes with and without dielectric coatings. Water Resources Research. 32: 271-279, 1996.

FERRÉ P A.; REDMAN J D.; RUDOLPH D L. and KACHANOSKI R G. The dependence of the electrical conductivity measured by time domain reflectometry on the water content of a sand. Water Resources Research. 34: 1207-1213, 1998.

GARDNER W H. Water content. In: KLUTE A., ed. Methods of soil analysis, Part 1: Physical and Mineralogical methods. 2. Madison, ASA and SSSA, 1986. p.479-492.

GRAYBILL F A and IYER H K. Regression analysis: concepts and applications. Belmont, Duxbury Press, 1994. 701p.

HALL P G. and ROSE M A. Dielectric properties of water adsorbed by kaolinite clays. Trans. Faraday Soc. 1221-1233, 1977.

HEIMOVAARA T J.; BOUTEN W. and VERSTRATEN J M. Frequency domain analysis of time domain reflectometry waveforms 2. A four-component complex dielectric mixing model for soils. Water Resources Research. 30: 201-209, 1994.

HERKELRATH W N.; HAMBURG S P. and MURPHY F. Automatic, real-time monitoring of soil moisture in a remote field area with time domain reflectometry. Water Resources Research. 27: 857-864, 1991.

HODNETT M G.; OYAMA M D.; TOMASELLA J. and MARQUES A DE O. Comparisons of long-term soil water storage behaviour under pasture. In: GASH J H C.; NOBRE C A.; ROBERTS J M. and VICTORIA R L, eds. Amazonian deforestation and climate. Chichester, John Wiley & Sons, 1986. p.57-78.

HOOK W R. and LIVINGSTON N J. Propagation velocity errors in time domain reflectometry measurements of soil water. Soil Science Society of America Journal. 59: 92-96, 1995.

JACOBSEN O H. and SCHJØNNING P. A laboratory calibration of time domain reflectometry for soil water measurement including effects of bulk density and texture. Journal of Hydrology. 151: 147-157, 1993.

JACOBSEN O H and SCHJØNNING P. Comparison of TDR calibration functions for soil water determination. In: PETERSEN L W. and JACOBSEN O H. (eds.). Danish institute of plant and soil science, Tjele, 1995. p.25-34.

KIM D J.; VANCLOOSTER M.; FEYEN J. and VEREECKEN H. Simple linear model for calibration of time domain reflectometry measurements on solute concentration. Soil Science Society of America Journal. 62: 83-89, 1998.

LEDIEU J.; RIDDER P DE.; CLERCK P DE. and DAUTREBANDE S. A method of measuring soil moisture by time-domain reflectometry. Journal of Hydrology. 88: 319-328, 1986.

LIDE D R. Handbook of chemistry and physics. 80.ed. Boca Raton, CRC, 1999. np.

MALICKI M A.; PLAGGE R. and ROTH C H. Improving the calibration of dielectric TDR soil moisture determination taking into account the solid soil. European Journal of Soil Science. 47: 357-366, 1996.

MORAIS F I.; PAGE A L. and LUND L J. The effect of pH, salt concentration, and nature of electrolytes on the charge characteristics of Brazilian tropical soils. Soil Science Society of America Journal. 40: 521-527, 1976.

OR D. and WRAITH J M. Temperature effects on soil bulk dielectric permittivity measured by time domain reflectometry: A physical model. Water Resources Research. 35: 371-383, 1999.

PEPIN S.; LIVINGSTON N J. and HOOK W R. Temperature-dependent measurement errors in time domain reflectometry determinations of soil water. Soil Science Society of America Journal. 59: 38-43, 1995.

PERSSON M. and BERNDTSSON R. Texture and electrical conductivity effects on temperature dependency in time domain reflectometry. Soil Science Society of America Journal. 62: 887-893, 1998.

PETERSEN L W.; THOMSEN A.; MOLDRUP P.; JACOBSEN O H. and ROLSTON D E. High-resolution time domain reflectometry: sensitivity dependency on probe-design. Soil Science. 159: 149-154, 1995.

PRESS W.; TEUKOLSKY S A.; VETTERLING W T. and FLANNERY B P. Numerical recipes in Fortran - The art of scientific computing. 2.ed. Cambridge, Cambridge University Press, 1992. 963p.

ROBISON D A.; BELL J P. and BACHELOR C H. Influence of iron and titanium on water content determination by TDR. In: PETERSEN L.W. and JACOBSEN O.H. (eds.) .Danish institute of plant and soil science, Tjele, 1994. p.63-70.

ROTH C H.; MALICKI M A. and PLAGGE R. Empirical evaluation of the relationship between soil dielectric constant and volumetric water content as the basis for calibrating soil moisture measurements by TDR. Journal of Soil Science. 43: 1-13, 1992.

ROTH K.; SCHULIN R.; FLÜHLER H. and ATTINGER W. Calibration of time domain reflectometry for water content measurement using a composite dielectric approach. Water Resources Research. 26: 2267-2273, 1990.

ROTHE A.; WEIS W.; KREUTZER K.; MATTHIES D.; HESS U. and ANSORGE B. Changes in soil structure caused by the installation of time domain reflectometry probes and their influence on the measurement of soil moisture. Water Resources Research. 33: 1585-1593, 1997.

SCHROTH G.; DA SILVA L F.; WOLF M A.; TEIXEIRA W G. and ZECH W. Distribution of throughfall and stemflow in multi-strata agroforestry, perennial monoculture, fallow and primary forest in central Amazonia, Brazil. Hydrological Processes. 13: 1423-1436, 1999 a.

SCHROTH G.; DA SILVA L F.; SEIXAS R.; TEIXEIRA W G.; MACÊDO J L V. and ZECH W. Subsoil accumulation of mineral nitrogen under monoculture and polyculture plantations in a ferralitic Amazonian upland soil. Agriculture, Ecosystems and Environment. 75: 1423-1436, 1999 b.

SEYFRIED M S. and MURDOCK M D. Calibration of time domain reflectometry for measurement of liquid water in frozen soils. Soil Science. 161: 87-98, 1996.

STELL R G.; TORRIE J H. and DICKEY D A. Principles and procedures of statistics a biometrical approach. 3.ed. New York, Mc-Grawn Hill, 1997. 666p.

TEIXEIRA W G.; FACCIN O P.; SCHROTH G.; AZEVEDO C P. and HUWE B. Calibração de TDR para avaliação da umidade do solo num latossolo amarelo textura muito argilosa - avaliação de campo. In: congresso brasileiro de ciência do solo, 26., 1997. SBCS - EMBRAPA / SNLCS, Rio de Janeiro, 1997. CD-ROM

TEIXEIRA W G.; MARQUES J D.; SCHROTH G. and HUWE B. Sampling procedures and mode of insertion into the soil of TDR probes on determination of volumetric soil water content (θ) C. Revistra Brasileira de Ciência do Solo. 00: 00-00, 2001. – (accepted to be published)

TOMMASELLI J T G and BACCHI O O S. Calibração de um TDR utilizando modelos empíricos para cinco solos paulistas. In: Congresso latino americano de ciência do solo, 13., 1996. SBCS, Campinas, 1996. CD-ROM.

TOPP G C.; DAVIS J L. and ANNAN A P. Electromagnetic determination of soil water content: measurements in coaxial transmission lines. Water Resources Research. 16: 574-582, 1980.

TOPP G C. and DAVIS J L. Measurements of soil water content using time-domain reflectometry (TDR): a field evaluation. Soil Science Society of America Journal. 49: 19-24, 1985.

WHALLEY W R. Consideration on the use of time-domain reflectometry (TDR) for measuring soil water content. European Journal of Soil Science. 44: 1-9, 1993.

WEITZ A M.; GRAUEL W T.; KELLER M. and VELDKAMP E. Calibration of time domain reflectometry technique using undisturbed soil samples from humid tropical soils of volcanic origin. Water Resources Research. 33: 1241-1249, 1997.

WHITE I.; KNIGHT S J.; ZEGELLIN S J. and TOPP G C. Comments on 'Considerations on the use of time-domain reflectometry (TDR) for measuring soil water content' by W.R. Whaley. European Journal of Soil Science. 45: 503-508, 1994.

WRAITH J M. and OR D. Temperature effects on soil bulk dielectric permittivity measured by time domain reflectometry: Experimental evidence and hypothesis development. Water Resources Research. 35: 361-369, 1999.

YU C.; WARRICK A W.; CONKLIN M H.; YOUNG M H. and ZREDA M. Two- and three-parameter calibrations of time domain reflectometry for soil moisture measurement. Soil Science Society of America Journal. 33: 2417-2421, 1997.

YU C.; WARRICK A W. and CONKLIN M H. Derived functions of time domain reflectometry for soil moisture measurement. Water Resources Research. 35: 1789-1796, 1999.

ZEGELIN S J.; WHITE I. and RUSSEL G F. A critique of the time domain reflectometry technique for determining field soil-water content. In: TOPP G C.; REYNOLDS W D. and GREEN R E., eds. Advances in measurements of soil physical properties: bringing theory into practice. Madison, SSSA, 1992. p.187-208.

Table A-5.1 Measured gravimetric water content, dielectric number of soil; bulk density and porosity in different depths in an clayey Ferralsol in the central Amazon.

	Depth [cm]	θ_{Grav}	ε	BD [Mg kg^{-1}]	porosity ϕ		Depth [cm]	θ_{Grav}	ε	BD [Mg kg^{-1}]	porosity ϕ
1	30	0.468	23.81	1.27	0.49	41	90	0.498	26.45	1.22	0.51
2	30	0.4526	24.55	1.25	0.5	42	90	0.517	28.22	1.25	0.5
3	30	0.4604	23.45	1.27	0.49	43	90	0.5	28.42	1.26	0.5
4	30	0.426	21.23	1.21	0.52	44	90	0.511	28.92	1.28	0.49
5	30	0.419	21.49	1.18	0.53	45	90	0.502	28.32	1.3	0.48
6	30	0.429	20.37	1.2	0.52	46	90	0.476	28.92	1.21	0.52
7	30	0.424	20.54	1.18	0.53	47	90	0.471	27.92	1.18	0.53
8	30	0.394	22.54	1.19	0.52	48	90	0.505	29.02	1.3	0.48
9	30	0.441	21.92	1.28	0.49	49	90	0.459	24.18	1.22	0.51
10	30	0.425	23.81	1.22	0.51	50	90	0.462	24.64	1.22	0.51
11	30	0.458	24.46	1.33	0.47	51	90	0.471	25.11	1.23	0.51
12	30	0.468	22.9	1.27	0.49	52	90	0.474	24.55	1.24	0.5
13	30	0.462	25.78	1.3	0.48	53	90	0.4807	26.12	1.21	0.52
14	30	0.472	25.4	1.32	0.47	54	150	0.4537	28.22	1.19	0.52
15	30	0.465	25.3	1.29	0.48	55	150	0.4924	27.92	1.16	0.54
16	30	0.427	24.09	1.18	0.53	56	150	0.4782	27.82	1.14	0.54
17	30	0.423	23.72	1.17	0.53	57	150	0.4885	28.72	1.19	0.52
18	30	0.416	25.49	1.13	0.55	58	150	0.4769	28.52	1.16	0.54
19	30	0.44	25.21	1.21	0.52	59	150	0.479	29.02	1.18	0.53
20	30	0.446	21.92	1.2	0.52	60	150	0.519	30.46	1.25	0.5
21	30	0.453	24.09	1.22	0.51	61	150	0.532	31.61	1.29	0.48
22	30	0.474	26.45	1.3	0.48	62	150	0.504	29.43	1.27	0.49
23	30	0.456	25.59	1.25	0.5	63	150	0.495	27.52	1.26	0.5
24	30	0.345	15.15	1.06	0.58	64	150	0.494	28.22	1.27	0.49
25	30	0.378	19.03	1.17	0.53	65	150	0.503	27.62	1.28	0.49
26	30	0.419	20.11	1.31	0.48	66	150	0.5	30.04	1.24	0.5
27	90	0.4548	23.26	1.19	0.52	67	150	0.477	29.84	1.21	0.52
28	90	0.4499	22.1	1.2	0.52	68	150	0.48	29.22	1.2	0.52
29	90	0.4867	24.74	1.2	0.52	69	150	0.496	26.64	1.24	0.5
30	90	0.408	20.45	1.11	0.56	70	150	0.476	28.02	1.23	0.51
31	90	0.432	21.57	1.16	0.54	71	150	0.463	28.72	1.17	0.53
32	90	0.423	21.4	1.16	0.54	72	150	0.487	28.62	1.24	0.5
33	90	0.486	26.55	1.16	0.54	73	150	0.466	29.12	1.22	0.51
34	90	0.496	26.35	1.22	0.51	74	150	0.464	26.45	1.22	0.51
35	90	0.5	25.68	1.25	0.5	75	150	0.466	26.35	1.21	0.52
36	90	0.504	28.02	1.28	0.49	76	150	0.455	24	1.2	0.52
37	90	0.534	29.43	1.28	0.49	77	150	0.48	26.55	1.29	0.48
38	90	0.511	28.32	1.05	0.58	78	150	0.445	26.74	1.19	0.52
39	90	0.511	27.62	1.11	0.56						
40	90	0.51	28.72	1.2	0.52						

BD is bulk density

Table A- 5.2 Measured gravimetric water content, dielectric number of soil ; bulk density and porosity near different species of plant in an clayey Ferralsol in the central Amazon.

N. treat	θ_{Grav}	ε	BD	ϕ	N. treat.	θ_{Grav}	ε	BD	ϕ	N. treat.	θ_{Grav}	ε	BD	ϕ
1 PP	0.222	9.63	0.82	0.67	53 P	0.411	25.02	1.06	0.58	105 PP	0.3976	22.46	0.73	0.71
2 PP	0.238	10.04	0.81	0.68	54 P	0.398	23.08	1.04	0.58	106 PP	0.4021	18.87	0.95	0.62
3 PP	0.233	8.55	0.86	0.66	55 P	0.344	18.71	1.04	0.58	107 PP	0.3402	16.73	0.85	0.66
4 PP	0.236	9.75	0.85	0.66	56 P	0.308	17.12	0.97	0.61	108 PP	0.3814	20.07	1	0.6
5 PP	0.231	9.98	0.84	0.66	57 P	0.326	16.5	1.01	0.6	109 PP	0.405	23.13	0.87	0.65
6 PP	0.239	10.28	0.73	0.71	58 P	0.38	21.92	1.13	0.55	110 PP	0.3795	20.97	0.78	0.69
7 PP	0.234	12.63	0.87	0.65	59 M	0.287	15.08	0.65	0.74	111 PP	0.3662	19.49	1	0.6
8 PP	0.27	10.28	1.06	0.58	60 M	0.296	15.82	0.68	0.73	112 PP	0.4132	20.5	0.97	0.61
9 PP	0.298	14.36	1.22	0.51	61 M	0.267	13.73	0.62	0.75	113 PP	0.4775	25.4	1.04	0.58
10 PP	0.264	9.75	1.03	0.59	62 M	0.337	15.6	0.79	0.68	114 PP	0.4672	25.35	1.16	0.54
11 PP	0.281	12.11	1.03	0.59	63 M	0.414	25.4	0.85	0.66	115 PP	0.447	25.3	1	0.6
12 PP	0.283	13.52	0.83	0.67	64 M	0.397	23.17	0.81	0.68	116 C	0.3467	16.08	1	0.6
13 PP	0.251	13.87	0.96	0.62	65 M	0.415	24	0.9	0.64	117 C	0.394	20.67	0.94	0.62
14 PP	0.273	12.37	1	0.6	66 M	0.385	19.95	0.85	0.66	118 C	0.4028	20.28	1	0.6
15 PP	0.264	11.14	1	0.6	67 M	0.34	17.51	0.87	0.65	119 C	0.461	26.89	0.93	0.63
16 PP	0.295	11.91	1	0.6	68 M	0.384	17.19	0.94	0.62	120 C	0.4193	23.17	1.04	0.58
17 PP	0.299	11.85	1.04	0.58	69 M	0.3	14.08	0.71	0.72	121 C	0.4136	22.23	0.97	0.61
18 PP	0.28	13.52	0.78	0.69	70 M	0.306	12.11	0.73	0.71	122 C	0.4148	22.86	1	0.6
19 PP	0.322	15.67	0.94	0.62	71 M	0.254	11.91	0.65	0.74	123 C	0.4569	27.47	1	0.6
20 PP	0.33	18.46	1.11	0.56	72 M	0.274	12.3	0.71	0.72	124 C	0.415	23.4	1.04	0.58
21 PP	0.268	13.73	0.86	0.66	73 M	0.391	20.37	0.83	0.67	125 C	0.4294	21.4	0.98	0.61
22 PP	0.2027	9.46	0.71	0.72	74 M	0.477	25.49	0.94	0.62	126 C	0.4363	25.92	0.91	0.64
23 PP	0.254	12.84	0.76	0.7	75 M	0.401	21.75	0.98	0.61	127 C	0.4271	25.21	1.03	0.59
24 PP	0.262	13.59	0.72	0.71	76 M	0.273	10.77	0.65	0.74	128 C	0.4113	22.23	0.95	0.62
25 PP	0.33	16.5	0.86	0.66	77 M	0.282	12.63	0.76	0.7	129 C	0.4668	24.04	0.98	0.61
26 PP	0.368	17.82	0.98	0.61	78 B	0.348	19.7	0.75	0.7	130 C	0.391	22.63	1.04	0.58
27 PP	0.353	15.15	1.02	0.59	79 B	0.336	15.67	0.77	0.69	131 C	0.382	19.57	0.96	0.62
28 PP	0.272	13.66	0.93	0.63	80 B	0.369	16.96	0.67	0.73	132 C	0.3736	19.16	1.05	0.58
29 PP	0.318	15.89	0.91	0.64	81 B	0.429	19.86	0.74	0.7	133 C	0.3897	18.75	0.93	0.63
30 PP	0.234	11.85	0.82	0.67	82 B	0.453	21.66	0.94	0.62	134 C	0.4449	24.6	0.95	0.62
31 PP	0.292	16.58	0.91	0.64	83 B	0.465	24.36	0.91	0.64	135 C	0.4413	22.01	0.98	0.61
32 PP	0.29	16.12	0.86	0.66	84 B	0.457	25.68	0.89	0.64	136 C	0.42	22.68	1.03	0.59
33 PP	0.301	14.29	0.95	0.62	85 B	0.487	25.68	1	0.6	137 C	0.4152	24.13	0.96	0.62
34 PP	0.291	13.31	0.93	0.63	86 B	0.383	22.9	0.69	0.72	138 C	0.419	24.64	1.07	0.57
35 PP	0.272	11.78	0.96	0.62	87 B	0.465	26.16	0.87	0.65	139 C	0.406	23.58	1.02	0.59
36 PP	0.275	14.57	0.98	0.61	88 B	0.417	22.19	0.77	0.69	140 C	0.4312	21.84	0.95	0.62
37 PP	0.272	11.65	0.96	0.62	89 B	0.472	25.78	0.86	0.66	141 C	0.4463	21.4	1.47	0.41
38 PP	0.262	14.15	0.94	0.62	90 B	0.455	22.72	0.72	0.71	142 C	0.4104	18.63	1.32	0.47
39 P	0.37	21.49	0.97	0.61	91 B	0.437	21.49	0.63	0.75	143 C	0.4049	20.45	1.52	0.39
40 P	0.394	22.37	0.93	0.63	92 B	0.479	25.4	0.77	0.69	144 C	0.3944	20.37	1.54	0.38
41 P	0.418	21.66	1	0.6	93 B	0.355	16.2	0.88	0.65	145 C	0.4486	26.79	1.43	0.43
42 P	0.398	23.36	1.02	0.59	94 B	0.302	14.79	0.78	0.69	146 C	0.4422	23.49	1.48	0.41
43 P	0.367	19.78	1.1	0.56	95 B	0.351	16.05	0.9	0.64	147 C	0.4269	23.08	1.47	0.41
44 P	0.37	18.22	1.13	0.55	96 PP	0.4007	24.32	0.95	0.62	148 C	0.414	20.62	1.47	0.41
45 P	0.355	17.67	1.04	0.58	97 PP	0.4219	22.28	0.99	0.6					
46 P	0.378	19.78	1.05	0.58	98 PP	0.461	23.49	0.79	0.68					
47 P	0.378	17.04	1.06	0.58	99 PP	0.4486	26.69	0.92	0.63					
48 P	0.37	18.22	1.08	0.57	100 PP	0.3861	18.71	0.9	0.64					
49 P	0.366	20.97	1.18	0.53	101 PP	0.3681	21.14	0.95	0.62					
50 P	0.372	21.31	1.02	0.59	102 PP	0.323	17.7	0.71	0.72					
51 P	0.396	18.71	1.05	0.58	103 PP	0.4185	20.24	1.03	0.59					
52 P	0.425	24.18	1.1	0.56	104 PP	0.3579	20.92	0.93	0.63					

P – pueraria, PP – peach palm, C – Cupuacu; M – Matá – matá and B -- bacaba.

6 LAND USE EFFECTS ON HYDRAULIC PROPERTIES

6.1 INTRODUCTION

Determination of hydraulic properties may be required to solve many questions in agriculture research. Studies involving water fluxes and chemical transport through the soil profile; changes in soil water storage, water balance studies and soil-plant-water relations need accurate estimations of soil hydraulic properties. Hydraulic properties are spatially and temporally variable, consequently, reliable soil hydraulic characterisation is complex and time-consuming. Furthermore, many hydraulic properties are better represented by functions (i.e., unsaturated hydraulic conductivity and soil water retentivity) instead by the mean values. Besides, the results are dependent on the methods used and soil and climate conditions at the time of determination.

Soil hydraulic properties are easily altered by natural events such as rainfall, faunal and microbial activity, and by management practices such as harrowing, ploughing, cultivating, draining, fertilisation and use of cover crops. The change of cohesive forces between the soil constituents, determined by alteration of characteristics such as pH, CEC, iron and aluminium oxides and organic matter, can affect the mechanical and consequently the hydraulic properties of the soil (El Swaify, 1980; Assouline et al., 1997; Silva et al., 1999). Other factors that can also interfere in the water transport processes into the soil vadose zone are the mineralogy of the solid particles (Iwata, 1996) the nature of the ions present (Kutilek et al., 1973), and initial volumetric water content (Hillel, 1998).

Temperature effects are normally considered too small to be of importance, especially in comparison with the spatial and temporal variability encountered in the field. However, the effect of temperature on the function K (h) was analysed by Stoffregen et al. (1999) which show that the temperature dependence is independent of water pressure head, and can be described by an exponential function. However, the experimental data did not agree with the expected values of the theory, and the hydraulic conductivity can be doubled by varying the temperature by about 15°C, when all other factor remain equal. Matthieu and Pieltain (1998) presented factors of correction to permit comparison between infiltration tests using water at different temperatures. The magnitude of the temperature effect on the hydraulic properties is not completely understood, and similar conditions should be maintained during the evaluation process to permit comparisons.

In general, most undisturbed tropical forest soils are characterised by a rich organic matter layer on the surface with considerable biotic activity which apparently opens large channels in the soil and allows for rapid infiltration of water. In addition, the forest canopy and litter effectively intercept raindrops, slowing their kinetic energy during high intensity thunderstorms, which are frequent in tropical climates.

The removal of vegetation and introduction of mechanised tillage operations result in disturbance and exposure of soil to the direct impact of raindrops and more intensive cycles of wetting and drying. Deforestation frequently cause a rapid decline in the infiltration rate (Lal, 1979; 1989; Côrrea, 1985), which could lead to runoff and erosion processes, especially in hill slope agriculture fields. The ability of a soil to transmit water at a rate comparable to that of rainfall intensity is an important property that maintains an adequate soil water balance and controls runoff and erosion. Land use systems with perennial crops have a potential for erosion control by providing a permanent soil cover of tree canopies, litter and eventually cover crops, in addition of the role of trees as runoff-barriers and the beneficial aspects in the maintenance of a stabile structure with high inputs of organic matter (Young, 1997). Although, these positive effects of perennial land use systems have been verified in many experiments, we still have to demonstrate this function under other climate conditions, soil types and management regimes. The hypothesis that land use system with perennial crops maintain favorable infiltration rates due to bio-channels and better soil structure than annual food-crop-systems was proven in a long-term agroforestry experiment established on an Alfisol in western Nigeria. The decline in the infiltration rate, evaluated with a double ring infiltrometer, was less in the agroforestry than in the food-crop-systems with either plow-till or no-till treatments (Lal, 1989).

On an Oxic Paleustalf, a study including *Leucaena leucocephala*, *Gliricida sepium*, *Alchornea cordifolia* and *Dactyladenia bartieri* found that the water infiltration was superior in the hedgerow plots as compared to the control without trees (Hulugalle and Kang, 1990).

Hedgerow intercropping with Senna *spectabillis* on a Typic Kandiudult in southern Cameroon increased infiltration rates measured with the double ring infiltrometer (Hululgalle and Ndi, 1993). In northern Zambia, on an Orthic Ferralsol, an evaluation of the infiltration rate using the inverse falling head method showed high values in alley cropping with *Leucaena leucocephala* (Dalland et al., 1993).

The variability due the presence of macropores or soil cracks commonly found in some soil classes in the tropics can enhance the naturally high soil hydraulic variability (Beven and Germann, 1982; Bouma et al., 1982). Other sources of inaccuracy in the evaluation of hydraulic properties arise from the measurement technique itself, such as soil disturbance during installation of the equipment or irregular hole diameters for the auger (Amoozegar and Warrick, 1986). Because of the high variability of soil hydraulic properties, it is better for many purposes to have several points with smaller precision than just a few highly accurate data. Certainly, both properties are desirable but not easily obtained.

The variability of the hydraulic properties in the field needs to be taken into account when choosing the measurement method and the number of repetitions. If they are insufficient, straightforward treatment effect can be misinterpreted or not detected.

In this chapter, firstly, a review about the equations used to calculate the soil hydraulic functions and field methods more appropriate to evaluate hydraulic properties on tropical soils is provided. Specific sources of errors and procedures to avoid or alleviate them are pointed out. Secondly, results about saturated hydraulic conductivity are shown. The measurements are carried out using the classical laboratory method of soil cores and the field method of disc infiltrometer. Furthermore, comparisons between land use systems and statistical methods to analyse data with log normal distribution are presented and exemplified. Thirdly, to evaluate the unsaturated hydraulic conductivity the results from an instantaneous profile method experiment is analysed. A detailed handling of data is presented, and the results in terms of homogeneity of the hydraulic properties within the profile are discussed. Moreover, measurements with tension infiltrometer were carried out to compare the unsaturated hydraulic conductivities between land use systems and between positions within the land use systems. The scaling theory and the statistical techniques of piecewise continuous regression are briefly described and used to analyse the results. Finally, the ability of the new method of inverse simulation to assess hydraulic functions and to mathematically describe the water dynamics for clayey Ferralsols at several depths is investigated.

Theory and literature review

6.1.1 Equations for calculating water fluxes

A brief review over the equations used to estimate the hydraulic properties and water fluxes into the soil are presented below. More detailed mathematical explications are given by Jury et al. (1991), Kutilek and Nielsen (1994), Libardi (1995), and Hillel (1998), among others.

6.1.1.1 Saturated flow

Darcy's law for water transport in saturated soil states that the flux density (q) through a given soil segment is equal to the hydraulic conductivity of that soil multiplied by its hydraulic gradient.

$$q = -Ks\frac{dH(z)}{dz} \qquad \approx -Ks\left[\frac{H_2 - H_1}{Z_2 - Z_1}\right] \qquad [6.1]$$

Here q is the flux density (LT^{-1} – cm day^{-1}), Ks the saturated hydraulic conductivity (LT^{-1} - cm day^{-1}); ΔH the hydraulic gradient (L – cm) (i.e., the difference between two water potentials applied to two points in a soil segment), and L is the distance between the two points (L – cm) on the segment where the flux is applied (e.g. between Z_2 and Z_1). The negative sign means that water flows in the direction of decreasing potential (Kutilek and Nielsen, 1994).

6.1.1.2 Unsaturated flow

The steady-state unsaturated flux in soil is normally calculated with the Darcy-Buckingham, which in the finite difference form (for vertical flux) and expressed in function of q is given by Equation 6.2

$$q = -K(\theta)\left[\frac{dH(z)}{dz}\right] \quad = -K(\theta)\left[\frac{\partial(h-z)}{\partial z}\right] \quad = -K(\theta)\left[\frac{\partial(h)}{dz} - 1\right] \qquad [6.2]$$

Here q (z, t) is the flux density, as defined previously but now related to the unsaturated hydraulic conductivity which is a function of the volumetric soil water content (θ) [$L^3\ L^{-3} - m^3\ m^{-3}$]. The variable z is the vertical depth (L – cm), a space coordinate here taken as positive in downward direction, and H (z, t) the total pressure head (L – cm).

The Equation of Darcy-Buckingham describes one-dimensional, isothermal, nonhysteretic unsaturated flow (Kutilek and Nielsen, 1994; Hillel, 1998), which is fully applicable to steady unsaturated flow (i.e., when q and θ are constant during time). However, in many situations nonsteady flow exists (i.e.; $dq / dt \neq 0$ and $d\theta / dt \neq 0$). In such situations, two equations are needed to describe the flux density and the change of water content in the soil.

The filling or emptying of the soil pores can be described by the equation of continuity (the law of mass conservation), which in a simple statement applied for changes of water content in soil says that the difference between the amount of water entering into a determined volume of soil and the amount leaving it must be equal to the change in water content of this volume. Kutilek and Nielsen (1994) and Hillel (1998) give details about the equation of continuity applied to soil hydraulic problems. A form of the continuity equation applied to water fluxes into the soil is

$$\frac{\partial\theta}{\partial t} = -\left(\frac{\partial q_x}{\partial x} + \frac{\partial q_y}{\partial y} + \frac{\partial q_z}{\partial z}\right) \quad [6.3]$$

Here, x, y and z represent the three dimensional water flux variation in space. The other parameters are as previously described.

The combination of the continuity equation (Eq.6.3) and the Darcy-Buckingham equation (Eq. 6.2) lead to the so-called Richard's Equation. In one dimension (vertical direction) this is

$$\frac{\partial\theta}{\partial t} = \frac{\partial}{\partial z}\left[K(\theta)\frac{\partial H}{\partial z}\right] \quad [6.4]$$

The solution of the Richard's Equation needs many additional assumptions, and many complications arise because the hysteric and highly variable hydraulic properties of natural soils. Many of these limitations are discussed in this chapter.

6.1.2 Measuring soil hydraulic properties in tropical soils

6.1.2.1 Saturated hydraulic conductivity and infiltration

The term "infiltration rate" refers to the vertical entry of freely available water into a soil surface. It should not be confused with hydraulic conductivity[1], which is a measure of the ability of a

[1] The term permeability that is some time found as synonym for hydraulic conductivity is not correct. Permeability is an intrinsic property of soil and has the dimension L^2 while hydraulic conductivity has the dimension LT^{-1} (Jury et al., 1991).

soil to transmit water in a 3-dimensional system. The infiltration rate tends to be numerically equal to the saturated hydraulic conductivity if the hydraulic gradient of the soil is unity. This condition is frequently approximated for homogenous and isotropic soils; it is discussed further in the section about the instantaneous profile method. For many practical problems of large-scale significance, the mean flow path over a sufficiently large area is approximately one-dimensional in the vertical direction, especially in relatively homogeneous soils (Stephens, 1996).

In tropical climates, the exposure of the soil surface frequently leads to the formation of a superficial soil crust. To verify if such a thin, superficial layer of low permeability controls the infiltration rate, measurements should be made both under natural surface conditions and after the surface layer has been carefully removed.

Worms tend to move upwards and crawl out of the soil when the surface is covered with water (Bouwer, 1986). The resulting open wormholes can greatly increase infiltration rates, particularly if the test is carried out over a long time. Prewetting the site before the measurements alleviates this trouble frequently encountered in the tropics. The temperature and chemical composition of the water used for infiltration measurements should be the same as those of the soil water to avoid dissolution of soil air in the infiltrating water (Bouwer, 1986), and changes of the flocculation status of the clay particles (Hillel, 1998). If possible, rainwater from the site should be used to avoid such problems.

Disc infiltrometers or ring infiltrometers consist of one or two concentrical metal cylinders that are pushed or driven a small distance into the soil. The cylinder(s) are filled with water, and the infiltration rate is measured until it reaches a constant value (Bouwer, 1986). The simplicity and low cost of the method are its main advantages. As the head of water pounded on the soil surface affects the infiltration rate, a constant water level should be maintained in the cylinder with a float valve or a marriotte siphon arrangement. To prevent leakage between the cylinders, equal water levels must be maintained in both cylinders.

A multiple automated system can be constructed to allow simultaneous measurements with several devices (Matula and Dierksen, 1989; Maheshwari, 1996). The use of a double ring, with measurements confined to the inner ring, may minimise errors due to non-vertical flow at the edge of the cylinder. However, to assure vertical flow the radius of the outer cylinder would have to be infeasible large, which may be a restrictive factor to carry out the measurements. Fortunately, Bouwer (1986) pointed out that the double ring is not essential and measurements conducted with a large disk alone are not different from measurements carried out with a double ring infiltrometer (except when a surface crust exists). The best way to reduce the effect of lateral divergence is increasing the size of the disk. Soils with a restricting layer deeper in the profile can cause overestimation of the infiltration rate, because the lateral flow above this layer may exceed the rate that occurs when the entire soil surface is inundated and all water has to move straight down through the soil and the restricting layer (Bouwer, 1986; Kutilek and Nielsen, 1994). In this situation it is preferable to use another technique such as the bore hole permeameter (see below). Beside lateral flow of infiltrating water, several other factors can affect the results from double ring measurements. The soil compaction by the insertion of the cylinders can lead to a reduction of the true infiltration rate. On the other hand, the measured infiltration rate will be overestimated if a surface crust or other restricting layer at or near the surface is disrupted by the installation of the infiltrometer, or if there is imperfect contact between the restricting layer and the inside cylinder wall (Bouwer, 1986).

The commonly used equations to describe and to extrapolate infiltration results are the Green-Ampt Equation, Philip's two parameter Equation, the Equations of Kostiakov and Horton. The applicability and utility of these different equations are discussed by Jury et al. (1991), Kutílek and Nielsen (1994); Libardi (1995) and Hillel (1998). Recently, methods to calculate infiltration from a single ring infiltrometer using scaling approaches have been published (Wu and Pan, 1997; Wu et al., 1999).

Rainfall simulators or sprinkler infiltrometers are arrangements of droppers or nozzles supplying the soil surface with a uniform inflow of water such that the flux density at the soil surface is kept at a constant level (Peterson and Bubenzer, 1986; Kutílek and Nielsen, 1994). The principal advantage in comparison with the ring infiltrometers is a better simulation of the infiltration process under natural rainfall conditions (Bouwer, 1986; Wallace, 1996). The relatively large sample area of these infiltrometers should increase the representivity of the measurements. Small systems are available (Asseline and Valentin, 1978; Mathieu and Pieltain, 1998) which may be useful for small-scale applications in land use systems research.

The Guelph permeameter, borehole infiltrometer or well permeameter is a subsurface technique consisting of a mariotte flask that is lowered into a well or borehole augered into unsaturated soil until the desired depth of measurement. The mariotte flask maintains a constant depth of water in the hole as a means of measuring the rate of water flow into the surrounding unsaturated soil (Elrick and Reynolds, 1992). The hole should be excavated using a screw-type or bucket auger. It should be cylindrical and have a flat bottom at least 20 cm above the water table (Reynolds, 1993). Specific factors that can affect the accuracy of the measurements with well permeameters include smearing, remoulding, and/or compaction of the well surfaces during augering, gradual siltation of the well and well collapse during the measurement (Elrick and Reynolds, 1992; Reynolds, 1993). On clayey soils, scratching the bottom and side of the hole with a sharp pointed instrument or metal brush normally alleviates the smearing and compaction caused during augering. On sandy soils, the collapse of the well during the measurement is the principal constraint to the use of this technique, whereas in silty soils the gradual siltation (clogging of the soil pores with silt particles) can be partially alleviated by protecting the bottom of the hole with coarse sand or fine gravel (Reynolds, 1993). Solar heating of the head space in the water reservoir can also affect the accuracy of the mariotte-based well permeameter, but this can be alleviated by performing the measurements under a tent. Elrick and Reynolds (1992), Reynolds (1993) and Stephens (1996) give a further discussion of the Guelph method and procedures for calculating hydraulic parameters.

6.1.2.2. Unsaturated hydraulic conductivity

Most of the water movements above the water table in the field, including water and nutrient fluxes to plant roots, rainfall infiltration and leaching of nutrients through the soil profile, occur while the soil is unsaturated and are thus controlled by unsaturated hydraulic conductivity. Field measurements of unsaturated hydraulic conductivity are generally preferred to laboratory measurements if the site is sufficiently accessible, has reasonable homogeneity, and level topography, is not too stony, and has predominantly vertical flow during drainage (Hillel et al., 1972; Green et al., 1986).

Tension infiltrometer or disc permeameter consist of a porous baseplate, which establishes hydraulic continuity with the soil through a nylon membrane. It is connected to a mariotte reservoir that allows supplying the soil surface with water at a constant and regulated tension. The soil water potential under the infiltrometer is controlled by air entry into the mariotte flask through tubes of different lengths, with tension infiltrometers normally operating in the range of 0 to -20 cm. The infiltration rate is measured as the water flow into the soil and the water level falls in the bubble tower. The data can be recorded manually or automatically (Ankeny, 1992; Elrick and Reynolds, 1992).

Tension infiltrometers have been used to characterise near-saturated hydraulic properties, sorptivity, macroscopic capillary length, characteristic pore size (Ankeny, 1992; Reynolds, 1993; Stephens, 1996), soil structural conditions at the soil surface as a function of short-term variations in weather conditions (White and Perroux, 1989), and effects of tillage practices (Ankeny et al., 1991; Messing and Jarvis, 1993). The near-saturated hydraulic conductivity and sorptivity obtained using tension infiltrometry have been used to distinguish infiltration through macropores from that through the soil matrix (Watson and Luxmoore, 1986; Wilson and Luxmoore, 1988; Messing and Jarvis, 1993). The method involves supplying water to the soil surface at different potentials to exclude a range of macropores from the flow whose contribution to infiltration can thus be quantified.

A good soil surface preparation and hence good contact between the infiltration disc and the soil is essential. The hydraulic conductivity of the contact material should be greater than or equal to the hydraulic conductivity of the soil over the range of pressure heads set on the tension infiltrometer. The pore water pressure head at which the contact material spontaneously saturates should be less than the minimum pressure head set on the infiltrometer membrane. The supply membrane must be visible during the infiltration to permit examination for air leaks. Perroux and White (1988) concluded that 3-5 mm thickness of single grain contact material having a fine sand texture and a hydraulic conductivity of about 10^{-5} m s^{-1} should be adequate for most agricultural soils and the usual range of tension infiltrometer pressure heads (e.g., 0 to – 150 mm water tension).

For measurements near saturation the infiltration disc must be level, otherwise the potential varies across the supply surface. Close to saturation, small changes in soil tension lead to dramatic changes of the infiltration rate and sometimes to higher variability in structured soils. The contact material can have a large influence on the pore water pressure head and hydraulic head gradient at the soil surface, and this can have a substantial impact on the validity of tension infiltrometer results (Reynolds and Zebchuk, 1996). Solar heating of the headspace in the mariotte reservoir should be avoided by shading. According to Reynolds (1993), the main factors affecting the accuracy of tension infiltrometer measurements are soil heterogeneity, soil collapse under the infiltrometer during the measurement, inadequate hydraulic contact between infiltrometer and soil, and the hydraulic properties and thickness of the contact material. A shortcoming of the technique is the time necessary to reach steady flow at low tensions in clayey soils, which can make manual recording impracticable. In this situation, an automated infiltrometer should be used.

The Instantaneous Profile Method or IPM method requires measurements of volumetric water content (θ) and hydraulic head (H) [(which is the sum of matric (h) and gravitational pressure head (z)] as a function of time and depth, under the conditions that evapotranspiration and absorption of water by roots are prevented. From these measurements, it is possible to obtain instantaneous values of the potential gradients and fluxes operating within the profile. Accordingly, when the water flux density and the gradient of the hydraulic head at the same time and depth are measured, the hydraulic conductivity can be calculated as the only unknown in the Richard Equation. Hydraulic conductivities can be determined for any distinct soil layer as a function of volumetric water content and/or pressure head. The data set collected with this method is also well suited for the inverse parameter optimization approach. It is probably the most widespread nonsteady-state field method.

The so called "unit gradient method", which presumes that the gradient of the matrix potential is practically zero and only the gravitational gradient operates the flux, is used in several field methods to calculate K (e.g. Davidson et al., 1969; Libardi et al, 1980; Sisson et al., 1980; Luxmoore et al., 1981). However, the validity of this assumption is frequently questioned (Ahuja et al. 1988; Reichardt et al, 1993) and in some conditions the unit gradient is in fact not observed (Hillel et al., 1972; Aragão Junior et al., 1983; Ahuja et al., 1988; Prevedelo, 1994). Although gradients near unity are frequently observed during internal drainage, the validity of the unit gradient approach should be verified. Common causes of divergence from the unit gradient include entrapped air within the narrow pore space when an initially dry soil is wetted, and the occurrence of horizontal flows (Collis-George, 1977; Mbagwu, 1995). The unit gradient methods of Libardi (1980), Sisson et al. (1980) and Chong et al. (1981) normally lead to similar results and work well for the wet range (Libardi, 1980; Luxmoore et al., 1981; Jones and Wagenet 1984; Comegna et al., 1996). Moreover, Bacchi and Reichardt (1991; 1993), analysing the methods of Libardi et al. (1980) and Sisson et al. (1980), showed that although these methods have been developed on a completely different theoretical basis, they are identical when using an exponential equation to relate K to θ.

6.1.2.3 Indirect methods and inverse solution

The direct measurement of hydraulic properties in situ is expensive, time consuming and labour intensive, and often the measured data remains unreliable or unrepresentative (Reichardt et., 1998; van Genuchten et al., 1999; Jong van Lier and Libardi, 1999). Therefore, several empirical and semi-empirical approaches based on pore size distribution (see review of Mualem, 1992) and particle size distribution (e.g., Arya et al., 1999; Schaap and van Genuchten, 1999) have been made to estimate hydraulic functions based on more easily measurable parameters.

An estimation method that describes the soil water relationship based on other soil characteristics is called pedo-transfer functions (Tietje and Tapkenhinrichs, 1993). Although, pedotransfer functions have shown reasonable agreement with experimental data for many temperate soils, they do not give reasonable predictions for some tropical soils as showed by Tomasella and Hodenett (1997, 1998).

The most common indirect methods to estimate hydraulic functions are the parametric models of Brooks and Corey (Mualen, 1992), Campbell (1974) and the coupling of the equation of van Genuchten with the model of Mualem or Burdine (van Genuchten, 1980). However, results to date indicate that these parametric models are relatively efficient for many coarse and medium textured soils, but predictions for fine-textured and structured soils like clayey Ferralsols remain unreliable (Durner, 1994; Tomasella and Hodnett, 1996).

In the inverse methods, analytical equations are first assumed to describe the soil hydraulic properties. Assigning values to the parameters in these equations makes it possible to solve the water flow equation for the same initial and boundary conditions as encountered in experiments. The final hydraulic properties are calculated by using interactive procedures and simulating the flow processes numerically. Inverse modelling is a relatively complex procedure that provides a quick method for soil hydraulic characterisation. Its successful application requires suitable experimental procedures as well as advanced numerical flow codes and optimisation algorithms. The majority of efforts in inverse methods refers to laboratory experiments (Hoppmans et al., 2001; Durner et al., 1999).

Dane and Hruska (1983) conducted the first application of the inverse problem to IPM experiment in which the parameters of Van Genuchten-Mualem (afterwards called VGME) soil hydraulic functions were optimised. Tomasella and Hodnett (1996) also applied inverse procedures to fit the parameters of VGME for an IPM experiment in a clayey Ferralsol. Santini and Romano (1992) also investigated the feasibility of the inverse method to estimate unsaturated properties for the IPM experiment. They showed good stability of the results and carried out sensitivity analyses for designing an optimal field experiment.

The inverse numerical solutions of the water flow equation require identical information of the forward problem in numerical simulation. Time and geometric information, initial conditions, and boundary conditions. In addition, specific information specific to the inverse problem are needed (e.g., the initial parameter estimates, position of the observation points and measurement times with corresponding data and weighting factors). Additionally, some convergence parameters need to be defined. The general inverse simulations may be performed using computer programs such like Hydrus 1-D code (Simunek et al., 1998) or ESHPIM code (Zurmühl and Durner, 1998). The success of inverse modelling depends on the suitability and quality of the experimental design, the choice of boundary conditions, the location and time resolution of the sensors, accuracy of the experimental data, the suitability of the transient flow model and hydraulic functions and the robustness of the optimisation algorithm as determined by its convergence to a global minimum (Hopmanns et al., 2001).

6.2 MATERIALS AND METHODS

6.2.1 Study area and site history

The study area and the site history of the selected plots have been described in details in Chapter 2.

6.2.2 Soil sampling and the location of the soil profile

The soil sampling scheme as well as the steel cylinders to collect samples for the evaluation of saturated hydraulic conductivity in laboratory were the same as described in Chapter 3 for the determination of bulk density. After completion of infiltration measurements the soil cores were taken in 3 to 5 replications directly below the area where the disc of the infiltrometer was installed. The land use systems and the positions evaluated are shown in Table 6.16. The instantaneous profile experiment was conducted in the middle of the experiment, between the block A and B.

6.2.3 Saturated hydraulic conductivity

6.2.3.1 Constant head method

The measurement of the hydraulic conductivity of saturated soils using the constant head method in the laboratory is based on the direct application of the Darcy equation to a saturated soil column of uniform cross-sectional area. A hydraulic head difference is imposed on the soil column, and the resulting flux of water is measured. Finally, saturated hydraulic conductivity (Ks) [L T^{-1}- cm day^{-1}) is calculated using Equation 6.5.

$$Ks = \frac{V \times l}{[A \times t(H_2 - H_1)]} \qquad [6.5]$$

Where V [L^3 - cm^3] is the volume of water that flows through the sample of cross-sectional area A [L^2 - cm^2] during the time t [T - day^{-1}] and (H_2 – H_1) is the hydraulic head difference [L - cm] imposed across the sample of length (l) [L - cm].

The measurements of Ks were carried out in a special apparatus constructed at the Soil physics laboratory at Embrapa – Amazonia Ocidental, very similar to those described by Klute and Dirksen, (1986) and Reynolds (1993). The measurements were carried out for about 4 hours with measurements being recorded at each 30 min. The hydraulic head difference was maintained constant at 1 cm height using a mariotte system.

6.2.3.2 Disc infiltrometer

The disc infiltrometer equipment is explained in detail below in the section about unsaturated conductivity, and it can be visualised in Figure 6.3. The localisation of the area evaluated was the same as for the tension infiltrometer described in Table 6.16.

The 1-Dimensional vertical approach of the fluxes was calculated using directly the Darcy's law [Eq. 6.1], which for this specific situation can be represented by the Equation 6.6.

$$Ks = \frac{Qi}{\pi r^2} \qquad [6.6]$$

Where Qi is the infiltration rate [L T^{-1} – cm day^{-1}] in quasi-steady state, and r is the radius of the inner ring [L - cm].

The calculation in 3-D approach using Ankeny's equations is explained below in the tension infiltrometer section. Logarithmic transformation using natural logarithms was used, because the raw data deviated significantly from the normality in most of the cases (see, data analysis section for details about lognormal distribution).

6.2.4 Unsaturated hydraulic conductivity

6.2.4.1 Tension infiltrometer

The tension infiltrometer was installed at ≈ 40 cm from the trunk of the respective trees that were grown either in monoculture or in association, as well as under the leguminous cover crop, *Pueraria phaseoloides*. Measurements and soil samples were also collected close to the dominant species in the adjacent secondary forest, *Vismia spp.* Table 6.16 shows the sample points and their localisation relative to the land use systems evaluated.

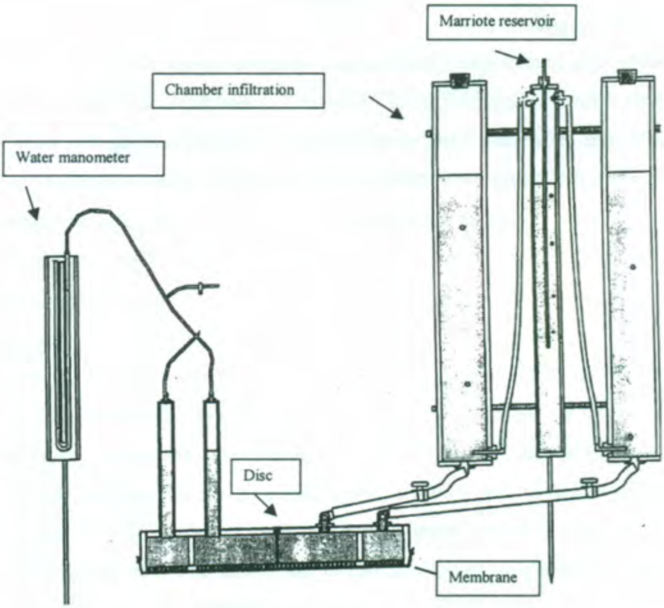

Figure 6.1 Scheme of the disc infiltrometer.

A double ring tension infiltrometer constructed by Umwelt-Geräte-Technik GmbH – Müncheberg – Germany was used to evaluate the unsaturated hydraulic conductivity. This disc infiltrometer has a special design (Figure 6.1) where the infiltrometer was constructed separately from the water tower, making it more stable and accurate under windy conditions and also avoiding the collapse of the soil structure near saturation. Moreover, it allows to perform, in addition to the three-dimensional analysis in unsaturated and saturated hydraulic conditions, also a one-dimensional analysis for saturated hydraulic conductivity, when the tension infiltrometer was used like a simple double ring infiltrometer with the outer ring functioning as a small buffer system. The base radii were 77.5 mm and 124 mm for the inner and outer ring, respectively.

At each infiltration site, an area approximately with the same diameter as the ring was cleared and levelled with the help of water levels. Compactions and disturbances were avoided with carefully preparations and roots were cut with scissors. To delimit the surface infiltration area and to prevent lateral surface flow of pounded water, a sharpened steel ring with 25-cm diameter and 1.0 cm height was pushed 0.5 cm into the soil.

The evaluation was started when bubbling was observed in the mariotte reservoir. The time to approach steady-state infiltration rates (Q)[$L^3\ T^{-1}$ – $cm^3\ h^{-1}$] varied from ca. 2 hours near 50 mm of h to less than 5 minutes near saturation. Data were collected manually reading the water levels in the mariotte reservoirs when the values were stable (not varied during three consecutive readings), then it was recorded as a pair value of Q and water pressure head (h) [L – cm]. The water pressure head or tension was evaluated with a double U water-manometer (see, detail in Figure 6.1).

A broadcloth-covered 400-mesh nylon filter (with a bubbling point ≈ 25 cm of water) was used as porous membrane for hydraulic contact with the soil and covered the base of the tension infiltrometer. A thin layer of fine sand was applied and levelled to the soil surface to provide a smoother contact between the membrane on the base of the tension infiltrometer and the soil surface. Fine sand, with diameter between 0.5 – 0.02 mm (K saturated about 5000 cm d^{-1}) was used as a contact material. A layer of maximal 5 mm thickness was applied on the soil surface and levelled using a special equipment, then the disc was installed and the level was checked by using water balances. Unsaturated measurements at approximately 50, 40, 30, 20, 10 mm of h were followed by measurement of saturated hydraulic conductivity at 0 h. An ascending sequence of supply pressure was adopted, since a descending sequence may cause hysteresis with progressive drainage occurring close to the disc while wetting continues at the infiltration front (Reynolds and Elrick, 1991). The measurements were performed under a tent to protect the mariotte reservoir from the direct sunbeam and also to reduce temperature variations.

The paired K and h values were obtained from Q at successive matric potential0 (h – values) using the theory outlined by Ankeny et al., (1991) with modification of Jarvis and Messing (1995). The Ankeny's solution is based on the Wording's solution for a three-dimensional infiltration from a disc source with a constant pressure head at the soil surface (Wooding, 1968), it is also assumed that the relation K (h) can be described by the exponential function of Gardner (Eq. 6.7).

$$K = K_{fs}\exp(\alpha h) \qquad [6.7]$$

Where K_{fs} is the field-saturated hydraulic conductivity [L T^{-1} - cm day^{-1}] and α is the empirical fitting exponential slope [L - cm^{-1}]. The α parameter is calculated by measuring the steady-state flow rate at two different supply potentials (such h_i and h_{i+1}) and solving Equation 6.8.

$$\alpha_{i+1/2} = \frac{\ln\dfrac{Q_i}{Q_{i+1}}}{h_i - h_{i+1}} \quad i = 1,..., n\text{-}1 \qquad [6.8]$$

Where Q_i is the steady-state infiltration rate [L^3 T^1 - cm^3 day^{-1}] measured at the tension h [L - cm] and Q_{i+1} is the subsequent evaluation rate at the tension h_{i+1}. The notation ½ denotes the estimated value of α is at the midpoint between successive supply pressure heads h.

Finally, hydraulic conductivity is calculated using Equation 6.9, where r [L - cm] is the radius of the disc infiltrometer.

$$K_{i+1/2} = \frac{\sqrt{Q_i \times Q_{i+1}}}{\left(1 + \dfrac{4}{\pi r \alpha_{i+1/2}}\right)} \quad i = 1,..., n\text{-}1 \qquad [6.9]$$

The denominator term in the Equation 6.9 represents the geometric mean of infiltration rates (Qi and Q_{i+1}) between adjacent supply potentials $[h_i + h_{i+1}]/2$. Two additional paired values of K and h were obtained assuming that the largest and smallest supply potentials, respectively, equal $\alpha_{3/2}$ and $\alpha_{n-½}$ respectively (Jarvis and Messing, 1995).

6.2.4.2 Instantaneous profile method (IPM)

The IPM method was carried out on a plot of 5 x 5 m, where the vegetation was previously eliminated in a radius of about 20 m from the centre of the plot. Therefore, the water processes in the centre of the plot were practically unaffected by its boundaries and water absorption by plant roots was improbable. Within this plot, TDR probes were installed at each 10 cm until 100 cm. A serie of tensiometers was also installed near the TDR probes at the same depths. The plot was ponded with water, until saturation had been reached, which was showed by tensiometer readings. Then the soil surface was covered by a plastic sheet to avoid evaporation. Additionally, a tent was constructed to prevent the entering of rainwater and to reduce thermal effects. The clayey Ferralsols in the central Amazon have very deep soil profiles that permits free vertical drainage.

The calculation of K performed in this study was based on the method of Hillel et al. (1972) and modifications given by Libardi et al. (1980) and Libardi (1995) as explained above. During the initial stages of drainage, the time lags between measurements were some minutes, then hours; after the second day measurements were taken every morning. The experiment was carried out for 28 days until variations of θ in the deeper layers had become too small to be reliably measured.

A numerical solution of the one-dimensional form of the Richard equation [Eq. 6.4.] was used to calculate the fluxes in IPM. The initial and boundary conditions that allow the solution of this differential equation are assumed to be:

$$q = 0 \qquad t \geq 0 \qquad z = 0 \qquad [6.10]$$

$$\theta = \theta\,(z) \qquad t = 0 \qquad z > 0 \qquad [6.11]$$

$$\theta = \theta_i \qquad t > 0 \qquad z = \propto \qquad [6.12]$$

Here q is the soil water flux [L T^{-1} - cm h^{-1}], t the time [T – h], z is the depth [L – cm] and the subscript i stands for initial conditions.

The total water content change per unit time is obtained by integrating the Richard Equation between successive soil moisture profiles down to depth z

$$\int_{z_1}^{z}\frac{\partial\theta(z,t)}{\partial t}\cdot dz = \int_{z_1}^{z}\frac{\partial}{\partial z}\left[K(\theta)\frac{\partial H(z,t)}{\partial z}\right]dz \qquad [6.13]$$

Since $z_1 = 0$ as an assumed referential on the soil surface, and because the boundary condition 6.10., Eq. 6.13 simplifies to Equation 6.14

$$\int_{0}^{z}\frac{\partial\theta(z,t)}{\partial t}\cdot dz = \left[K(\theta)\frac{\partial H(z,t)}{\partial z}\right]_z \qquad K(\theta) = \int_{0}^{z}\frac{\partial\theta(z,t)}{\partial t}dz \bigg/ \frac{\partial H(z,t)}{\partial z} \qquad [6.14]$$

In case of unity gradient, this simplifies further to Equation 6.15

$$K(\theta) = \int_{0}^{z}\frac{\partial\theta(z,t)}{\partial t}dz \qquad [6.15]$$

Because of the boundary condition [6.10], a simpler method for integrating Equation 6.15 than using finite differences, as proposed by Hillel et al., (1972), is simply to taken the partial derivative of the water storage functions [W (z, t) – Eq. 6.20] at selected times (Libardi, 1995 pg.382).

$$K(\theta)\big|_z = \frac{\partial Wz}{\partial t} \qquad [6.16]$$

For the calculation of fluxes in the IPM experiments, the use of smoothing functions before the derivations may be necessary to reduce the influence of the inherent fluctuations, noises and outliers in the data. These deviations arise from the natural soil heterogeneity and the limits of precision and accuracy of TDRs and tensiometers. Smoothed data in the IPM method prior of differencing was used by Ahuja (1980), Libardi et al. (1980), Luxmoore et al. (1981), Reichardt et al. (1998) and Jong van Lier and Libardi (1999).

Katul et al. (1993) and Scheibke (1998) investigated the influence of different smoothing techniques on the estimation of K in IPM experiments. Scheibke (1998) used differential error analysis and concluded that the smoothing procedures for IPM have to be done twice, for the measured data and for the calculated K values. Therefore, the variations of θ during time were smoothed by fitting the measured θ data to the Equations 6.17 to 6.19.

Linear	$y = \alpha + \beta x$	[6.17]
Logarithmic	$y = \alpha + [\beta * \ln(t)]$	[6.18]
Power	$y = \alpha\, t^{\beta}$	[6.19]

Here y represents the measured values of θ and x represents the time (t). The best equation was selected based on the higher coefficient of correlation [r^2] (See, Appendix 5-A for details about its calculations). Then, the mean water storage (W) for a specific layer was estimated for the depths of 10; 20; 40; 60; 80 and 90 cm by Equation 6.20.

$$W_{z,t_i} = \left(\frac{1}{n} \sum_{i}^{n} \theta_i \right) z \qquad [6.20]$$

Here, n is the number of layers evaluated and z is the position reference [L - cm] of the last layer considered and t_i is the time [T - h] in the i^{th} interval. The depths 30, 50, 70 and 100 cm were eliminated because either a tensiometer or a TDR was damaged or gave unrealistic results during the measurement period.

Then the values of W (t_i) were fitted for each depth z to the same equations [Eq. 6.17 to 6.19]. Again, the selection of the best equation was based on the higher r^2 value.

The water fluxes were calculated using the derivative of the fitted equation for W (z, t) at the 28 subsequent times as listed in Table 6.5. The values obtained (Table 6.10) are already the flux density Q or the K values, since the unit gradient was verified ($\partial H/\partial z = -1$; see, Figure 6.9).

Further, Equation 6.21 was selected for describing K (θ) and the experimental data were fitted using regression analysis.

$$K(\theta) = K_o e^{\beta[(\theta-\theta_o)]} \qquad [6.21]$$

Here, β is an empirical constant and K_o and θ_o are the hydraulic conductivity and water content values at the beginning of the drainage process or a fitted parameter. Equation 6.21 was used to analyse IPM experiments by Davidson et al. (1969); Libardi et al. (1980); Reichard et al., (1998) and Jong van Lier and Libardi (1999). Since the values of K_o do not necessarily equal the hydraulic conductivity at the saturation Ks, it should not be compared to field measurements. Equation 6.21 is a linear model in a ln K vs. $(\theta-\theta_o)$ plot. Hence, the parameters K_o and β represent the slope and intercept, respectively. These analyses were carried out with standard procedures of regression analysis. As a measure of goodness of fit, r^2 and the standard error were used.

The equations of hydraulic conductivity as a function of volumetric water content [K (θ)] or in function of the relative saturation [K(Se)] is frequently preferred because these functions are less affected by hysteresis compared to the function [K(h)] (Mualen, 1986; Roth, 1996; Hillel, 1998). This is because the water phase with different values of θ can correspond to the same value of h, because "h merely determines the local form of the water-air interface but generally not the entire geometry of the water phase" (Roth, 1996). Hysteresis is mainly due to complicated shapes of capillary pores in soil. The wetting curve always has lower water content for a given potential than the drying curve.

Since the water content (θ) of the subsoil layers did not decrease markedly from the values close to saturation during the experiment, the precision of the TDR probes was not good enough to detect the variations in θ. However, variations in the water phase were clearly identified by the tensiometer measurements of h (Table 6.5). The most reliable and precise measurement of h by water-mercury tensiometers partially compensates for the inaccuracies from a probably higher hysteresis effect in the function K (h). Therefore, the functional relationships between K and h were also fitted using the Equation 6.22.

$$K(h) = K_0 e^{[\lambda(h_o-h)]} \qquad [6.22]$$

The fitted equations K (θ, z) and K (h, z) were then tested for parallelism, concurrence and concordance between the layers. Piecewise continuous regressions were performed when linear procedures did not lead to a reasonable fit of the parameters. Details about the regression procedures and statistical analysis are given in the data analysis section.

6.2.5 Indirect and inverse method

The inverse modelling was performed using the Hydrus –1D code (Simunek et al., 1998). The Hydrus 1-D code, beside the reduction of the deviation between the calculated space-time variables (e.g., observed pressure head and water content in a time serie) it permit also to include soil hydraulic data independently measured (e.g. θ vs. h, or K vs. θ or K vs. h). Furthermore, penalty functions, which make use of prior knowledge about the values of some parameters, can also be included in the objective function. Weighting coefficients are used to minimise differences in absolute values and number of data involved. The objective function conducted by the inverse algorithm implemented in the Hydrus -1D code is accomplished by using the Levenberg-Marquardt nonlinear minimisation method.

In the inverse methods, performed by Hydrus 1-D code analytical functions are first assumed to describe the soil hydraulical properties. Assigning values to the parameters in these functions makes it possible to solve the water flow equation for the same initial and boundary conditions as encountered in the experiments. The functional relationships of van Genuchten – Mualem (VGME) for K (θ), θ (h) and K (h) was presumed to be able to describe the data collected in the IPM experiment. The VGME are shown below

$$\frac{K(\theta)}{Ks} = Se^{\tau}\left[1-\left(1-Se^{1/m}\right)^{m}\right]^{2} \qquad \text{for} \qquad m = 1-(1\text{-}n), \qquad n > 1 \qquad [6.23]$$

Here, Se is the effective saturation expressed by Eq. 6.23

$$Se = \frac{\theta-\theta r}{\theta s-\theta r} \qquad \text{or} \qquad Se = \left[1+(\alpha\cdot h)^{n}\right]^{-1+1/n} \qquad [6.24]$$

The pore connectivity parameter (τ) in the Eq. 6.22 was assume to be 0.5 as an average found for many soils by Mualem (1986). However, other workers have shown that the τ parameter can assume different optimal values (Wösten and van Genuchten, 1988; Tomasella and Hodnett, 1996) and it is nowadays commonly considered a fit parameter to be optimised.
Equation 6.25 expresses the VGME equation as function of h

$$\frac{K(h)}{Ks}=\frac{\left\{1-(\alpha|h|)^{n-1}\left[1+(\alpha|h|)^{n}\right]^{-m}\right\}^{2}}{\left[1+(\alpha|h|^{n})\right]^{\frac{m}{2}}} \qquad [6.25]$$

The above equations contain six independent parameters: θr, θs, α, n and Ks and τ, which are all previously defined. The Hydrus -1D code estimated them simultaneously by using interactive procedures.

6.2.5.1 Inverse solution of the IPM experiment

Simultaneous measurements of θ and h monitored in the IPM experiment were used in the inverse method. The field set-up and the measurements procedures were described in the IPM section. The data sets of θ^* (t, z); h (t, z) is shown in Table 6.7 and 6.5. The smoothed θ^* values were used instead of the original values because inverse solution presumes error free data (Hoppmans et al., 2001). Experimental data with noise tend to destabilise the inverse solution by creating several local minima (Simunek and van Genuchten, 1997).

Initial estimates of the hydraulic functions were found by fitting the field data θ (h) using the RETC code to the van –Genuchten unimodal approach. The initial estimates were then sequentially optimised for each layer changing the parameter in order to find a better fit between the soil profiles estimates and measured. As initial boundary condition the measured values of matric potential (h) evaluated at the top and the bottom of the code was linearly interpolated within the whole profile. Water flow boundary conditions were set to atmospheric conditions, but the values of precipitation evaporation and transpiration were set to zero. The soil profile of 100 cm depth was divided into four layers with different hydraulic properties and four subregions for calculating water balances (Figure

6.13). The soil profile was discretized using a grid with 101 nodes, using the same space in the whole profile. Observation nodes for which values of pressure head and water content are saved at each time step were implemented to describe the depths of 10, 20 40 and 60 cm. These depths coincide with the depths where the TDRs and tensiometers were installed in the field. Therefore, some comparisons between estimates and observed values are possible. The times selected for output results were the same as those manually recorded in the IPM experiment.

As bottom boundary condition free drainage was selected. A summary of the initial and boundary conditions implemented is shown below

$h(z, 0) = -1$ to -10 (linearly interpolated) $\quad\quad$ $-100\ \text{m} \leq z \leq 0$

$Q(0, t) = 0$ $\quad\quad$ $0 \leq t \leq 428\ \text{h}$

Here, t is time (T - hours), z the depth of the profile (L - cm) and Q is the water flux ($L^3\ T^{-1}$ – $cm^3\ h^{-1}$).

6.2.6 Data analysis

6.2.6.1 Analysis of lognormal distributions

Logarithmic transformation was used to improve the efficiency of estimates of the mean, because the raw data deviated significantly from normality in most cases. Lognormal distributions of measured data in nature are not uncommon. This is a consequence of the fact "*that many environmental variables cannot take on negative values and are, hence, constrained by zero*" (Parkin and Robinson, 1992).

The high variability of natural processes translates into high uncertainty regarding statistical estimation and inference processes. More specifically, high uncertainty results in wide confidence intervals, and low power associated with hypothesis-testing procedures. This suggests that better quantification of the variability, or at least the recognition that high variability exists, is necessary to optimise the statistical and experimental design.

In many cases, the high variability exhibited by natural processes is manifested in positively skewed distributions. A variable is considered to be lognormally distributed if the logarithm of the variable is normally distributed (Steel et al., 1997). The "sample mean" of a lognormally distributed data set should be calculated by taking the antilogarithm of the average of the log-transformed sample values. It represents the sample geometric means, which is an estimator of the population median, and not the sample mean (Parkin and Robison, 1992). For symmetric distributions mean and median will have the same value, however, for an asymmetric distribution, such as the lognormal distribution, these parameters have different values. The mean and the median of a lognormal distribution actually convey different information about the distribution. The mean is the centre of gravity of the distribution, while the median is the centre of probability of the distribution (Parkin and Robinson, 1992).
The log transformation was done using natural logarithms

$$y_i = \ln(x_i) \qquad x = i,\ldots, n \qquad [6.26]$$

The mean and the variance of the ln-transformed data were calculated with Equation 6.27 and 6.28, respectively.

$$\bar{y} = \frac{1}{n}\sum_{i=1}^{n}\ln(x_i) \qquad [6.27]$$

$$s^2 = \frac{1}{n-1}\sum_{i=1}^{n}(\ln(x_i) - \overline{y})^2 \qquad [6.28]$$

The geometric mean (GM) is computed as Equation 6.29

$$GM = \exp\left(\frac{1}{n}\sum_{i}^{n} y_i\right) = \sqrt[n]{x_1 x_2 x_3 ... x_n} = \sqrt[n]{\prod_{i=1}^{n} x_i} \qquad [6.29]$$

The symbol Π is the product operator, which symbolises the multiplication of x in the terms that follow it.

The estimates of the population mean (m) and the variance (s^2) were calculated with the maximum likelihood method (Parkin and Robinson, 1992; Warrick, 1998) Equation 6.30 and 6.31, respectively

$$m = \exp\left(\overline{y} + \frac{s^2}{2}\right) \qquad [6.30]$$

and

$$s^2 = \exp \cdot \left(2\overline{y} + s^2\right) \cdot \left[\exp(s^2) - 1\right] \qquad [6.31]$$

To express the data after transformation, the means should be transformed back y' into linear scale by using their antilogarithms $[y' = \exp^{(y)}]$. The back transformed mean of a logarithmically transformed parameter [i.e., geometric mean (GM)] is an estimator of the population median (Parkin and Robinson, 1992) instead of the mean as suggested by Sokal and Rohlf (1995). The true mean can be calculated using Equation 6.30; in case of a lognormal distribution. The confidence intervals assuming a normal distribution of the back transformed variable (y') can be calculated by the method shown in the Appendix 3-A. The confidence intervals for the median are computed in the logarithmic scale, then transformed back into the linear scale (Sokal and Rohlf, 1995). This leads often to asymmetric limits around the median.

For natural logarithm, the confidence interval is calculated as follow

$$y' = \exp(y \cdot \pm \cdot t_{\alpha,\cdot n-1} \sqrt{s^2 / n}) \qquad [6.32]$$

Here, t is the value of the student distribution with confidence level α of probability, and n-1 is the degree of freedom for the t distribution (n is the number of samples composing the mean) and s is the standard deviation.

6.2.6.2 Testing the equality of a set of linear models

Comparing simple linear regression equations or testing the identity of linear equations are statistical analyses that permit to identify whether the slopes of two or more regression lines differ significantly. Normally, the following sequence of tests is performed. Firstly, the identity of slopes is tested, if they are not significantly different then it is tested if the several sets of data are likely to be from the same population (i.e., if both intercepts and slopes are not significantly different). The use of statistical tests to compare linear regressions, concerning comparisons of hydraulic functions in this chapter, permits to answer question such as:

Does a variation of the pressure head (h) in different depths a change in the hydraulic conductivity in the same magnitude? To answer this question we need to test whether the slopes are different or not. (See below, hypothesis 6.34 and test 6.35).

Are there significant differences between the hydraulic functions evaluated at different depths of a soil profile? For instance, this comparison may permit, to represent the whole profile by only one function, if no significant differences between the functions exist. To answer this question it should be first tested if the slopes are the same (see, hypothesis 6.34 and Eq. 6.35) and then if the intercepts are the same (hypothesis 6.36 and Eq. 6.37). An overall statistic, that tests both hypotheses together is also possible (hypothesis 6.39 and Eq. 6.40). However, if the overall test shows a difference, it may be still necessary to employ the previous tests, if one wants to determine whether the differences are due to different slopes or intercepts. If the tests do not indicate significant differences among depths, a reduction of the parameters by pooling the data together in a unique equation that represents all the pooled depths (or the whole profile) might be possible.

The statistical tests for the equality of the slopes (i.e., parallelism), the equality of intercepts (i.e., concurrence) and an overall test (i.e., concordance) among k linear equations are given by Graybill (1976), Seber (1977), Regazzi (1996) and Zar (1999).

Considering the linear equation as

$$y = \alpha_i + \beta_i x + \varepsilon \qquad [6.33]$$

Where, α represents the intercept, β the slope and ε denotes the errors terms.

The statistical hypothesis to test whether the slopes are the same is (i.e., if the regression lines are parallel) is

$$H_o \;\; \beta_1 = \beta_2 = \ldots = \beta_n \qquad [6.34]$$

The statistical test to compare slopes is

$$F = \left(\frac{\dfrac{SS_c - SS_p}{k-1}}{\dfrac{SS_p}{df_p}} \right) \qquad [6.35]$$

Here SS_c denotes the "common" sum of residuals, SS_p is the sum of residuals of a pooled regression, k the number of equations being compared, and df_p the degree of freedom of the pooled residuals. The F value estimated by Equation 6.35 should be compared with the $F_{[\alpha,\, k-1,\, dfp]}$ critical value calculated from the F distribution. Here, α is the level of significance, the other parameters are as defined previously. The F values can be found in practically all books of basic statistic (e.g., Snedecor and Cochran, 1989; Steel et al., 1997; Zar, 1999). If the estimated F value is lower than the critical value of the F distribution with the appropriate degrees of freedom at the significant α level, then the hypothesis H_o should not be rejected, (i.e., the slopes are not different). If H_o is rejected (F estimated > F crit) it means that at least a significant difference among the slopes exists, which can be identified using contrast analysis or multicomparison tests (see, Appendix 3-A for details about multicomparison tests).

In order to test if the intercepts are identical (i.e., if the lines intercept the y axis at the same point) the hypothesis is

$$H_o \ \alpha_1 = \alpha_2 = \dots = \alpha_n \qquad [6.36]$$

The test statistic to compare intercepts is

$$F = \left(\frac{\frac{SS_t - SS_c}{k-1}}{\frac{SS_c}{df_c}} \right) \qquad [6.37]$$

Here, SS_t is the total sum of squares, and df_c is the degree of freedom of the common residuals. The other parameters were previously defined. The F value estimated by the Equation 6.37 should be compared with the critical F value $_{[\alpha, k-1, dfc]}$

To test both parameters in an overall test, the hypothesis is

$$H_o \ \alpha_1 = \alpha_2 = \dots = \alpha_n \text{ and } \beta_1 = \beta_2 = \dots = \beta_n \qquad [6.38]$$

The overall test for coincidental regression is

$$F = \left(\frac{\frac{SS_t - SS_p}{2(k-1)}}{\frac{SS_p}{df_p}} \right) \qquad [6.39]$$

The parameters of the Equation 6.39 were all previously defined. The F value estimated by the Equation 6.39 should be compared with the critical F $_{[\alpha, 2(k-1), dfp]}$ value. If this value is not significant (F estimated > F critical), then all k regressions are assumed to estimate the same population, and the best estimate of that population is a pooled regression (Zar, 1999).

A Fortran Code (Slope) was written by the author to calculate these statistics, which permits to compare the regression lines for parallelism (Eq. 6.35), concurrence (Eq. 6.37), and coincidence (Eq. 6.39). Further, the regression parameter (α and β) are also calculated. The code is given in Appendix 6.A.

6.2.6.3 Piecewise continuos regression for two segments

The results in Chapter 4 show that the clayey Ferralsols have a bimodal pore size distribution instead of a conceptualised soil with a continuous unimodal pore size distribution. Furthermore, the results show a discontinuity in the functional relationship between K and h. Therefore, it may be more appropriate to consider the function K (h) in discrete intervals and to express the relation by a two-line regression model. Therefore, the paired data (K, h) obtained from each sequence of infiltration were then fitted by means of a piecewise continuous regression (with two segments).

A difficulty in fitting a piecewise continuous regression is to determine the break point or joint point, which separates the two domains. Since its position is unknown, it has to be estimated by interactive methods of nonlinear squares.

The piecewise regression analysis was used by Ahuja et al. (1980) in an IPM experiment, and it has been used to fit data from tension infiltrometer measurements in a soil with multi-domains fluxes (Keng and Lin, 1982; Messing and Jarvis, 1993; Jarvis and Messing, 1995; Mohanty, 1999)

The exponential model of Gardner (Eq. 6.7) was linearized and rearranged so that Kr = ln (K Kfs^{-1}). The slopes, the intercept for the second segment, and the water pressure head at the break point (hp) were determined by non linear least square techniques. A conceptualised piecewise continuous regression is illustrated in Figure 6.2. A simple computational protocol was developed to estimate the unknown parameter (α_1, α_2 and hp) using the non-linear least square method of Levenberg - Marquardt in the program Sigma plot 6.0 (SPSS Inc, USA)

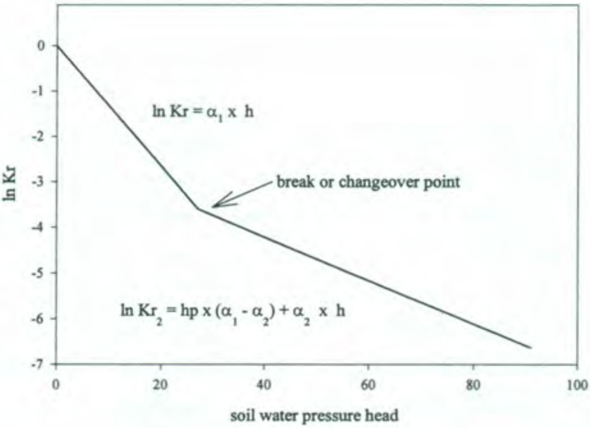

Figure 6.2 Scheme of a piecewise continuous regression

$$\mathrm{Kr} = \begin{cases} \mathrm{K_1(h)} \cdot \cdot \mathrm{if} \cdot \cdot \mathrm{h} \le \mathrm{hp} \\ \mathrm{K_2(h)} \cdot \cdot \mathrm{if} \cdot \cdot \mathrm{h} \ge \mathrm{hp} \end{cases}$$

where

$$\mathrm{K_1(h)} = \alpha_1 \mathrm{h}$$

$$\mathrm{K_2(h)} = \mathrm{h_p}(\alpha_1 - \alpha_2) + \alpha_2 \cdot \mathrm{h} \qquad [6.40]$$

Here α_1 and α_2 are the slopes of segment 1 and 2 respectively. The function K_1 (h) summarises the unsaturated hydraulic function governed by the gravitational process, and K_2 (h) segment the relation which is basically governed by the flux in capillary pores. The value of hp can be interpreted as a matric pressure head that divides operationally the two flow domains, i.e., the critical h where flow changes from gravity dominated to capillary dominated flow or vice versa (Keng and Lin, 1982; Shouse and Mohanty, 1998). The mathematically and statistically simpler piecewise regression, however, not a smooth function may have advantages over the others empirical power or exponential equations normally used to fit hydraulic parameters. Furthermore, the segments, and the break point in the piecewise continuous regression can be statistically compared (Seber, 1977; Keng and Lin, 1982; Draper and Smith, 1998).

6.2.6.4 Scaling theory

Miller and Miller (1956) introduced scaling factors derived from similitude analysis in soil science. Their original geometric similitude concept for scaling hydraulic properties is based on capillary laws and viscous flow laws, and it presumes that for different locations, the geometry of the pores is the same with differences only in a characteristic length. Therefore, it can be characterised completely by scale factors (Figure 6.3). Hence, it implies a constant porosity that limits the use of the original scaling concept for many natural soils (Warrick et al. 1977). The original scaling concept was changed, and nowadays scaling methods are based on similarities between soil hydraulic functions instead of similarities between respective geometries (Simmons et al. 1979, Tillotson and Nielsen, 1984; Jury et al., 1987; Hopmans, 1987; Nielsen et al., 1998). Scale factors are calculated by regression methods, and scaling methods based on regression analysis are called *"functional normalisation techniques"* (Simmons et al., 1979; Tillotson and Nielsen, 1980), further they do not require similar media. Although these scale factors are not directly related to Miller scaling and have no explicit physical meaning, they are useful to express the variability by a single parameter. The purpose of scaling is to reduce the number of parameters needed to characterise the variability of soil properties.

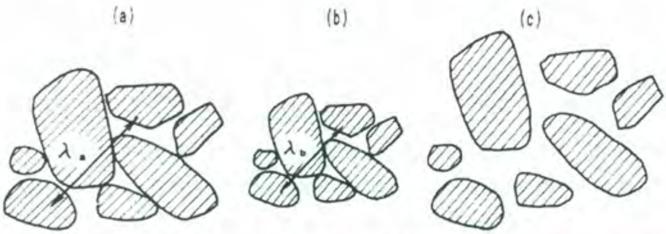

Figure 6.2 Concept of similitude of Miller and Miller. The porous media (a) and (b) are similar. (Adapted from Miyazaki, 1993).

In this study, the usefulness of the scaling theory was investigated in combining with piecewise-regression in order to describe and reduce the spatial variability of hydraulic conductivity functions.

The scaling theory was used in a *"hybrid media scaling"* combining the original concept of Miller and the functional normalisation. It was based on the scaling technique proposed by Shouse and Mohanty (1998), however some modifications are explained below. Similar approaches were used for analysing data from tension infiltrometer by Messing and Jarvis, (1993) and Mohanty (1999).

In this the paired data $(K_{i,} h_i)_{i,\dots, N}$ obtained by tension infiltrometry under the different positions within the land use systems were scaled. Application of the scaling method requires a set of reference parameters. There are several methods for determining the reference parameters, such as using the field-average parameter values, using parameters for an arbitrary site within the transect, measuring the parameters at a site independent of the transect, or using previously measured data (Shouse et al., 1992).

To define the reference model, measured data $[K_r (h), h]$ were arbitrarily chosen, and Equation (6.40) was fitted by non linear regression, giving hp = 21 mm, and α_1 = -0.1342 and α_2 = -0.0803. Paired $[K_r (h), h)]_{i = 1,\dots,N,\, x = 1,\dots, x]}$ data points were subsequently scaled to the reference curve using the regression analysis. The scale factors α_x for a certain infiltration sequence at position [x], consisting on N data points (i.e., water pressure heads steps) was then found by minimising the sum of squared differences (SS) between the reference relative hydraulic conductivity curve and the scaled data point (Eq. 6.41).

$$SS = \sum_{i=1}^{i=N} \left[\alpha_x h_i - h_i^{ref}\right]^2 \qquad [6.41]$$

A computational code was developed to calculate α_x by computing the Equation 6.42 and 6.43

$$\alpha_{i,x} = \frac{h_{i,x}^{ref}}{h_{i,x}} \qquad i = 1, \dots, N \qquad [6.42]$$

$$\alpha_x = \frac{1}{N} \sum_{i=1}^{i=N} \alpha_{i,x} \qquad [6.43]$$

Here, h^{ref} is the water pressure head at the reference curve; α_x is the scaling factor for a certain infiltration sequence at a position [x] consisting of N steps. Once α_x for a position x is known, scaled values $h^*_{i,x}$ $(= \alpha_x h_{i,x})$ are calculated for all water pressure head steps (i = 1,...,N).

6.3 RESULTS AND DISCUSSION

6.3.1 Saturated hydraulic conductivity (K_s)

6.3.1.1 Soil core method or constant head method

Descriptive statistics of K_s evaluated in the laboratory with the constant head method are shown in Table 6.1. The complete data set is shown in the Appendix 6.A.

The statistical parameters show a high variability of K_s with a minimum value of 96 cm d^{-1} to a maximum value of 12456 cm d^{-1} in the raw data. The raw K_s data show an asymmetric distribution, indicated by the positive skeweness values (Table 6.1). Therefore, the data were logarithmically transformed in order to normalise their distribution. The distribution of the logarithmic transformed data is more symmetrical, what is indicated by the value of skweness around zero. The closer the skweness value is to zero, the greater is the likelihood for a normal distribution (Hays, 1981). The large variance and coefficient of variation of the data in Table 6.1 reflects not only the true variability of K_s, but also bias introduced by the sampling method. Two extreme cases are possible when sampling the clayey Ferralsols to evaluate K_s with the constant head method. First, samples could be compacted by hammering and therefore give minimum values. Conversely, samples containing pores that were open on both sides in the soil sample (i.e., open-ended macropores) gave maximum values. The open-ended macropores over the length of the soil core caused piping effects (Mohanty et al., 1994). In soils with macropores like the clayey Ferralsols in the central Amazon, evaluation of K_s in detached samples, where the continuity of the macropores outside the length of the soil sample are not taken into account, lead to unreliable results.

Representative elementary volume (REV) [1]

Another factor that limits the interpretation of the data from soil core method refers to the soil volume sampled (in the present experiment 100 cm^3). This volume is probably not large enough to encompass the REV of the saturated hydraulic conductivity for the clayey Ferralsol.

Table 6.1 Saturated hydraulic conductivity - K_s [$cm\ d^{-1}$] evaluated by constant head method in laboratory using soil samples collected on a clayey Ferralsol in the central Amazon.

Number	Common name	Samples	Minimum	Maximum	Median	Mean	95% CI Upper	95% CI Lower	C.V %	Skewness	GM
1.00	*Cupuaçu*	13	921.4	14665.4	4032.0	4146.2	6314.2	1978.3	90	2.3	3157.3
2.00	Annatto	13	288.0	15624.0	1872.0	3779.0	6501.4	1056.6	120	2.0	2145.0
3.00	Brazil nut	12	1008.0	9360.0	2856.0	3523.1	5064.0	1982.3	70	1.4	2895.7
4.00	Peach palm – F	13	192.0	3528.0	768.0	1264.3	1932.8	595.8	90	0.8	828.6
5.00	Peach palm – P	13	288.0	13296.0	2040.0	3551.4	6114.2	988.6	120	1.5	1797.7
6.00	Pueraria	13	240.7	4560.0	1029.1	1350.3	2059.2	641.4	90	2.0	1011.4
7.00	Cupuaçu	13	2383.4	11208.0	4032.0	4929.1	6436.8	3421.4	50	1.5	4457.9
8.00	Grasses and pueraria	13	607.2	12456.0	1040.2	2293.2	4221.2	365.2	140	3.1	1455.9
9.00	Peach palm – F(m)	14	576.0	4519.9	2537.9	2505.9	3154.3	1857.6	40	0.1	2223.7
10.00	Peach palm – F(ma)	14	144.0	2664.0	856.9	1070.1	1552.9	587.4	80	0.7	752.6
11.00	Peach palm –P(m)	14	360.0	9528.0	1623.5	2607.7	4144.4	1071.0	10	1.8	1737.2
12.00	Peach palm –P(ma)	14	264.0	3912.0	1200.0	1664.7	2460.9	868.6	80	0.7	1151.9
13.00	Vismia	14	96.0	4728.0	2016.0	2432.9	3338.4	1527.5	60	0.3	1728.1
				Ln K_s [$cm\ d^{-1}$]							
1.00	*Cupuaçu*	13	6.80	9.60	8.30	8.05	8.51	7.60	9	0.24	8.02
2.00	Annatto	13	5.70	9.70	7.50	7.68	8.35	7.00	15	0.21	7.59
3.00	Brazil nut	12	6.90	9.10	7.95	7.97	8.38	7.55	8	0.14	7.95
4.00	Peach palm – F	13	5.30	8.20	6.60	6.72	7.32	6.12	15	0.04	6.65
5.00	Peach palm – P	13	5.70	9.50	7.60	7.50	8.26	6.74	17	0.17	7.40
6.00	Pueraria	13	5.50	8.40	6.90	6.92	7.39	6.45	11	0.06	6.88
7.00	Cupuaçu (m)	13	7.80	9.30	8.30	8.42	8.69	8.15	5	0.54	8.39
8.00	Grasses and pueraria (m)	13	6.40	9.40	6.90	7.27	7.79	6.75	12	1.39	7.24
9.00	Peach palm – F(m)	14	6.40	8.40	7.85	7.71	8.03	7.40	7	-1.09	7.69
10.00	Peach palm – F(mb)	14	5.00	7.90	6.70	6.63	7.17	6.09	14	-0.28	6.56
11.00	Peach palm –P(m)	14	5.90	9.20	7.40	7.46	8.00	6.93	12	0.21	7.41
12.00	Peach palm –P(mb)	14	5.60	8.30	7.10	7.06	7.59	6.52	13	0.02	6.99
13.00	Vismia	14	4.60	8.50	7.60	7.47	8.09	6.86	14	-1.70	7.37

SE = standard error of the mean.
m = monoculture; b = among the palms; F = Peach palm for fruits production; P = Peach palm for palm heart production

[1] A practical definition of a REV is the smallest volume of soil that contains a representation of microscopic variations in all forms and proportions present in the system (Bear, 1972). Therefore, it is dependent of the physical quantity investigated but also on the soil variability under study. Generally, values of REV for capacity or static parameters differ from those for transport parameters. Moreover, values of a REV of the same property for different soils are not identical (Warrick, 1998).

The sampling volume needed to characterise the saturated hydraulic conductivity of a clayey soil with macropores was studied by Lauren et al., (1988). They found that K saturated measurements made on detached cylinders in the laboratory were extremely unreliable and not at all comparable with those made in the field. The discrepancy was primarily explained, because of short-circuiting of water flow through macrovoids that were continuous through the cylinders.

Relationships between K saturated and core height were also demonstrated by Anderson and Bouma (1973).

In spite of bias of the method, the higher magnitude of the geometric means (GM) of K_s values in Table 6.1 in relation to the field values of saturated hydraulic conductivity (K_{fs}) (Table 6.2) may be due to the fact that vertical macropores were filled with water under laboratory conditions. Because most of the entrapped air was removed gradually by saturating the core from the bottom. Moreover, the differences between the land use systems may be caused by the presence or absence of macropores in different soil cores. Analysing the K_s values in this way, reduced values of K_s near the peach palms [GM around 800 cm d^{-1}] and the higher values of K_s near the trunks of cupuaçus [GM > 3000 cm d^{-1}] agree with the results of Chapters 3 and 4. Where a reduced range of macropores was found near the peach palms, and a higher total porosity was found near the trunks of cupuaçus.

The discussion was done using GM (an estimate of the median) instead of arithmetic means, because GM yields a best estimate of the central tendency of lognormal distributions (Bower and Asce, 1969). GM is frequently used for analyses of K saturated data (Mohanty et al., 1998; Reynolds et al. 2000).

In conclusion, although the traditional soil core method with small cores may give some information about K saturated, this method is not appropriate for the clayey Ferralsols. It produces highly variable results because of the small sample size, the presence or absence of open-ended macropores, and variable soil compaction during core extraction. The limitation of the soil core method reported here agrees with the findings of Anderson and Bouma (1973), Lauren et al. (1988), Mohanty et al. (1994) and Reynolds et al. (2000).

6.3.1.2 Field saturated hydraulic conductivity (K_{fs})

A descriptive analyses of the data set (original values and log transformed) from the disc infiltrometer calculated with the direct application of Darcy's law (1-dimensional analysis) and the Ankeny method (3-dimensional analysis) is shown in Table 6.2. The complete data set is shown in Appendix 6 A. The results of K_{fs} (Table 6.2) are much less variable than the results from the soil core method (Table 6.1). This is probably related to the fact that in natural conditions the macropores terminate in the subsoil, and the water had to flow from these filled macropores into the surrounding matrix. Also, the sample volume assessed by the disc probably approximated the minimum REV for K saturated in the clayey Ferralsol. The smaller disturbance of the original structure of the soil in relation to the detached soil core from the constant head method may also be responsible for the higher precision of K_{fs}. The K_{fs} results are discussed based on the GM of the raw data due to lognormal distribution as explained above. A brief example of the calculation of statistical moments in log normal distributions is given at the end of this section. Details about log normal distributions are given in data analysis section. In Table 6.2 the results of the logarithmic transformation in the reduction of the CV are shown.

In the agroforestry system, the soil under the pueraria show the highest values of K_{fs} followed by those near the trunks of cupuaçu. K_{fs} near the peach palms tends to shows reduced values (the minimum values), which agrees with the results found using the soil cores and partially confirm the presence of greater percentage of micropores (Chapter 4). Conversely, these reduced values contrast with the reduced values of bulk density found near the palms [ca. 0.80 Mg m^{-3} – Chapter 3]. These results indicated that bulk density is for many land use systems (or position within the complex agroforestry system) a misleading parameter to infer about hydraulic conductivity (e.g., normally low bulk density correlates with high hydraulic conductivity).

In agroforestry system several factors, such different patterns in throughfall and stemflow (Schroth et al., 1999), nutrients (Chapter 3, and Schroth et al., 2000 a, b) and physical properties (Chapter 3 and 4) created a deterministic or systematic variability within small distances of the same plot. This variability is a result of different plant species with contrasting characteristics (i.e. growth, litter production, root distribution and different soil management). The systematic variability is introduced by different land use system management, and is simultaneously and concurrently superposed on changes in soil properties that vary randomly. Therefore, it becomes extremely complex to interpret parameters such like K_{fs} in complex land use systems for predictive use.

An expected reduction of the K_{fs} between cupuaçus growing in monoculture as a consequence of higher soil dispersion, (Chapter 2) and a reduction of total porosity (Chapter 3) was not found (Table 6.2 and 6.4). The high values of K_{fs} found in the more compact soil covered by grasses and pueraria may be explained that the presence of a small number of macropores (fissures), while comprising a small portion of the total porosity, lead to great K_{fs} (Beven and German, 1982; Mbagwu, 1995).

Luxmoore et al. (1981) and Bouma et al. (1982) show that only few macropores are enough to lead to high values of K_{fs}. Wilson and Luxmoore (1988) estimated that 96 % of water flux was transmitted through the macropores (< 0.02 mm of radius) which constituted only 0.32 % of the total soil volume. Dunn and Philips (1991) reported a value of 83 % of the saturated flux through 0.10 % of the total soil volume. These calculations assume that macropore flow follows Poiseuille's law and the capillary equation. Although these assumptions are not strictly valid, such calculations of field measurements are still helpful in a relative sense. The capillary equation does not apply to the largest macropores simply because these are no capillaries.

Table 6.2 Saturated hydraulic conductivities evaluated under field conditions (K_{fs}) on a clayey Ferralsol in the central Amazon. Results calculated with Ankeny's method [3-D] and with the direct application of Darcy's law [1-D].

Land use system and specie	Saturated Hydraulic conductivity K_{fs} [cm d^{-1}]									
	3 D					1D				
	Mean	Minimum	Maximum	GM	CV⁺	Mean	Minimum	Maximum	GM	CV
Cupuaçu	39.0	12.0	52.7	32.1	60	48.9	11.6	75.9	37.3	68
Annatto	57.0	2.9	101.3	27.1	88	75.8	2.5	135.7	31.2	89
Brazil nut	24.0	3.3	45.9	15.1	89	34.5	4.6	60.3	22.3	81
Peach palm – F	11.6	4.7	23.2	9.1	87	24.4	4.6	60.0	13.4	126
Peach palm – P	27.0	7.0	41.6	21.1	66	32.3	4.9	54.8	21.6	78
Pueraria	32.0	18.1	50.0	29.3	51	45.4	25.5	62.6	42.5	41
Cupuaçu	115.2	65.1	205.3	100.4	68	136.2	73.5	231.7	121.4	68
Grasses and pueraria	108.8	34.5	187.8	87.7	70	130.3	55.7	191.4	115.3	53
Peach palm – F(m)	30.0	10.4	64.9	21.5	100	43.9	15.7	92.8	32.3	97
Peach palm – F(ma)	24.5	6.2	56.3	15.7	112	29.5	9.3	65.0	20.5	104
Peach palm –P(m)	31.0	2.9	56.9	17.7	87	37.6	3.7	69.6	21.6	88
Peach palm –P(ma)	25.2	2.2	39.4	14.4	80	31.6	1.2	51.7	13.6	85
Vismia	76.0	26.7	168.6	53.8	105	90.6	27.6	197.2	63.5	102
	Ln K [cm d^{-1}]									
	3 D					1D				
Cupuaçu	3.47	2.49	3.96	3.39	24	3.61	2.61	4.09	3.51	24
Annatto	3.30	1.08	4.62	2.75	59	3.44	0.91	4.91	2.72	64
Brazil nut	2.72	1.19	3.83	2.43	50	3.10	1.53	4.10	2.85	44
Peach palm – F	2.21	1.55	3.14	2.11	38	2.60	1.53	4.09	2.39	51
Peach palm – P	3.05	1.94	3.73	2.93	32	3.07	1.60	4.00	2.85	42
Pueraria	3.38	2.89	3.91	3.35	15	3.75	3.24	4.14	3.73	12
Cupuaçu	4.61	4.18	5.32	4.58	14	4.73	4.30	5.45	4.78	13
Grasses and pueraria	4.47	3.54	5.24	4.42	19	4.75	4.02	5.25	4.72	13
Peach palm – F(m)	3.07	2.34	4.17	2.97	32	3.48	2.75	4.53	3.40	26
Peach palm – F(mb)	2.75	1.83	4.03	2.61	41	3.02	2.23	4.17	2.91	34
Peach palm –P(m)	2.87	1.08	4.04	2.48	55	3.07	1.30	4.24	2.73	51
Peach palm –P(mb)	2.67	0.80	3.67	2.18	61	2.61	0.15	3.95	1.30	82
Vismia	3.97	3.28	5.13	3.91	25	4.15	3.32	5.28	4.07	24

GM = geometric mean; ⁺ CV = coefficient of variation around the arithmetic mean.
m = monoculture; b = between palms;
F = Peach palm for fruits production;
P = Peach palm for palm heart production

Calculations based on Poiseuille's law are erroneous because water flow in macropores is not laminar (Chen and Waganet, 1992), and macropores need not be filled to conduct water (Philips et al., 1989; Beven and German, 1981). Therefore, the high values of K_{fs} found in the more compact soil covered by grasses and pueraria may be explained that the presence of a small number of macropores, while comprising a small portion of the total porosity, lead to great K_{fs} (Beven and German, 1982; Mbagwu, 1995).

An intense macrofauna activity in the secondary forest (Römbke and Garcia, 2001) are probably related to the high values of saturated hydraulic conductivity. The true K_{fs} for this site would even be higher. Due the fact that , positions with "big holes" originating from the intense activity of earthworms were avoided for practical reasons. Those position, certainly, have a very high K_{fs}.

A comparison between the saturated hydraulic conductivity obtained through different methods (i.e., the soil core, 1D and 3D calculations) shows that although differences in magnitude were found between the field method and laboratory methods, many trends were similar. As discussed above in the soil core method, a clear tendency of reduction of the infiltration rate near the peach palms could be identified. Nevertheless, the magnitude of the K_{fs} values was still relatively high. Therefore, only intermittent ponded areas after very intense rains could be observed, especially in the monoculture of peach palm.

The values of K_{fs} estimates using the 1-D and 3-D approach are similar (Table 6.2). Some variation is probably related to pockets of entrapped air, and horizontal flow of water due to the reduced radius of the outer ring.

The values obtained for K_{fs} in the presented study (Table 6.2 and 6.4) are considerably lower than previously reported values evaluated in clayey Ferralsols in the central Amazon (Table 6.3). This great variability between the results are probably not only a consequence of different land use systems or the natural soil variability but it may be also a consequence of the different methods, boundary conditions and the calculation methods used. When measurements of K saturated are performed in the field to be used in comparisons among different treatments, the conditions of the measurements such as water quality, temperature, soil moisture, surface conditions, lengths of inundation and infiltration flow system, should be reported in detail to allow reliable comparisons and interpretation of the results.

Table 6.3 Saturated hydraulic (K) conductivity evaluated with different methods at the soil surface on clayey Ferralsol in the central Amazon

Authors	Method	Land use system evaluated	K (cm d^{-1})[†]
Nortcliff and Thornes, 1981	Constant head [+]	Primary Forest	156 – 322
Corrêa, 1985 a	Constant head [+]	Traditional tillage	800
		No tillage	395
		Rotavator system	724
		Primary forest	1197
Corrêa, 1985 b	Double ring	Mechanized conventional	359
		No tillage	174
		Rotavator	323
		Primary forest	1500
Medina, 1985	Double ring	Land clearing – Mechanized	34
		Land clearing – Manual	269
		Primary forest	708
Medina e Leite 1985	Double ring	Rubber tree with pueraria	684
		Rubber tree with grasses	792
		Rubber tree with coffee	1416
		Secondary forest	545
		Primary forest	535
Tomassela and Hodnett, 1996	Ring Permeater	Pasture	159 [43 – 528]

[+] Laboratory method; † Arithmetic mean

The values more appropriate for some comparisons (Table 6.2) are those evaluated by Tomasella and Hodnett (1996) who also used a similar disc infiltrometer. Their results agree in magnitude with the values found in the present study. The magnitude of the results are lower than those obtained by ponding water in the double ring method. This may be due not only by a reduced conductance caused by the contact sand and the porous membrane of the infiltrometer (Reynolds and Zebchuk, 1996), but and principally because the clayey Ferralsols show a positive air entry point (i.e., when the soil matrix potential is zero some pores still empty). Because of presence of large macropores in this clayey Ferralsol, K changes dramatically with even small changes in pressure head (i.e., changes in two orders of magnitude occur with a millimetric variation of the pressure head near saturation and with small water pressures).

Most of the studies and mathematical equations about K are developed on soils with relatively low water intake rates in the temperate regions (e.g. Brooks and Corey; Campbel and van Genuchten-Mualen model, see discussion about this model in the inverse methods section). In these soils a flat region of the functions that relate K with θ or h near saturation is normally found. Further, K is normally taken as a constant value for $h \geq 0$.

Figure 6.4 shows an example of measured K_{fs} where this flat region is not found and the K_{fs} values continues to increase with increasing h for positive values. In the clayey Ferralsols, small changes of h near the saturation or with positive pressure head lead to significant changes in the infiltration rates.

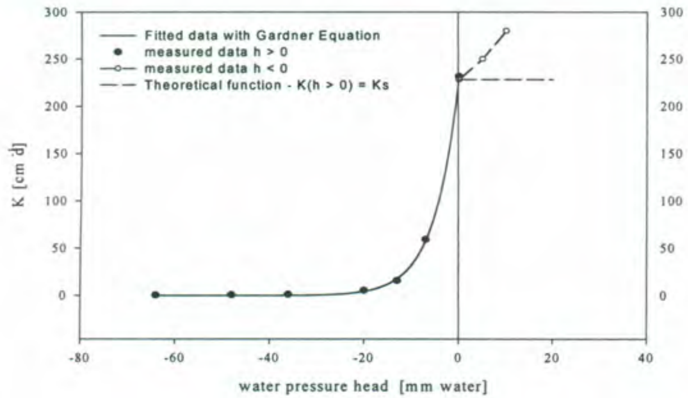

Figure 6.4 Relationship between hydraulic conductivity and matric pressure head evaluated with tension infiltrometer on the soil surface of an clayey Ferralsol in the central Amazon. The line of a theoretical function K(h) for a theoretical soil without macropores is also plotted.

This phenomenon was also reported by Logdson et al. (1993) and McCoy et al. (1994) in a study on evaluation of K in macroporous soils. If this phenomenon is not taken into account, it could lead to serious overestimation when modelling soil water fluxes, especially in situations of the occurrence of ponding. Therefore, hydraulic models that assume a negative air-entry pressure point, must be modified to be appropriate for simulation studies. The disc infiltrometer available in this study did not permited further measurements of this phenomenon because of the extremely high fluxes that made the readings and refilling of the reservoir unfeasible.

The K_{fs} values evaluated with disc infiltrometer are better characterized indicating that the value was measured at a water pressure near zero [e.g. K_{fs} ($h \approx 0$)], and it should be pointed out that they do not represent the maximum infiltration rate on clayey Ferralsols. More reliable methods for field conditions, and a mathematical theory to describe K saturated in soils with macropores are subject to further investigations.

As discussed above, K saturated values are frequently lognormal distributed, and the analysis of log normal distribution is in many studies misleading. Transforming the logarithmically transformed values (normally used in statistical analysis) back for the linear scale is usually done by taking the antilogarithm of the mean of the ln transformed values. This is equivalent to an estimation of the geometrical mean of a log normal distribution and not of an arithmetic mean. Fortunately, in most studies of soil hydrology the geometric mean will be the most appropriate representation of the central tendency (Bower and Asce, 1969). In some circumstances (e.g., when mass calculation is involved, Parkin and Robinson, 1992) the arithmetic mean is more appropriate. Furthermore, highly variable parameters such as K saturated are better understood and more completely described if the probability density function (pdf) is estimated. Stochastic modelling, or statistical modelling analyses, which include a component to examine the uncertainty of simulation result, need estimates of the mean and variance of the parameters. The maximum likelihood method was used to estimate these moments for the K_{fs} (Eq. 6.30 and 6.31). The results are shown in Table 6.4, and give a complete description of K_{fs} ($h \approx 0$). They will be used in ongoing water simulation studies.

Table 6.4 Saturated hydraulic conductivity [K_{fs} ($h \approx 0$)] evaluated with disc infiltrometer in a clayey Ferralsols in the central Amazon.

Land use system	Specie	Mean[T]	Variance
		$cm\ d^{-1}$	$cm^2\ d^{-2}$
Agroforestry	Cupuaçu	46.06	2249.64
Agroforestry	Annatto	176.61	1296350.05
Agroforestry	Brazil nut	38.42	8056.56
Agroforestry	Peach palm -F	12.85	165.49
Agroforestry	Peach palm –P	33.74	1771.19
Agroforestry	Pueraria	33.40	332.03
Monoculture	Cupuaçu	121.81	7106.15
Monoculture	Grass	126.85	17601.12
Monoculture	Peach palm - F	34.50	1869.81
Monoculture	Peach palm – aF	30.13	2434.72
Monoculture	Peach palm – P	61.55	42146.29
Monoculture	Peach palm – aP	53.33	36309.10
Secondary Forest	Vismia	88.03	13742.67

[T] The probability density function is log normal.
F = Peach palm for fruits production; P = Peach palm – for palm heart production
a = between palms

6.3.2 Unsaturated hydraulic conductivity (K)

6.3.2.1 Instantaneous profile method (IPM)

In the clayey Ferralsols in the central Amazon, when only internal drainage is allowed, the variation of θ is very slow and below the precision of the TDR. The measured data set with volumetric soil water (θ) and matrix potential (h) in the IPM experiment is shown in Table 6.5. The measured data show some noise behaviour especially in the θ measurements, because the precision of the TDR technique is not sufficient to evaluate variation lower than about 2 % (see, Chapter 5). It should be stressed that none of the available methods to evaluate θ in field conditions show a precision higher than 2 %. Concurrently, soil variability also contributed to the noise behaviour of the results between depths. Therefore, smoothing function were used to fit the functional relationship between θ and t for each depth [θ*(t, z)]. The results show that between the equations tested [Eq. 6.17 to 6.19] the power equation is the best option for the depths of 10, 20, 40 cm. However, the linear equation fitted better the deeper layers (Table 6.5). The linear variation in the deeper layers is related to the small variation of θ. Table 6.7 shows the estimated [θ* (z, t)] data with respect to time for each depth calculated using the selected function presented in Table 6.6.

Table 6.8 shows the coefficients and statistical parameters of the equations tested to relate soil water storage (W) to (z, t). The power equation was selected for all depths and used to estimate a new W* with respect to time for each depth (Table 6.9).

Table 6.5 Volumetric water content (θ) and matrix potential (h) in different depths evaluated in a IPM experiment in an clayey Ferralsol in the central Amazon.

Time	θ (Volumetric water content – $m^3\ m^{-3}$)						h [matrix potential – cm]					
Accumulated hours	Depth											
	10	20	40	60	80	90	10	20	40	60	80	90
0	0.4056	0.4416	0.4956	0.4213	0.5204	0.4990	-13.4	-10.9	-14.9	-13.8	-6.4	-1.4
3.50	0.4011	0.4303	0.4900	0.4146	0.5170	0.4968	-22.2	-24.8	-23.7	-30.1	-26.5	-24.1
21.25	0.3954	0.4168	0.4833	0.4101	0.5046	0.4866	-41.1	-48.7	-45.1	-52.8	-49.2	-48.0
47.25	0.3887	0.4112	0.4844	0.4123	0.5080	0.4911	-53.7	-63.8	-61.5	-66.7	-63.1	-64.4
69.33	0.3864	0.4067	0.4810	0.4078	0.5046	0.4889	-61.2	-71.4	-71.6	-74.2	-66.8	-65.7
93.50	0.3853	0.4067	0.4787	0.4157	0.5137	0.4866	-70.1	-80.2	-79.1	-79.3	-73.1	-72.0
117.33	0.3864	0.4078	0.4787	0.4112	0.5114	0.4855	-75.1	-86.5	-84.2	-84.3	-79.4	-75.7
141.67	0.3808	0.4033	0.4776	0.4078	0.5125	0.4855	-78.9	-89.0	-91.7	-86.8	-84.5	-82.0
165.33	0.3808	0.4022	0.4742	0.4056	0.5103	0.4833	-83.9	-95.3	-94.2	-93.1	-85.7	-83.3
189.42	0.3808	0.4022	0.4742	0.4067	0.5024	0.4697	-86.4	-99.1	-99.3	-94.4	-90.8	-88.3
212.80	0.3740	0.3966	0.4720	0.4044	0.5024	0.4697	-91.5	-104.2	-103.1	-100.7	-97.1	-94.6
237.92	0.3763	0.3988	0.4720	0.4044	0.5024	0.4731	-92.7	-106.7	-106.8	-103.2	-99.6	-95.9
261.17	0.3785	0.4011	0.4754	0.4078	0.5024	0.4754	-97.8	-111.7	-110.6	-105.7	-102.1	-99.7
286.42	0.3797	0.4022	0.4686	0.3999	0.4934	0.4697	-99.0	-113.0	-114.4	-112.0	-99.6	-103.5
309.33	0.3763	0.3988	0.4720	0.4022	0.4956	0.4731	-104.1	-116.8	-116.9	-113.3	-105.9	-103.5
333.33	0.3774	0.3999	0.4731	0.3988	0.4968	0.4709	-105.3	-119.3	-119.4	-115.8	-108.4	-104.7
357.33	0.3763	0.3999	0.4731	0.3999	0.4956	0.4709	-107.9	-123.1	-122.0	-117.1	-110.9	-108.5
381.67	0.3774	0.4011	0.4720	0.3999	0.5001	0.4709	-112.9	-125.6	-124.5	-120.9	-114.7	-113.5
407.17	0.3774	0.3999	0.4697	0.3943	0.4923	0.4641	-112.9	-128.1	-127.0	-122.1	-116.0	-113.5

Table 6.6 Selection of smoothing equations to fit volumetric soil water content (θ) in function of time for different depths [θ (t, z)]

Depht	Model	r^2	d.f.	F	Sig	b_0	b_1
0 – 10	Linear	0.69	17	37.47	0.0001	0.394	-6.00E-05
0 – 10	Log	0.94	17	271.25	0.0001	0.4079	-5.30E-03
0 – 10	*Power*	0.94	17	252.45	0.0001	0.4082	-0.0135
10 - 20	Linear	0.54	17	19.88	0.0001	0.4189	-6.00E-05
10 – 20	Log	0.96	17	456.51	0.0001	0.4391	-7.00E-03
10 – 20	*Power*	0.97	17	462.75	0.0001	0.4393	-0.0167
20 – 40	Linear	0.73	17	45.94	0.0001	0.4859	-5.00E-05
20 – 40	Log	0.92	17	206.33	0.0001	0.4966	-4.20E-03
20 – 40	*Power*	0.92	17	197.09	0.0001	0.4967	-0.0087
40 – 60	Linear	0.82	17	79.23	0.0001	0.4154	-5.00E-05
40 – 60	Log	0.69	17	37.43	0.0001	0.4225	-3.40E-03
40 – 60	*Power*	0.68	17	36.5	0.0001	0.4226	-0.0083
60 – 80	Linear	0.72	17	42.72	0.0001	0.5144	-5.00E-05
60 – 80	Log	0.60	17	25.61	0.0001	0.5224	-3.80E-03
60 – 80	*Power*	0.60	17	25.15	0.0001	0.5226	-0.0076
80 – 90	Linear	0.84	17	87.03	0.0001	0.4932	-7.00E-05
80 – 90	Log	0.74	17	48.42	0.0001	0.505	-0.0055
80 – 90	*Power*	0.73	17	46.8	0.0001	0.5054	-0.0113

Italicised letter indicate the selected equations

Table 6.7 Volumetric soil water content [$\theta* - m^3\ m^{-3}$] estimated in different depth profiles in relation to different times in the IPM experiment.

Accumulated hours	Depth [cm]					
[h]	0-10	0-20	0-40	0-60	0-80	0-90
0	0.4079	0.4391	0.4966	0.4154	0.5144	0.4932
3.50	0.4013	0.4303	0.4913	0.4152	0.5142	0.4930
21.25	0.3917	0.4177	0.4838	0.4143	0.5133	0.4917
47.25	0.3875	0.4121	0.4804	0.4130	0.5120	0.4899
69.33	0.3854	0.4094	0.4788	0.4119	0.5109	0.4883
93.50	0.3838	0.4073	0.4775	0.4107	0.5097	0.4867
117.33	0.3826	0.4057	0.4766	0.4095	0.5085	0.4850
141.67	0.3816	0.4044	0.4758	0.4083	0.5073	0.4833
165.33	0.3808	0.4033	0.4751	0.4071	0.5061	0.4816
189.42	0.3801	0.4024	0.4746	0.4059	0.5049	0.4799
212.80	0.3795	0.4016	0.4741	0.4048	0.5038	0.4783
237.92	0.3789	0.4008	0.4736	0.4035	0.5025	0.4765
261.17	0.3784	0.4001	0.4732	0.4023	0.5013	0.4749
286.42	0.3779	0.3995	0.4728	0.4011	0.5001	0.4732
309.33	0.3775	0.3990	0.4725	0.3999	0.4989	0.4715
333.33	0.3771	0.3984	0.4722	0.3987	0.4977	0.4699
357.33	0.3767	0.3979	0.4719	0.3975	0.4965	0.4682
381.67	0.3764	0.3975	0.4716	0.3963	0.4953	0.4665
407.17	0.3761	0.3970	0.4714	0.3950	0.4940	0.4647

Table 6.8 Selection of smoothing equations to fit soil water storage (W) in function of time for different depths [W (t, z)] in the IPM experiment

Depth	Model	r^2	d.f.	F	Sig.	b_0	b_1
0-10	Linear	0.68	17	36.57	0.0001	3.9363	-0.0005
0-10	Log	0.91	17	161.71	0.0001	3.9793	-0.0331
0-10	*Power*	*0.90*	*17*	*151.96*	*0.0001*	*3.978*	*-0.0085*
0-20	Linear	0.67	17	34.5	0.0001	8.1351	-0.0012
0-20	Log	0.91	17	161.86	0.0001	8.2371	-0.0768
0-20	*Power*	*0.90*	*17*	*151.82*	*0.0001*	*8.2337*	*-0.0095*
0-40	Linear	0.67	17	35.08	0.0001	17.3142	-0.0022
0-40	Log	0.90	17	160.5	0.0001	17.4951	-0.1371
0-40	*Power*	*0.90*	*17*	*152.01*	*0.0001*	*17.49*	*-0.008*
0-60	Linear	0.78	17	58.97	0.0001	25.711	-0.0033
0-60	Log	0.86	17	103.97	0.0001	25.8949	-0.1826
0-60	*Power*	*0.85*	*17*	*98.91*	*0.0001*	*25.8899*	*-0.0072*
0-80	Linear	0.84	17	89.71	0.0001	35.6534	-0.0043
0-80	Log	0.81	17	73.13	0.0001	35.8243	-0.2236
0-80	*Power*	*0.81*	*17*	*70.18*	*0.0001*	*35.8199*	*-0.0063*
0-90	Linear	0.89	17	143.53	0.0001	40.8253	-0.0051
0-90	Log	0.76	17	53.48	0.0001	40.9551	-0.2487
0-90	*Power*	*0.75*	*17*	*51.5*	*0.0001*	*40.9512*	*-0.0062*

Italicised letters indicate the selected equation.

Table 6.9 shows the soil water storage (W) calculated for each depth using the θ^* data (Table 6.7) in the Equation 6.20. The relationships [W, (t, z)] were smoothed with respect to time for each depth generating the smoothed functional relationships $W^*(z, t)$ (Table 6.10)

Tensiometers were used in the IPM experiment to evaluate the hydraulic gradient and their possible fluctuation in time. Figure 6.5 shows profiles of the total potential (H) and matric potential (h) as a function of time. Only small deviations are observed from the unit gradient (particularly for the depth of 10 cm in the dry period). However, in practice, these deviations are not significant in the flux calculations since the fluxes in the dry range are too small. Concluding, these results permit the use of a unit gradient approach in the flux calculation for this clayey Ferralsol. Moreover, it is also an indication of the predominance of vertical flow. Certainly, when the interests lay in the dry range, the assumption of the unit gradient may yield inaccurate K values. Since the unit gradient was verified, taking the derivative of the functional relationships W^* (z, t) at selected times gives already values of the instantaneous flux which equals K (Table 6.10).

Table 6.9 Storage water content (W) in different depth in function of time for different depths in the IPM experiment – After smoothing of θ (t, z)].

Accumulated hours	Depth					
[h]	0-10	0-20	0-40	0-60	0-80	0-90
	W [mm]					
0	4.08	8.47	17.91	26.39	36.37	41.50
3.50	4.01	8.32	17.64	26.07	36.04	41.18
21.25	3.92	8.09	17.24	25.61	35.53	40.69
47.25	3.88	8.00	17.07	25.40	35.28	40.42
69.33	3.85	7.95	16.98	25.28	35.14	40.27
93.50	3.84	7.91	16.91	25.19	35.02	40.14
117.33	3.83	7.88	16.87	25.12	34.93	40.02
141.67	3.82	7.86	16.82	25.05	34.84	39.91
165.33	3.81	7.84	16.79	24.99	34.76	39.81
189.42	3.80	7.83	16.76	24.95	34.69	39.72
212.80	3.80	7.81	16.74	24.90	34.62	39.63
237.92	3.79	7.80	16.71	24.85	34.55	39.54
261.17	3.78	7.79	16.69	24.81	34.48	39.45
286.42	3.78	7.77	16.67	24.77	34.42	39.37
309.33	3.78	7.77	16.65	24.73	34.36	39.29
333.33	3.77	7.76	16.64	24.70	34.31	39.21
357.33	3.77	7.75	16.62	24.66	34.25	39.13
381.67	3.76	7.74	16.61	24.63	34.19	39.05
407.17	3.76	7.73	16.59	24.59	34.14	38.97

Table 6.10 Instantaneous hydraulic conductivity K [cm h^{-1}] in function of time for different layers evaluated with IPM method on a clayey Ferralsol in the central Amazon.

Accumulated hours	Layers [cm]					
	0-10	10-20	20-40	40-60	60-80	80-90
	$\partial W/\partial t^{\dagger}$					
	K[cm d^{-1}]					
0	8.43908	19.61236	34.84103	46.24599	55.75402	62.70029
3.50	0.02294	0.05300	0.09499	0.12667	0.15353	0.17275
21.25	0.00372	0.00858	0.01542	0.02059	0.02500	0.02814
47.25	0.00166	0.00383	0.00689	0.00921	0.01119	0.01259
69.33	0.00113	0.00260	0.00468	0.00626	0.00761	0.00856
93.50	0.00084	0.00192	0.00346	0.00463	0.00563	0.00634
117.33	0.00066	0.00153	0.00276	0.00368	0.00448	0.00504
141.67	0.00055	0.00126	0.00228	0.00305	0.00371	0.00417
165.33	0.00047	0.00108	0.00195	0.00261	0.00317	0.00357
189.42	0.00041	0.00094	0.00170	0.00227	0.00277	0.00311
212.80	0.00036	0.00084	0.00151	0.00202	0.00246	0.00277
237.92	0.00033	0.00075	0.00135	0.00181	0.00220	0.00248
261.17	0.00030	0.00068	0.00123	0.00165	0.00200	0.00225
286.42	0.00027	0.00062	0.00112	0.00150	0.00182	0.00205
309.33	0.00025	0.00057	0.00104	0.00139	0.00169	0.00190
333.33	0.00023	0.00053	0.00096	0.00129	0.00157	0.00176
357.33	0.00022	0.00050	0.00090	0.00120	0.00146	0.00164
381.67	0.00020	0.00046	0.00084	0.00112	0.00137	0.00154
407.17	0.00019	0.00044	0.00079	0.00105	0.00128	0.00144

† First derivative of the power functions $\partial W/\partial t = [b \times bo \times t^{(b-1)}]$.

The variations of K in function of θ for all depths are illustrated in a scatter plot in Figure 6.6; which shows that K in the unsaturated range is by about five orders of magnitude lower than near saturation. Moreover, two typical behaviours can be identified: i) a linear one for the superficial layers and ii) a curvilineous for the deeper layers. This is probably related to fact that, when the evaluation started in the IPM experiment the first layers had already drained the water from the large pores (see first values of the data in Table 6.6) while in the deeper layers the drainage process was still in progress in a broad range of radius of pores. It is obvious that the concentration of macropores in the first layers contributes to this phenomenon.

The functional relationships between K and θ (Figure 6.6) were estimated by linear regression using the linear form of the Equation 6.5. Further, ln K was plotted as a function of (θ_0 - θ) in Figure 6.6 b and c. The coefficients and statistical results of the fitted equations ln K (z, θ_0-θ) show a very good fit for the depths of 10; 20 and 40 cm, but significant deviations were found for the depths of 60, 80 and 90 cm (indicated by a small r^2). That deviations is probably due the fact that the linearization of these functions was not able to fit the distinct behaviour of the water fluxes in the two different domains in the deeper layers. A probable explanation is that near saturation both domains were transmitting water, but after a pressure head of [40 mm] only the micropore domains were operating. This can be further elucidated remembering that water flow is governed by different physical forces (e.g., gravity, capillarity, and absorption) in each pore group (e.g. macropores, mesopores, and micropores). For example, gravity may dominate the flow process in the macropores, whereas capillary forces will dominate flow in the micropores. Because of differences in the governing forces, the hydraulic conductivity can increase/decrease several orders of magnitude across one or more threshold soil water pressure head(s) separating the different flow regions (Mohanty, 1999).

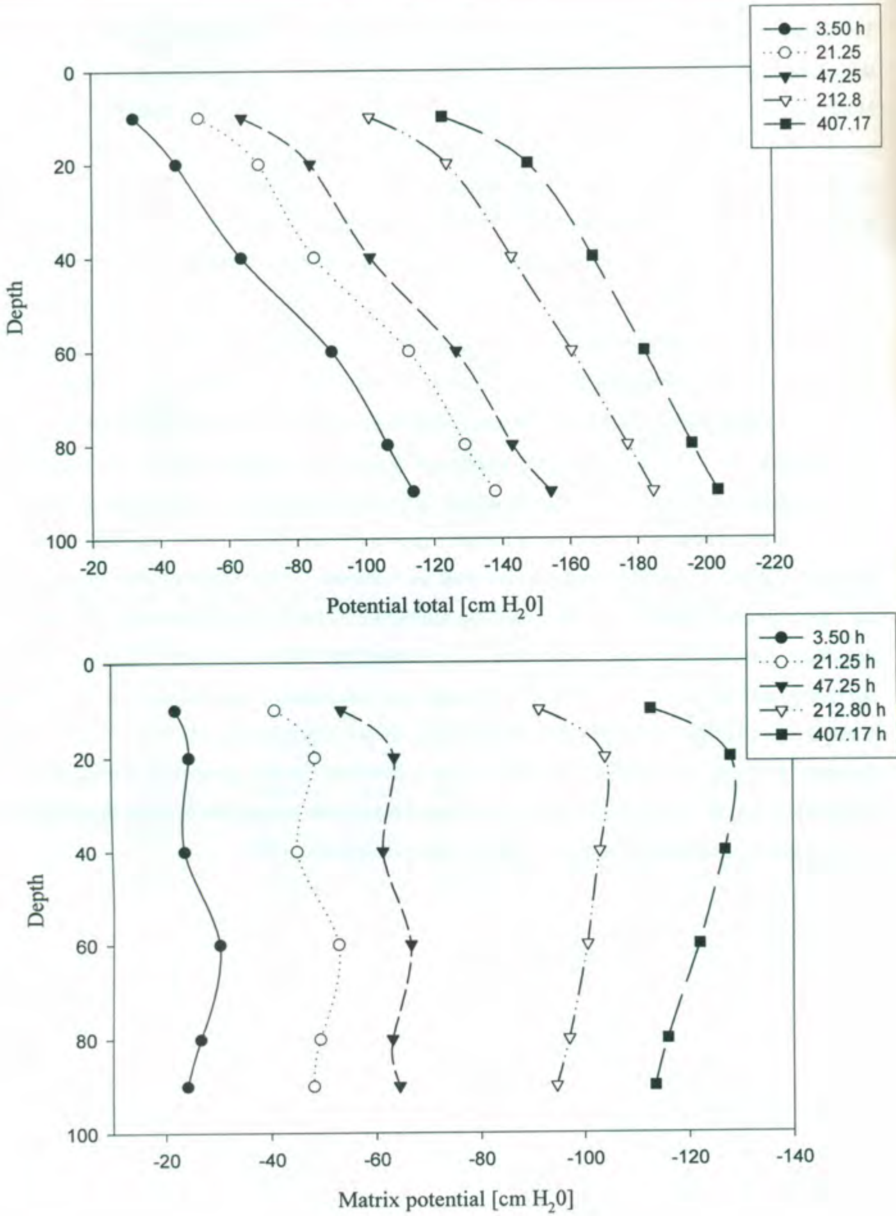

Figure 6.5 Total potential and matric potential evaluated in the IPM experiment.

The similarities of the linear equations (Figure 6.6 and Table 6.11) were tested in relation to parallelism and concordance.

Table 6.11 Parameters of the Equation ln K (θ) = ln Ko + β (θ–θ$_o$) for different depths on a soil profile in a clayey Ferralsols.

Depth	θ_0	K_0^+	λ	Std. Error	R^2
0-10	0.4079	-0.2129	190.0662	0.0056	0.99
10-20	0.4391	0.6344	144.2777	0.0039	0.99
20-40	0.4966	1.2143	240.0519	0.0066	0.99
40-60	0.4154	-1.7964	163.4216	0.6507	0.73
60-80	0.5144	-1.6024	163.2759	0.6501	0.73
80-90	0.4932	-1.4868	116.6923	0.6482	0.73

+ The first paired data was eliminated in the regression analysis

The results showed that these functions are distinct for intercept coefficients as well as for slopes (Table 6.12). Therefore, they should not be pooled in a single equation, representing the whole profile. For the layers of 10, 20 and 40 cm depth distinct equations should be used.

Table 6.12 Parameter estimated for testing the differences between the equations for common intercept and parallelism for the depths of 0-10; 10-20 and 20-40 cm.

Testing for difference among regression				
Source	F cal.	df, df†	$F_{(\alpha = 0.05)}$	p
Common intercept	298	2, 50	3.18	1.00
Parallelism	52242	2, 48	3.19	1.00

† Degrees of freedom of numerator and denominator for F distribution.

A visual inspection of the piecewise equation for the deeper layers shows that the equations have the same slopes. Moreover, the values of the pressure head in the break point (hp) in the piecewise equation are interpreted as the h that divides operationally the two domains. The hp values are similar for the three depths analyzed (Table 6.13). The fluxes which occur between the aggregates (i.e., macropores fluxes) and in the aggregates (i.e., micropore fluxes) could be better represented by a piecewise continuous functions (Figure 6.6 c and Table 6.13).

Table 6.13 Parameters of the piecewise equations for the three depths on a soil profile on a clayey Ferralsol.

Layer	θ_0	K_0^+	β_0	K_1^+	β_1	θ_{bp}	Std. Error	r^2
40-60	0.4154	-3.1066	73.5811	-1.8410	231.7811	-0.0076	0.0528	0.99
60-80	0.5144	-2.9114	73.5159	-1.7101	231.5757	-0.0076	0.0528	0.99
80-90	0.4932	-2.7186	55.84895	-1.5092	186.5652	-0.0093	0.0535	0.99

+ The first paired data were eliminated in the regression analysis.

The parallelism visualised in the Figure 6.6(c) can be interpreted in the sense that the clayey Ferralsol has as homogeneous hydraulic behaviour (i.e., a variation in h results in the same magnitude of variation on K for different depths). The parallelism of the hydraulic functions may permit a reduction of the number of parameters needed to describe the hydraulic properties of the clayey Ferralsols. The offset in the hydraulic functions between the depths is related to the different porosities. A similar trend was observed in a study carried out on a clayey Ferralsol by Tomasella and Hodnett (1996).

Some indications of the existence of a fluffy horizon located between two more compacted ones (see, Chapter 3 and 4) are reconfirmed here. The curve at the depth of 60 cm is situated near the curves of the more superficial depths (Figure 6.6), as a consequence of the presence of macropores in these depths (see, Chapter 4). The increase of the values of K with depth is a consequence of an increase of the actual values of θ with depth.

Accuracy of the prediction of K (θ) with IPM

The accuracy, precision and validation of the results evaluated in the direct measurements by the IPM have been questioned (Reichardt et al, 1998; Falleiros et al., 1998; Jong van Lier and Libardi, 1999). However, some studies as Chong et al. (1981), Jones and Wagenet (1984) and Comegna et al. (1996) obtained a relatively low CV for the water fluxes estimated using the parameters obtained in the IPM method. The error analyses carried out by Flühler et al. (1976), Reichardt et al. (1998) show that the estimation of K is very sensitive to experimental errors. Variation of 200% or more for very small deviations in θ can be found. Errors in K values obtained during the early stage of measurement in the IPM experiments arise from the flux measurement and at later times (small K values) error in water content is more serious (Green et al, 1986). Since θ shows a high spatial variability at small scale and cannot be measured in the field with errors of less than 3 - 4 % in the clay Ferralsol; the use of the Darcy – Buckinghan Equation, has a restricted use to monitor soil water dynamics.

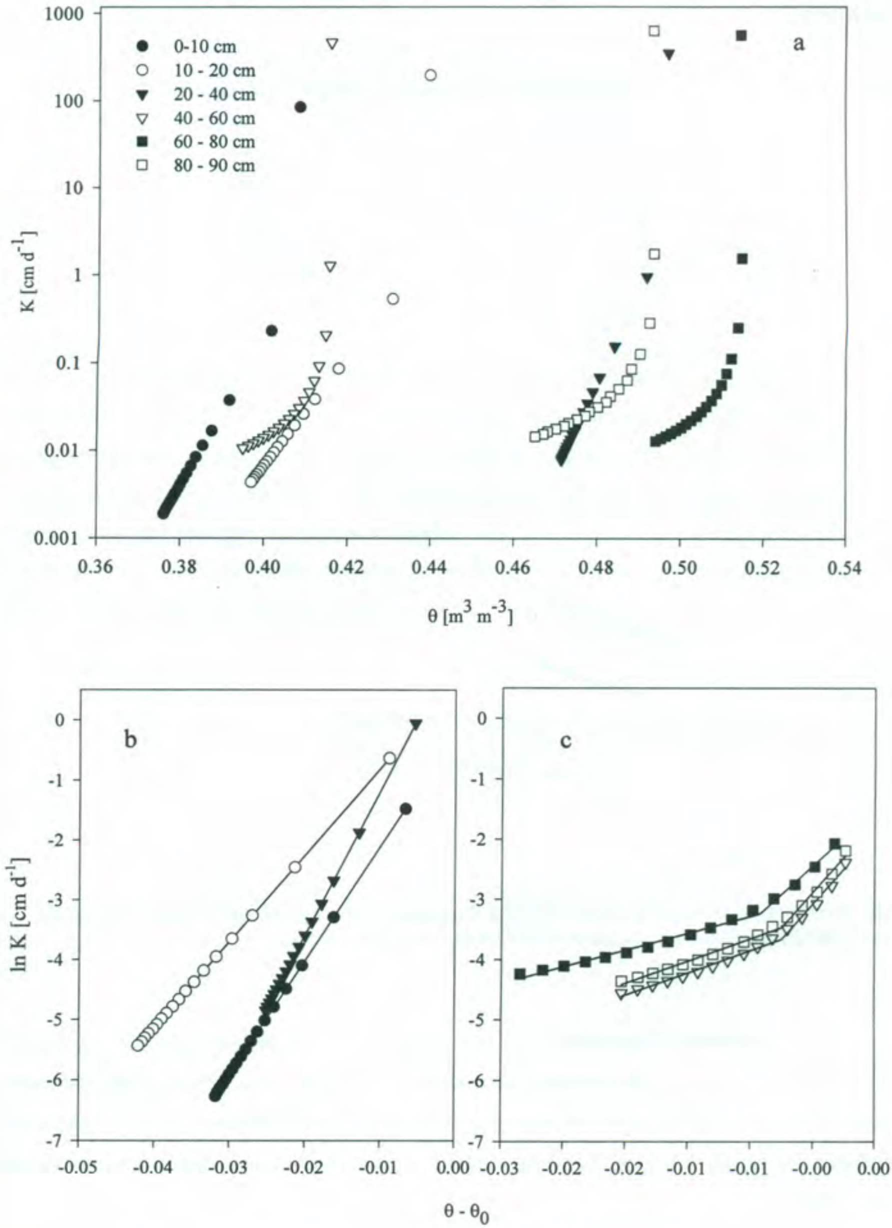

Figure 6.6 a) Relationship between hydraulic conductivity [K] and volumetric water content [θ] at different depths estimated in a IPM experiment on a clayey Ferralsol in the central Amazon. b) and c) are relationship between hydraulic conductivity [ln K] and volumetric water content [θ-θ_0].

The functions K (h)

The scatter plot of data for K and h evaluated at different depths is shown in Figure 6.7.

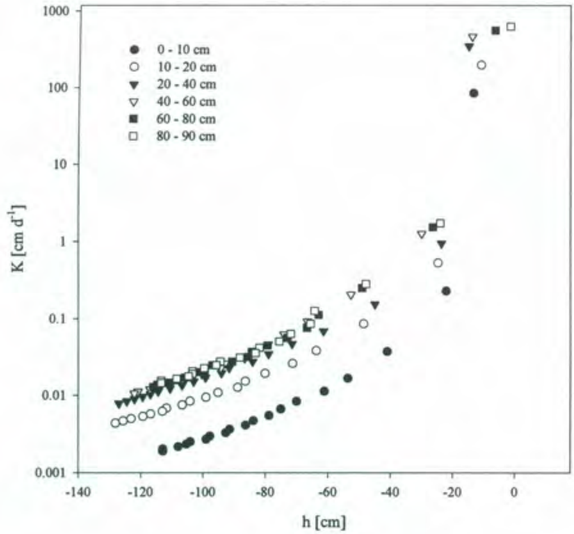

Figure 6.7 Relationship between unsaturated hydraulic conductivity [K] and matric pressure head [h] evaluated in IPM experiment on an clayey Ferralsol in the central Amazon

A reduced scatter is observed of the data K vs. h in comparison to the K vs. θ (Figure 6.7 and. Figure 6.6). In the analyses of the K (h) functions, no smoothing techniques were applied. The functional relationships between K and h were fitted using the linear form of the Equation 6.22. The parameters Ko and λ were determined by linear regression analyses. The coefficients and statistical indicators are shown in Table 6.14.

Table 6.14 Parameters of the Equation $\ln K(h) = \ln K_0 + [\lambda (h-h_o)]$ for different depths on a soil profile on a clayey Ferralsol.

Depths	h_0 [cm]	K_0^+	β	Std. Error	R^2
0-10	-13.4	-1.9201	0.0465	0.3012	0.94
10-20	-10.9	-0.7970	0.0421	0.2715	0.95
20-40	-14.9	-0.4680	0.0413	0.2697	0.95
40-60	-13.8	0.0473	0.2919	0.2754	0.95
60-80	-6.4	0.7201	0.0491	0.2715	0.95
80-90	-1.4	1.0314	0.0495	0.2669	0.95

+ The first paired data were eliminated in the regression

Figure 6.8 shows the fitted equation [K vs. h] and the measured data. The equations for the depths of 0-10; 10-20 and 20-40 cm were compared in relation to the slope and intercept (Table 6.15), showing that the equations have a similar slopes ($p > 0.10$). Therefore, these functions can be represented by only one function where only the intercept needs to be changed to represent different depths. This approach can be used in simulation models and error analysis, where a reduction of the parameters is a vital task. Some deviation in the inclination of the curve in the dry range can surely better fitted by piecewise equations if higher accuracy is required.

Table 6.15 Parameter estimates for testing the differences between the equations for common intercept and parallelism for the depths of 0-10, 10-20 and 20-40 cm.

Testing for difference among regression				
Source	F cal.	df, df†	$F_{(\alpha = 0.05)}$	p
Common intercept	203.29	5, 101	3.18	1.00
Parallelism	1.94	5, 96	2.30 (1.90‡)	1.00

† Degrees of freedom of numerator and denominator for the F distribution ;
‡ F value at $\alpha = 0.10$

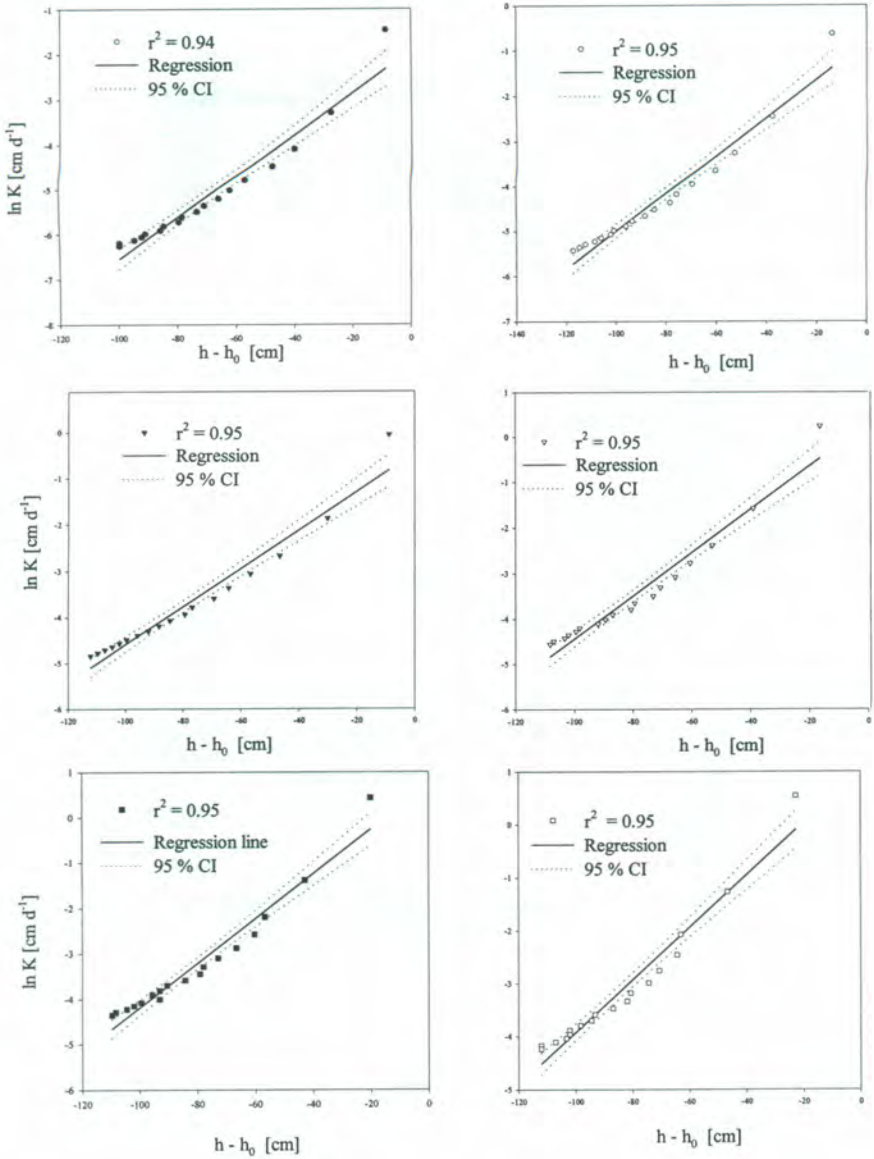

Figure 6.8 Relationship between the hydraulic conductivity [ln K] and matric potential [h-h$_0$] at different depths evaluated in a IPM experiment on a clayey Ferralsol in the central Amazon.

6.3.2.2 Tension infiltrometer (TI)

Table 6.16 shows the scope of infiltration measurements carried out with TI. The complete data set is shown in Appendix 6-A. Figure 6.9 (a) shows that K (h) values vary by three to four orders of magnitude between 0-70 mm of water pressure head (h). Figure 6.9 (b) shows that calculating logarithmic values of the relative hydraulic conductivity Kr [Kr = K (h)/Ks] results in reducing of the variability of the data. The calculation of Kr alleviates any gravity dominated macropore flow near saturation, which has little or no influence on water flow under unsaturated conditions (Shouse and Mohanty, 1998; Mohanty, 1999). Figure 6.9 (c) shows that assuming geometric similarity among the locations, h could be successfully scaled. The reference function fitted to the data is also shown. In an overall analysis of the K data, a breakpoint that operationally divides the flux is located near 20 mm of h. Wilson and Luxmoore (1988) found also a division ≈ 20 mm of h to separate macropore from micropore flow, while Luxmoore and Wilson (1989) found a division about ≈ 30 mm, and Jarvis and Messing (1985) around ≈ 40 mm.

Table 6.16 Scope of inflitration measurements conducted with the tension infiltrometer

Number	Land use system	common name	Replicate infiltration sequence	Tension steps	Total data Q (h) for K analysis
1	Agroforestry	Cupuaçu	3	4-7	17
2	Agroforestry	Annatto	3	4-7	17
3	Agroforestry	Brazil nut	2	6	12
4	Agroforestry	Peach palm – F	2	7	14
5	Agroforestry	Peach palm – P	3	6-7	20
6	Agroforestry	Pueraria	3	6-8	21
7	Monoculture	Cupuaçu	3	6-7	20
8	Monoculture	Grasses and pueraria	3	4-7	17
9	Monoculture	Peach palm – F(m)	3	6-7	20
10	Monoculture	Peach palm – F(mb)	3	6-7	19
11	Monoculture	Peach palm – P(m)	3	5-7	18
12	Monoculture	Peach palm –P(mb)	3	6-7	20
13	Secondary forest	Vismia	3	7	21
		TOTAL	37	-	237

m = monoculture; b = between the palms; F = Peach palm for fruits production; P = Peach palm – for palm heart production

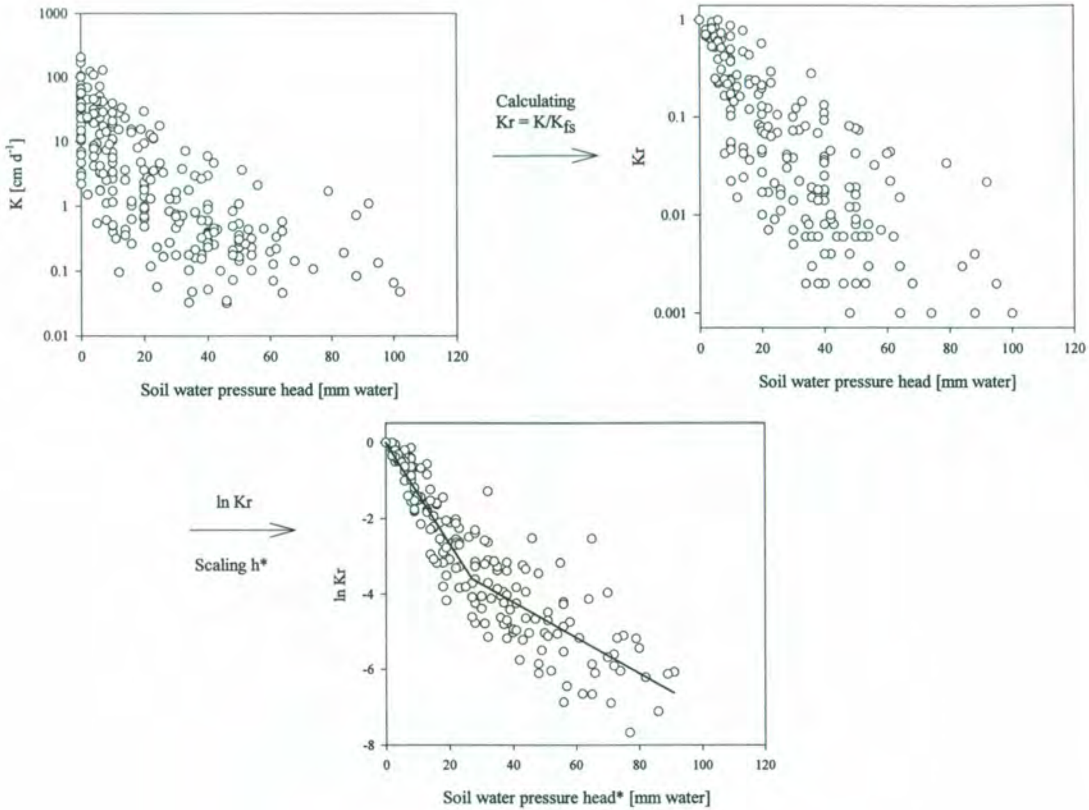

Figure 6.9 Scatter of unsaturated hydraulic conductivity evaluated in different land use system on a clayey Ferralsol in the central Amazon. Effects of using relative hydraulic conductivity and scaling theory in the reduction of variability.

Table 6.17 shows the CV of the scale factors for the different land use systems and positions evaluated. These CV values, which ranged from 10 to 51 %, are much smaller than those previously reported by Warrick et al. (1997) but are in the same range as those found by Hopmans (1987) and Messing and Jarvis (1995). The rather small to moderate degree of spatial variability in the scale factors probably reflects the fact that a representative measurement volume was encompassed by the relative large disc radius, as well as a reduced disturbance of the soil during preparation of the site where the disc was installed.

Table 6.17 Coefficient of variation of the scale factors.

Localization	Mean	Coefficient of variation [%]
	Agroforestry	
Cupuaçu	1.348	29
Annato	1.316	39
Brazil nut	0.883	51
Peach palm F	1.037	35
Peach palm – PH	1.128	11
Pueraria	1.438	43
	Monocultures	
Cupuçu	1.592	10
Grasses	1.184	22
Peach palm – F	1.816	33
between Peach palm F	1.893	21
Peach palm – PH	1.391	24
between Peach palm - PH	1.148	14
Vismia	1.265	20

F = fruit; PH = palm heart

A comparison between the results from the monoculture of peach palm for fruits and palm heart did not show relevant differences in the form of the curve. Therefore, the data are pooled and analysed together. Figure 6.10 illustrates the similarity of the relationships between K and h for those positions. Table 6.18 shows the piecewise equations fitted for each monoculture, and the equation fitted with all data pooled.

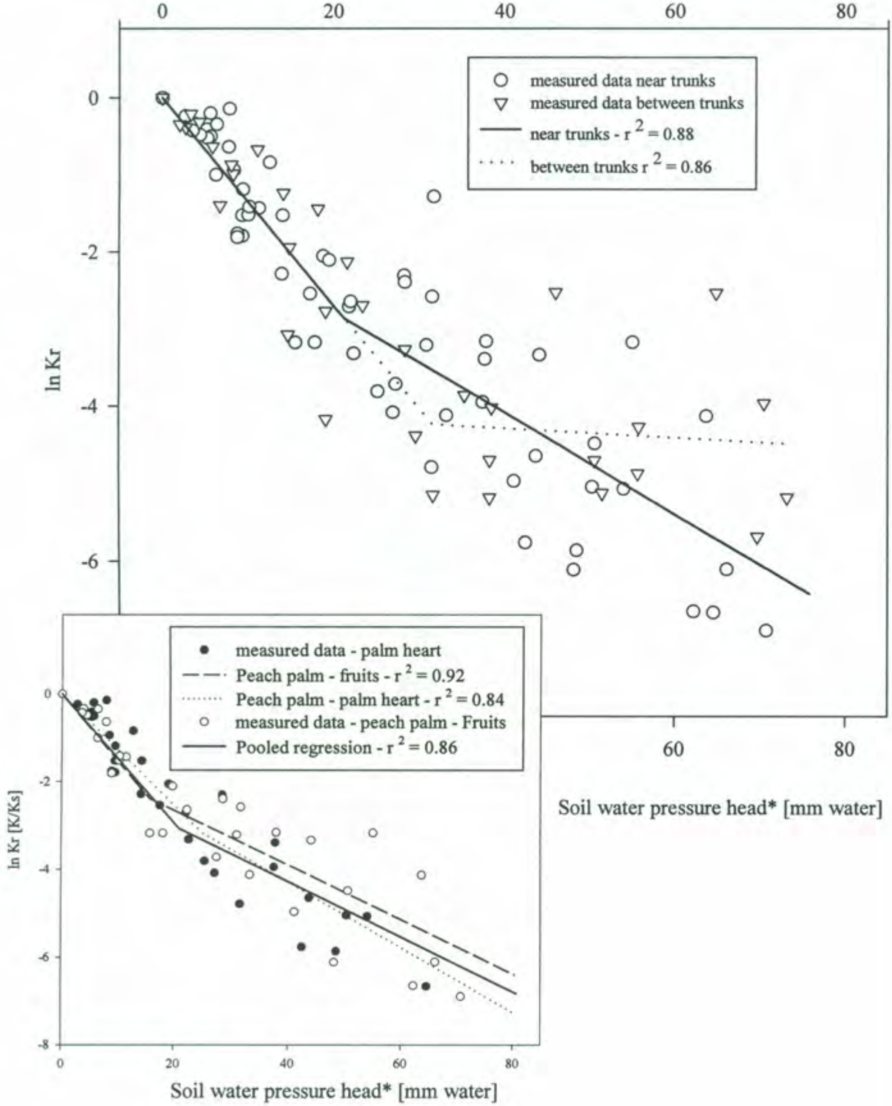

Figure 6.10 Unsaturated hydraulic conductivity of the soil surface evaluate at 0.40 and 1.20 m from the trunks of peach palms growing in monoculture for fruit production and palm heart production. The small figure shows the similarity of the hydraulical functions measured at 1.20 m from the trunks of peach palm for fruits and peach palm for palm heart production.

Table 6.18 Coefficients and statistical parameters of the piecewise regression for the position among the peach palms in monoculture.

Treatment	n	α_1	α_2	β_2	bp	s	r^2
Peach palm - Fruits	19	-0.1672	-0.0084	-4.3036	27	0.6220	0.92
Peach palm – Palm heart	20	-0.1182	-0.0001	-3.7913	32	0.6925	0.84
Pooled regression	39	-0.1345	-0.0060	-4.0514	31	0.7412	0.86

Further, Figure 6.10 shows that in the monoculture of peach palm, the functions near the trunks and far away from the trunks show a similar behaviour. But this changes for h greater than ≈ 20 mm with the position near the trunk showing a more significant reduction of K. This partly agrees with the finding in Chapter 4, where a greater concentration of micropores near these palms was found. The compaction of the soil between the peach palms, while reducing total porosity (see, Figure 4.1 in the Chapter 4) and specifically reducing macroporosity (Table 5.4 in Chapter 5) actually increased the number of small pores. Therefore, positions under the influence of the peach palm roots show a reduced K in the capillary range. Moreover, the lower inclination of the K function for h in the range of 30 – 70 mm in the position between the plants probably indicated that pores with radii in the range of 0.5 to 0.21 mm practically did not exist (i.e. estimated with Eq. 4.18 – Chapter 4).

A high infiltration rate near the peach palm was expected because of the large amount of water that arrives from stemflow (e.g., 100 l of stemflow in a 24 mm rainfall – Schroth et al., 1999), which does not remain on soil surface, quickly infiltrated, probably, along both dead root channels and fauna tunnels. These macropores, although occupying a small percentual of the pore volume, are very effective in conducting water at high potentials. Some intermittent ponding conditions were observed between the palms in monoculture after strong rainfall events. Peach palm appears to be sensitive to aeration conditions (see, Chapter 4). Therefore, the monitoring of the K functions in this land use system can be an important factor for management decisions.

Table 6.19 shows the coefficients and statististical parameters of the piecewise functions K (h) for different land use systems and positions. Although, measurements of the function of K (h) with TI have shown great spatial (Logsdon and Jaynes, 1993; Mohanty et al., 1994) and temporal (Messing and Jarvis, 1993; Angulo-Jamarillo et al., 1997; Logsdon, 1997) variability, trends can be observed in the present study.

Preliminary analyses showed that the measurements near the trunks of cupuaçu growing in agroforestry or monoculture show similar results. Therefore the data were pooled and analysed together. Similar results were found for the evaluation of K near the trunks of peach palms growing in monoculture and agroforestry; these were pooled in a unique function. The K values between the peach palms in the monocultures for fruits and palm hearts were also pooled. Table 6.19 shows that h values ranged from 15 – 45 mm with a mean around 20 mm. Some of these functions were chosen to be plotted and discussed in more details.

Table 6.19 Coefficients and statistical parameters of the functional relationship between K(h) piecewise continuous regression

Specie	n	α_1	α_2	β_2	bp	s	r^2
Cupaçu †	39	-0.1361	-0.0319	-3.4488	33	0.5459	0.93
Brazil nut	12	-0.1522	-0.0016	-3.0120	20	0.4851	0.89
Annatto	17	-0.1481	-0.0531	-1.6150	17	0.4754	0.96
Pueraria	21	-0.1567	-0.0440	-2.0416	18	0.4744	0.94
Grasses	17	-0.1342	-0.0803	-1.1662	22	0.5144	0.96
Peach palm – Fruit†	34	-0.1539	-0.0618	-1.4312	15	0.7477	0.88
Peach palm - Palm heart†	38	-0.1282	-0.0740	-1.3417	25	0.6854	0.90
Peach palm among trunks †	39	-0.1345	-0.0060	-4.0514	31	0.7412	0.86
Vismia	21	-0.1250	-0.0039	-5.4034	45	0.4871	0.96

† pooled data

Figure 6.11 shows that within the monoculture of cupuaçu, the positions between the plants (incompletely covered by grasses) have a lower unsaturated K compared to the values found near the trunks of cupuaçu for h > 50 mm. Although both values assumed greater magnitude. Cupuaçu appears to create a higher near saturated hydraulic conductivity near the trunks, probably due to a large concentration of fine roots near the soil surface (Haag, 1997). Figure 6.11 also shows the K (h) function for pueraria (evaluated in the agroforestry system). Pueraria is normally recommended as cover crop for monocultures in the central Amazon, and its effect on the maintenance and enlargement of the mesoporosity (Chapter 4) is probably an explanation for its higher hydraulic conductivity in those ranges of h.

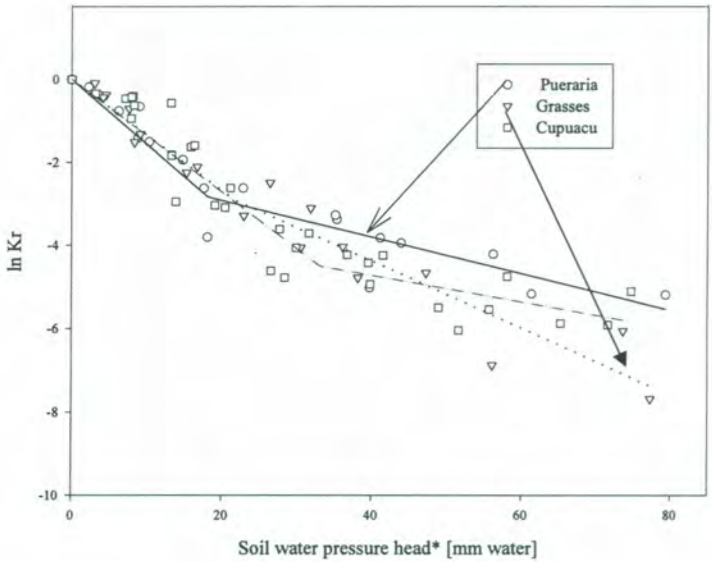

Figure 6.11 Unsaturated hydraulic function near different species of plants growing in a clayey Ferralsol in the central Amazon. Doted line represent the function for soil covered by grasses, solid line by pueraria and dash line by cupuaçu

Figure 6.12 shows the scatter plot of all K data measured within the agroforestry system at different positions. In spite of the spatial variability of the surface hydraulic properties, the influence of intrinsic factors (e.g. soil porosity, pore continuity) and deterministic factors (e.g., plant species, pattern in throughfall and stemflow, specific fertilisers and different rate for each species) differences could be tentatively identified.

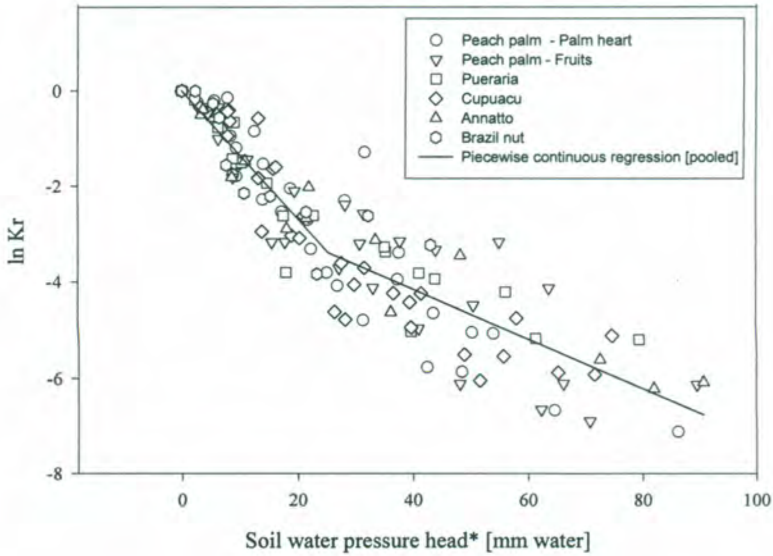

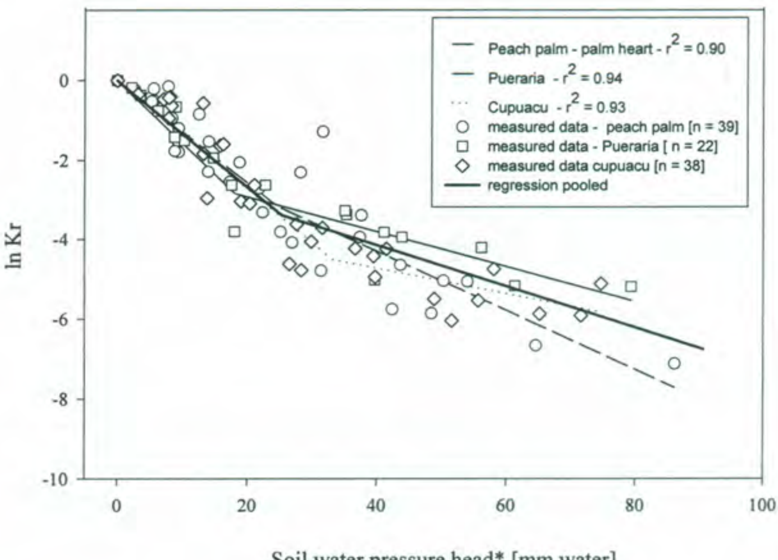

Figure 6.12 Unsaturated hydraulic conductivity evaluated near different species of plant growing in an agroforestry system on a clayey Ferralsol in the central Amazon.

The source of variability in the soil properties was partially discussed in the results of saturated hydraulic conductivity in this chapter and in Chapter 4. Figure 6.12 shows that using a pooled function with all K values in agroforestry it will subestimate the water fluxes in some positions and overestimate them in other. Because of some function are below and some functions are above the pooled function. For instance, for h ≈ 60 mm K is about two orders of magnitude greater in the soil under the cover crop pueraria than in the soil near the trunks of peach palms. Mallants et al. (1996) demonstrated that the use of nonoptimal K functions underpredicted the cumulative drainage by more than 30 % for a macropore soil.

The measurements with TI were carried out using very small increments (i.e., mm) in h near saturation. Therefore, the K values below 10 mm of h should be interpreted in a qualitative manner, because of possible inaccuracies in the applied h. Also, a very intense bubbling (due to high infiltration rates) in the chamber reservoir made it very difficulty to read accurately the water level. Moreover, in this soil variations of millimetres near saturation change the infiltration substantially. Measurements with values of h around 70 mm or higher are very difficult to obtain in the clayey Ferralsols by TI measurements, because they are very time-consuming. Consequently, the likelihood of precipitation events, and changes in soil structure above the disc (probably because of macrofauna movements) make these measurements not feasible. The measurement of unsaturated hydraulic functions are also very helpful in terms of supplying a matching factor (Luckner et al., 1989; van Genuchten and Leij, 1999), rather than the use of saturated K to transform relative values of K into absolute ones when using indirect methods of estimation of hydraulic properties (see discussion in the Inverse method section). This is because saturated K of macroporous soils may be unrelated to the unsaturated K in the region near saturation (Clothier and Smetten, 1990)

The accuracy of field determinations with TI is affected primarily by soil heterogeneity, soil collapse under the infiltrometer during the measurement, inadequate hydraulic contact material (Reynolds and Zebchuk, 1996) or by the solar heating of the head space in the mariotte reservoirs (Elrick and Reynolds, 1992; White et al., 1992). In the materials and methods section, all precautions to avoid or alleviate these sources of inaccuracies are detailed. It should be noticed that when the measurements were carried out under the central Amazonian conditions, the protection of the marriotte reservoirs from the direct sun was a fundamental factor for reliable measurements. Moreover, a good preparation of the soil surface which allows using only a fine layer of the contact material. Further, the installation of the disc levelled is fundamental for the measurements with at small h. Roots should be carefully scissored, otherwise the membrane is easily damaged and the soil is disturbed.

Comparisons between the TI results and the results from the IPM method are only possible in a qualitative way. The ranges of h evaluated by both methods do not overlap. Moreover, the TI measurements were carried out in ascending change of h (from negative to saturation), whereas the IPM method is a measurement of a draining process. The infiltration process is somewhat more complicated than drainage since wetting and draining are occurring simultaneously (Logsdon, 1999).

Laboratory and field evaluation of soil water retentivity [θ(h)]

A discussion about the evaluation of the soil water retentivity function [θ(h)] using field and laboratory data is presented here.

Figure 6.13 shows the results of θ vs. h determined with soil samples in the laboratory and field data at four depths. The laboratory procedures are described in Chapter 4 and the field data are from the IPM experiment, previously discussed in this chapter. The results show good agreement between field and laboratory data only for the depth of 10 cm. A tendency of the laboratory data to overestimate the field values can be seen for the depths of 20 and 60 cm (deeper layers not illustrated in Figure 6.13 also show this tendency). Compaction caused by sampling procedures may explain the higher values of θ (at the same h) for the laboratory data, owing to the reduction of pore radii that can hold more water at those potentials. Similar results were found by Dane(1980) and Luxmoore et al. (1981).

Figure 6.13 shows that, for the depth of 60 cm, a variation of about 100 cm in h (between 100 to 200 cm), corresponded only to a variation in θ of 0.03 $m^3\ m^{-3}$ (see details in Figure 6.13). This fact is also observed for deeper layers (data in Table 6.6) and reflects a lack of pores with radii between 15 and 7 μm.

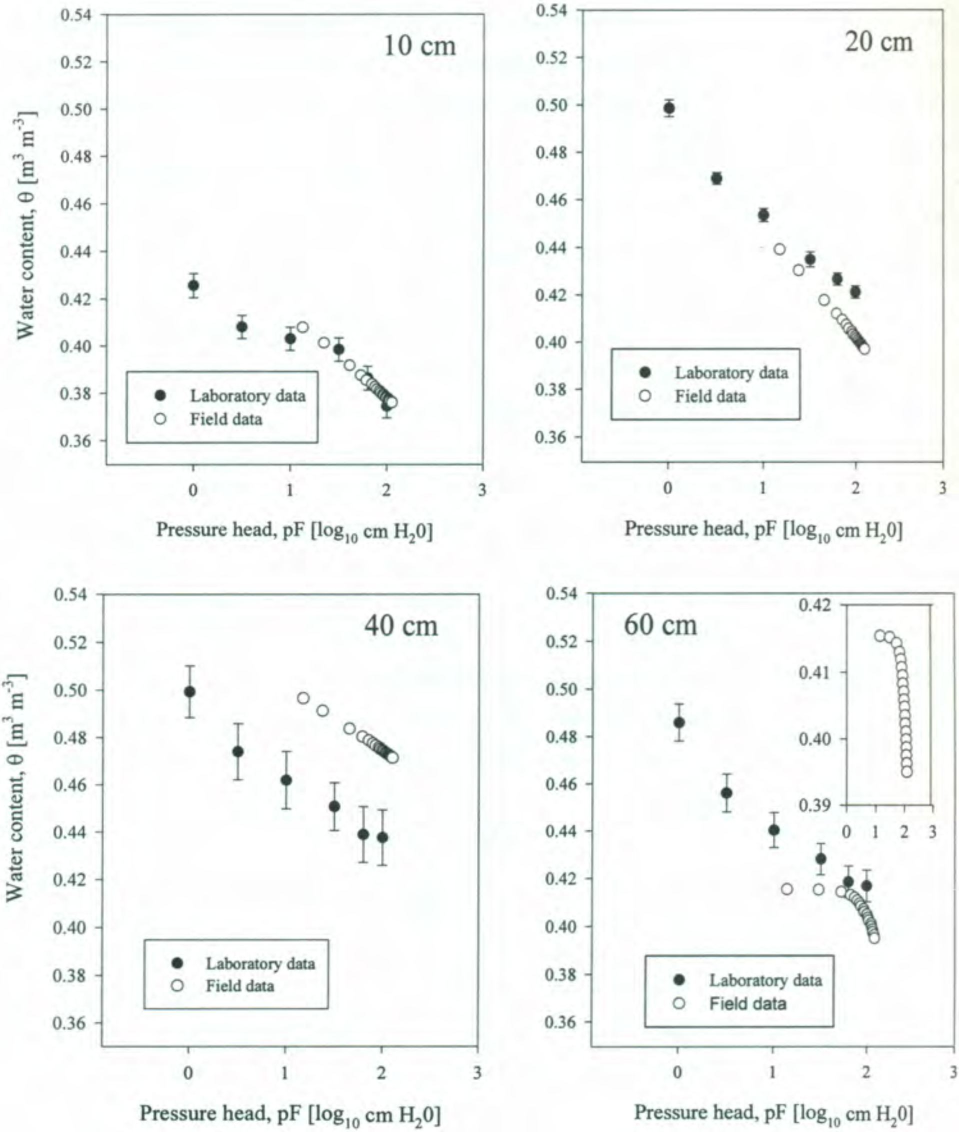

Figure 6.13 Laboratory and field data relating volumetric water content and matric pressure head for a clayey Ferralsol in the central Amazon. Errors bars represent standard error of mean.

The reasons for underestimation of the laboratory θ values compared to the field data for the depth of 40 cm is not very clear. It could simply be due to soil variability. The profile to collect the samples was dug about 3 m apart from the place where the TDRs and tensiometers were installed. The soil variability and the representativeness of the soil cores were discussed in the section of saturated hydraulic properties in this chapter.

Many factors (underlined words) may explain the differences between field and laboratory results. They are discussed focussing on the specific problems of this data set and some generalisation is made for the general problem for the clayey Ferralsol.

The volumes sampled in the measurement of θ and h in the field were not coincident. In addition, the instruments were separated to avoid measurement interference. Determining the REV for each specific soil can help to decide about the minimal soil volume to be measured. Then, if a sensor assesses this minimal REV, it should be not a serious problem to work with different sampled volumes.

Calibration of the instruments is often an essential factor for accurate data. In this project, a specific calibration for the TDR readings was developed and all tensiometers were checked before they were installed in the field. The specific accuracy of the TDR measurements for field evaluation in the clayey Ferralsols is discussed in detail in Chapter 5. The accuracy of tensiometers used was about 2 hPa (working with water-mercury manometers). The ceramic cups had a conductance in the order of 3 X 10^{-5} cm^2 s^{-1}. A tensiometer constructed with such a cup and a mercury water manometer will have a response time of 40 to 60 seconds. Factors for correction should be used in some specific situations when the changes in the pressure head are very fast. In a typical IPM experiment, or at least for the clayey Ferralsols, changes in the pressure head are very slow, after a few hours the response time effects assume lower importance.

Tensiometers often misbehave in the field due to temperature fluctuations (especially day/night variations), because water and air in the tensiometer expand and contract. This was controlled by insulating the tensiometers and doing the evaluation under standard conditions (e.g., early morning). The possible effects of variation of temperature in SWRC as determined in the laboratory were discussed in Chapter 4. A further factor influencing the θ vs. h results is its wetting and drying history through the phenomenon of hysteresis, which implies that soil that reached a certain h by wetting will have a lower θ than soil that reached the same h by drying. Iwata et al. (1995) and Hillel (1998) give a detailed discussion of this phenomenon. However, the hysteresis effect is presumed to be not significant in the results, because the drainage, which is essentially a drying process, was applied in both experiments in the field and in the laboratory. Moreover, the difference between field data and laboratory data may be due to the incomplete wetting of field soil volumes because of air-entrapment. The errors arriving from the laboratory method itself are discussed in Chapter 4. On the dry range, the water retention phenomena are controlled basically by absorption phenomena (Corey, 1992), probably invalidating the use of the capillary laws for the dry range. Most of the phenomena cited above are expected to be important in soil with macropores and soils with high amounts of clay, which are exactly the characteristics of the clayey Ferralsols in the central Amazon. Therefore, field data may be more representative for the real characteristics of the soil retentivity. Unfortunately, many factors difficult the measurement of field data, such as methods to make measurements at higher potentials.

6.3.3. Inverse simulation

Table 6.20 shows the final parameters of the VGME for five layers into which the soil profile was divided to perform the inverse method (Figure 6.14). The initial parameters were estimated using the RETC code for the unimodal VGME (Eq. 6.23 to 6.25).

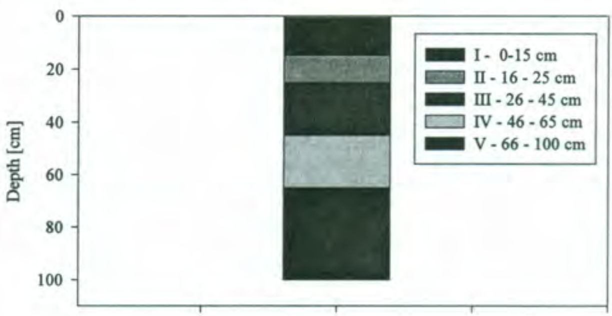

Figure 6.14 Profile specification and distribution of soil layers to perform the inverse solution of Richard's equation for a IPM experiment by the Hydrus-1D code.

Table 6.20 Estimated hydraulic parameters for soil water retention curves for different depths in clayey Ferralsols in the central Amazon.

Parameters	Depth [cm]				
	0-15	16-25	26-45	46-65	66-100
θ_s (m^3 m^{-3})	0.29	0.29	0.30	0.29	0.30
θr (m^3 m^{-3})	0.42	0.45	0.54	0.44	0.50
α (cm-1)	0.09	0.09	0.08	0.09	0.09
n	1.14	1.14	1.14	1.14	1.14
K(cm h^{-1})	15	20	40	40	35
τ	-0.580	-0.125	-0.125	-0.125	-0.300

The unimodal VGME had enough flexibility to fit reasonably well the field data. A better fit could be succeeded optimising the VG equation without constraining the m parameter or employing the bimodal approach (see, Chapter 4). However, it was preferred to perform the inverse simulation with the unimodal approach, because the increase of the number of parameters is directly related to considerable numerical problems in the inverse solution (Russo et al., 1991; Santini et al. 1995; Zurmühl and Durner, 1998). The parameters shown in Table 6.20 differ from the parameters presented for the laboratory data in Chapter 4 (Table 4.6). The probable reasons of this discrepancy between field and laboratory data, besides those previously discussed, refer to the fact that the range of values measured under field conditions is small compared with the laboratory range. Although, laboratory experiments have the advantage of being precise and comprise a large range of values, their use instead field data often leads to soil hydraulic properties that are not representative for the field. For this reason, only the field data were used in the inverse simulation.

The primary objective of the inverse simulation was to assure a good agreement between measured and predicted θ profiles [θ (t, z)]. Therefore, in order to obtain a better fit, the hydraulic parameters for each layer were then sequentially optimised in a Bayesian approach (i.e., which constrained the range for each parameter with a maximum and a minimum value). Some alterations in the optimised results were done arbitrarily to the optimisation results (i.e., calibration procedures) to assure accurate θ profiles. The comparisons between estimated and measured profiles are shown in Figure 6.15 and 6.16. When comparing the profiles until the depth of 60 cm, with exception of the first two times [t = 0 and 3.5 hours], the results are surprisingly good. The inverse simulation and VGME were able to fit and describe the drainage processes of the clayey Ferralsol. Simulations showed that starting with hydraulic parameters (θs, θr, α, n, K and τ), that differed too much from the final value, probably moved the optimisation processes into the wrong direction for a long time and many times caused overflow and division by zero error. Therefore, is advantageous to have a reliable range of the parameters that encompasses the possible values. This empirical adjustment of the hydraulic parameters was tedious, and the Hydrus 1-D code was not able to optimise all of them simultaneously (perhaps by an ill-posed problem or the excessive number of parameters). A high sensitivity was observed for the K values, and it was considered a fit parameters without physical meaning. The high sensitivity of the VG-Mualem to the parameter K was shown previously by van Genuchten and Nielsen (1985) and Luckner et al. (1989). If K would be taken at a conductivity value somewhat less than saturation as recommended by Luckner et al. (1989) this sensitivity would probably be reduced. Many of the hydraulical parameters were strongly correlated, and it appears that arbitrary changes in one parameter can only be successfully done if the other parameters are changed simultaneously, otherwise the model becomes very unstable.

Comparison between measured and simulated K vs. θ relations

Figure 6.16 shows the relationship between the inversely estimated hydraulic conductivity K vs. θ. The agreement with the results calculated directly in the IPM method (see, Table 6.10 and Figure 6.10) is good.. Romano and Santini et al. (1992) also reported successful inverse modelling of results from an IPM experiment using the simpler Davidson Equation [Eq. 6.21.]

Although the hydraulic conductivity (Figure 6.10 and 6.16) and the soil profiles (Figure 6.15 and 6.17) show good agreement between measured and estimated data, the soil water retention curve is not so accurate, because the optimal initial fitted values were changed in optimisation approaches. This is probably related to the fact that, although VGME gives an excellent fit for experimental water retention data in most unimodal soils. However, for aggregated soils having bi- modal pore-size distributions it does not work very well (Othmer et al., 1991, Durner et al., 1994; Tomasella and Hoodnet, 1996; Mallants et al., 1997). Therefore, if the models are not accurate to describe the SWRC, the resulting fitting parameters may compromise the accuracy of one or both hydraulic functions. It may be advantageous to use parametric models for K (θ) or K (h) that are not coupled with θ (h) function, otherwise to fit them separately. Although in the Hydrus-1D code the hydraulic functions are coupled, the general inverse modelling approach does not require the coupling of the soil hydraulic functions, and some studies suggest that improved parameter optimisation results are obtained by fitting the hydraulic functions separately (Durner et al., 1999).

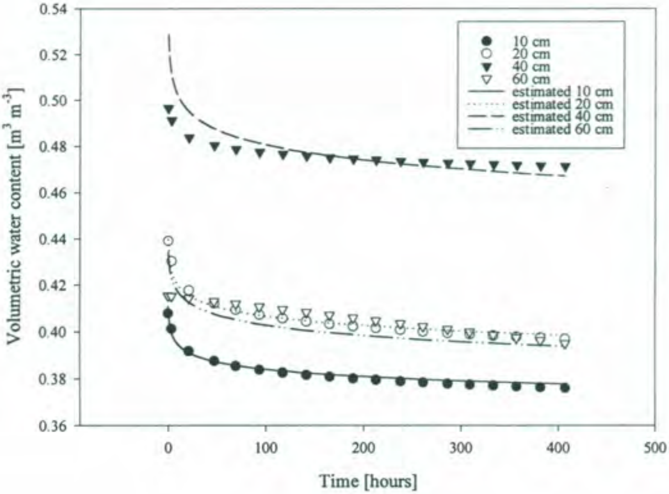

Figure 6.15 Experimental and inversely estimated values of volumetric water content for different depths in function of time of a IPM experiment conducted on a clayey Ferralsol in the central Amazon.

It should be stressed that uniqueness of the resolution is not assured. Many parameters were correlated and the estimated confidence intervals were excessively large for some parameters. It was not feasible to test the non-uniqueness by solving repeatedly the problem using different initial parameter estimates as suggested by Hoppmans et al., (2001), because the description of the profile involved many parameters. The hydraulic parameters shown in Table 6.20 also differed from the values determined for a very similar profile in a clayey Ferralsol in the central Amazon by Tomassela and Hoodnet (1996); in contrast the hydraulic function are quite similar for some comparable depths. A simplification of the description of the soil profile (e.g. reducing the number of layers) could have permitted more detailed statistical analysis. However, reducing parameters would have the cost of a reduced accuracy of the estimated profiles [θ (z, t)]. Russo et al. (1991) pointed out that the larger number of parameters in the van Genuchten model might increase the likelihood of non-uniqueness and instability of the inverse solution. Nevertheless, the results show the feasibility of the inverse method, together with its flexibility and advantages. It requires a complex computational effort for the solution and may show inherent sources of uncertainty. However, the success of the inverse modelling in the clayey Ferralsol should be cautiously interpreted and it is probably related to the fact that the data used are from an IPM experiment, where the predominant flow was through micropores. Therefore the results are valid only for the range studied and extrapolation of the results should not be attempted, especially near saturation. The Hydrus 1-D code allows to include independently measured information about hydraulic parameters in the objective function (i.e., the K(h) evaluated with tension infiltrometer). Therefore, the range where the hydraulic functions apply could be extended, some preliminary analyses were performed and the results are promising. However, a lack of information about the hydraulical properties of the subsoil of the clayey Ferralsols in the central Amazon limited further investigations.

Hydraulic conductivity and water movement in the unsaturated zone in the clayey Ferralsol is about five orders of magnitude higher near saturation than at 200 cm of h (see, Figure 6.7 and 6.16).

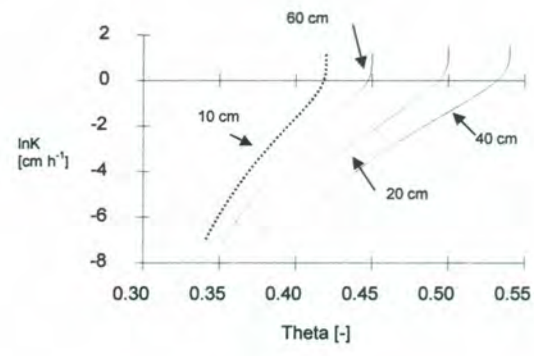

Figure 6.16 Unsaturated hydraulic conductivity estimated with inverse modelling.

The VGME that depends of many parameters in a strongly non-linear manner would make it difficult to obtain accurate estimates of hydraulic conductivity throughout the entire water content range. Probably the use of simpler relationships, for specific ranges, could fit the variable field data with equal reliability and might provide simple analytical solutions and statistical analysis. Recently, Poulsen et al. (1998) proposed a one parameter equation for the range comprised only between 0 and 350 kPa. The use of many parameters makes the modelling and the statistical analysis too involved.

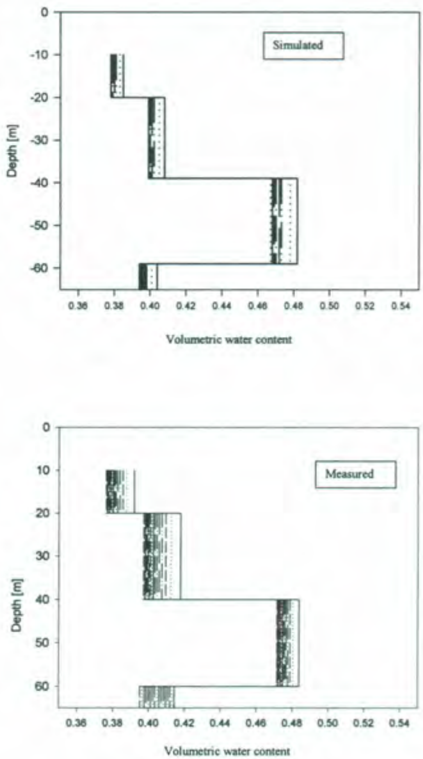

Figure 6.17 Profiles of volumetric water content measured and inversely estimated for an IPM experiment conducted on a clayey Ferralsol in the central Amazon. The lines represent selected times of evaluation or simulation.

6.4 CONCLUSIONS

Evaluation of saturated hydraulic conductivity

Soil core method (K_s)

The use of the soil core method for evaluating saturated hydraulic conductivity is limited because of the smaller sample size, the presence or absence of open-ended macropores, and variable soil compaction during core extraction. Although, some trends may be identified, the reduced reliability of the results for structured soil lead to this method to be inappropriate for determination of saturated hydraulic conductivity for the clayey Ferralsol.

Field evaluation of saturated hydraulic conductivity with disc infiltrometer (K_{fs})

The results of K_{fs} are much less variable than the results from the soil core method. This is, probably, related to less disturbance on the original structure, and that the sample volume assessed by the disc probably approximate of minimum REV for K evaluation in the clayey Ferralsol.

The values obtained for K_{fs} were considerably lower than previously reported values for the clayey Ferralsols in the central Amazon.

In the agroforestry system the K_{fs}, in the soil under the cover crop (pueraria) shows the highest value of K_{fs} followed by the values of K_{fs} evaluated near the trunks of cupuaçus. K_{fs} near the peach palms tends to show reduced values. Conversely, these reduced values contrast with the reduced values of bulk density found near these palms. These results indicated that bulk density is for many land use systems a misleading parameter to infer about hydraulic conductivity.

An expected reduction of the K_{fs} between cupuaçus (as a consequence of higher soil dispersion, and a reduced porosity) was not identified.

The presence of large macropores in the clayey Ferralsol, leads to dramatically changes of "saturated hydraulic conductivity" near saturation. The values of K continue increasing markedly with increasing matric pressure head for small positive values. This phenomenon which is not well described by the common hydraulic models, and if not taken into account could lead to serious overestimation when modelling soil water fluxes, especially in situation of occurrence of ponding conditions.

The K_{fs} values measured with the disc infiltrometer at approximately zero matric pressure ($h \approx 0$) does not represent the maximum infiltration rate on the clayey Ferralsols.

More reliable methods for field measurements and a mathematical theory to describe saturated hydraulic conductivity in soil with macropores is subject for further investigations.

Evaluation of unsaturated hydraulic conductivity (K)

<u>Tension infiltrometer (TI)</u>

Tension infiltrometers are relatively cheap, robust and a simpler field method to evaluate unsaturated hydraulic conductivity in clayey Ferralsols. Since K near saturation is highly variable, the data were better analysed using the relative hydraulic conductivity and the scaling theory.

The use of piecewise continuous regression analysis allowed the estimation of a changeover point, located between 15 ~ 40 mm of h, which operationally separate two domains that govern the hydraulic conductivity of the clayey Ferralsol.

K changes by three to four orders of magnitude between 0 - 70 mm of water pressure head. Effect of land use systems and different species of plants on unsaturated hydraulic functions were identified, these differences if not taken into account could be a source of error in water and solute transport studies.

The soil near the trunks of cupuaçu shows higher values of hydraulic conductivity near saturation. This fact is probably related to a developed fine roots system near the surface. Conversely, near trunks of peach palms were found reduced values of unsaturated hydraulic conductivity.

A limitation of the TI method is the small range, in which they operate. However, data from TI can be combined with data derived from other methods to obtain an overview of a large unsaturated range.

Instantaneous profile method (IPM)

The functions between K and θ estimated by using the linear form of the exponential model of Davidson et al. (1969) show a very good fit with the measured data for the depths of 10, 20 and 40 cm, but significative deviations for the depths of 60, 80 and 90 cm.

Similarities of the equations K(θ) or K(h) were tested in relation to parallelism and concordance in order to reduce the number of equation needed to describe the water fluxes in a soil profile.

The parallelism between some K (h) equations shows that the clayey Ferralsols have a similar hydraulic behaviour.

Evidence of the existence of a fluffy horizon located between two more compacted showed in the pore size distribution analyses were reconfirmed here.

Laboratory and field evaluation of soil water retentivity [θ(h)]

The results for the paired data θ vs. h show good agreement between field and laboratory data only for the depth of 10 cm. A tendency of the laboratory to overestimate the field values is observed for most depths. Compaction caused by sampling procedures may explain the higher values of θ (at the same h) for the laboratory data. A discussion of the many factors (soil variability, the volumes sampled, calibration of the instruments, accuracy of tensiometer and its response time, temperature fluctuation, hysteresis and air-entrapment) that biased the accuracy of the determination of soil retentivity was shown for this specific study.

Inverse simulation

The inverse simulation using the unimodal van Genuchten –Mualem Equation were able to fit and describe accurately the drainage processes [i.e., the evolution of θ in profiles [θ (t, z)]] until the depth of 60 cm. However, to obtain this accurate description of the water dynamic a detailed discretization of the soil profile was needed.

The agreement between the hydraulic conductivity estimated with the inverse method and the results calculated in the IPM method are also good. Although, the soil water retention curve is not so accurate, because the optimal values were changed in the optimisation and calibration procedures. Therefore, it may be advantageous to use parametric models for K (θ) or K (h) that is not coupled with the θ (h) function, otherwise to fit them separately.

The results show the feasibility of the inverse method, together with its flexibility and advantages. However, the success of the inverse modelling in the clayey Ferralsol should be cautiously interpreted, and it is probably related to the range of the data used. Where the predominant flow was probably only through the domain of micropores.

The K functions estimated by inverse methods are valid only for θ range studied, and extrapolation should not be attempted, especially near saturation and for deeper layers. The ability of the inverse method to estimate the hydraulic functions within a wide range embracing also fluxes near saturation is subject for further investigations. Preliminary results involving results from different experiments using the inverse method are promising.

General conclusions about hydraulic properties

The uncertainties of determination of water fluxes near saturation by use of K (θ) or K (h) functions arise because its exponential behaviour (i.e., in the linear models, slopes with very higher values) near saturation. This problem is extreme in highly structured soils, like the clayey Ferralsols in the central Amazon. It has a consequence that a small change in θ or h can change K dramatically. Regardless of the equation used, it is an intrinsic characteristic of the clayey Ferralsol (and other well structured soils). Therefore, in the estimation of water fluxes near saturation this phenomenon is extremely expressive and may lead to higher uncertainties in the estimated values.

Using hydraulic equation that depends on many parameters in strongly non-linear manner, make difficult to assess the uncertainties of the estimations and to use them in numerical simulation. The use of many parameters makes the modelling and the statistical analysis too involved. On the other hand, it is unrealistic to try to obtain accurate estimates of the hydraulic conductivity throughout the entire water content range using a single and simple equation for this soil. Probably, an option for modelling water fluxes in structured soils like the clayey Ferralsols in the central Amazon, is to develop linear piecewise models, with only one or two parameters for specific ranges with distinct hydraulic behaviour (e.g. the domain of macropore flux; capillary flux and adsorptive domain). The piecewise equation may fit the variable field data with equal reliability that then more elaborate smoothed functions, further they may provide simple analytical solutions and feasible statistical analysis.

6.5 REFERENCES

AHUJA L R.; GREEN R E.; CHONG S K. and NIELSEN D R. A simplified functions approach for determining soil hydraulic conductivities and water characteristics *in situ*. Water Resources Research. 16: 947-953, 1980.

AHUJA L R.; BARNES B B.; CASSEL D K.; BRUCE R R. and NOFZIGER D L. Effect of assumed unit gradient during drainage on the determination of unsaturated hydraulic conductivity and infiltration parameters. Soil Science. 145: 235-243, 1988.

AMOOZEGAR A. and WARRICK A W. Hydraulic conductivity of saturated soils: Field methods. In: KLUTE A., ed. Methods of soil analysis. Part 1. Physical and mineralogical methods. 2. Madison, American Society of Agronomy & Soil Science Society of America, 1986. p.735-735.

ANDERSON J L. and BOUMA J. Relationships between saturated hydraulic conductivity and morphometric data of an argilic horizon. Soil Science Society of America Journal. 37: 408-413, 1973.

ANGULO-JARAMILLO R.; MORENO F..; CLOTHIER B E.; THONY J L.; VACHAUD G.; FERNADEZ-BOY E. and CAYUELA J A. Seasonal Variation of hydraulic properties of soils measured using a tension disk infiltrometer. Soil Science Society of America Journal. 61: 27-32, 1997.

ANKENY M D.; AHMED M.; KASPAR T C. and HORTON R. Simple field method for determining unsaturated infiltration measurement. Soil Science Society of America Journal. 55: 467-470, 1991.

ANKENY M D. Methods and theory for unconfined infiltrometer measurements. In: TOPP G.C..; REYNOLDS W.D.. and GREEN R.E., eds. Advances in measurements of soil physical properties: bringing theory into practice. Madison, SSSA, 1992. p.123-141.

ARAGÃO JUNIOR T C.; MAGALHÃES C A. and CASTRO P T. Determinação da condutividade hidráulica em um solo podzólico-vermelho-amarelo em condições de campo. Pesquisa Agropecuária brasileira. 18: 805-810, 1983.

ARYA L M.; LEIJ F J.; VAN GENUCHTEN M TH. and SHOUSE P J. Scaling parameter to predict the soil water characteristic from particle-size distribution data. Soil Science Society of America Journal. 63: 510-519, 1999.

ASSELINE J. and VALENTIN C. Construction et mise au poin d'un infiltromètre à aspersion. Cah. ORSTON. 15: 321-348, 1978.

ASSOULINE S.; TAVARES FILHO J. and TESSIER D. Effect of compaction on soil physical and hydraulic properties: experimental results and modeling. Soil Science Society of America Journal. 61: 390-398, 1997.

BACCHI O O S. and REICHARDT K. Análise comparativa de dois métodos simplificados de determinação da condutividade hidraulica de solo. Revista Brasileira de Ciência do Solo. 15: 249-252, 1991.

BACCHI O O S. and REICHARDT K. On simple methods for unsaturated soil hydraulic conductivity determination. Scientia Agricola. 50: 326-328, 1993.

BEAR Y. Dynamics of fluids in porous media. New York. Dover Pulb.764. 1972

BEVEN K. and GERMANN P. Macropores and water flow in soils. Water Resources Research. 18: 1311-1325, 1982.

BOUMA J.; BELMANS C. and DEKKER L W. Water infiltration and redistribution in a silt loam subsoil with vertical worm channels. Soil Science Society of America Journal. 46: 917-921, 1982.

BOUMA J. Measuring the hidraulic conductivity of soil horizons with continuous macropores. Soil Science Society of America Journal. 46: 438-441, 1982.

BOUWER H. and ASCE M. Planning and interpreting soil permeability measurements. Journal of the irrigation and drainage division. IR3: 391-403, 1969.

BOUWER H. Intake rate: cylinder infiltrometer. In: KLUTE A., ed. Methods of soil analyis. Part 1- Physical and mineralogical methods. 2. Madison, American Society of Agronomy, Inc., 1986. p.825-844.

CAMPBELL G.S. A simple method for determining unsaturated conductivity from moisture retention data. Soil Science. 117: 311-314, 1974.

CHEN C. and WAGENET R J. Simulation of water and chemicals in macropore soils. Part I Representation of the equivalent macropore influence and its effects on soil water flow. Journal of Hydrology. 130: 105-126, 1992.

CHONG S K.; GREEN R E. and AHUJA L R. Simple in situ determination of hydraulic conductivity by power fucntion description of drainage. Water Resources Research. 17: 1109-1114, 1981.

CLOTHIER B E. and SMETTEM K R J. Combining laboratory and field measurements to define the hydraulic properties of soil. Soil Science Society of America Journal. 54: 299-304, 1990.

COLLIS-GEORGE N. Infiltration equations for simple soil systems. Water Resources Research. 13: 395-403, 1977.

COMEGNA V.; DAMIANI P.; D'ANNA F. and RUGGIERO C. Comparison of different field methods for determining the hydraulic conductivity curve of a volcanic Vesuvian soil. Georderma. 73: 231-244, 1996.

COREY A T. Pore-size distribution. In: VAN GENUCHTEN M TH.; LEIJ F J. and LUND L J (eds.). Workshop Indirect methods for estimating the hydraulic properties of unsaturated soils, 1., 1992. University of California, Riverside, 1992. p.37-44.

CORRÊA J C. Características físicas de um latossolo amarelo muito argiloso (typic Acrorthox) do Estado do Amazonas, sob diferentes sistemas de preparo do solo. Pesquisa Agropecuária brasileira. 20: 1381-1387, 1985.

DALLAND A.; VÅJE P I.; MATTHEWS R B. and SINGH B R. The potential of alley cropping in improvement of cultivation systems in the high rainfall areas of Zambia. III. Effects on soil chemical and physical properties. Agroforestry Systems. 21: 117-132, 1993.

DANE J.H. Comparison of field and laboratory determined hydraulic conductivity values. Soil Science Society of America Journal. 44: 228-231, 1980.

DANE J H. and HRUSKA S. In-situ determination of soil hydraulic properties during drainage. Soil Science Society of America Journal. 47: 619-624, 1983.

DAVIDSON J M.; STONE L R.; NIELSEN D R. and LARUE M E. Field measurement and use of soil properties. Water Resources Research. 5: 1312-1321, 1969.

DRAPER N R and SMITH H. Applied regression analysis. 3.ed. New York, Wiley, 1998. 820p.

DUNN G H. and PHILLIPS R E. Macroporosity of a well-drained soil under no-till and convetional tillage. Soil Science Society of America Journal. 55: 817-823, 1991.

DURNER W. Hydraulic conductivity estimation for soils with heterogeneous pore structure. Water Resources Research. 30: 211-223, 1994.

DURNER W.; PRIESACK E.; VOGEL H J. and ZURMÜHL T. Determination of parameters for flexible hydraulic functions by inverse modeling. In: VAN GENUCHTEN M TH and LEIJ F J (eds.). Workshop Characterization and Measurements of the Hydraulic Properties of Unsaturated Porous Media. 1997. University of California, Riverside, 1999. p.817-829.

EL-SWAIFY S A. Physical and mechanical properties of Oxisols. In: THENG B K G, ed. Soils with variable charge. Lower Hutt, New Zealand Society of Soil Science, 1980. p.303-324.

ELRICK D E. and REYNOLDS W D. Methods for analyzing constant head well permeameter data. Soil Science Society of America Journal. 56: 320-323, 1992.

FALLEIROS M C.; PORTEZAN O.; OLIVEIRA J C M.; BACCHI O O S. and REICHARDT K. Spatial and temporal variability of soil hydraulic conductivity in relation to soil water distribution, using an exponential model. Soil Technology. 45: 279-285, 1998.

FLÜHLER H.; ARDAKANY M S. and STOLZY L H. Error propagation in determining hydraulic conductivities from sucessive water content and pressure head profiles. Soil Science Society of America Journal. 40: 830-836, 1995.

GRAYBILL F A. Theory and application of the linear model. Belmont, Wadsworth Publishing Company, 1976. 704p.

GREEN R E.; AHUJA L R. and CHONG S K. Hydraulic conductivity, diffusivity, and sorptivity of unsaturated soils: field methods. In: KLUTE A., ed. Methods of soil analysis - Part 1 Physical and mineralogical methods. 2. Madison, American Society of Agronomy, 1986. p.771-798.

HAAG D. Root distribution patterns in a polycultural system with local tree crops on an acid upland soil in central Amazonia, University of Bayreuth, 1997. 86p. (Diplomarbeit)

HAYS W L. Statistics for the social sciences. 3.ed. New York, Holt, Rinehart and Wiston, 1981. 713p.

HILLEL D.; KRENTOS V D. and STYLIANOU Y. Procedure and tes of an internal drainage method for measuring soil hydraulic characteristics *in situ*. Soil Science. 114: 395-400, 1972.

HILLEL D. Environmental soil physics. San Diego, Academic press, 1998. 771p.

HOPMANS J W. A comparison of various methods to scale soil hydraulic properties. Journal of Hydrology. 93: 241-256, 1987.

HOPMANS J W.; SIMUNEK J.; ROMANO N. and DURNER D. Simultaneous determination of water transmission and retention properties - Inverse methods. In: DANE J.H. and TOPP G C, eds. Methods of soil analysis, Part 1: Physical Methods. 3. Madison, Soil Science Society of America, 2001. p.-np. (manuscript in preparation)

HULUGALLE N R. and KANG B T. Effect of hedgerow species in alley cropping systems on surface soil physical properties of an Oxic Paleustalf in south-western Nigeria. Journal of Agricultural Science. 114: 301-307, 1990.

HULUGALLE N R.. and NDI J N. Effects of no-tillage and alley cropping on soil properties and crop yieds in a typic Kandiudult of southern Cameroon. Agroforestry Systems. 22: 207-220, 1993.

IWATA S .; TABUCHI T. and WARKENTIN B P. Soil-water interactions. 2.ed. New York, Marcel Dekker, 1995. 440p.

JARVIS N J. and MESSING I. Near-saturated hydraulic conductivity in soils of contrasting texture measured by tension infiltrometers. Soil Science Society of America Journal. 59: 27-34, 1995.

JONES A J. and WAGENET R J. In situ estimation of hydraulic conductivity using simplified methods. Water Resources Research. 20: 1620-1626, 1984.

JONG VAN LIER Q. and LIBARDI P L. Variabilidade dos parâmetros da equação que relaciona a condutividade hidráulica com a umidade do solo no método do perfil instantâneo. Revista Brasileira de Ciência do Solo. 23: 1005-1014, 1999.

JURY W A.; RUSSO D. and SPOSITO G. The spatial variability of water and solute transport properties in unsaturated soil. II. Scaling models of water transport. Hilgardia. 55: 33-56, 1987.

JURY W A.; GARDNER W R. and GARDNER W H. Soil physics. 5.ed. New York, John Wiley & Sons, 1991. 328p.

KATUL G G.; WENDROTH O.; PARLANGE M B.; PUENTE C E.; FOLEGATTI M V. and NIELSEN D R. Estimation of in situ hydraulic conductivity function from nonlinear filtering theory. Water Resources Research. 29: 1063-1070, 1993.

KENG J C W. and LIN C S. A two-line approximation of hydraulic conductivity for structured soils. Canadian Agricultural Engineering. 24: 77-80, 1982.

KLUTE A. and DIRKSEN C. Hydraulic condictivity and diffusivity: Laboratory methods. In: KLUTE A., ed. Methods of soil analysis. Part 1. Physical and mineralogical methods. 2. Madison, American Society of Agronomy; Soil Science Society of America, 1986. p.687-734.

KUTÍLEK M. The influence of clay minerals and exchangeable cations on soil moisture potential. In: HADAS A.; SWARTZENDRUBER D.; RITJEMA P E.; FUCHS M. and YARON B., eds. Physical aspects of soil water and salts in ecosystems. Berlin, Springer, 1973. p.153-160.

KUTÍLEK M. and NIELSEN D R. Soil hydrology. Cremlingen-Destedt, Catena, 1994. 370p.

LAL R.; WILSON G F. and OKIGBO B N. Changes in properties of an alfisol produced by various cover crops. Soil Science. 127: 377-382, 1979.

LAL R. Agroforestry systems and soil surface management of a tropical alfisol: IV. Effects on soil physical and mechanical properties. Agroforestry Systems. 8: 197-215, 1989.

LAUREN J G.; WAGENET R J.; BOUMA J. and WOSTEN J HM. Variability of saturated hydraulic conductivity in a glossaquic hapludalf with macropores. Soil Science. 145: 20-28, 1988.

LIBARDI P L.; REICHARDT K.; NIELSEN D R. and BIGGAR J W. Simple field methods for estimating soil hydraulic conductivity. Soil Science Society of America Journal. 44: 3-7, 1980.

LIBARDI P L. Dinâmica da água no solo. Piracicaba, ESALQ, 1995. 497p.

LOGSDON S D.; M$_C$COY E L.; ALLMARAS RR. and LINDEN D R. Macropore characterisation by indirect methods. Soil Science. 155: 316-324, 1993.

LOGSDON S D. and JAYNES D B. Methodology for detemining hydraulic conductivity with tension infiltrometers. Soil Science Society of America Journal. 57: 1426-1431, 1993.

LOGSDON S D. Transient variation in the infiltration rate during measurement with tension infiltrometer. Soil Science. 162: 233-241, 1997.

LUCKNER L M T.; VAN DER PLOEG RR. and NIELSEN D R. A consistent set of parametric models for the two-phase flow of immiscible fluids in the subsurface. Water Resources Research. 25: 2187-2193, 1989.

LUXMOORE R J.; GRIZZARD T. and PATTERSON M R. Hydraulic properties of fullerton cherty silt loam. Soil Science Society of America Journal. 45: 692-698, 1981.

MAHERSHWARI B L. Development of an automated double ring infiltrometer. Australian Journal of Soil Research. 34: 709-14, 1996.

MALLANTS D.; TSENG P H.; TORIDE N.; TIMMERMAN A. and FEYEN J. Evaluation of multimodal hydraulic functions in characterizing a heterogeneous field soil. Journal of Hydrology. 195: 172-199, 1997.

MATHIEU C. and PIELTAIN F. Analyse physique des sols. Paris, Lavoisier, 1998. 275p.

MATULA S. and DIRKSEN C. Automated regulating and recording system for cylinder infiltrometer. Soil Science Society of America Journal. 53: 299-302, 1989.

MBAGWU J S C. Saturated hydraulic conductivity in relation to physical properties of soils in the Nsukka plains, southeastern Nigeria. Geoderma. 68: 51-66, 1995.

McCOY E L.; BOAST R C.; STEHOWER R C. and KLADIVKO E J. Macropore hydraulics. Taking a sledgehammer to classical theory. In: LAL R.. and STEWART B A, eds. Soil processes and water quality. BocaRaton, Lewis Publishers, 1994. p.303-348.

MESSING I. and JARVIS N J. Temporal variation in the hydraulic conductivity of a tilled clay soil as measured by tension infiltrometers. Journal of Soil Science. 44: 11-24, 1993.

MILLER E E. and MILLER R D. Physical theory for capillary flow phenomena. J. Appl. Phys. 27: 324-332, 1956.

MIYAZAKI T. Water flow in soils. New York, Marcel Dekker, 1993. 296p.

MOHANTY B P.; KANWAR R S. and EVERTS C J. Comparison of saturated hydraulic conductivity measurement methods for a Glacial-Till soil. Soil Science Society of America Journal. 58: 672-677, 1994.

MOHANTY B P. Scaling hydraulic properties of a macroporous soil. Water Resources Research. 35: 1927-1931, 1999.

MUALEN Y. Modelling the hydraulic conductivity on unsaturated porous media. In: VAN GENUCHTEN M TH.; LEIJ F J. and LUND L J (eds.). Workshop Indirect methods for estimating the hydraulic properties of unsaturated soils, 1997. University of California, Riverside, 1992. p.15-36.

MUALEN Y. Hydraulic conductivity of unsaturated soils: prediction and formulas. In: KLUTE A-, ed. Methods of soil analysis. Part 1 Physical and mineralogical methods. 2. Madison, ASA/ SSSA, 1986. p.799-824.

NIELSEN D R.; HOPMANS J W. and REICHARDT K. An emerging technology for scaling field soil-water behavior. In: SPOSITO G, ed. Scale dependence and scale invariance in hydrology. Cambridge, Cambridge Univ. Press, 1999. p.136-165.

OTHMER H.; DIEKKRÜGER B. and KUTÍLEK M. Bimodal porosity and unsaturated hydraulic conductivity. Soil Science. 152: 139-150, 1991.

PARKIN T B. and ROBINSON J A. Analysis of lognormal data. In: STEWART B, ed. Advances in soil science. New York, Springer Verlag, 1992. p.193-233.

PERROUX K M. and WHITE I. Designs for disc permeameters. Soil Science Society of America Journal. 52: 1205-1215, 1988.

PETERSON A E. and BUBENZER G D. Inatke rate: Sprinkler infiltrometer. In: KLUTE A., ed. Methods of soil analysis, Part 1: Physical and Mineralogical methods. 2. Madison, ASA and SSSA, 1986. p.845-870.

PHILLIPS R E.; QUISENBERRY V L.; ZELEZNIK J M. and DUNN G H. Mechanism of water enty into simulated macropores. Soil Science Society of America Journal. 53: 1629-1635, 1989.

POULSEN T G.; MOLDRUP P. and JACOBSEN O H. One-parameter models for unsaturated hydraulic conductivity. Soil Science. 163: 425-435, 1998.

PREVEDELLO C L.; REICHARDT K.; CORDEIRO D G.; MELO E FR Q. and SCHEFFER M. Gradiente unitário do potencial hidráulico como fonte de erro na obtenção da condutividade hidráulica em solo não saturado. Pesquisa Agropecuária brasileira. 29: 275-280, 1994.

REGAZZI A J. Teste para verificar a identidade de modelos de regressão. Pesquisa Agropecuária brasileira. 31: 1-17, 1996.

REICHARDT K. Unit gradient in internal drainage experiments for the determination of soil hydraulic conductivity. Scientia Agricola. 50: 151-153, 1993.

REICHARDT K.; PORTEZAN O.; LIBARDI P L.; BACCHI O O S.; MORAES S O.; OLIVEIRA J C M. and FALLEIROS M C. Critical analysis of the field determination of soil hydraulic conductivity fucntions using the flux-gradient approach. Soil & Tillage Research. 48: 81-89, 1998.

REYNOLDS W D. and ELRICK D E. Determination of hydraulic conductivity using a tension infiltrometer. Soil Science Society of America Journal. 55: 633-639, 1991.

REYNOLDS W D. Unsaturated hydraulic conductivity: field measurement. In: CARTER M.R, ed. Soil Sampling and methods of analysis. Boca Raton, Lewis, 1993. p.633-644.

REYNOLDS W D. and ZEBCHUK W D. Use of contact material in tension infiltrometer measurements. Soil Technology. 9: 141-159, 1996.

REYNOLDS W D.; BOWMAN B T.; BRUNKE R R.; DRURY C F. and TAN C S. Comparison of tension infiltrometer, pressure infiltrometer, and soil core estimates of saturated hydraulic conductivity. Soil Science Society of America Journal. 64: 678-484, 2000.

RÕMBKE J and GARCIA M. Report Earthworms. Manaus, Relatório ShiFT 54 -Embrapa - CPAA, 2001. 21p.

ROTH K. Soil physics. Heildelberg, The author ,1996. 200 p.

RUSSO D.; BRESLER E.; SHANI U. and PARKER J C. Analysis of infiltration events in relation to determining soil hydraulic properties by inverse problem methodology. Water Resources Research. 27: 1361-1373, 1991.

SANTINI A.; ROMANO G.; CIOLLARO G. and COMEGNA V. Evaluation of a laboratory inverse method for determing unsaturated hydraulic properties of a soil under different tillage practices. Soil Science. 160: 340-351. 1995

SANTINI A.; ROMANO G.; CIOLLARO G. and COMEGNA V. A field method for determining soil hydraulic properties. In: Congress of hydraulics and hydraulic constructions held in Florence., 1992. Tecnoprint, Bologna, 1992. p.117-139. 1992

SCHAAP M G.; LEIJ F J. and VAN GENUCHTEN M TH. A bootstrap-neural network approach to predict soil hydraulic parameters. In: VAN GENUCHTEN M TH.; LEIJ F J. and WU L (eds.). Workshop Characterization and Measurements of the Hydraulic Properties of Unsaturated Porous Media. University of California, Riverside, 1999. p.1237-1250.

SCHEIBKE R. Die Bestimmung der ungesättigten hydraulischen Leitfähigkeit in Böden mit der Augenblickprofilmethode, University of Bayreuth, 1998. 131p. (Doctor)

SCHROTH G.; SILVA L F DA.; WOLF M A.; TEIXEIRA W G. and ZECH W. Distribution of throughfall and stemflow in multi-strata agroforestry, perennial monoculture, fallow and primary forest in central Amazonia, Brazil. Hydrological processes. 13: . 13: 1423-1436. 1999.

SCHROTH G, TEIXEIRA W. G., DA SILVA L F, SCHALLER, M.; MACÊDO J L V AND ZECH, W. Effect of five tree crops and a cover crop in multi-strata agroforestry at two fertilization levels on soil fertility and soil solution chemistry in central Amazonia. Plant and Soil. 221:143-156. 2000 a.

SCHROTH G; SEIXAS R.; SILVA L F DA.; TEIXEIRA W. G. and ZECH W. Nutrient concentrations and acidity in ferralitic soil under perennial, fallow and primary forest in central Amazonia. European Journal of Soil Science. 51: 219-231, 2000 b.

SEBER G A F. Linear regression analysis. New York, John Wiley & Sons, 1977. 465p.

SHOUSE P J. and MOHANTY B P. Scaling of near-saturated hydraulic conductivity measured using disc infiltrometers. Water Resources Research. 34: 1195-1205, 1998.

SHOUSE P J.; SISSON J B.; ELLSWORTH T R. and JOBES J A. Estimating in situ unsaturated hydraulic properties of vertically heterogeneous soils. Soil Science Society of America Journal. 56: 1673-1679, 1992.

SILVA R B.; LIMA J M. and DIAS JUNIOR M.S. Efeitos da adsorção de fosfato em parâmetros físicos e na compressibilidade de solos tropicais. Revista Brasileira de Ciência do Solo. 23: 219-226, 1999.

SIMMONS C S.; NIELSEN D R. and BIGGAR J W. Scaling of field-measured soil water properties. I. Methodology II. Hydraulic conductivity and flux. Hilgardia. 47: 74-173, 1979.

SIMUNEK J.; SEJNA M. and VAN GENUCHTEN M TH. The Hydrus 1 D software package for simualting the one-dimensional movement of water, heat and multiple solutes in variably saturated-media - Version 2.0. Golden, International ground water modeling center, 1998. 178p.

SIMUNEK J. and VAN GENUCHTEN M TH. Estimating unsaturated soil hydraulic properties from multiple tension disc infiltrometer data. Soil Science. 126: 383-398, 1997.

SISSON J B.; FERGUSON A H. and VAN GENUCHTEN M TH. Simple method for predicting drainage form field plots. Soil Science Society of America Journal. 44: 1147-1152, 1980.

SNEDECOR G W. and COCHRAN W G. Statistical methods. 8.ed. Ames, The Iowa state university press, 1989. 593p.

SOKAL R R. and ROHLF F J. Biometry. 3.ed. New York, W. H. Freeman, 1995. 887p.

STELL R G.; TORRIE J H. and DICKEY D A. Principles and procedures of statistics a biometrical approach. 3.ed. New York, Mc-Grawn Hill, 1997. 666p.

STEPHENS D B. Vadose zone hydrology. Boca Raton, Lewis Publishers, 1996. 339p.

STOFFREGEN H.; WESSOLEK G. and RENGER M. Effect of temperature on hydraulic properties. In: VAN GENUCHTEN M TH.; LEIJ F J. and WU L (eds.). Workshop Indirect methods for estimating the hydraulic properties of unsaturated soils, 2., 1997. University of California, Riverside, 1999. p.497-506.

TIETJE O. and TAPKENHINRICHS M. Evaluation of pedo-transfer functions. Soil Science Society of America Journal. 57: 1095, 1993.

TILLOTSON P M. and NIELSEN D R. Scale factors in soil science. Soil Science Society of America Journal. 48: 953-959, 1984.

TOMASELLA J. and HODNETT M G. Soil hydraulic properties and van Genuchten parameters for an Oxisol under pasture in Central Amazonia. In: GASH J H C.; NOBRE C A.; ROBERTS J M. and VICTORIA R L., eds. Amazonian deforestation and climate. West Sussex, John Wiley, 1996. p.101-124.

TOMASELLA J. and HODNETT M G. Estimating unsaturated hydraulic conductivity of Brazilian soils using soil-water retention data. Soil Science. 162: 703-712, 1997.

VAN GENUCHTEN M. TH. A closed-form equation for predicting the hydraulic conductivity of unsaturated soils. Soil Science Society of America Journal. 44: 892-898, 1980.

VAN GENUCHTEN M TH. and NIELSEN D R. On describing and predicting the hydraulic properties of unsaturated soils. Annales Geophysicae. 3: 615-618, 1985.

VAN GENUCHTEN M TH and LEIJ F J. Estimating the hydraulic properties on unsaturated soils. In: VAN GENUCHTEN M TH.; LEIJ F J. and WU L. (eds.). Workshop Indirect methods for estimating the hydraulic properties of unsaturated soils, 2., 1997. University of California, Riverside, 1999. p.1-13.

WALLACE J S. The water balance of mixed tree-crop system. In: ONG C.K. and HUXLEY P., eds. Tree-crop interactions - a physiological approach. Wallingford, CAB, 1996. p.189-234.

WARRICK A.W.; MULLEN G J. and NIELSEN D R. Scaling field-measured soil hydraulic properties using a similar media concept. Water Resources Research. 13: 355-362, 1977.

WARRICK A. Spatial variability. In: HILLEL, D., ed. Environmental soil physics. San Diego, Academic Press, 1998. p.655-675.

WATSON K W. and LUXMOORE R J. Estimating macroporostiy in a forest watershed by use of a tension infiltrometer. Soil Science Society of America Journal. 50: 578-582, 1986.

WHITE I. and PERROUX K M. Estimation of unsaturated hydraulic conductivity from field sorptivity measurements. Soil Science Society of America Journal. 51:1093-1101.

WHITE I.; SULLY M J. and PERROUX K M. Measurement of surface soil hydraulic properties: disc permeameters, tension infiltrometers and other techniques. In: TOPP W D.; REYNOLDS W D. and GREEN R E., eds. Advances in measurements of soil physical properties: bringing theory into practice. Madison, SSSA, 1992. p.69-10.

WILSON G V. and LUXMOORE R J. Infiltration, macroporosity, and mesoporosity distributions on two forested watersheds. Soil Science Society of America Journal. 52: 329-335, 1988.

WOODING R A. Steady infiltration from a shallow circular pond. Water Resources Research. 4: 1259-1273, 1968.

WÖSTEN J H M. and VAN GENUCHTEN M TH. Using texture and other soil properties to predict the unsaturated soil hydraulic functions. Soil Science Society of America Journal. 52: 1762-1770, 1988.

WU L.; PAN L.; MITCHEL J. and SANDEN B. Measuring saturated hydraulic conductivity using a generalized solution for single-ring infiltrometer. Soil Science Society of America Journal. 63: 788-792, 1999.

WU L. and PAN L. A generalized solution to infiltration from single-ring infiltrometers by scaling. Soil Science Society of America Journal. 61: 1318-1322, 1999.

YOUNG A. Agroforestry for soil management. 2.ed. Wallingford, CAB, 1997. 320p.

ZAR J H. Biostatistical analysis. 4.ed. Prentice-Hall, 1999. 663p.

ZURMÜHL T. and DURNER W. Determination of parameters for bimodal hydraulic functions by inverse modeling. Soil Science Society of America Journal. 62: 874-880, 1998.

Table A- 6.1 Saturated hydraulic conductivity evaluated with disc infiltrometer – Field method – K [cm d^{-1}]

K(3D)	1D	Block	K(3D)	1D	Block
52.7094	75.9800	3	205.2831	228.1720	2
12.0185	11.6000	2	75.6718	109.0400	1
52.1590	59.0000	1	34.5198	55.6800	3
101.2647	135.7200	3	187.7908	191.4000	2
2.9301	2.4940	2	103.9386	143.8400	1
66.8709	89.3200	1	14.7441	23.2000	3
22.89	38.51	3	10.4057	15.6600	2
3.29	4.64	2	64.89	92.8	1
45.89	62	1	11.0518	14.2100	3
23.2000	59.9700	1	6.2255	9.2800	2
6.8282	8.7000	3	56.2595	64.9600	1
4.7164	4.6400	2	33.1643	39.4400	3
6.9570	4.9300	3	2.9314	3.6772	2
32.4647	54.8100	2	56.8540	69.6000	1
41.6137	37.1200	1	33.9134	41.7600	3
18.0761	25.5200	3	2.2200	1.1600	2
27.8736	48.0240	2	39.4416	51.7360	1
49.9993	62.6400	1	32.8484	46.9800	3
65.1303	71.9200	3	28.1306	27.6080	2
			168.6136	197.2000	1

Table 6.2 A – Saturated hydraulic conductivity evaluated with constant head method. Q [cm h^{-1}]

Treatment	Block A [1]					Block B [2]					Block C [3]				
	1	2	3	4	5	6	7	8	9	10	11	12	13	14	15
1	82.48	53.6	38.39	.	.	204	169	258	194.35	611.06	217	106	81	168	63
2	30.2	236.08	26.69	.	.	651	58	96	97.00	435	12	78	194	72.00	61
3	69.16	57.06	102.02	.	.	390	42	127	186.33		111	198	271	80.00	128
4	20.06	51.87	82.88	.	.	118	147	81	32.00	87	12	8	17	10.00	18
5	17.52	42.88	41.27	.	.	398	375	94	554.00	147	12	44	98	85.00	15
6	17.52	42.88	10.03	.	.	70	37	116	59	24	61	33	49	190	22
7	99.31	134.29	147.32	.	.	295	162	311	116	120	264	467	168	199	187
8	43.34	38.5	25.3	.	.	89	43	157	35	28	51	80	106	519	27
9	188.33	98.49	122.97	142	.	168	113	81	74	133	61	24	75	133	48
10	14.39	14.11	48.41	22.34	.	51	111	80	61	62	6	23	8	102	21
11	76.22	59.07	397	97.87	.	55	81	39	91	43	15	282	210	57	18
12	148.43	76.91	28.5	20.26	.	25	153	59	142	66	11	163	41	21	16
13	60.37	74.3	197	110.55	.	90	4	18	78	36	72	131	158	194	196

The treatment number are coded following Table 3.2.

Table A – 6.3 – Tension infiltrometer measurements

Tension [mm]	Infiltration rate [cm d^{-1}]	Specie	Tension [mm]	Infiltration rate [cm h^{-1}]	Specie	Tension [mm]	Infiltration rate [cm d^{-1}]	Specie	Tension [mm]	Infiltratio n rate [cm d^{-1}]	Specie
0	0.0827	PueraAGA	20	0.0733	BrazilNutB	8	0.1827	VismiaC	28	0.0098	PupuF AGC
5	0.0915	PueraAGA	40	0.0155	BrazilNutB	20	0.0516	VismiaC	40	0.0393	PupuF AGC
14	0.0451	PueraAGA	61	*	BrazilNutB	30	0.0131	VismiaC	50	*	PupuF AGC
23	0.0470	PueraAGA	0	0.3045	BrazilNutC	40	0.0002	VismiaC	0	0.2150	PupuF MA
33	0.0423	PueraAGA	6	0.0641	BrazilNutC	0	0.1034	CupuAGA	5	0.0582	PupuF MA
51	0.0135	PueraAGA	10	0.0243	BrazilNutC	20	0.1750	CupuAGA	16	0.1140	PupuF MA
79	0.0300	PueraAGA	20	0.0194	BrazilNutC	32	0.0454	CupuAGA	40	0.0595	PupuF MA
92	*	PueraAGA	30	0.1790	BrazilNutC	43	*	CupuAGA	58	0.0568	PupuF MA
0	0.2333	PueraAGB	40	0.0001	BrazilNutC	0	0.1833	CupuAGB	68	0.0063	PupuF MA
4	0.2172	PueraAGB	0	0.2248	Pupu AGA	4	0.0494	CupuAGB	88	0.0426	PupuF MA
10	0.0515	PueraAGB	5	0.2652	Pupu AGA	10	0.2207	CupuAGB	100	*	PupuF MA
20	0.0359	PueraAGB	9	0.1116	Pupu AGA	20	0.0303	CupuAGB	0	0.1822	PupuF MB
40	0.0288	PueraAGB	21	0.0524	Pupu AGA	40	0.0405	CupuAGB	5	0.5901	PupuF MB
50	0.0159	PueraAGB	36	0.1142	Pupu AGA	50	*	CupuAGB	8	0.1696	PupuF MB
64	*	PueraAGB	42	0.0860	Pupu AGA	0	0.4398	CupuAGC	14	0.0152	PupuF MB
0	0.6592	PueraAGC	52		Pupu AGA	6	0.1377	CupuAGC	26	0.0289	PupuF MB
5	0.1833	PueraAGC	0	0.0471	Pupu AGB	10	0.0673	CupuAGC	50	*	PupuF MB
10	0.0152	PueraAGC	10	0.2912	Pupu AGB	20	0.0446	CupuAGC	0	0.7072	PupuF MC
22	0.0052	PueraAGC	16	0.2232	Pupu AGB	30	0.0470	CupuAGC	4	0.1342	PupuF MC
34	0.0161	PueraAGC	22	0.0817	Pupu AGB	42	0.0347	CupuAGC	8	0.0394	PupuF MC
44	*	PueraAGC	32	0.0758	Pupu AGB	54	*	CupuAGC	14	0.0317	PupuF MC
0	0.1602	PueraMA	40	0.0062	Pupu AGB	0	0.1852	CupuM A	26	0.0010	PupuF MC
6	0.1497	PueraMA	54	*	Pupu AGB	6	0.2571	CupuM A	34	0.0014	PupuF MC
12	0.1471	PueraMA	0	0.2418	Pupu AGC	12	0.5249	CupuM A	46	*	PupuF MC
22	0.0805	PueraMA	6	0.0669	Pupu AGC	14	0.0938	CupuM A	0	0.1290	AMPupuFA
42	0.0085	PueraMA	10	0.0191	Pupu AGC	22	0.0962	CupuM A	4	0.2682	AMPupuFA
74	0.0327	PueraMA	20	0.0723	Pupu AGC	38	*	CupuM A	10	0.1725	AMPupuFA
102	*	PueraMA	30	0.0651	Pupu AGC	0	0.1953	CupuMB	23	0.0040	AMPupuFA
0	0.3974	PueraMB	40	*	Pupu AGC	7	0.2185	CupuMB	38	0.0156	AMPupuFA
3	0.2349	PueraMB	0	0.2817	Pupu MA	13	0.1434	CupuMB	62	0.0091	AMPupuFA
6	0.1387	PueraMB	2	0.5836	Pupu MA	20	0.0869	CupuMB	84	*	AMPupuFA
19	0.0799	PueraMB	7	0.1459	Pupu MA	36	0.0446	CupuMB	0	0.5311	AMPupuFB
26	0.0866	PueraMB	20	0.0499	Pupu MA	48	0.0279	CupuMB	7	0.0964	AMPupuFB
34	0.0491	PueraMB	36	0.0436	Pupu MA	64	*	CupuMB	12	0.0128	AMPupuFB
53	*	PueraMB	48	0.0180	Pupu MA	0	0.2018	CupuMC	24	0.0296	AMPupuFB
0	0.0721	PueraMC	64	*	Pupu MA	6	0.7662	CupuMC	35	0.0152	AMPupuFB
4	0.2637	PueraMC	0	0.1781	Pupu MB	10	0.0272	CupuMC	46	*	AMPupuFB
10	0.1114	PueraMC	6	0.0109	Pupu MB	20	0.0470	CupuMC	0	0.6801	AMPupuFC
20	0.0693	PueraMC	10	0.0084	Pupu MB	30	0.0297	CupuMC	4	0.0814	AMPupuFC
30	0.0606	PueraMC	16	0.0538	Pupu MB	42	0.0128	CupuMC	10	0.0427	AMPupuFC
40	0.0182	PueraMC	36	*	Pupu MB	54	*	CupuMC	24	0.0068	AMPupuFC
50	*	PueraMC	0	0.1288	Pupu MC	0	0.2027	UrucumA	38	0.1273	AMPupuFC
0	0.2935	VismiaA	4	0.7237	Pupu MC	7	0.2892	UrucumA	48	*	AMPupuFC
4	0.0803	VismiaA	6	0.2257	Pupu MC	10	0.0320	UrucumA	0	0.1078	AMPupuA
10	0.1251	VismiaA	10	0.2070	Pupu MC	25	0.0663	UrucumA	7	0.0866	AMPupuA
25	0.0732	VismiaA	16	0.0387	Pupu MC	56	0.0292	UrucumA	23	0.1257	AMPupuA
40	0.0629	VismiaA	36	*	Pupu MC	95	*	UrucumA	38	0.0531	AMPupuA
50	0.0424	VismiaA	0	0.1344	PupuF AGB	0	0.2037	UrucumB	48	0.0297	AMPupuA
88	*	VismiaA	6	0.0892	PupuF AGB	6	0.0235	UrucumB	62	*	AMPupuA
0	0.0318	VismiaB	10	0.0933	PupuF AGB	40	0.0056	UrucumB	0	0.4917	AMPupuB
4	0.2094	VismiaB	16	0.0238	PupuF AGB	61	*	UrucumB	2	0.2086	AMPupuB
10	0.2160	VismiaB	31	0.0446	PupuF AGB	0	0.4993	UrucumC	5	0.0176	AMPupuB
19	0.0690	VismiaB	50	0.0288	PupuF AGB	2	0.3349	UrucumC	11	0.0620	AMPupuB
28	0.0589	VismiaB	60	*	PupuF AGB	6	0.4525	UrucumC	16	0.0154	AMPupuB
40	0.0225	VismiaB	0	0.3548	PupuF AGC	10	0.0944	UrucumC	34	0.0365	AMPupuB
54	*	VismiaB	4	0.1920	PupuF AGC	20	0.0424	UrucumC	48	*	AMPupuB
0	0.4859	VismiaC	8	0.0382	PupuF AGC	40	0.0598	UrucumC	0	0.3225	AMPupuC
2	0.2567	VismiaC	20	0.0251	PupuF AGC	50	*	UrucumC	2	0.0331	AMPupuC
-	-	-	-	-	-	0	0.0189	BrazilNutB	8	0.2044	AMPupuC
-	-	-	-	-	-	6	0.1969	BrazilNutB	18	0.0670	AMPupuC
-	-	-	-	-	-	14	0.0471	BrazilNutB	28	0.1012	AMPupuC

Letter identify the blocks

THE Fortran code – Slope – To test identity of models

Fortran 90

```
        Parameter(Nmax=20)
        real x,y,A,B,C,SS,FS,FE,FO
        real slope(Nmax),slope1(Nmax),elev(Nmax)
        character*33 names(Nmax)
        integer ne,DFp,DFc
        call inicio(ne,names,Nmax)
        call calculo(ne,names,FS,FE,FO,slope,slope1,elev,Nmax,DFp,DFc)
        call out(FS,FE,FO,slope,slope1,elev,names,ne,Nmax,DFp,DFc)
        end

        subroutine inicio(ne,names,Nmax)
        character*33 names(Nmax)
        integer ne
        logical ex
10   continue
     write(*,*) 'SLOPE - Fortran code to compare linear regressions'
     write(*,*) '________________________________________________'
        write(*,*)
        write(*,*)
        write(*,*) 'HOW MANY FILES DO YOU HAVE ?'
        read(*,*) Nm
        write(*,*) 'WRITE THE NAMES OF THE FILES - (Name.ext)'
        do i=1,Nm
        write(*,*) ' NAME OF THE FILE ',i,'?'
        read(*,*) names(i)
        inquire(file=names(i),exist=ex)
        if(ex.eqv..false.)then
        write(*,*) 'FILE DOES NOT EXIST TYPE AGAIN'
        go to 10
        stop
        endif
        end do
102     close(1)
        ne=i-1
        return
        end

        subroutine calculo(ne,names,FS,FE,FO,slope,slope1,elev,Nmax,DFp,DFc)
        integer ne,DF,DFp,Nt,DFt,DFc
        character*33 names(Nmax)
        real xm,ym,A,B,C,x(100),y(100),SS,SSp
        real xm1,ym1,xmt,ymt,Ac,Bc,Cc,At,Bt,Ct,xym,xm2
        real Num,Den,FE,FD,FO,FS,slope(Nmax),slope1(Nmax),elev(Nmax)
        SSp=0.
        DFp=0
        xmt=0.
        ymt=0.
        Nc=0
        Ac=0.
        Bc=0.
        Cc=0.
        do k=1,ne
          open(1,file=names(k),status='unknown')
          do i=1,10000
            read(1,*,end=100) xx,yy
          end do
100       continue
```

```
    close(1)
    N=i-1
    open(1,file=names(k),status='unknown')
    do i=1,N
      read(1,*) x(i),y(i)
    end do
    close(1)
    xm=0.
    ym=0.
    xym=0.
    xm2=0.
    do i=1,N
      xm=xm+x(i)
      ym=ym+y(i)
      xym=xym+x(i)*y(i)
            xm2=xm2+x(i)**2
    end do
    xm1=xm/N
    ym1=ym/N
    xmt=xmt+xm
    ymt=ymt+ym
    Nc=Nc+N
    A=0.
    B=0.
    C=0.
    do i=1,N
      A=A+(x(i)-xm1)**2
      C=C+(y(i)-ym1)**2
      B=B+(x(i)-xm1)*(y(i)-ym1)
    end do

    SS=C-B**2/A
    DF=N-2
    SSp=SSp+SS
    DFp=DFp+DF
    slope(k)=B/A
    elev(k)=ym1-slope(k)*xm1
    Ac=Ac+A
    Bc=Bc+B
    Cc=Cc+C
    slope1(k)=xym/xm2
  end do

  xmt=xmt/Nc
  ymt=ymt/Nc
  SSc=Cc-Bc**2/Ac
  DFc=Nc-Ne-1
  Nt=0

  do k=1,ne
    open(1,file=names(k),status='unknown')
    do i=1,10000
      read(1,*,end=101) xx,yy
      At=At+(xx-xmt)**2
      Ct=Ct+(yy-ymt)**2
      Bt=Bt+(xx-xmt)*(yy-ymt)
      Nt=Nt+1
    end do
101 continue
    close(1)
  end do
  SSt=Ct-Bt**2/At
  DFt=Nt-2
```

```
      Num=(SSc-SSp)/(ne-1)
      Den=SSp/DFp
      FS=Num/Den
      Num=(SSt-SSc)/(ne-1)
      Den=SSc/DFc
      FE=Num/Den
      FO=((SSt-SSp)/(2.*(ne-1)))/(SSp/DFp)

      return
      end

      subroutine out(FS,FE,FO,slope,slope1,elev,names,ne,Nmax,DFp,DFc)
      real FS,FE,FO,slope(Nmax),slope1(Nmax),elev(Nmax)
      character*33 names(Nmax)
      integer ne,DFp,DFc
      open(1,file='out.lis',status='unknown')
      write(1,*) 'TEST FOR PARALLELISM'
      write(1,*)
      write(1,*) 'Multiple comparisons among slopes'
      write(1,*) 'FS= ',FS
      write(1,*) 'F critical (',ne-1,',',DFp,')'
      write(1,*)
      write(1,*)
      write(1,*) 'TEST FOR CONCURRENCE'
      write(1,*)
      write(1,*) 'Multiple comparisons among intercepts'
      write(1,*) 'FE= ',FE
      write(1,*) 'F critical (',ne-1,',',DFc,')'
      write(1,*)
      write(1,*)
      write(1,*) 'TEST FOR COINCIDENCE'
      write(1,*)
      write(1,*) 'An Overall test for coincidental regressions'
      write(1,*) 'FO= ',FO
      write(1,*) 'F critical (',2*(ne-1),',',DFp,')'
      write(1,*)
      write(1,*)
      write(1,*) 'FS, FE or FO should be compared with critical values
&of F'
      write(1,*)
 write(1,*) 'IF FE, FS or FO > F critical, reject Ho'
      write(1,*)
 write(1,*)
 write(1,*) 'REGRESSION PARAMETERS'
      write(1,*)
      write(1,*) 'Intercepts'
      write(1,*)
      Do k=1,ne
      write(1,*) names(k),'intercept = ',elev(k)
      end do
      write(1,*)
      write(1,*) 'Slopes'
      write(1,*)
      Do k=1,ne
      write(1,*) names(k),'slope = ',slope(k)
      end do
      close(1)
      return
      end
```

7 GENERAL CONCLUSIONS AND ASPECTS TO BE FURTHER INVESTIGATED

This Chapter will neither review extensively specific aspect of the results nor discuss the feasibility of the methods investigated. These results and conclusions are described at the end of the respective chapter were they are presented. Here, I will draw some conclusion in an attempt to interpret the results in a comprehensive manner. In addition, I suggest some aspects which should be further investigated.

7.1 Soil physical and hydraulical parameters investigated

Bulk density and the index of flocculation proved to be useful physical indicators for monitoring the soil quality. The use of fertiliser and lime affected the stability of small aggregates, and the evaluation of the index of flocculation indicates changes in the natural aggregation of the clay particles. Bulk density measurements ranged from 0.8 to 1.1 Mg kg^{-1}. These lower values indicated a strongly aggregated soil. Further, bulk density values are not inversely correlated with infiltration rates as normally expected. As a consequence of the flocculation and the aggregation present in the Ferralsols, these soils behave like sand in terms of water infiltration near saturation. But, they behave like clay soils at higher tensions with respect to infiltration rates and water holding capacity. This unusual behaviour of the clayey Ferralsols, combining the properties of sand and clay, in combination with a bimodal pore size distribution lead to the failure of many pedotransfer functions which use texture or bulk density as input parameter to determine hydraulic properties. Further studies about the phenomena of flocculation and aggregation related with organic matter, and especially, the dynamic of the iron oxides should be promoted.

The pore size distribution and its intricate geometry and continuity control the water dynamics. Therefore, the knowledge of porosity properties and how they change as a result of soil management are a key factor to maintain the Ferralsols with good soil physical qualities. Methodological studies about evaluation of pore size distribution, continuity, stability, and factors responsible for the formation and destruction of the pore system are fascinating topics for further studies.

The most common calibration functions to relate the soil dielectric number (ε) to volumetric water content (θ) lead to serious errors in the estimations of θ in the clayey Ferralsols, unless a specific calibration is used. The failure of the calibration functions are related to the unusual combination of low bulk density [ca. 1.00 Mg kg^{-1}] with a high amount of clay particles [> 600 g kg^{-1}]. The use of physically-based models to relate ε to θ will be optimised with a better knowledge of the amount of water that are bound to clay particles and water that is free in the soil. Investigations of the relationship between specific soil surface and ε may give not only a better accuracy of the θ estimation, but it also may permit to define in a better way the residual water content (θ_r), which is a parameter used in many hydraulic models. The direct use of ε values instead to calibrate it to θ in many studies concerning water dynamic is also a possibility to be investigated.

The uncertainties of determination of water fluxes near saturation by use of $K(\theta)$ or $K(h)$ functions arise because of its exponential behaviour (i.e., in linear models, slopes with very high values) near saturation. This problem is extreme in highly structured soils, like the clayey Ferralsols. It has a consequence that a small change in θ or h can change K dramatically. Regardless of the equation used, it is an intrinsic characteristic of the clayey Ferralsol (and other well structured soils). Therefore, in the estimation of water fluxes near saturation this phenomenon is extremely expressive and may lead to higher uncertainties in the estimated values. Using hydraulic equations that depends of many parameters in a strongly non-linear manner, make it difficult to assess the uncertainties of the estimations and to use them in numerical simulations. The use of many parameters makes the modelling and the statistical analysis too involved. On the other hand, it is unrealistic to try to obtain accurate estimates of the hydraulic conductivity throughout the entire water content range using a single and simple equation for this soil. Probably an option for modelling water fluxes in structured soils, like the clayey Ferralsols in the central Amazon, is to developed linear piecewise models, with few parameters for specific ranges with distinct hydraulic behaviour (e.g. the domain of macropore flux; capillary flux and adsorptive domain). The piecewise equation may fit the variable field data with equal reliability then the more elaborate smoothed functions, further they may provide simple analytical solutions and feasible statistical analysis. Preliminary results using the inverse method combining results from different methods have been promising.

7.2 Soil quality and sustainability of land use systems

A brief discussion concerning general aspects on the three agricultural systems, secondary and primary forest sites investigated is presented above. However, as described in the introduction of this study, the concept of land sustainability involve economic and social demands, the term sustainability is used here in this Chapter in a restrict sense concerning only biophysical aspects.

For the monoculture of cupuaçus, the results show that the maintenance of the soil covered between the plant in the first years of the establishment of a plantation, when large space between the plants occurs, is fundamental to keep the soil structure in good quality. *Pueraria phaseoloides* appears to be a very good option, as a cover crop plant, to maintain or recuperate the porosity of the clayey Ferralsol.

In the monocultures of peach palm a reduction of the hydraulic conductivity could be observed. Since peach palm is sensitive to deficient soil aeration, the monitoring of hydraulical properties may be used as indicator of critical levels of aeration. However, for the hydraulic or physical parameters as indicators of soil quality to be more useful, critical values limiting the growth of peach palms must be established. The reduction of the soil conductivity is apparently caused by compression of the soil by the root system. This phenomenon may be more serious in less permeable soils than the Ferralsols.

In the Agroforestry systems intricate patterns created by the different characteristics of the plants and by the specific management for each species create spot areas around stems with different soil properties. The evaluation of the soil quality parameters in a more complicated system like the agroforestry need an elaborated sampling scheme, which allows estimating the area of these spots around the species. The sampling scheme will identify extreme values and may permit to calculate weighted-average means for the whole system. The weighted means allow comparison between land use systems. Moreover it also permits to speculate about combination of plants and management to achieve an ideal structure. The creation of data bases with information about tree and crop performance as response to management practices and other parameters, will enable us to perform simulations of future or imaginary scenarios which can be used in land use planning to define a suitable combination of plants and management practices.

The secondary forest appears to create efficient mechanisms to recuperate the soil qualities, and many parameters in this system approximate the values found in the primary forest. Further investigation, in addition to forms of increasing the rate of biomass accumulation, may include the processes that happen in the soil covered by the secondary forest. A better understanding of the natural mechanisms of soil reclamation may allow us to find a form to reduce the time for secondary vegetation to recuperate the soil quality, and consequently may reduce the intervals between rotation areas in the slash-and-burn system.

The primary forest shows an optimal combination of soil physical and hydraulic characteristics to preserve the scarce nutrients in the clayey Ferralsols. The bimodal pore system, permit to drain water quickly by the macropores during intense rainfalls by passing the soil matrix. The remaining water in the soil flows slowly enhancing time for the nutrients in solution to be adsorbed by the soil matrix or uptaken by the plant roots. The optimal functioning of this system in terms of reduction of leaching in the soil matrix is related to the intense precipitations, which occurs frequently in the central Amazon.

Based on the findings in this study inferences about practices to optimise the use of fertiliser or to reduce the leaching of pesticides to the groundwater are delineated. Controversially to as that is normally said, the macropore fluxes can reduce the leaching rates if the nutrients are in the soil matrix, and the water does not flow through the matrix. Based on this statement, the investigation of forms to incorporate the nutrients into the soil matrix assumes importance. Studies about methods of incorporating fertilisers directly in the soil matrix; parcel of fertilisers in many applications; use of fertiliser finely granulated that will react more quickly with the soil matrix (or the opposite); and the adequate moisture of the soil for the fertiliser distribution, should be encouraged.

A better forecasting of water fluxes in the clayey Ferralsol will be possible if we known under which conditions water flows in the macropores. Certainly, it is not a trivial problem because this process is not only dependent on the precipitation rate but also on the current moisture of the soil. Further, there is still a requirement for better mathematical equations for describing macropore fluxes. However, if this can be achieved, the judicious use of fertiliser and pesticides may be predicted and prescribed, and as a consequence the macropore system may contribute to reduce leaching.

It is doubtful if the clayey Ferralsols can support a productive land use system for a long period without external inputs. Conversely, the most of the smallholder farmers in the central Amazon cannot afford high monetary investment for the agriculture production. A paradox problem is posed, and need be equalised to achieve an alternative land use system to the slash-and-burn system. Obviously, that the implementation of suitable agricultural systems for the central Amazon is not only dependent on suitable agronomic techniques but also from the social and economic policies.

Bayreuther Bodenkundliche Berichte (BBB)

Bisher erschienene Bände:

Band 1: Kögel I., Organische Stoffgruppen in Waldhumusformen und ihr Verhalten während der Streuzersetzung und Humifizierung. 1987, 131 S., vergriffen.

Band 2: Joneck M., Untersuchungen zur Wasser- und Stoffdynamik in einem hängigen Einzugsgebiet des Rotmains. 1987, 143 S., DM 18,50.

Band 3: Hantschel R., Wasser- und Elementbilanz von geschädigten, gedüngten Fichtenökosystemen im Fichtelgebirge unter Berücksichtigung von physikalischer und chemischer Bodenheterogenität. 1987, 219 S., vergriffen.

Band 4: Kweton A., Bodenerosion und Wasserhaushalt im Haraz-Gebirge, Arabische Republik Jemen. 1988, 141 S., DM 19,50.

Band 5: Grosser L., Untersuchungen zu Vegetation, Böden und Landnutzungsmöglichkeiten in der Gebirgsregion Haraz/Arabische Republik Jemen. 1988, 226 S., DM 32,00.

Band 6: Hempfling R., Charakterisierung verschiedener Waldhumusformen und ihrer Dynamik durch analytische Pyrolyseverfahren. 1988, 126 S., DM 19,00.

Band 7: Simmleit N., Charakterisierung und Differenzierung von Fichten (Picea abies) durch multivariate chemometrische Auswertung von biometrischen, chemischen und pyrolytischen Analysen. 1988, 196 S., DM 29,50.

Band 8: Beudert G., Morphologische, naßchemische und ^{13}C-NMR-spektroskopische Kennzeichnung der organischen Substanz von Waldhumusprofilen nach Dichtefraktionierung. 1988, 133 S., DM 19,00.

Band 9: Haber J., Beziehungen zwischen dem Humusgehalt/Humusvorrat bayerischer Bergwaldböden und steuernden Standorts- und Bestandesfaktoren. 1988, 296 S., vergriffen.

Band 10: Guggenberger G., Chromatographische (GPC, RP-HPLC) und spektroskopische (IR, ^{13}C-NMR) Kennzeichnung wasserlöslicher organischer Bodensubstanzen aus Waldhumus. 1989, 110 S., DM 18,00.

Band 11: Kaupenjohann M., Chemischer Bodenzustand und Nährelementversorgung immissionsbelasteter Fichtenbestände in NO-Bayern. 1989, 202 S., vergriffen.

Band 12: Lebert M., Beurteilung und Vorhersage der mechanischen Belastbarkeit von Ackerböden. 1989, 131 S., DM 25,00.

Band 13: Ziegler F., Zum Einfluß von Regenwürmern (*Eisenia fetida*; Lumbricidae) und mineralischer Substanz auf die Zersetzung von Buchenstreu (*Fagus sylvatica*) und Gerstenstroh (*Hordeum vulgare*) im Modellversuch. 1990, 164 S., DM 34,00.

Band 14: Suttner T., Zur mikrobiellen Aktivität bayerischer Böden in Abhängigkeit von der Nutzung und unter besonderer Berücksichtigung des bodenbiologischen Transformationsvermögens. 1990, 164 S., vergriffen.

Band 15: Gunzelmann M., Die Quantifizierung und Simulation des Wasserhaushalts von Einzelaggregaten und strukturierten Gesamtböden unter besonderer Berücksichtigung der Wasserspannungs/Wasserleitfähigkeitsbeziehung von Einzelaggregaten. 1990, 180 S., DM 37,00.

Band 16: Baer U., Zum Einfluß wasserlöslicher organischer Substanzen auf die Adsorption und Desorption von Herbiziden. 1990, 90 S., DM 20,00.

Band 17: Zech W. (Hrsg.), Exkursionsführer (Supplementband NO-Bayern) zur Jahrestagung der Deutschen Bodenkundlichen Gesellschaft 1991 in Bayreuth. 1991, 273 S., DM 42,00.

Band 18: 15 Jahre bodenkundliche Forschung an der Universität Bayreuth. 1991, kostenlos.

Band 19: Drechsel P., Bodengesellschaften Zentralsomalias: Ökologie und Genese. 1991, 119 S., DM 24,00.

Band 20: Durner W., Vorhersage der hydraulischen Leitfähigkeit strukturierter Böden. 1991, 208 S., vergriffen.

Band 21: Mineralstoffversorgung tropischer Waldbäume, Symposium Universität Bayreuth, Juli 1989. 1991, 150 S., DM 30,00.

Band 22: Türk T., Die Wasser- und Stoffdynamik in zwei unterschiedlich geschädigten Fichtenstandorten im Fichtelgebirge. 1992, 252 S., DM 43,00.

Band 23: Schaaf W., Elementbilanz eines stark geschädigten Fichtenökosystems und deren Beeinflussung durch neuartige basische Magnesiumdünger. 1992, 204 S., DM 38,00.

Band 24: Kögel-Knabner I., Forest soil organic matter: structure and formation. 1992, 103 S., DM 21,00.

Band 25: Maxin C., Sorption Polyzyklischer Aromatischer Kohlenwasserstoffe (PAK) an die wasserlösliche organische Substanz in Böden (WOBS). 1992, 109 S., DM 24,00.

Band 26: Guggenberger G., Eigenschaften und Dynamik gelöster organischer Substanzen (DOM) auf unterschiedlich immissionsbelasteten Fichtenstandorten. 1992, 195 S., vergriffen.

Band 27: Totsche K.U., Co-Transport in Böden: Konzeption und Bau einer Laborbodensäulenanlage und Modellentwicklung. 1992, 97 S., DM 19,00.

Band 28: Rothammel B., Modellierung des Einflusses wichtiger Steuergrößen auf den boden- und gewässerchemischen Zustand ausgewählter Einzugsgebiete des Frankenwaldes. 1992, 121 S., DM 23,00.

Band 29: Kaiser K., Salz- und Säureeffekte auf die Zusammensetzung der Bodenlösung und die Sorptionseigenschaften saurer Waldböden. 1992, 137 S., DM 27,00.

Band 30: Hartmann C., Die Ertragsbildung und Stickstoffixierung der Weißen Süßlupine (*Lupinus albus* L.) in Abhängigkeit von Genotyp, Standort und Anbaumaßnahmen. 1992, 182 S., DM 34,00.

Band 31: Drechsel P., Beziehungen zwischen Standort, Ernährungszustand und Wuchsleistung von Teak (*Tectona grandis* L.f.) im humiden Westafrika. 1992, 252 S., DM 48,00.

Band 32: Zech W., Reuschel S., Wohlfromm J., Humuschemische Veränderungen während der Fermentation von Fichtenrinde. 1993, 107 S., DM 21,00.

Band 33: Sandhage-Hofmann A., Feinwurzeldynamik unterschiedlich geschädigter kalkalpiner Fichtenbestände (Wank-Massiv). 1993, 243 S., DM 54,00.

Band 34: Drechsel P., DRIS - Diagnosis and Recommendation Integrated System - in Theorie und Praxis. Eine SPSS-orientierte Anleitung. 1994, 72 S., DM 14,00.

Band 35: Außendorf M., Säulenversuche zur Aufklärung der Schwermetalldynamik auf einem mit Kompost gedüngten sauren Waldboden. 1994, 102 S., DM 19,00.

Band 36: Zurmühl T., Validierung konvektiv-dispersiver Modelle zur Berechnung des instationären Stofftransports in ungestörten Bodensäulen. 1994, 204 S., DM 47,00.

Band 37: Schroth G., Above- and below-ground interactions in alley cropping with Gliricidia sepium as compared to conventional and mulched sole cropping on a high base status soil in the West African rainforest zone. 1994, 178 S., DM 32,00.

Band 38: Totsche K. U., Co-Transport und Co-Sorption in Böden: Experimentelle Befunde - Modellentwicklung - Numerische Simulation. 1995, 145 S., DM 22,00.

Band 39: Pöhhacker R., Steuerungsfaktoren des Streuabbaus. Einfluß von Temperatur, Sauerstoffverfügbarkeit und Substratqualität auf Streuzersetzung und Humifizierung - ein Modellversuch. 1995, 132 S., DM 20,00.

Band 40: Bäumler R., Dynamik gelöster Stoffe in verschiedenen Kompartimenten kleiner Wassereinzugsgebiete in der Flyschzone der Bayerischen Alpen - Auswirkungen eines geregelten forstlichen Eingriffs. 1995, 133 S., DM 20,00.

Band 41: Ludwig R., Modellierung des Matrix- und Makroporenflusses einer Versuchsdeponie. 1995, 96 S., DM 15,00.

Band 42: Forster J.C., Nutzungseinflüsse auf Struktureigenschaften von Gebirgsböden.

Band 43: Deschauer H., Eignung von Bioabfallkompost als Dünger im Wald. Untersuchungen zu den Auswirkungen einer Bioabfalldüngung auf den Elementumsatz, die Schwermetalldynamik und das Verhalten von polyzyklischen aromatischen Kohlenwasserstoffen in einem humus- und nährstoffarmen Kiefernbestand. 1995, 169 S., DM 25,00.

Band 44: Hartmann R., Polyzyklische Aromatische Kohlenwasserstoffe (PAK) in Waldböden. 1995, 117 S., DM 18,00.

Band 45: Lang F., Molybdän auf sauren Waldstandorten. Vorräte, Mobilität und DOC-Sorptionskonkurrenz. 1995, 92 S., DM 14,00.

Band 46: Pichler M., Polyzyklische aromatische Kohlenwasserstoffe (PAK) in Partikelgrößenfraktionen von Waldböden. Untersuchungen zu Verteilung und Dynamik an Standorten unterschiedlicher biologischer Aktivität. 1995, 123 S., DM 19,00.

Band 47: Heid P., Muerte misteriosa - Untersuchungen zu neuartigen Schäden an *Coffea arabica* L. in Costa Rica. 1995, 126 S., DM 19,00.

Band 48: Wilcke W., Kleinräumige chemische Heterogenität in Böden: Verteilung von Aluminium, Schwermetallen und polyzyklischen aromatischen Kohlenwasserstoffen in Aggregaten. 1996, 136 S., DM 21,00.

Band 49: Kaiser K., Sorption gelöster organischer Substanzen (DOM) in Waldböden. 1996, 141 S., DM 22,00.

Band 50: Blessing U., Kennzeichnung der PAK-Dynamik zweier Kleineinzugsgebiete im Flysch (Tegernseer Alpen). 1996, 96 S., DM 15,00.

Band 51: Bäumler R., Kemp-Oberhettinger M., Zech W., Bodengenetische Untersuchungen zur Moränenstratigraphie im Langtang-Tal (Zentralnepal) und im Solu/Khumbu (Ostnepal). 1996, 91 S., DM 22,00.

Band 52: Miltner A., Umsetzungen organischer Bodensubstanz unter dem Einfluß von Mineralphasen. 1997, 110 S., DM 18,00.

Band 53: Amelung W., Zum Klimaeinfluß auf die organische Substanz nordamerikanischer Prärieböden. 1997, 140 S., DM 24,00.

Band 54: Weigand H., Mobilität gelöster organischer Substanz (DOM) in porösen Medien: Auswirkung transportmodifizierender Prozesse auf die Ergebnisse von Durchbruchsexperimenten. 1997, 78 S., DM 12,00.

Band 55: Ott J., Messung und Charakterisierung von Gasdiffusionskoeffizienten in künstlichen und natürlich gelagerten Böden. 1997, 116 S., DM 18,00.

Band 56: Vandré R., Ammoniakausgasung aus Gülle nach der Ausbringung. Faktoren und Möglichkeiten der Minderung. 1997, 84 S., DM 13,00.

Band 57: Lehmann J., Tree-crop interactions in a runoff agroforestry system in Northern Kenya. 1997, 151 S., DM 23,00.

Band 58: Ippisch O., Modellentwicklung zum gekoppelten Transport von Wasser, Wärme und Gasen in Abraum aus dem Braunkohletagebau. 1997, 70 S., DM 11,00.

Band 59: Neufeldt H., Land-Use Effects on Soil Chemical and Physical Properties of Cerrado Oxisols. 1998, 174 S., DM 27,00.

Band 60: Westerhof R., Short-Term Effects of Land Use Systems on Nutrient Availability and Structural Stability in the Cerrado Region in Brazil. 1998, 116 S., DM 18,00.

Band 61: Guggenberger G., Transformation und Funktion der organischen Bodensubstanz. 1998, 279 S., DM 42,00.

Band 62: Kammerer G., Untersuchung anorganischer Schwefel-Festphasen in sauren Unterbodenhorizonten und auf Mineraloberflächen. 1998, 107 S., DM 17,00.

Band 63: Droppelmann K.J., Resource Capture in a Runoff Agroforestry System in Northern Kenya. 1999, 138 S., DM 21,00.

Band 64: Rodionov A., Einfluß von Klima und Nutzung auf Humuseigenschaften russischer Steppenböden. 1999, 94 S., DM 15,00.

Band 65: Geosciences in High Asia, Symposium Dushanbe, October 1998. 1999, 217 S., DM 33,00.

Band 66: Eusterbrock L., Polyzyklische aromatische Kohlenwasserstoffe (PAK) und polychlorierte Biphenyle (PCB) in urbanen Böden Bayreuths. 1999, 99 S., DM 15,00.

Band 67: Dittmar C., Radialzuwachs der Rotbuche (*Fagus sylvatica* L.) auf unterschiedlich immissionsbelasteten Standorten in Europa. 1999, 208 S., DM 31,00.

Band 68: Glaser B., Eigenschaften und Stabilität des Humuskörpers der „Indianerschwarzerden" Amazoniens. 1999, 196 S., DM 30,00.

Band 69: Lilienfein J., Water and Nutrient Dynamics in Differently Used Ecosystems of the Brazilian Savanna. 2000, 191 S., DM 29,00.

Band 70: Solomon D., Land Use Effects on Organic Matter and Associated Nutrients in Soils of East African Highlands: Tanzania and Ethiopia. 2001, 211 S., DM 32,00.

Band 71: Ludwig R., Mathematische Modellierung der durch Pyritoxidation induzierten Stofftransporte in Braunkohleabraumkippen in gasförmiger und flüssiger Phase. 2001, 104 S., DM 16,00.

Bayreuther Bodenkundliche Berichte (BBB)

Herausgeber: Lehrstuhl für Bodenkunde und Bodengeographie
der Universität Bayreuth
im Selbstverlag

Schriftleitung: Ludwig Haumaier

zu beziehen über: Sekretariat
Lehrstuhl für Bodenkunde und Bodengeographie
Universität Bayreuth
D-95440 Bayreuth

Fax: 0921/552246
e-mail: wolfgang.zech@uni-bayreuth.de

Bayreuther Forum Ökologie (bfö)

Bisher erschienene Bände:

BITÖK (Hrsg.) (1993) Stickstoff-, Schwefel- und Wasserhaushalt naturnaher Ökosysteme: Forschungskonzept des BITÖK 1993/94. Bayreuther Forum Ökologie **1**, 66 S.

Buchmann, N. (1993) Wege und Umsetzungen von ^{15}N-Ammonium und ^{15}N-Nitrat in einem Fichtenjungbestand (*Picea abies* (L.) KARST.). Bayreuther Forum Ökologie **2**, 246 S.

Deml, R. (1993) Sekundärstoffe und Verteidigung von Augen- und Schadspinnern (Lepidoptera, Saturniidae und Lymantriidae): Eine chemisch-ökologische Studie. Bayreuther Forum Ökologie **3**, 181 S.

Steidle, J. (1993) Das Abdominaldrüsensekret von *Bledius* (Coleoptera, Staphylinidae, Oxytelinae): Seine Zusammensetzung, Funktion und Anpassung. Bayreuther Forum Ökologie **4**, 164 S.

Hilker, M. (1993) Chemische Ökologie juveniler Entwicklungsstadien der Blattkäfer (Coleoptera, Chrysomelidae). Bayreuther Forum Ökologie **5**, 186 S.

Scheidler, M. (1994) Untersuchungen zur Bedeutung von Schadstoffbelastung und Kalkdüngung für die Collembolengemeinschaften in Nordbayerischen Fichtenforsten. Bayreuther Forum Ökologie **6**, 175 S.

Schmitt, M. (1994) Denitrifikation in saurer Nadelstreu. Bayreuther Forum Ökologie **7**, 130 S.

Huth, A. (1994) Untersuchungen zur Biogenese der Wehrsekrete ausgewählter Oxytelinenarten (Coleoptera, Staphylinidae). Bayreuther Forum Ökologie **8**, 163 S.

Burkhardt, J. (1994) Dünne Wasserfilme auf Fichtennadeln und ihr Einfluß auf den Stoffaustausch zwischen Atmosphäre und Pflanze. Bayreuther Forum Ökologie **9**, 135 S.

Beierkuhnlein, C. (1994) Waldquellfluren im Frankenwald - Untersuchungen zur reaktiven Bioindikation. Bayreuther Forum Ökologie **10**, 253 S.

Durka, W. (1994) Isotopenchemie des Nitrat, Nitrataustrag, Wasserchemie und Vegetation von Waldquellen im Fichtelgebirge (NO-Bayern). Bayreuther Forum Ökologie **11**, 197 S.

Koppisch, D. (1994) Nährstoffhaushalt und Populationsdynamik von *Calamagrostis villosa* (CHAIX.) J.F. GMEL., einer Rhizompflanze des Unterwuchses von Fichtenwäldern. Bayreuther Forum Ökologie **12**, 187 S.

Ostendorf, B. (1995) Räumlich-differenzierte Modellierung von Ökosystemen. Bayreuther Forum Ökologie **13**. 141 S.

Köckenberger, W. (1995) Wasser- und Nährstofftransport im Keimling von *Ricinus communis* L. - Erfassung der Flüsse durch Modellierung und Anwendung zerstörungsfreier NMR-Bildgebungsverfahren. Bayreuther Forum Ökologie **14**, 136 S.

BITÖK (Hrsg.) (1995): BITÖK-Forschungsbericht 1994. Bayreuther Forum Ökologie **15**, 266 S.

BITÖK (Hrsg.) (1995): Vorhersage und Erklärung des Verhaltens und der Belastbarkeit von Ökosystemen unter veränderten Umweltbedingungen. Forschungskonzept des BITÖK 1995-97. Bayreuther Forum Ökologie **16**, 279 S.

Höft, M.G. (1995): Aut-ecological studies on *Tabernaemontana pachysiphon* STAPF and *Rauvolfia mombasiana* STAPF (Apocynaceae) in the Shimba Hills (Kenya) with special Reference to their Alkaloid Contents. Bayreuther Forum Ökologie **17**, 139 S.

Manderscheid, B. und Göttlein, A. (eds.) (1995): Wassereinzugsgebiet 'Lehstenbach' - das BITÖK-Untersuchungsgebiet am Waldstein (Fichtelgebirge, NO-Bayern). Bayreuther Forum Ökologie **18**, 84 S.

Alewell, Ch. (1995): Sulfat-Dynamik in sauren Waldböden - Sorptionsverhalten und Prognose bei nachlassenden Depositionen. Bayreuther Forum Ökologie **19**, 185 S.

Achtziger, R. (1995): Die Struktur von Insektenlebensgemeinschaften an Gehölzen: Die Hemipteren-Fauna als Beispiel für die Biodiversität von Hecken- und Waldrandökosystemen. Bayreuther Forum Ökologie **20**, 216 S.

Lükewille, A. (1995): Rekonstruktion der Boden- und Gewässerversauerung in der Langen Bramke (Harz) - Modellierung der Sulfat-Dynamik mit MAGIC (Adsorption) und dem LB-Modell (Ausfällung). Bayreuther Forum Ökologie **21**, 189 S.

Hemp, A. (1995): Die Dolomitkiefernwälder der Nördlichen Frankenalb - Entstehung, synsystematische Stellung und Bedeutung für den Naturschutz. Bayreuther Forum Ökologie **22**, 189 S.

Berger, A. (1995): Wirkungen von Angebot und Bedarf auf den Stickstoff- und Magnesiumhaushalt von Fichten-Keimlingen (*Picea abies* (L.) Karst.). Bayreuther Forum Ökologie **23**, 270 S.

Matschonat, G. (1995): Zur NH_4^+-Sorption und NH_4^+-Fixierung in europäischen Waldböden. Bayreuther Forum Ökologie **24**, 151 S.

Beierkuhnlein, C. (1995): Bibliographie naturschutzrelevanter Publikationen und Examensarbeiten der Fakultät für Biologie, Chemie und Geowissenschaften der Universität Bayreuth. Bayreuther Forum Ökologie **25**, 93 S.

Ostendorf, B., Boyns, M. (1996): Spatial Information System (SIS) - Documentation of a C++ program library for modeling using spatial data. Bayreuther Forum Ökologie **26**, 66 S.

Vogg, G. (1996): Frosthärtung und Enthärtung von immergrünen Nadelbäumen: Auswirkungen auf den Photosyntheseapparat und die photosynthetische Leistungsfähigkeit. Bayreuther Forum Ökologie **27**, 103 S.

BITÖK (Hrsg.) (1996): BITÖK-Forschungsbericht 1995. Bayreuther Forum Ökologie **28**, 285 S.

Bruckner, G. (1996): Deposition und oberirdische Aufnahme von gas- und partikelförmigem Stickstoff aus verschiedenen Emissionsquellen in ein Fichtenökosystem. Bayreuther Forum Ökologie **29**, 230 S.

Falter, R. (1996): Quecksilber in Ökosystemen, Bestimmung von organischen Quecksilberspezies mit einer neuentwickelten HPLC-Methode. Bayreuther Forum Ökologie **30**, 167 S.

Lauerer, M. (1996): Wachstum, Kohlenstoff- und Stickstoffhaushalt von *Nicotiana tabacum* mit reduzierter Nitratreduktase-Aktivität. Bayreuther Forum Ökologie **31**, 179 S.

Küsel, K. (1996): Anaerober Abbau von organischem Kohlenstoff in Waldböden - Acetat als Bindeglied anaerober und aerober Prozesse. Bayreuther Forum Ökologie **32**, 157 S.

Stickroth, H. (1996): Einfluß der Mahd auf den Phytophagen-Parasitoiden-Komplex beim Wiesenpippau (*Crepis biennis* L.). Bayreuther Forum Ökologie **33**, 199 S.

Schricker, K. (1996): Mikrobielle Aktivitäten und Populationen in Abhängigkeit vom Wasserpotential und anderen Bodenparametern. Bayreuther Forum Ökologie **34**, 215 S.

Limmer, C. (1996): N_2-Fixierung in Waldböden. Bayreuther Forum Ökologie **35**, 80 S.

Frank, C. (1996): Nitrifikation und N-Mineralisation in sauren und Dolomit-gekalkten Nadelwaldböden im Fichtelgebirge. Bayreuther Forum Ökologie **36**, 152 S.

Frankl, R. (1996): Zur Vegetationsentwicklung in den Rottauer Filzen (Südliche Chiemseemoore) im Zeitraum von 1957 bis 1992. Bayreuther Forum Ökologie **37**, 257 S.

Kaupp, H. (1996): Atmosphärische Eintragswege und Verhalten von polychlorierten Dibenzo-p-dioxinen und -furanen sowie polyzyklischen Aromaten in einem Maisbestand. Bayreuther Forum Ökologie **38**, 224 S.

Liepert, C. (1996): Chemische Mimikry bei Blattlausparasitoiden der Gattung *Lysiphlebus* (Hymenoptera, Aphidiidae). Bayreuther Forum Ökologie **39**, 180 S.

Richert, E. (1996): Waldränder in Süddeutschland - Struktur, Dynamik und Bedeutung für den Naturschutz. Bayreuther Forum Ökologie **40**, 283 S.

BITÖK (Hrsg.) (1997): BITÖK-Forschungsbericht 1996. Bayreuther Forum Ökologie **41**, 290 S.

Melchior. W. (1997): Wasser- und Nährstofftransport in Geweben. Bayreuther Forum Ökologie **42**, 135 S.

Karsten, G. (1997): Mikrobielle Populationen und Prozesse im Darm von Regenwürmern (Oligochaeta, Lumbricidae). Bayreuther Forum Ökologie **43**, 292 S.

Freese, G. (1997): Insektenkomplexe in Pflanzenstengeln - Eine vergleichende Analyse zu Diversität, Gildenstruktur, Ressourcennutzung und „life-history„-Strategien am Beispiel ausgewählter krautiger Pflanzen. Bayreuther Forum Ökologie **44**, 203 S.

Faust, E. (1997): Die Modellierung atmosphärischer Stickstoff-Deposition in einen Koniferenbestand. Bayreuther Forum Ökologie **45**, 113 S.

Vollrath, B. (1997): SO_2-Entgiftung, Kationen-Versorgung und Photosynthese von ungedüngten und unterschiedlich stickstoffgedüngten Fichten an stark SO_2-belasteten Standorten im Erzgebirge. Bayreuther Forum Ökologie **46**, 207 S.

Peiffer, S. (1997): Umweltgeochemische Bedeutung der Bildung und Oxidation von Pyrit in Gewässersedimenten. Bayreuther Forum Ökologie **47**, 104 S.

Falge, E. M. (1997): Die Berechnung der Kronendachtranspiration von Fichtenbeständen (*Picea abies* (L.) KARST.) mit unterschiedlichen Modellierungsansätzen. Bayreuther Forum Ökologie **48**, 231 S.

Alsheimer, M. (1997): Xylemflußmessungen zur Charakterisierung raum-zeitlicher Heterogenitäten in der Transpiration montaner Fichtenbestände (*Picea abies* (L.) KARST.). Bayreuther Forum Ökologie **49**, 143 S.

Hochwald, S. (1997): Populationsökologie der Bachmuschel (*Unio crassus*). Bayreuther Forum Ökologie **50**, 181 S.

Lindemann, J. (1997): Quantifizierung biogeochemischer Eisen- und Sulfat-Umsetzungen in einem Quellmoor und deren Beitrag zur Säureneutralisierung in einem Einzugsgebiet des Frankenwaldes. Bayreuther Forum Ökologie **51**, 271 S.

Kastner-Maresch, A. (ed.) (1998): Proceedings of a Workshop on Ecosystem Modelling. Bayreuther Forum Ökologie **52**, 243 S.

Bauer, G. (1998): Stickstoffhaushalt und Wachstum von Fichten- und Buchenwäldern entlang eines europäischen Nord-Süd-Transektes. Bayreuther Forum Ökologie **53**, 183 S.

Reinhard, J. (1998): Nahrungssuche und Nahrungsaufnahme der Erdtermite *Reticulitermes santonensis* (Isoptera, Reticulitermitidae): Rolle chemischer Signale. Bayreuther Forum Ökologie **54**, 106 S.

Marmann, P. (1998): Der interne Stickstoffkreislauf von Esche (*Fraxinus excelsior* L.) und Birke (*Betula pendula* ROTH.) bei unterschiedlicher Wasserversorgung. Bayreuther Forum Ökologie **55**, 239 S.

BITÖK (Hrsg.) (1998): Forschungsbericht 1995-97. Bayreuther Forum Ökologie **56**, 268 S.

Scheibke, R. (1998): Die Bestimmung der ungesättigten hydraulischen Leitfähigkeit in Böden mit der Augenblicksmethode - Fehleranalyse, Feldexperiment und Simulation. Bayreuther Forum Ökologie **57**, 191 S.

Husseneder, C. (1998): Populationsgenetik und soziogenetische Organisation der Termite *Schedorhinotermes lamanianus*. Bayreuther Forum Ökologie **58**, 134 S.

Betz, H. (1998): Untersuchungen zur Ausbreitungsökologie des Wolligen Reitgrases (*Calamagrostis villosa* (CHAIX.) J. F. GMEL.). Bayreuther Forum Ökologie **59**, 207 S.

Schultze, B. (1998): Optimierung der Messung bodenhydraulischer Eigenschaften durch inverse Simulation von Ausfluß- und Rückflußexperimenten an Bodensäulen. Bay reuther Forum Ökologie **60**, 133 S.

Nunnenmacher, L. (1998): Blattläuse auf Kopfsalat und deren Kontrolle durch gezielte Beeinflussung der Lebensgrundlagen ihrer Prädatoren. Bayreuther Forum Ökologie **61**, 148 S.

Peine, A. (1998): Saure Restseen des Braunkohletagebaus - Charakterisierung und Quantifizierung biogeochemischer Prozesse und Abschätzung ihrer Bedeutung für die seeinterne Neutralisierung. Bayreuther Forum Ökologie **62**, 141 S.

Sturm, N. (1998): Steuerung, Skalierung und Umsatz der Wasserflüsse im Hartheimer Kiefernforst (*Pinus sylvestris* L.). Bayreuther Forum Ökologie **63**, 190 S.

BITÖK (Hrsg.) (1999): Vegetationsökologische, ethnobotanische und -faunistische Beiträge über Äquatorial-Afrika - Mount Kenya, Kilimanjaro, Äthiopien, Elfenbeinküste. Bayreuther Forum Ökologie **64**, 244 S.

Wolf, F. (1999): Berechnung von Information und Komplexität in Zeitreihen - Analyse des Wasserhaushaltes von bewaldeten Einzugsgebieten. Bayreuther Forum Ökologie **65**, 164 S.

Lauf, J. (1999): Entwicklung von Methoden zur Bestimmung des natürlichen Stickstoff-Isotopenverhältnisses von NH_3, NO und NO_2 in Umgebungsluft. Bayreuther Forum Ökologie **66**, 106 S.

Michalzik, B. (1999): Flüsse und Dynamik von gelösten organischen Stickstoffverbindungen (DON) in einem Fichtenwaldökosystem. Bayreuther Forum Ökologie **67**, 190 S.

Burkhardt, B. (1999): Eiablageverhalten, Gallentyp und Fitness von *Urophora*-Arten (Diptera: Tephritidae) bei unterschiedlicher Wirtsqualität. Bayreuther Forum Ökologie **68**, 182 S.

Beierkuhnlein, C. (Hrsg.) (1999): Rasterbasierte Biodiversitätsuntersuchungen in nordbayerischen Landschaftsräumen. Bayreuther Forum Ökologie **69**, 206 S.

Lange, H (1999): Charakterisierung ökosystemarer Zeitreihen mit nichtlinearen Methoden. Bayreuther Forum Ökologie **70**, 112 S.

Beierkuhnlein, C. & Gollan, T. (Hrsg.) (1999): Ökologie silikatischer Waldquellen in Mitteleuropa. Bayreuther Forum Ökologie **71**, 256 S.

Chang, S.-C. (1999): The effect of stemflow on element fluxes and soil nitrogen transformations in a mixed beech/oak stand in the Steigerwald, Germany. Bayreuther Forum Ökologie **72**, 108 S.

Lenuweit, U. (1999): Latexlectine von *Euphorbia cyparissias* L., *E. esula* L. und *E. virgata* W. & K. und ihre Funktion als pflanzliche Abwehrstoffe gegen phytophage Insekten. Bayreuther Forum Ökologie **73**, 148 S.

May, C. (1999): Nutzung von Ammonium und Nitrat durch Rotbuche (*Fagus sylvatica* L.) und Traubeneiche (*Quercus petraea* [L.] KARST.). Bayreuther Forum Ökologie **74**, 112 S.

Scherer, M. (1999): Effects of plant diversity on ecosystem processes in experimental grassland communities. Bayreuther Forum Ökologie **75**, 195 S.

Dieffenbach, A. (2000): In situ-Bodenlösungschemie in der Rhizosphäre von Fichten-Feinwurzeln. Bayreuther Forum Ökologie **76**, 129 S.

Dörwald, W. (2000): Ein Framework für interaktive individuenbasierte Modelle. Bayreuther Forum Ökologie **77**, 87 S.

BITÖK (Hrsg.) (2000): Forschungsbericht 1999. Bayreuther Forum Ökologie **78**, 395 S.

Stuhrmann, M. (2000): Verbleib eingetragenen Stickstoffs in Waldböden entlang eines klimatischen Transektes durch Europa. Bayreuther Forum Ökologie **79**, 154 S.

Sahin, H. (2000): Auswaschung saurer Verwitterungsprodukte der Pyritoxidation aus einer Abraumhalde des Schieferbergbaus in Thüringen. Bayreuther Forum Ökologie **80**, 153 S.

Balzer, S. (2000): Populationsökologische Untersuchungen an *Dactylorhiza sambucina* (L.) SOÓ im Frankenwald, Nordost-Bayern. Bayreuther Forum Ökologie **81**, 241 S.

Henzler, T. (2001): Die Funktion von Wasserkanälen in pflanzlichen Zellmembranen und ihre Bedeutung für den Wassertransport in Wurzeln. Bayreuther Forum Ökologie **82**, 141 S.

Schwesig, D. (2001): Biogeochemistry of Mercury and Methylmercury in Two Forested Catchments in Bavaria, Germany. Bayreuther Forum Ökologie **83**, 135 S.

BITÖK (2001): Forschungsbericht 2000. Bayreuther Forum Ökologie **84**, 420 S.

Mertens, M. (2001): Die Anwendung der Fuzzy-Set-Theorie auf die Modellierung von Stickstoffbilanzen im Weißenstädter Becken. Bayreuther Forum Ökologie **85**, 215 S.

Taube, J. (2001): Vorkommen von Pflanzenschutzmitteln im Bioabfall und Verhalten ausgewählter Pflanzenschutzmittel bei der Bioabfallbehandlung in anaeroben und aeroben Prozessen. Bayreuther Forum Ökologie **86**, 199 S.

Zimmermann, H. M. (2001): Die Rolle apoplastischer Transportbarrieren bei der radialen Wasser- und Ionenaufnahme in Maiswurzeln (*Zea mays* L.) Bayreuther Forum Ökologie **87**, 160 S.

Schwörer, U. (2001): Fouragierstrategien und Ressourcennutzung von Blattlausparasitoiden unter ungünstigen abiotischen Bedingungen. Bayreuther Forum Ökologie **88**, 209 S.

zu beziehen über: Bayreuther Forum Ökologie (bfö)

Herausgeber: Bayreuther Institut für Terrestrische Ökosystemforschung (BITÖK) im Selbstverlag

Redaktion: BITÖK - Wissenschaftliches Sekretariat
Dr. Pedro Gerstberger, Dr. Thomas Gollan

Bestellungen an: BITÖK - Wissenschaftliches Sekretariat
Universität Bayreuth
D - 95440 Bayreuth
Tel.: 0921/55 - 57 00 Fax: 0921/55 - 57 99
e-mail: bitoek@bitoek.uni-bayreuth.de

⇨ Ein **Übersichtsprospekt** mit sämtlichen Kurz-Zusammenfassungen wird auf Anfrage gerne kostenlos zugesandt bzw. ist im **Internet** verfügbar:

http//:www.bitoek.uni-bayreuth.de/Bestellungen/DE.html